Upregulation of inflammatory mediators during diabetic cardiomyopathy and possible amelioration with cinnamic acid

by

Anupama Nair
10BB15A39021

A thesis submitted to the
Academy of Scientific & Innovative Research
for the award of the degree of

DOCTOR OF PHILOSOPHY
in
SCIENCE

Under the supervision of
Prof. (Dr) K G Raghu

CSIR-National Institute for Interdisciplinary Science and Technology
(NIIST), Thiruvananthapuram, Kerala, 695019, India

Academy of Scientific and Innovative Research
AcSIR Headquarters, CSIR-HRDC campus, Sector 19, Kamla Nehru Nagar,
Ghaziabad, U.P. – 201 002, India

February 2021

DECLARATION

I hereby declare that the work incorporated in this thesis entitled, "*Upregulation of inflammatory mediators during diabetic cardiomyopathy and possible amelioration with cinnamic acid*", submitted to the Academy of Scientific and Innovative Research (AcSIR) in fulfilment of the requirements for the award of the Degree of *Doctor of Philosophy* in *Biological Sciences*, embodies original research work carried out by me under the supervision of Prof (Dr) KG Raghu, Senior Principal Scientist, Agro-Processing and Technology Division, CSIR-National Institute for Interdisciplinary Science and Technology (CSIR-NIIST), Thiruvananthapuram, Kerala, India. I, further declare that this work has not been submitted to any other University or Institution in part or full for the award of any degree or diploma.

Anupama Nair

Dr. K.G. Raghu

राष्ट्रीय अंतर्विषयी विज्ञान तथा प्रौद्योगिकी संस्थान
NATIONAL INSTITUTE FOR INTERDISCIPLINARY SCIENCE AND TECHNOLOGY
वैज्ञानिक तथा औद्योगिक अनुसंधान परिषद् | Council of Scientific and Industrial Research
डस्ट्रियल इस्टेट पी. ओ. पाप्पनकोड, तिरुवनंतपुरम, भारत - 695 019 | Industrial Estate P.O., Pappanamcode, Thiruvananthapuram, India-695 019

CERTIFICATE

This is to certify that the work incorporated in this Ph.D. thesis entitled, "*Upregulation of inflammatory mediators during diabetic cardiomyopathy and possible amelioration with cinnamic acid*", submitted by Anupama Nair to the Academy of Scientific and Innovative Research (AcSIR) in fulfillment of the requirements for the award of the Degree of *Doctor of Philosophy* in Biological Sciences, embodies original research work carried-out by the student. We, further certify that this work has not been submitted to any other University or Institution in part or full for the award of any degree or diploma. Research materials obtained from other sources and used in this research work have been duly acknowledged in the thesis. Image(s), illustration(s), figure(s), table(s) etc., used in the thesis from other source(s), have also been duly cited and acknowledged.

Anupama Nair 12/02/21
Anupama Nair
12-02-2021

12/02/2021
Dr. K G Raghu
12-02-2021

Tel: 91 471 2490874 Fax: 91 471 2491895, 2491712, 2490389, (D) 2515239/256/384 E-mail: spo@niist.res.in, Website: http/www.niist.res.in

STATEMENTS OF ACADEMIC INTEGRITY

I, **Anupama Nair,** a Ph.D. student of the Academy of Scientific and Innovative Research (AcSIR) with Registration No. 10BB15A39021 hereby undertake that, the thesis entitled "*Upregulation of inflammatory mediators during diabetic cardiomyopathy and possible amelioration with cinnamic acid*" has been prepared by me and that the document reports original work carried out by me and is free of any plagiarism in compliance with the UGC Regulations on *"Promotion of Academic Integrity and Prevention of Plagiarism in Higher Educational Institutions (2018)"* and the CSIR Guidelines for *"Ethics in Research and in Governance (2020)"*.

12/02/21

12-02-2021
Thiruvananthapuram

It is hereby certified that the work done by the student, under my supervision, is plagiarism-free in accordance with the UGC Regulations on *"Promotion of Academic Integrity and Prevention of Plagiarism in Higher Educational Institutions (2018)"* and the CSIR Guidelines for *"Ethics in Research and in Governance (2020)"*.

12/02/2021

Dr. KG Raghu
12-02-2021
Thiruvananthapuram

Acknowledgements

First and foremost, it's my pleasure to express a deep sense of thanks and gratitude to my supervisor Dr. K.G.Raghu, Senior Principal Scientist, CSIR-NIIST for having given me an opportunity to do PhD under his guidance. His valuable suggestions, creative ideas, timely advice and assistance throughout has helped me immensely in my research. I also thank him for his motivation at times of hardships and also for providing me necessary lab facilities to complete this work. I thank you for the leadership and commitment to put in extra work to achieve my goals.

My gratitude also extends to Dr. A. Ajayaghosh, Director and Dr. Suresh Das, former Director, CSIR-NIIST, Trivandrum, for allowing me to be a part of this institution and also for providing necessary facilities for carrying out my work. I would also like to express my sincere gratitude to former heads of Agroprocessing and Technology Division, Dr. A. Sundaresan, Mr. M.M. Sreekumar and Dr. Dileepkumar BS, for their support and encouragement.

I would also like to thank the Doctoral Advisory Committee: Dr. Madhavan Nampoothiri, Dr. Priya S. and Dr. K.V. Radhakrishnan for their valuable suggestions and support. I wish to extend my sincere thanks to Dr. P. Jayamurthy, Smt. M. V. Reshma, Dr. P. Nisha, Mr. V.V. Venugopal, Dr. Beena Joy, Mr. D.R. Soban Kumar, and Ms. Divya Mohan for their help and support in one or other way. All the former and present members of Agroprocessing and Technology Division have been extremely helpful and co-operative and I am thankful to one and all for their kind gesture.

I also wish to thank the AcSIR coordinators Dr. Mangalam S Nair, Dr. Luxmi Verma and Dr. Suresh C.H. for helping me in fulfilling AcSIR requirements.

I express my sincere thanks to the Director, Jubilee Mission Medical College and Research Institute (JMMC&RI), Thrissur for having given me an opportunity to conduct my animal study in the Small Animal Research Facility, JMMC&RI. I wish to thank Dr. Rajankutty K, Head, Small Animal Research Facility for having helped us in all our animal experiments. I also would like to thank Dr. Varghese PR, Research Coordinator, Dr. Ranjith S, Adjunct faculty, Dr. Alex George, Dr. Mathew John, Dr. Sureshkumar and Evelyn Maria for allowing me to utilize their lab facilities. I also extend my gratitude to Mrs. Gracy and

Kalyani MS of the animal house for continuously supporting me throughout my animal study.

My sincere thanks goes to all my former labmates Dr. Antu K Antony, Dr. Reshma PL, Dr. Vandana S, Dr. Riya MP, Dr. Anusree SS, Dr. Prathapan A, Dr. Nisha VM, Dr. Soumya RS, Dr. Priyanka A, Dr. Vineetha VP, Dr. Priya Rani, Ms Kavitha Sasidharan, and Mr. Vinod J.S. and all those who have given me proper directions to do my work and for teaching me to use the facilities. I also would like to thank Dr. Syama HP, Dr. Dhanya R, Dr. Shamla L, Dr. Shilpa G and Ms. Saranya for having given me valuable suggestions.

My appreciation extends to my present lab colleagues for having helped me in various ways. Initially, I would like to thank Ms. Preetha Rani MR who has always been with me through the thick and thin of my entire PhD. My special thanks also goes to Dr. Sindhu G for her valuable suggestions. I express my gratitude to Dr. Salin Raj P, Dr. Shyni G.L., Dr. Genu George, Dr. Soumya RS, Ms. Sreelekshmi Mohan, Ms. Sruthi CR, Ms. Swapna Sasi, Ms. Poornima MS, and Ms. Roopasree OJ for supporting, encouraging and helping me in various phases of my PhD. I would also like to thank Mr. Billu Abraham, Dr. Jubi Jacob, Dr. Varsha K, Ms. Lekshmi K, Ms Lakshmi S, Ms Anagha Nair, Ms Eveline Anto, Ms Reshmitha TR, Ms Anusha, Ms Tanya M.S., Mr. Pratheesh S Nair, Mr. Sreejith and all other friends of Agroprocessing and Technology Division, CSIR-NIIST for having helped me throughout.

It is my pleasure to thank all the members of library, administrative, academic programme committee and technical staff of NIIST for their help and support.

I also extend my sincere thanks to my seniors and all friends in other divisions of NIIST for their help and support.

I am also indebted to Council of Scientific and Industrial Research (CSIR) and Department of Health Research (DHR), ICMR, for financial assistance in the form of research fellowship and Young Scientist fellowship.

A special thanks to my family for their prayers, affection and support which helped me in successful completion of my research work.

Finally, I humbly bow before the almighty God for showering his blessings upon me and giving me the strength and patience to reach this important milestone in my academic life.

Anupama Nair

Table of Contents

List of Figures

List of Tables

Abbreviations

ANP	: Atrial natriuretic peptide
ATP	: Adenosine triphosphate
BNP	: B-type natriuretic peptide
BSA	: Bovine serum albumin
CK-MB	: Creatine phosphokinase-MB
CRP	: C-reactive protein
CVD	: Cardiovascular diseases
DCFH-DA	: Dichloro-dihydro-fluorescein diacetate
DCM	: Diabetic cardiomyopathy
DMEM	: Dulbecco's modified eagle medium
DRP1	: Dynamin related protein 1
DMSO	: Dimethyl sulfoxide
EDTA	: Ethylene diamene tetraacetic acid
FBS	: Foetal bovine serum
FIS1	: Fission protein 1
FITC	: Fluorescein isothiocyanate
GPx	: Glutathione peroxidase
GSH	: Reduced glutathione
GSK-3β	: Glycogen Synthase Kinase-3 β
ICAM	: Intracellular adhesion molecule
IκBα	: Inhibitor of Nuclear factor of kappa B
IL-1β	: Interleukin -1 beta
IL-6	: Interleukin - 6
IL-10	: Interleukin- 10
iNOS	: Inducible nitric oxide synthase
JNK	: c-Jun N-terminal kinase
LDH	: Lactate dehydrogenase
MCP-1	: Monocyte chemo-attractant protein
MCUR1	: Mitochondrial calcium uniporter 1

MFN2	: Mitofusin-2
MAPK	: Mitogen activated protein kinases
MTT	: 3-(4, 5-dimethylthiazol- 2-yl)-2,5-diphenyl tetrazolium bromide)
MyD88	: Myeloid differentiation primary response 88
NAD	: Nicotinamide adenine dinucleotide
NBT	: Nitroblue tetrazolium
NF-κβ	: Nuclear factor-κβ
O-GlcNAc	: O- linked β- N- acetylglucosamine
OPA1	: Optic atrophy 1
PBS	: Phosphate buffered saline
PI	: Propidium iodide
PVDF	: Polyvinylidene difluoride
qRT-PCR	: Quantitative real time polymerase chain reaction
RIPA buffer	: Radio immunoprecipitation buffer
ROS	: Reactive oxygen species
SDS	: Sodium dodecyl sulphate
SGOT	: Serum glutamic oxaloacetic transaminase
SOD	: Superoxide dismutase
STL2	: Soluble interleukin 1 receptor-like 1
STZ	: Streptozotocin
TBA	:Thiobarbituric acid
TGF-β	: Transforming growth factor-β
TLR4	: Toll like receptor
TNF-α	: Tumour necrosis factor-α
TNNI3K	: Cardiac troponin I interacting kinase (TNNI3K)
NLRP3	: NLR family pyrin domain containing 3
TxNIP	: Thioredoxin interacting protein

Chapter 1

Introduction and Literature Survey

1.1 Diabetes mellitus

Metabolic syndromes refer to a cluster of diseases that increases the risk of heart diseases. High blood pressure, a large waistline, low HDL cholesterol, high LDL levels, high triglyceride levels and high fasting blood glucose levels are some of the risk factors associated with metabolic syndromes. Diabetes mellitus (DM) is a chronic metabolic disease in which high levels of blood glucose leads to severe damage to the heart, kidneys, blood vessels, eyes and nerves (World Health Organisation, 2020). The three main types of diabetes are Type 1 DM, Type 2 DM and gestational diabetes. In type 1 DM the elevated blood glucose levels or hyperglycemia are due to the inability of pancreas to make insulin while type 2 DM is characterised by the inability of cells to utilise the insulin produced by the body and the most common form of diabetes among adults (International Diabetes Federation, 2020). Gestational diabetes is distinguished by the occurrence of high blood glucose during pregnancy which causes complications to both mother and child (International Diabetes Federation, 2020). In 2019, approximately 463 million adults were living with diabetes and the figures are expected to rise to 700 million by 2045 (International Diabetes Federation, 2019). The low and middle income countries are the worst affected (International Diabetes Federation, 2020 & World Health Organisation, 2020).

1.1.1 Complications of diabetes

Diabetes can lead to complications in many parts of the body (Fig. 1) which are mentioned below. Diabetics are also prone to developing infections.

- Cardiovascular disease- Diabetes affects the heart and blood vessels leading to coronary artery disease and stroke. The risk factors for the cardiovascular complications include hypertension, high cholesterol and high blood glucose levels.
- Diabetic nephropathy- The small blood vessels in the kidneys are severely affected during diabetes. This leads to decreased efficiency of kidneys.

- Diabetic neuropathy- Damage to the nerves is another common complication of diabetes. The most adversely affected are the extremities, particularly the feet. This is also known as peripheral neuropathy which is mainly characterised by pain, tingling and numbness in the affected area.
- Diabetic retinopathy- High blood glucose levels along with high blood pressure and cholesterol leads to some form of eye disease or retinopathy leading to reduced eye vision or blindness.
- Oral complications- Periodontitis or gum inflammation is another complication of high blood glucose. It results in tooth loss and is also associated with increased risk of cardiovascular disease.
- Pregnancy complications- Diabetes during pregnancy leads to overweight in the fetus. This results in complications during delivery and increased trauma for the mother and child. Such children are also at a higher risk of developing diabetes in future.

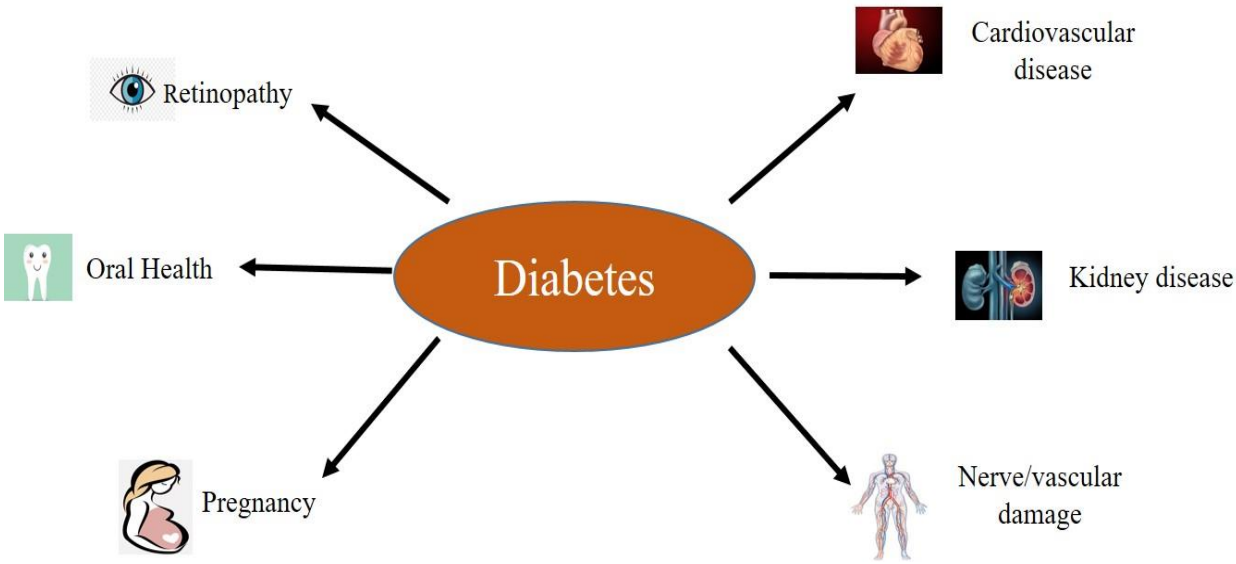

Fig. 1.1 Complications of diabetes

1.2 Cardiovascular diseases

Cardiovascular diseases (CVDs) include disorders of the heart and blood vessels and there are different types of CVDs like coronary heart disease, cerebrovascular disease, peripheral arterial disease, rheumatic heart disease, and congenital heart disease. CVDs account for the increased risk of mortality worldwide. At least 17.9 million people die of CVDs every year which accounts for 31% of all global deaths (World Health

Organization, 2019). The main factors responsible for the onset of these diseases include physical inactivity, tobacco use, unhealthy diet and the harmful use of alcohol. These risk factors are manifested as increased blood sugar levels, elevated blood pressure, overweight and obesity which are detrimental to good heart health. Again low and middle income countries are more vulnerable to CVDs (World Health Organization, 2019). In addition to these there are underlying determinants of CVD like globalization, urbanisation and aging. Diabetes is expected to affect 300 million people with a prevalence of 5.4% by 2025 (King et al., 1998).

1.2.1 Prevalence of cardiovascular disease in India.

CVDs have also become the leading cause of mortality in India (Reddy et al., 2005). The past two decades have witnessed a pronounced epidemiological transition in India from infectious diseases to non-communicable diseases (NCDs) (Institute for Health Metrics and Evaluation (IHME) 2010). However, at present the pandemic of Covid-19 has resulted in many deaths. Still we cannot underestimate the impact of NCDs. NCDs have become a global threat, India being no exception, affecting the sustainable development on the whole. The burden of non-communicable diseases has risen rapidly in India simultaneously with an increase in the aging of population. CVDs account for the major portion of non-communicable disease burden. There are many multisectoral national policies that aims to prevent and control the burden from NCDs. In India the National Health Policy 2017 targets to reduce 25% premature cardiovascular deaths by 2025 (Ministry of Health and Family Welfare, 2012). According to a recent study by Prabhakaran et al., the cases of cardiovascular diseases in India increased from 25·7 million (95% UI 25·1–26·0) in 1990 to 54·5 million (53·7–55·3) in 2016 (Prabhakaran et al., 2018). The frequency of CVD cases was highest in Kerala followed by Punjab and Tamil Nadu (Fig. 2). Also the death rate due to cardiovascular diseases in India increased from 1·3 million (95% UI 1·2–1·4) in 1990 to 2·8 million (2·6–2·9) in 2016 (Prabhakaran et al., 2018). From their study it is revealed that particularly Kerala is more vulnerable to ischemic heart disease and stroke. According to the Global Burden of Disease study age-standardized estimates (2010), 24.8%, i.e. approximately a quarter, of all deaths in India are due to CVD (Institute for Health Metrics and Evaluation (IHME) 2010). This situation immediately urges the country to adopt various population level strategies to reduce the risk factors.

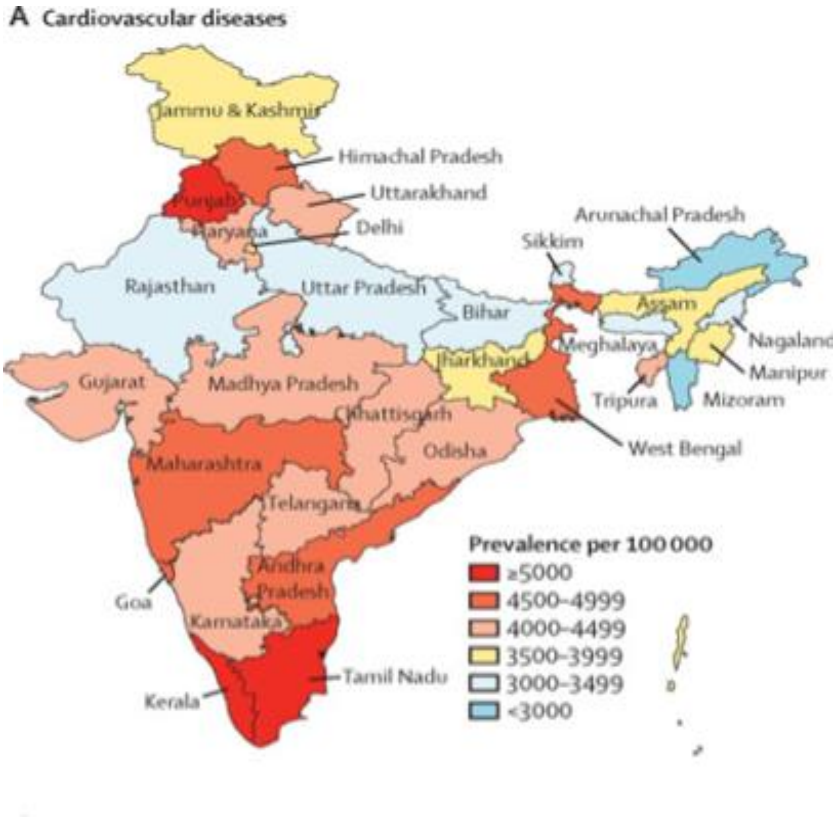

Fig. 1.2 Prevalence of cardiovascular diseases in India (Prabhakaran et al., 2018)

1.3 Diabetic cardiomyopathy

Diabetic cardiomyopathy (DCM) includes a collection of abnormalities that alter the structure and function of the myocardium in the absence of other risk factors, such as coronary artery disease, hypertension, and valvular heart disease (Liu et al., 2014). The existence of DCM was initially proposed by Rubler et al., in 1972 (Rubler et al., 1972). DCM constitutes nearly 12 % of T2DM patients (Bertoni et al., 2004). The sustaining hyperglycemic and hyperlipidemic conditions during diabetes results in the development of oxidative stress, inflammation, mitochondrial dysfunction and activation of renin angiotensin aldosterone system, all of which ultimately results in DCM (Bugger and Abel, 2014; Jia et al., 2016; Jia et al., 2018) in both T1DM and T2DM. However, hyperinsulinemia and hyperglycemia are considered to be the main culprits to induce the adaptive and maladaptive response that leads to heart failure during DCM in T2DM (Poornima et al., 2006); Terashima and Goto, 2002). There are reports about the association between high levels of glycated haemoglobin and increased risk of heart

failure in T2DM than in T1DM. Type 1 diabetic hearts showed increased cardiomyocyte autophagy while the same was subdued in type 2 diabetes (Kanamori et al., 2015). The aberrant insulin signalling in the myocardium is a characteristic of DCM (Battiprolu et al., 2013). Extensive studies are going on to investigate the structural, functional, and metabolic changes that occur in the diabetic myocardium. Left ventricular hypertrophy, interstitial fibrosis and apoptosis, are associated with structural changes occurring in the myocardium during chronic diabetes (Isfort et al., 2014). The functional changes include diastolic and systolic dysfunction and impaired contractile reserve (Nunes et al., 2012).

Initially, DCM shows no symptoms and is characterized by an increased fibrosis and stiffness. In the primary stages, early diastolic filling of the heart is reduced and it is followed by an increased atrial filling and enlargement and LV end-diastolic pressure (Westermeier et al., 2016) . The second stage of diabetic cardiomyopathy is manifested as hypertrophy, cardiac remodeling, advancing cardiac diastolic dysfunction, followed by appearance of clinical symptoms of heart failure with normal ejection fraction (Jia et al., 2016). The advanced stages of DCM is mainly characterised by systolic and diastolic dysfunction along with reduced cardiac ejection fraction, and an extended left ventricular chamber (Jia et al., 2016). However, the increased levels of natriuretic peptides and O-linked N-acetylglucosamine (O-GlcNAc), facilitate the diagnosis of heart failure (Jia et al., 2016).

1.3.1 Epidemiology of diabetes associated heart failure

Patients with diabetes are more susceptible to developing heart failure than those without diabetes (Dei Cas et al., 2015). According to the reports of the Framingham Heart Study there is a 5-fold increased risk of heart failure in women with diabetes than in men (Kannel et al., 1974). Another report from United Kingdom National Diabetes Audit, the most common complication for T2DM is heart failure. There was a significant variation in the left ventricular wall thickness and mass between diabetic and normal patients according to a population based surver conducted in the Cardiovascular Health Study (Devereux et al., 2000) and Multi-Ethnic Study of Atherosclerosis (Bertoni et al., 2006).

According to recent findings, bringing the glucose levels down to normal does not guarantee the restoration of the cardiovascular disease risk to the level of non-diabetics (Kenny and Abel, 2019). The observations that blood glucose lowering might not be sufficient to prevent increased hospitalization and mortality from HF, reinforce the

possibility that there are other factors apart from glycemia responsible for the increased risk of heart failure in diabetes, or that independent mechanisms might exist linking anti-hyperglycemic therapies and LV remodeling (Kenny and Abel, 2019). In addition to the structural and functional changes that occur with diabetic cardiomyopathy, a complex underlying and intertwined pathophysiology exists which may contribute to heart failure in the scenario of diabetes, some of which may be amenable to pharmacological therapy (Kenny and Abel, 2019).

1.3.2 Pathophysiology of diabetic cardiomyopathy

One of the major factor responsible for DCM is the alteration in myocardial substrate utilisation. Normally, the heart mainly uses fatty acids and glucose along with other substrates like lactate and amino acids in order to obtain energy, thus providing metabolic flexibility. Fatty acid uptake is mediated by CD36 and fatty acid translocase (FAT) while glucose uptake which is an insulin dependent mechanism is mediated by GLUT4 (Aroor et al., 2012; Jia et al., 2016). However during DCM, CD36 translocates to the sarcolemma but GLUT 4 remains internalised in an intracellular location due to insulin resistance (Battiprolu et al., 2013). This preferential localisation of CD36 to the myocytes' sarcolemma is one among the main culprits during DCM facilitating more lipid accumulation in the heart (Fig. 2). Myocardial fatty acid oxidation is also mediated by another protein called peroxisome proliferator activated receptor α (PPARα) which is responsible for the activation of genes involved in cardiac fatty acid utilization (Aoyama et al., 1998; Barger and Kelly, 2000). Studies in mice with cardiac overexpression of PPARα simulated the metabolic derangements of the diabetic heart (Young et al., 2001). Thus there is a substrate switch from glucose towards free fatty acids leading to decreased cardiac efficiency. This excessive lipid accumulation is detrimental to the cardiomyocytes (Borghetti et al., 2018). This substrate shift is usually accompanied by impaired oxidative phosphorylation and mitochondrial proton leak leading to an overproduction of ROS (Jia et al., 2018). The limited antioxidant capacity of heart adds insult to injury by increasing the mitochondrial ROS production which leads to NO destruction and thus reducing the bioavailability of NO, which is one of the hallmark of DCM (Marso et al., 2016) . Studies show that in CD36 knockout mice the FFA uptake is reduced by 70 % in cardiomyocytes (Habets et al., 2007) and another study shows that CD36 deficiency prevents lipotoxic injury to cardiomyocytes (Yang et al., 2007). Several lipid metabolites like ceramides and diacylglycerols which are the formed as a result of

non-oxidative lipid metabolism also contribute to DCM (Jia et al., 2016). In obese individuals insulin sensitivity is usually accompanied by elevated diacylglycerol content and PKC ε (protein kinase Cε) activation (Shulman and Samuel, 2016). A study in high fat diet fed mice showed an elevated levels of diacylglycerol which was closely associated with insulin resistance and diminished NO availability (Jornayvaz et al., 2011). Also impaired regulation of microRNAs like miRNA 451 also leads to myocardial steatosis (Costantino et al., 2019). Thus miRNAs also play an essential role in the progression of DCM.

Another pathophysiological consequence of DCM is hyperglycemia (Fig. 2). During hyperglycemia there is an overproduction of ROS which causes DNA damage and also triggers the production of advanced glycation end products (AGEs) (DeMarco et al., 2014). These are formed as result of nonenzymatic reactions between reducing sugars and the free amino groups present on macromolecules like proteins, lipids and nucleic acids (Goh et al., 2012). Hyperglycemia stimulates the AGE induced crosslinking of collagen molecules (Fig.2) leading to myocardial fibrosis and reduced myocardial relaxation (Jia et al., 2016). This further stimulates profibrotic and proinflammatory signalling leading to the formation of oxidative stress mediators (Yamagishi et al., 2012). AGEs were found to be an independent risk factor in postinfarction heart failure in 194 patients with acute coronary syndrome (Raposeiras-Roubín et al., 2012).

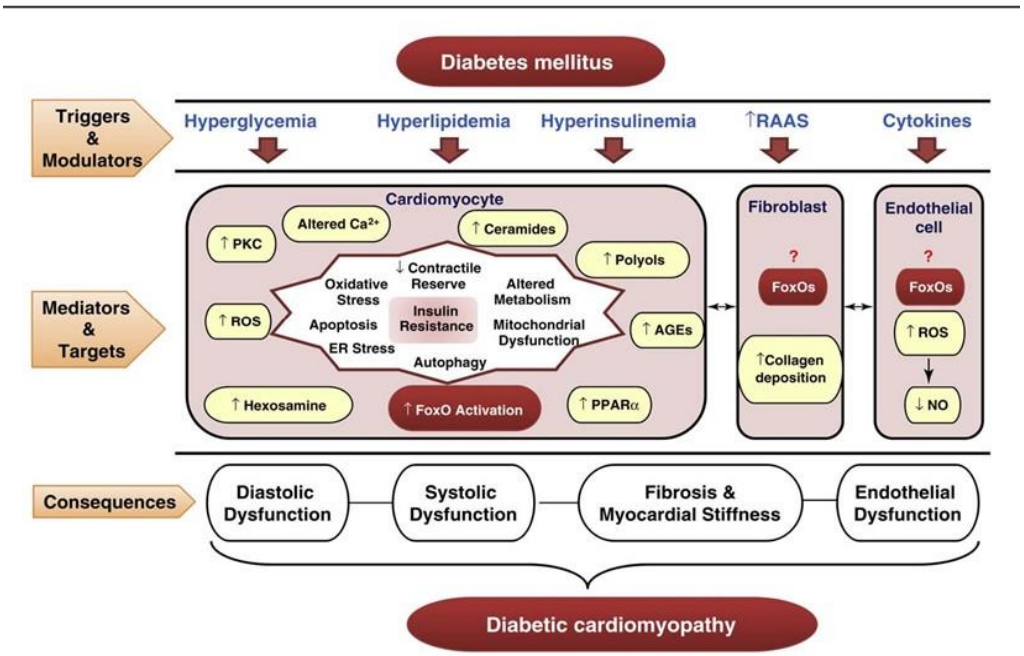

Fig. 1.3 Pathophysiology of diabetic cardiomyopathy (Battiprolu et al., 2010)

1.3.3 Clinical manifestation and diagnosis of DCM

The underlying mechanism for DCM may be distinct for the both type 1 and type 2 diabetes. However the important fact to be noted is that hyperinsulinemia which is present only in T2DM and absent from T1DM may be responsible for the differences in cardiac morphology found in subjects affected by both types of diabetes (Hölscher et al., 2016). At present there are no clinical manifestations or specific biomarkers present to identify DCM in patients with diabetes. Instead, a number of non-invasive imaging techniques like electrocardiography and magnetic resonance imaging are used nowadays to gather information about cardiac morphology and function (Lee and Kim, 2017). Doppler imaging techniques are used to quantify the diastolic and systolic dysfunction (Borghetti et al., 2018). Diabetic patients are shown to have more markers. The heart failure with normal ejection fraction in diabetic patients can be distinguished by the presence of biomarkers like endothelin 1, galectin 3 and carboxy terminal telopeptide of collagen 1 (Lindman et al., 2014). In addition many studies have found that normalization of glycemia might not restore risk of cardiovascular disease to the non-diabetic baseline (Kenny and Abel, 2019).

1.3.4 Alterations in myocardial function in diabetes

The pathogenesis of diabetic cardiomyopathy is multifactorial. Myocardial dysfunction during DCM mainly occurs as a result of changes in gene expression that affect excitation–contraction coupling (ECC) and cellular metabolism (Lebeche et al., 2008). Most of the underlying molecular mechanisms related to DCM have been unravelled using several rodent models (Poornima et al., 2006; Severson, 2004). The recurrence of fetal gene expression like overexpression of atrial natriuretic factor, α-actin; increased β-myosin heavy chain and reduced α-myosin heavy chain expression has been considered to be responsible for the characteristic phenotypic abnormalities of the myocardium (Dillmann, 1980).

1.3.4.1 Oxidative stress and diabetic cardiomyopathy

Oxidative stress occurs when there is an imbalance between the endogenous antioxidant system and the reactive free radicals (Cai and Kang, 2001). This change in the redox homeostasis is a major contributor to high glucose induced diabetic damage. The production of free radicals is escalated as a result of impaired lipid metabolism and chronic hyperglycemia (Arumugam et al., 2013). The most common free radicals include

reactive oxygen species (ROS) such as superoxide anions, hydroxyl radicals and reactive nitrogen species (RNS). They are known to cause DNA damage and thus increase cardiomyocyte apoptosis (Fig. 4) (Bordun et al., 2014). In addition ROS reacts with nitric oxide to produce peroxynitrite which triggers vasoconstriction, platelet activation and impaired coagulation ultimately leading to atherosclerosis (Bordun et al., 2014). Cai et al. reported that ROS and RNS lead to oxidative and nitrosative stresses thus leading to cardiomyopathy (Cai et al., 2006),. Cells have their innate mechanisms to scavenge these free radicals. These mechanisms include antioxidant enzymes such as superoxide dismutase, catalase, glutathione reductase, and thioredoxins. However, during pathological conditions, the innate antioxidant system fails to function properly and increases the intracellular levels of free radicals leading to oxidative damage (Piconi et al., 2003). A major source of ROS is mitochondria. Mitochondrial ROS production occurs mainly at complex 1 (NADH: ubiquinone oxidoreductase) and complex 3 (ubiquinone-cytochrome c reductase). The excess superoxide anions generated by the mitochondria is the precursor of most ROS and a mediator in oxidative chain reactions (Litvinova et al., 2015). Mitochondria are not the only source of ROS within a cell. NADPH oxidases, which are membrane bound enzymes, also contribute to the free radical pool inside a cell (Harper et al., 2004) The ultimate outcome of oxidative stress is cardiac hypertrophy, fibrosis, inflammation an extracellular matrix remodeling. Many studies have been reported showing the link between oxidative damage and diabetic injury in various organs. Recently there has been a study which suggested SIRT3 as a potential therapeutic target against DCM (Palomer et al., 2020). SIRT 3 is a deacetylase that protects against oxidative stress (Palomer et al., 2020). Another study revealed the potential of PGC-1 alpha/ HO-1 axis as a potential anti oxidative pathway that attenuated DCM in diabetic rats (Waldman et al., 2019). These studies indicate the essential role played by oxidative stress in the progression of DCM.

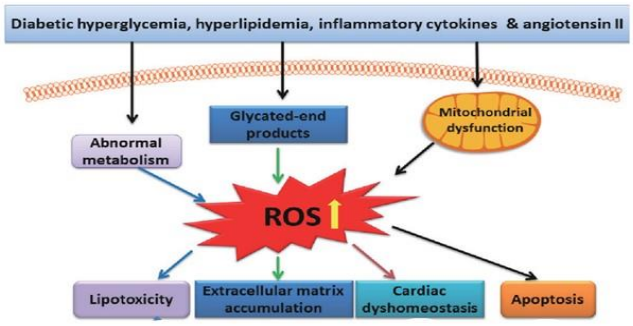

Fig. 1.4 Alteration in redox homeostasis during diabetic cardiomyopathy (Chen et al., 2014)

1.3.4.2 Mitochondria and cardiovascular diseases

Being the important source of free radicals in myocardial tissue, the importance of mitochondria in developing cardiovascular disease has been given much attention recently (Ren et al., 2010). In addition to the role of being the powerhouse of the cell, mitochondria are also essential regulators of cell life and death. The importance of mitochondria in metabolic syndromes is revealed by the fact that mitochondrial dysfunction plays a major role in developing complications in different organs during diabetes (Morino et al., 2006). Also it is responsible for developing T2DM by inducing insulin resistance in skeletal muscle, adipose tissue and pancreatic beta cell (Morino et al., 2006). A study has reported that in the hearts of obese mice ADP stimulated respiration (state 3 respiration) is highly impaired (Kuo et al., 1985). Anderson et al. reported mitochondrial dysfunction in the atrial tissue of diabetic patients (Anderson et al., 2009). Several animal and human studies have revealed the presence of damaged mitochondria in the diabetic hearts (Bugger and Abel, 2008; Tomita et al., 1996). For the proper functioning of the cell mitochondrial membrane potential maintained is -180mV. It is highly negative due to the chemiosmotic gradient of protons across the inner mitochondrial membrane which is essential for ATP synthesis. In pathological situations, the average mitochondrial membrane potential is altered with a loss in mitochondrial integrity. This situation also triggers ROS generation. A significant stimulation of ROS production occurs when the membrane potential across the inner mitochondrial membrane rises above a certain threshold value (Korshunov et al., 1997). Maintaining a

proper membrane potential also facilitates the calcium ion entry into the mitochondrion via the uniporter which is also essential for ATP synthesis.

The dependence of diabetic heart on fatty acids leads to increased delivery of fatty acid substrates to the mitochondria where β oxidation takes place. This constrained energy substrate preference causes the heart to depend entirely on mitochondrial fatty acid oxidation for ATP synthesis (Schilling 2015). The increased delivery of fatty acids causes mitochondrial uncoupling (Bugger and Abel, 2010) and changes the mitochondrial membrane potential. Uncoupling proteins or UCPs are H^+ translocases that mediate the transfer of protons into the mitochondrial matrix from the intermembrane space bypassing ATP synthase (Bugger and Abel, 2010). These UCPs increase oxygen consumption without a concomitant increase in mitochondrial ATP production (Schilling, 2015) which causes decreased mitochondrial efficiency. Although, mild uncoupling of respiration reduces mitochondrial superoxide production (Rousset et al., 2004) by the dissipation of mitochondrial membrane potential, continuous activation of uncoupling may severely affect cardiac function. There are different types of uncoupling proteins: UCP1, UCP2, UCP3, UCP4, UCP5 (Ledesma et al., 2002). Out of these five homologs, UCP2 and UCP3 are expressed in the heart (Gimeno et al., 1997). Thus targeting the uncouplers by inhibiting their action might be a useful strategy in preventing diabetic cardiomyopathy.

In mammalian cells, the genetic information is stored in two locations: nucleus and mitochondria. Alterations in mitochondrial genome organization disrupt mitochondrial function. Moreover, mitochondrial genome lacks histones and introns which make it more susceptible to mutagens (Linnane et al., 1989). Mutations in mitochondrial DNA also cause diabetes. Point mutation, most common mtDNA mutation that causes an A to G substitution at position 3243 encodes tRNA gene (Leu, UUR). In tissues such as muscle, A3243G mutation is commonly observed with lower replication rates (Maassen et al., 2004).Thus, it reduces the oxygen consumption by the tissue which is due to the decreased oxidative phosphorylation. This defect ultimately leads to mitochondrial dysfunction and mitochondrial diabetes (Sivitz and Yorek, 2010).

1.3.4.3 Inflammation and cardiovascular diseases

As mentioned earlier the increased fatty acid concentration, mitochondrial dysfunction and oxidative stress together lead to cardiomyocyte death, hypertrophy, inflammation and fibrosis (Hölscher et al., 2016). Recent evidences suggest that myocardial inflammation plays a pivotal role in the etiology of diabetic cardiomyopathy (Mann, 2015; Prabhu and Frangogiannis, 2016; Boudina and Abel, 2007). The myocardial inflammatory response which begins as an adaptive mechanism (Mann, 2015; Prabhu and Frangogiannis, 2016) turns into a maladaptive one under chronic pathological conditions. Chronic low grade inflammation or meta inflammation is considered to be associated with metabolic syndromes like T2DM and obesity (Filardi et al., 2012). In most of the studies demonstrating inflammation during diabetes there has been an elevated expression of inflammatory cytokines like TNF-α and IL-6, adhesion molecules like VCAM and ICAM, chemokines and increased infiltration of macrophages and leucocytes (Pan et al., 2014).

Cardiac hypertrophy, ventricular dysfunction and ECM remodeling which are some of the major outcomes of DCM are found in conjunction with the release of proinflammatory cytokines, chemokines and exosomes by inflammatory cells of the diabetic heart (Tan et al., 2019). Several inflammatory signalling pathways are activated in the heart during diabetes. Hyperglycemia, hyperlipidemia, ROS, angiotensin II and toll like receptors are some of the major contributing factors towards the upregulation of inflammatory pathways in the diabetic myocardium (Nunes et al., 2016; Tan et al., 2019). Together they promote the infiltration of macrophages and lymphocytes to the lesion site which then stimulate the production of the above mentioned inflammatory mediators (Tan et al., 2019). Inflammation leads to endothelial dysfunction which is the key factor responsible for the progression of DCM and other CVDs (Smail et al., 2019.)

The many signalling processes include the MAPK pathways like JNK, p38 MAPK and the ERK pathway which ultimately converge towards the NFkB pathway. The upregulation of these pathways create a state of inflammation that is closely associated with insulin resistance (Kaneto et al., 2004; Lorenzo et al., 2011; Nunes et al., 2012). There are evidences of correlation between progression of cardiac hypertrophy, fibrosis and ventricular dysfunction with activation of NFkB signalling pathway (Lorenzo et al., 2011). Viewing from the molecular level, most of the inflammatory mediators that induce

cardiac damage are produced as a result of NFkB upregulation (Nunes et al., 2016; Sun et al., 2004).

TLR activation and the inflammasome complex have been recently proposed to play a critical role in the pathogenesis of DCM (Fuentes-Antrás et al., 2014). There are many evidences related to the upregulation of TLRs during hyperglycemia and hyperlipidemia. TLRs are membrane anchored pattern recognition receptors present in various cells that play an important role in mediating immune response. The activation of TLRs ultimately converge towards NFKB upregulation. The role played by TLR4-mediated inflammatory signalling in the progression of DCM has been reported in animal models of T1DM and T2DM. Accumulating lines of evidence indicate the role of IL-1β, TNF-α and IL-6 in the development of cardiac dysfunction (Frati et al., 2017; Frieler and Mortenses, 2015; Mann, 2015). Similarly, exogenous administration of TNF-a is associated with cardiac dysfunction (Kubota et al., 1997). IL-6 levels were shown to have adverse effects on glucose metabolism. IL-6 infusion in obese mice decreased cardiac glucose metabolism by suppressing insulin signalling in heart (Ko et al., 2009). Also there are many studies showing the correlation between IL-6 and myocardial damage (Younce et al., 2010).

The detrimental effects of glucotoxicity and lipotoxicity is also manifested by the increase in expression of a multiprotein signaling complex known as nucleotide-binding oligomerization domain like receptor pyrin domain containing 3 (NLRP3) inflammasome. It regulates an inflammatory form of cell death (Filardi et al., 2019). NLRP3 inflammasome has now captured the attention of researchers because of the important role played by it during DCM. It has now been considered as a promising molecular marker for the development of targeted and specific therapies (Luo et al., 2017). The NLRP3 inflammasome have been known to be activated by a number of pathogens and host derived ligands like pathogen associated molecular patterns (PAMPs), bacterial toxins, danger associated molecular patterns (DAMPs), UV light, ATP and glucose (Schroder, Zhou, and Tschopp 2010). The two steps during NLRP3 activation includes an initial priming step that trigger NLRP3 expression and a second signal which is associated with structural modulation that induces the NLRP3 inflammasome assembly (Luo et al. 2017). NFkB plays an essential role in providing the first signal while the second signal is provided by certain ligands like thioredoxin interacting proteins (TxNIP) and oxidized mitochondrial DNA and also by deubiquitination. These were found

to be associated with modulating the oligomerization part of the inflammasome (Corsini et al., 2013; Martinon, 2010; Liao et al., 2013; Zhou et al., 2010). Association of CD36 with TLR4 is also a priming signal for the inflammasome assembly (Sheedy et al., 2013). Several studies have been conducted suggesting the role of glucotoxicity and lipotoxicity in the inflammasome activation. One of the major activator of NLRP3 inflammasome is glucose and several studies have been conducted for the same (Zu et al., 2015). The ROS overproduction that occurs during T2DM promotes NLRP3 inflammasome activation specifically by upregulating NF-Kb expression and TXNIP levels thus mediating the inflammasome induction and the complex oligomerization respectively (Martinon,. 2010). The major outcome of this ROS mediated NLRP3 inflammasome activation is the production of IL-1B and IL-18 both of which are substrates for caspase-1 which plays an essential role in triggering pyroptosis (Shalini et al., 2015). Pyroptosis is a caspase-1 mediated cell death characterised by membrane pore formation, cell swelling and release of proinflammatory mediators (Filardi et al., 2019; Luo et al., 2017) that aggravate the inflammatory scenario in the myocardium. Thus NLRP3 plays an essential role in the development of insulin resistance and thus diabetes.

1.3.4.4 Calcium and Diabetic cardiomyopathy

The impaired myocardial performance during diabetes is also due to reduced myocardial Ca^{2+} sensitivity (Liu et al., 2014). Intracellular calcium is an important ion which regulates myocardial contraction (Turan and Dhalla, 2014). The importance of calcium is evident from the reduced contractile protein Ca^{2+} ATPase activity in a diabetic scenario (Malhotra and Sanghi, 1997). This is usually accompanied by a shift in myosin isoenzyme composition from V1 to V3 and the dominance of fetal B- myosin heavy chain in the myocardium during hyperglycemia (Malhotra and Sanghi, 1997; Jia et al., 2018). This results in reduced contractility of heart as well as cardiac systolic dysfunction during diabetes (Jia et al., 2018; Pollack et al., 1986).

The reduced contractility of the myocardium is one of the major consequence of DCM. Myocardial contractility is primarily regulated by calcium cycling into and out of the cytoplasm of cardiac myocytes. SR is the storehouse of calcium and the majority of calcium in the cytoplasm comes from SR. However the release of calcium from SR is tightly regulated by the calcium ions that enter via L type calcium channels in the plasma membrane. The cardiac contraction is mainly facilitated by Ca^{2+} currents that enter the

cell via the phosphorylated L type channels. Ca^{2+} entry is regulated by phosphorylation of these channels. There are reports in mice where the overexpression of these channels lead to heart failure. This calcium induced calcium release is one of the major controller of myocardial contraction (Marín-García, 2010). Myocardial contraction is mainly initiated by binding of Ca^{2+} to a specific site on cardiac troponin C. According to a study conducted in streptozotocin induced diabetic rat model there was a diminished release of calcium ions from the sarcoplasmic reticulum ryanodine receptor thereby decreasing the upstroke phase of Ca^{2+} transient (Teshima et al., 2000). Similarly in another study it was found that there was a reduced ability for the sarcoplasmic reticulum (SR) to sequester Ca^{2+} which ultimately led to diastolic dysfunction. Atrial tissue of human diabetic hearts showed mitochondrial dysfunction due to calcium induced mitochondrial transmembrane pore opening (Anderson et al., 2009). Similarly ER stress during hyperglycemia which leads to accumulation of unfolded protein response is mainly caused by disturbances in calcium homeostasis. In addition, there are numerous studies on T1D and T2D in diabetic murine models emphasising the importance of various calcium ion transporters like sarcoplasmic reticulum Ca^{2+}-pump ATPase (SERCA) and sarcolemmal Ca^{2+} pump ATPase that are involved in excitation contraction coupling (Golfman and Dixon, 1998; Trost et al., 2002). According to recent studies, the activity of SERCA-2A and its inhibitor phospholamban appears to play a very important role in the pathogenesis of diabetes. There are also many clinical investigations which suggest that reduced myofilament Ca^{2+} sensitivity contributes to Ca^{2+} dysregulation in diabetic cardiomyocytes (Jweied et al., 2005). Although studies linked to cytosolic Ca^{2+} handling in human hearts is not available, based on other studies in animals, restoring Ca^{2+} levels in human cardiomyocytes might be a promising strategy to reduce the complications related to DCM (Dillmann, 2019).

1.3.5 Current therapies

There are evidences suggesting that obesity along with increased intake of refined food and less physical activity plays an important role in developing heart diseases and diabetes globally (Jia et al., 2018). So the first line of efficient therapeutic approach is to prevent the occurrence of diabetes by including lifestyle changes such as aerobic exercise and weight control. Bringing glycemia under control by insulin therapy reduces the consequences of DCM like hypertrophy, interstitial fibrosis, and left ventricular diastolic dysfunction in type 1 diabetic animal models (Tate et al., 2017). So any treatment

regimen should target on lowering blood glucose levels. The glucose lowering therapies have proved to be advantageous in reducing cardiovascular complications that arise due to diabetes (Jia et al., 2018). The most important examples include metformin, SGLT2 inhibitors and GLP1 receptor agonists all of which showed some beneficial effects in reducing the CVD risk in type 2 diabetic patients (Jia et al., 2016). According to the EMPA-REG OUTCOME trial, treatment with empaglifozin lowered myocardial infarction, stroke and other CVD associated mortalities. Also treatment with GLP-1 receptor agonists in high risk diabetic patients reduced CVD events and heart failure. However problem arises when these anti hyperglycemic therapies prove inefficient in reducing cardiovascular complications (Borghetti et al. 2018). For example a meta-analysis conducted in 2007 showed that the glucose lowering drug rosiglitazone increased the risk of myocardial infarction thus emphasizing the importance of meticulously studying the safety of this drug (Nissen and Wolski, 2007). However treatment with DPP-1V inhibitors and PPAR agonist increased the risk of heart failure in patients with type 2 diabetes mellitus, according to a meta-analysis of randomized control trials (Jia et al., 2018). In spite of the side effects of these drugs there are certain other drugs that can improve cardiac health beyond their ability to control glycemia (von Lewinski et al., 2017). The mechanisms by which these drugs exert their pleiotropic effects have not yet been explored.

1.3.5.1 GLP-1 receptor agonists

Glucagon like peptide is released from the gut after food intake. It belongs to incretin family and lowers hyperglycemia by increasing insulin secretion and suppressing glucagon expression in a glucose dependent manner. Several synthetic GLP-1 receptor agonists (GLP-1RAs) have been synthesized that have proved beneficial for T2DM patient. The major advantage of this drug is that it exerts its beneficial effect only in the context of hyperglycemia thereby lowering the risk of severe hypoglycaemia. The potential cardioprotective effects of GLP-1RAs are based on their ability to reduce the cardiovascular risk factors like hyperglycemia, and obesity. GLP-1 receptor is also shown to be present in the atrial tissue of rodents and non-human primates suggesting a direct beneficial effect of these drugs on the myocardium. Reduced infarct size and improved cardiac function is observed in several animal models of ischemic heart disease that have been infused with exogenous GLP-1 or treated with GLP-1RA.

1.3.5.2 Sodium glucose cotransporters 2 (SGLT2)

Recently, SGLT2 inhibitors provide a novel therapeutic strategy against T2DM. SGLT2 is a sodium glucose transporter that is present in the nephron of kidney that facilitates the reabsorption of glucose which is filtered by the glomeruli (Jabbour and Goldstein, 2008). The three SGLT2 inhibitors currently in use are dapaglifozin, canaglifozin and empaglifozin (ADA, 2017). All of these are effective in lowering blood glucose levels (Stenlof etal., 2013; White, 2015; Wilding et al., 2009). Interestingly many recent cardiovascular outcomes trials also revealed a strong cardioprotective signal of SGLT2 inhibition in high risk patients with T2DM (Kenny and Abel, 2019). According to the EMPA-REG OUTCOME trial, empaglifozin showed a reduction in mortality due to CVD and hospitalization from heart failure (Zinman et al., 2015). Similarly the CANVAS trial involving canaglifozin also reduced heart failure hospitalization (Neal et al., 2017). Thus SGLT2 inhibitors have proved to be efficient in reducing the risk of heart failure in T2DM. The proposed mechanisms by which these inhibitors exert their beneficial effects include increased natriuresis, reduced blood pressure and renal protection.

1.3.5.3 Metformin

Metformin is considered as the first line therapy in T2DM due to its high safety profile. It is one of the most widely used oral antihyperglycemic agent (Foretz et al., 2014). Its safety and efficiency as a monotherapy and also in combination with other antidiabetic agents have made it a potential drug for T2DM (Kenny and Abel, 2019). The United Kingdom Prospective Diabetes Study reported that the risk of myocardial infarction lowered by 39 % in patients with T2D on metformin (UKPDS, 1998). Metformin therapy showed better CVD risk reduction than insulin or sulfonylurea (SU) derivatives despite patients achieving similar glycemic control (Kenny and Abel, 2019; UKPDS, 1998). According to a recent analysis metformin also had a survival benefit in diabetic patients in heart failure compared with alternate glucose lowering regimens (Eurich et al., 2007). Although the cardioprotective mechanism of metformin is not fully understood one of the mechanism through which it exerts its beneficial effects is via the AMPK pathway. AMPK activation inhibits mTOR and represses protein synthesis thus suppressing cardiac hypertrophy (Horman et al., 2012). In a recent study involving a rat model metformin was shown to inhibit cardiac hypertrophy (Zhang et al., 2011). Metformin also inhibited transverse aortic constriction-mediated cardiac hypertrophy which was independent of AMPK pathway (Wu et al., 2019) and also provided

cardioprotection against ischemia induced heart failure (Gundewar et al., 2009). One of the major pathogenic mechanism of DCM is altered substrate utilization to free fatty acids. Metformin treatment partly increased myocardial glucose utilization by activating AMPK or by increasing myocardial insulin sensitivity (Horman et al., 2012). Similarly metformin treatment was also shown to attenuate cardiac fibrosis in mice subjected to transverse aortic constriction (Xiao et al., 2010). But a thorough investigation is required to find out whether similar changes also occur in a clinical setting. According to clinical studies metformin doesn't have a significant effect on myocardial substrate utilization and function. However, population cohort and observational studies have consistently revealed that metformin treatment is associated with a reduction in the prevalence of heart failure in diabetic subjects.

1.3.6 Herbal medicines used to treat cardiovascular diseases

Herbs have been an indispensable part of society since the beginning of human civilization and they have been valued since then for their culinary and medicinal properties. Although many pharmacological agents and anti-thrombotic drugs are in use for the treatment of CVDs, the role of dietary factors and herbal medicines are gaining more importance. Natural product derived drugs are used for prophylactic and curative purposes because of the perception that they are less toxic and have minimal side effects. According to WHO 80% of the world's population depends on natural products for healing (WHO, 2015). More than approximately 2000 plants have been known to be used in traditional systems of medicine and interestingly some of them prove to be beneficial to patients suffering from CVD and related complications (Cohen and Ernst, 2010). In many developed countries there are legitimate practices for use of such herbs- for example jinseng root, St. Johns wort, *Hypericum perforatum* and *Plantago major.* However in developed countries there are many regulatory policies for the sale of such herbals (Bandaranayake, 2006). Also in many countries herbal extracts are sold as dietary supplements.

The surge in the use of herbal medicines indicates that modern medicine is not fully successful in reducing the chronicity of many modern diseases. Approximately 50 % of FDA approved drugs are natural products or their derivatives (Williamson 2003). However there are also potential drug-herb interactions in CVD patients (Suroowan and Mahomoodally, 2015). There are a number of potent biologically active natural products

present in various herbal medicines. Herbal medicines have also helped in the preparations of commercial drug including ephedrine which is prepared from *Ephedra sinica*, digitoxin from *Digitalis purpurea*, salicin from *Salix alba*, and reserpine from *Rauwolfia serpentina*. Reserpine has been used for a long time to treat hypertension. Crataegus hawthorn included in Crataegus species is used as an important tonic particularly to treat angina. A study has identified a naturally occurring β-adrenergic blocking agent with partial agonism in a herbal remedy and also the discovery of the antineoplastic drug paclitaxel from Taxus brevifolia suggests the relevance of plants as a continuing source of medicine. However the major drawback of herbal remedies is that they have not been subjected to careful scientific evaluation to test their efficacy and toxicity. Also their importance has failed to be recognised globally due to multiple reasons.

1.3.6.1 Cinnamic Acid

Dietary polyphenols have gained considerable attention nowadays among scientists and researchers. They are considered as favourable agents for the prevention and management of diabetes and its complications due to their abundance in nature, less side effects and cost effectiveness than the currently used oral hypoglycemic agents (Hanhineva et al., 2010). In this study the molecule cinnamic acid is selected. Cinnamic acid (CiA) and its derivatives belong to the group of phenolic acids with wide distribution in a variety of foods (Adisakwattana, 2017).They are synthesized via the shikimate pathway in which phenylalanine and tyrosine are the precursor molecules (Tohge and Fernie, 2016). The well-known derivatives include cinnamic acid, caffeic acid, ferulic acid, isoferulic acid and hydroxycinnamic acid (Adisakwattana, 2017). Ferulic acid is seen abundantly in plants such as grains, pulses, rice and wheat bran (Mancuso and Santangelo, 2014). Similarly caffeic acid is seen in coffee (Butt and Sultan, 2011) and sweet potatoes (Sasaki et al., 2015). CiA is present in cinnamon, grapes, tea, spinach, citrus fruits, cocoa, celery and brassicas vegetables (Guzman, 2014). Also according to many pharmacokinetic studies, CiA can easily be absorbed from small intestine through various mechanisms including passive diffusion (El-Seedi et al., 2012), monocarbolxylic acid transporters (Konishi et al., 2004) and Na+-dependent career mediated transport mechanisms (Wolffram et al., 995). Also many studies have also shown that CiA is a good antioxidant (Sova, 2012), anti-inflammatory (De Cássia et al., 2014) and an anti-cancer agent (Anantharaju et al., 2016). Recently a study conducted in high fat diet induced

obese rats proved the anti-obesity and cardioprotective effects of CiA (Mnafgui et al., 2014). Similarly CiA and its derivatives were tested for their insulin secreting activity in INS-1 pancreatic β cells (Adisakwattana et al., 2008). Under high glucose concentration CiA increased insulin secretion in a concentration dependent manner (Hafizur et al., 2015). Hafizur et al., also proved that CiA , and not cinnmaladehyde, was the active principle of cinnamon that contributed to the antidiabetic activity (Hafizur et al., 2015). The ability of CiA in improving glucose tolerance and insulin secretion has revealed the compound's antidiabetic activity (Adisakwattana, 2017). Similarly another work by Kopp et al found that CiA enhanced adiponectin secretion and also resulted in the phosphorylation of AMPK in 3T3-L1 adipocytes (Kopp et al., 2014). The synergistic effects produced by the combination of CiA and its derivatives with oral hypoglycemic agents like metformin has been observed in 3T3-L1 adipocytes whereby the glucose uptake activity was increased. (Prabhakar and Doble, 2011). Although cinnamic acid shows anti diabetic effects and cardioprotective effects, the entire mechanism by which it acts has not been elucidated. In the present study we found the anti-inflammatory property of cinnamic acid and one of the many mechanism by which it exerts its cardioprotection during diabetes.

1.3.7 Hypothesis and Objectives

Diabetes induced cardiomyopathy is emerging as a major health problem in the public health. There is no ideal drug available to prevent the pathological changes occurring in the heart during diabetes. It is also known that control of blood sugar with continuous intake of diabetic drug is not much effective to protect the heart. So there is a need of drug which is exclusively for the benefit of heart during hyperglycemia. During initial stages of diabetes, the heart will withstand depletion of the availability of glucose through physiological adaptation. But after sometime pharmacological intervention is must. In order to design pharmacological intervention the knowledge of the mechanism responsible for DCM is essential. It is reported from various studies that inflammation is one of the pathological mechanism inducing DCM. The myocardial inflammatory response which begins as an adaptive mechanism turns into a maladaptive one under chronic pathological conditions. So unravelling the complex inflammatory mechanisms is necessary. So based on this hypothesis the present study aims to investigate the mechanism related to the origin of inflammation through different signalling pathways

including toll like receptors and the inflammasome complex during diabetes and how this inflammation leads to DCM.

The main objectives of this study are

- Investigation on alterations in redox homeostasis, mitochondrial function and calcium homeostasis in cardiomyoblasts (H9c2 cells) during glucotoxicity.
- Investigation on various inflammatory pathways (JNK, ERK, p38 MAPK, TLR4, NLRP3, GATA-4) in diabetes induced cardiomyopathy *in vivo*.
- Elucidation of molecular mechanism involved in diabetic cardiomyopathy emphasizing inflammation in *in vitro* model.
- Evaluation of efficacy of cinnamic acid against diabetic cardiomyopathy both in *in vitro* and *in vivo* study.

References

1. Adisakwattana S, Moonsan P, Yibchok-Anun S. Insulin-releasing properties of a series of cinnamic acid derivatives in vitro and in vivo. J. Agric. Food Chem. 2008 56 (17):7838-7844.
2. Adisakwattana S. Cinnamic acid and its derivatives: mechanisms for prevention and management of diabetes and its complications. Nutrients. 2017; 9:163.
3. American Diabetes Association. 8. Pharmacologic approaches to glycemic treatment. Diabetes Care. 2017; 40: S64-S74.
4. Anantharaju PG, Gowda PC, Vimalambike MG, Madhunapantula SV. An overview on the role of dietary phenolics for the treatment of cancers. Nutr. J. 2016; 15: 99.
5. Anderson EJ, Kypson AP, Rodriguez E, Anderson CA, Lehr EJ, Neufer PD. Substrate-specific derangements in mitochondrial metabolism and redox balance in the atrium of the type 2 diabetic human heart. J. Am. Coll. Cardiol. 2009; 54: 1891-1898.
6. Aoyama T, Peters JM, Iritani N, Nakajima T, Furihata K, Hashimoto T, et al. Altered constitutive expression of fatty acid-metabolizing enzymes in mice lacking the peroxisome proliferator-activated receptor alpha (PPARalpha). *J. Biol. Chem.* 1998; 273: 5678-5684.
7. Arumugam S, Karuppagounder V, Thandavarayan RA, Pitchaimani V, Sone H, Watanabe K. Diabetic cardiomyopathy and oxidative stress. diabetes: oxidative

stress and dietary antioxidants. Elsevier. 2013; http://dx.doi.org/10.1016/B978-0-12-405885-9.00003-6.

8. Bandaranayake WM. Quality control, screening, toxicity, and regulation of herbal drugs. modern phytomedicine. turning medicinal plants into drugs. Wiley. 2006; 25-57.
9. Barger PM, Kelly DP. PPAR signaling in the control of cardiac energy metabolism. Trends Cardiovasc. Med. 2000*;* 10: 238-245.
10. Battiprolu PK, Lopez-Crisosto C, Wang ZV, Nemchenko A, Lavandero S, Hill JA. Diabetic cardiomyopathy and metabolic remodeling of the heart. Life Sci*.* 2013; 92: 609-615.
11. Bertoni AG, Hundley WG, Massing MW, Bonds DE, Burke GL, Goff DC Jr. Heart failure prevalence, incidence, and mortality in the elderly with diabetes. Diabetes Care. 2004; 27: 699-703.
12. Bordun K-AM , Jassal DS, Dhalla NS. Metabolic alterations in diabetic cardiomyopathy. Diabetic cardiomyopathy biochemical and molecular mechanisms. Turan B and Dhalla NS. Springer New York Heidelberg Dordrecht London, 3-26.
13. Borghetti G, von Lewinski D, Eaton DM, Sourij H, Houser SR, Wallner M. Diabetic cardiomyopathy: current and future therapies. Beyond glycemic control. Front. Physiol. 2018; 9: 1514.
14. Boudina S, Abel ED. Diabetic cardiomyopathy revisited. Circulation. 2007; 115: 3213-3223.
15. Bugger H, Abel ED. Molecular mechanisms for myocardial mitochondrial dysfunction in the metabolic syndrome. *Clin. Sci.* 2008; 114: 195-210.
16. Bugger H, Abel ED. Mitochondria in the diabetic heart. Cardiovasc. Res. 2010; 88: 229-240.
17. Butt MS, Sultan MT. Coffee and its consumption: benefits and risks. *Crit. Rev. Food Sci. Nutr.* 2011; 51: 363-373.
18. Cai L, Wang Y, Zhou G, Chen T, Song Y, Li X, et al. Attenuation by metallothionein of early cardiac cell death via suppression of mitochondrial oxidative stress results in a prevention of diabetic cardiomyopathy. J. Am. Coll. Cardiol. 2006; 48: 1688-1697.
19. Cai L, Kang YJ. Oxidative stress and diabetic cardiomyopathy: a brief review.

Cardiovasc. Toxicol. 2001; 1:181-193.

20. Cohen PA, Ernst E. Safety of herbal supplements: a guide for cardiologists. *J. Cardiol. Therap.* 2010; 28: 246-253.
21. Corsini E, Galbiati V, Nikitovic D, Tsatsakis AM. Role of oxidative stress in chemical allergens induced skin cells activation. *Food Chem. Toxicol.* 2013; 61: 74-81.
22. Costantino S, Akhmedov A, Melina G, Mohammed SA, Othman A, Ambrosini S, et al. Obesity-induced activation of jund promotes myocardial lipid accumulation and metabolic cardiomyopathy. Eur. Heart J. 2019; 40: 997-1008.
23. de Cássia da Silveira E Sá R, Andrade LN, Dos Reis Barreto de Oliveira R, de Sousa DP. A review on anti-inflammatory activity of phenylpropanoids found in essential oils. Molecules. 2014; 19: 1459-1480.
24. Dei Cas A, Khan SS, Butler J, Mentz RJ, Bonow RO, Avogaro A, et al. Impact of diabetes on epidemiology, treatment, and outcomes of patients with heart failure. *JACC. Heart failure. 2015;* 3: 136-145.
25. DeMarco VG, Aroor AR, Sowers JR. The pathophysiology of hypertension in patients with obesity. *Nat. Rev. Endocrinol.* 2014; 10: 364-376.
26. Devereux RB, Roman MJ, Paranicas M, O'Grady MJ, Lee ET, Welty TK, et al. Impact of diabetes on cardiac structure and function: the strong heart study. Circulation. 2000 101:2271-2276.
27. Dillmann WH. Diabetes mellitus induces changes in cardiac myosin of the rat. *Diabetes. 1980;* 29: 579-582.
28. Dillmann WH. Diabetic cardiomyopathy what is it and can it be fixed? *Circ. Res.* 2019; 124: 1160-1162.
29. El-Seedi HR, El-Said AM, Khalifa SA, Göransson U, Bohlin L, Borg-Karlson AK, et al. Biosynthesis, natural sources, dietary intake, pharmacokinetic properties, and biological activities of hydroxycinnamic acids. J. Agric. Food Chem. 2012; 60: 10877-10895.
30. Eurich DT, McAlister FA, Blackburn DF, Majumdar SR, Tsuyuki RT, Varney J, et al. Benefits and harms of antidiabetic agents in patients with diabetes and heart failure: systematic review. BMJ. 2007; 335: 497.
31. Filardi T, Ghinassi B, Di Baldassarre A, Tanzilli G, Morano S, Lenzi A, et al. Cardiomyopathy associated with diabetes: the central role of the cardiomyocyte. *Int. J. Mol. Sci.* 2019; 20: 3299.

32. Foretz M, Guigas B, Bertrand L, Pollak M, Viollet B. Metformin: from mechanisms of action to therapies. *Cell Metab.* 2014; 20: 953-966.
33. Frati G, Schirone L, Chimenti I, Yee D, Biondi-Zoccai G, Volpe M, et al. An overview of the inflammatory signalling mechanisms in the myocardium underlying the development of diabetic cardiomyopathy. Cardiovasc. Res. 2017; 113: 378-388.
34. Frieler RA and Mortensen RM. Immune cell and other noncardiomyocyte regulation of cardiac hypertrophy and remodeling. *Circulation. 2015;* 131: 1019-1030.
35. Fuentes-Antrás J, Ioan AM, Tuñón J, Egido J, Lorenzo O. Activation of toll-like receptors and inflammasome complexes in the diabetic cardiomyopathy-associated inflammation. Int. J. Endocrinol. 2014; 2014: 847827.
36. Gimeno RE, Dembski M, Weng X, Deng N, Shyjan AW, Gimeno CJ, et al. Cloning and characterization of an uncoupling protein homolog: a potential molecular mediator of human thermogenesis. Diabetes. 1997; 46: 900-906.
37. Goh SY, Cooper ME. Clinical review: the role of advanced glycation end products in progression and complications of diabetes. *J. Clin. Endocrinol. Metab.* 2008; 93: 1143-1152.
38. Golfman L, Dixon IM, Takeda N, Lukas A, Dakshinamurti K, Dhalla NS. Cardiac sarcolemmal Na(+)-Ca2+ exchange and Na(+)-K+ ATPase activities and gene expression in alloxan-induced diabetes in rats. Mol. Cell Biochem. 1998; 188: 91-101.
39. Gundewar S, Calvert JW, Jha S, Toedt-Pingel I, Ji SY, Nunez D, et al. Activation of AMP-activated protein kinase by metformin improves left ventricular function and survival in heart failure. *Circ Res. 2009;* 104: 403-411.
40. Guzman JD. Natural cinnamic acids, synthetic derivatives and hybrids with antimicrobial activity. *Molecules. 2014;* 19: 19292-19349.
41. Habets DD, Coumans WA, Voshol PJ, den Boer MA, Febbraio M, Luiken JJ, et al. AMPK-mediated increase in myocardial long-chain fatty acid uptake critically depends on sarcolemmal CD36. *Biochem. Biophys. Res. Commun.* 2007; 355: 204-210.
42. Hafizur RM, Hameed A, Shukrana M, Raza SA, Chishti S, Kabir N, et al. Cinnamic acid exerts anti-diabetic activity by improving glucose tolerance in vivo and by stimulating insulin secretion in vitro. Phytomedicine. 2015; 22: 297-300.

43. Hanhineva K, Törrönen R, Bondia-Pons I, Pekkinen J, Kolehmainen M, Mykkänen H, et al. Impact of dietary polyphenols on carbohydrate metabolism. Int. J. Mol. Sci. 2010; 11: 1365-1402.
44. Harper ME, Bevilacqua L, Hagopian K, Weindruch R, Ramsey JJ. Ageing, oxidative stress and mitochondrial uncoupling. *Acta. Physiol. Scand.* 2004; 82: 321-331.
45. Hölscher ME, Bode C, Bugger H. Diabetic cardiomyopathy: does the type of diabetes matter? Int. J. Mol. Sci. 2016; 17: 2136.
46. Horman S, Beauloye C, Vanoverschelde JL, Bertrand L. AMP-activated protein kinase in the control of cardiac metabolism and remodeling. Curr. Heart Fail. Rep. 2012; 9:164-173.
47. Institute for Health Metrics and Evaluation (IHME). GBD profile : India. Global Burden of Disease Study 2010 (GBD 2010). 1-4.
48. Jabbour SA, Goldstein BJ. Sodium glucose co-transporter 2 inhibitors: blocking renal tubular reabsorption of glucose to improve glycaemic control in patients with diabetes. *Int. J. Clin. Pract. 2008;* 62: 1279-1284.
49. Jia G, DeMarco VG, Sowers JR. Insulin resistance and hyperinsulinaemia in diabetic cardiomyopathy. *Nat. Rev. Endocrinol.* 2016; 12: 144-153.
50. Jia G, Hill MA, Sowers JR. Diabetic cardiomyopathy: an update of mechanisms contributing to this clinical entity. Circ. Res. 2018; 122: 624-638.
51. Jornayvaz FR, Birkenfeld AL, Jurczak MJ, Kanda S, Guigni BA, Jiang, et al. Hepatic insulin resistance in mice with hepatic overexpression of diacylglycerol acyltransferase 2. *Proc. Natl. Acad. Sci. USA.* 2011; 108: 5748-5752.
52. Jweied EE, McKinney RD, Walker LA, Brodsky I, Geha AS, Massad MG, et al. Depressed cardiac myofilament function in human diabetes mellitus. Am. J. Physiol. Heart Circ. Physiol. 2005; 289: H2478-H2483.
53. Kanamori H, Takemura G, Goto K, Tsujimoto A, Mikami A, Ogino A, et al. Autophagic adaptations in diabetic cardiomyopathy differ between type 1 and type 2 diabetes. Autophagy. 2015; 11:1146-1160.
54. Kaneto H, Nakatani Y, Kawamori D, Miyatsuka T, Matsuoka TA. Involvement of oxidative stress and the JNK pathway in glucose toxicity. *Rev. Diabet. Stud.* 2004; 1: 165-174.
55. Kannel WB, Hjortland M, Castelli WP. Role of diabetes in congestive heart failure: the Framingham study. *Am. J. Cardiol. 1974;* 34: 29-34.

56. Kenny HC, Abel ED. Heart failure in type 2 diabetes mellitus: impact of glucose lowering agents, heart failure therapies and novel therapeutic strategies. Circ. Res. 2019; 124: 121-141.
57. King H, Aubert RE, Herman WH. Global burden of diabetes, 1995-2025: prevalence, numerical estimates, and projections. Diabetes Care. 1998; 21: 1414-1431.
58. Ko HJ, Zhang Z, Jung DY, Jun JY, Ma Z, Jones KE, Chan SY, et al. Nutrient stress activates inflammation and reduces glucose metabolism by suppressing AMP-activated protein kinase in the heart. Diabetes. 2009; 58: 2536-2546.
59. Konishi Y, Hitomi Y, Yoshioka E. Intestinal absorption of p-coumaric and gallic acids in rats after oral administration. J. Agric. Food Chem. 2004; 52: 2527-2532.
60. Kopp C, Singh SP, Regenhard P, Müller U, Sauerwein H, Mielenz M. Trans-cinnamic acid increases adiponectin and the phosphorylation of AMP-activated protein kinase through G-protein-coupled receptor signaling in 3T3-L1 adipocytes. Int. J. Mol. Sci. 2014 19; 15: 2906-2915.
61. Korshunov SS, Skulachev VP, Starkov AA. High protonic potential actuates a mechanism of production of reactive oxygen species in mitochondria. *FEBS Lett.* 1997; 416: 15-18.
62. Kubota T, McTiernan CF, Frye CS, Slawson SE, Lemster BH, Koretsky AP, et al.. Dilated cardiomyopathy in transgenic mice with cardiac-specific overexpression of tumor necrosis factor-alpha. *Circ. Res. 1997;* 81: 627-635.
63. Kuo TH, Giacomelli F, Wiener J. Oxidative metabolism of polytron versus nagarse mitochondria in hearts of genetically diabetic mice. *Biochim. Biophys. Acta.* 1985; 806: 9-15.
64. Lebeche D, Davidoff AJ, Hajjar RJ. Interplay between impaired calcium regulation and insulin signaling abnormalities in diabetic cardiomyopathy. Nat. Clin. Pract. Cardiovasc. Med. 2008; 5: 715-724.
65. Ledesma A, de Lacoba MG, Rial E. The mitochondrial uncoupling proteins. *Genome Biol.* 2002; 3: 3015.
66. Lee WS, Kim J. Diabetic cardiomyopathy: where we are and where we are going. *Korean J. Intern. Med. 2017;* 32: 404-421.
67. Liao PC, Chao LK, Chou JC, Dong WC, Lin CN, Lin CY et al. Lipopolysaccharide/adenosine triphosphate-mediated signal transduction in the

regulation of NLRP3 protein expression and caspase-1-mediated interleukin-1β secretion. *Inflamm. Res.* 2013; 62: 89-96.

68. Lindman BR, Dávila-Román VG, Mann DL, McNulty S, Semigran MJ, Lewis GD, et al. Cardiovascular phenotype in HFpEF patients with or without diabetes: A RELAX trial ancillary study. *J. Am. Coll. Cardiol. 2014;* 64: 541-549.
69. Linnane AW, Marzuki S, Ozawa T, Tanaka M. Mitochondrial DNA mutations as an important contributor to ageing and degenerative diseases. *Lancet.* 1989; 1: 642-645.
70. Litvinova L, Atochin DN, Fattakhov N, Vasilenko M, Zatolokin P, Kirienkova E. Nitric oxide and mitochondria in metabolic syndrome. Front. Physiol. 2015; 6: 20.
71. Liu Q, Wang S, Cai L. 2014. Diabetic cardiomyopathy and its mechanisms: Role of oxidative stress and damage. J. Diabetes Investig. 2014; 5: 623-634.
72. Lorenzo O, Picatoste B, Ares-Carrasco S, Ramírez E, Egido J, Tuñón J. Potential role of nuclear factor κB in diabetic cardiomyopathy. Mediators Inflamm. 2011; 2011:652097.
73. Luo B, Huang F, Liu Y, Liang Y, Wei Z, Ke H, et al. NLRP3 inflammasome as a molecular marker in diabetic cardiomyopathy. Front. Physiol. 2017; 8: 519.
74. Maassen JA, 'T Hart LM, Van Essen E, Heine RJ, Nijpels G, Jahangir Tafrechi RS, et al. Mitochondrial diabetes: molecular mechanisms and clinical presentation. Diabetes. 2004; 53: S103-S109.
75. Malhotra A, Sanghi V. Regulation of contractile proteins in diabetic heart. *Cardiovas. Res.* 1997; 34: 34-40.
76. Mancuso C, Santangelo R. Ferulic acid: pharmacological and toxicological aspects. *Food Chem. Toxicol. 2014;* 65: 185-195.
77. Mann DL. Innate immunity and the failing heart: the cytokine hypothesis revisited. *Circ. Res.* 2015; 116: 1254-1268.
78. Marín-García J. Cardiac function in heart failure: the role of calcium cycling. heart failure: bench to bedside, Contemporary Cardiology. Springer, New York, 2010; pp. 15-22.
79. Marso SP, Bain SC, Consoli A, Eliaschewitz FG, Jódar E, Leiter LA, et al.. SUSTAIN-6 Investigators. Semaglutide and cardiovascular outcomes in patients with type 2 diabetes. N. Engl. J. Med. 2016; 375:1834-1844.
80. Martinon F. Signaling by ROS drives inflammasome activation. Eur. J. Immunol.

2010; 40: 616-619.

81. Ministry of Health and Family Welfare, Government of India. National health policy 2017 - India.
82. Mnafgui K, Derbali A, Sayadi S, Gharsallah N, Elfeki A, Allouche N. Anti-obesity and cardioprotective effects of cinnamic acid in high fat diet- induced obese rats. J. Food Sci. Technol. 2015; 52: 4369-4377.
83. Morino K, Petersen KF, Shulman GI. Molecular mechanisms of insulin resistance in humans and their potential links with mitochondrial dysfunction. *Diabetes. 2006;* 55: S9-S15.
84. Neal B, Perkovic V, Mahaffey KW, de Zeeuw D, Fulcher G, Erondu N, et al. Canagliflozin and cardiovascular and renal events in type 2 diabetes. N. Engl. J. Med. 2017; 377: 644-657.
85. Nissen SE, Wolski K. Myocardial effect of rosiglitazone on the risk of infarction and death from cardiovascular causes. *N. Engl. J. Med. 2007;* 356: 2457- 2471.
86. Nunes S, Soares E, Pereira F, Reis F. The role of inflammation in diabetic cardiomyopathy. *Int. J. Interferon Cytokine* Mediat. Res. 2012; **4,**59-73.
87. Nunes S, Rolo AP, Palmeira CM, Reis F. *Diabetic* cardiomyopathy: focus on oxidative stress, mitochondrial dysfunction and inflammation. InTechOpen. 2017; doi: 10.5772/65915.
88. Palomer X, Román-Azcona MS, Pizarro-Delgado J, Planavila A, Villarroya F, Valenzuela-Alcaraz B, et al. SIRT3-mediated inhibition of FOS through histone H3 deacetylation prevents cardiac fibrosis and inflammation. Signal. Transduct. Target Ther. 2020; 5: 14.
89. Pan Y, Wang Y, Zhao Y, Peng K, Li W, Wang Y, et al. Inhibition of JNK phosphorylation by a novel curcumin analog prevents high glucose-induced inflammation and apoptosis in cardiomyocytes and the development of diabetic cardiomyopathy. Diabetes. 2014; 63: 3497-3511.
90. Piconi L, Quagliaro L, Ceriello A. Oxidative stress in diabetes. *Clin. Chem. Lab. Med. 2003;* 41: 1144-1149.
91. Pollack PS, Malhotra A, Fein FS, Scheuer J. Effects of diabetes on cardiac contractile proteins in rabbits and reversal with insulin. *Am. J. Physiol. 1986;* 251: H448-H454.
92. Poornima IG, Parikh P, Shannon RP. Diabetic cardiomyopathy: the search for a unifying hypothesis. Circ. Res. 2006; 98: 596-605.

93. Prabhakar PK, Doble M. Interaction of cinnamic acid derivatives with commercial hypoglycemic drugs on 2-deoxyglucose uptake in 3T3-L1 adipocytes. J. Agric. Food Chem. 2011; 59: 9835-9844.
94. Prabhakaran D, Jeemon P, Sharma M, Roth GA, Johnson C, Harikrishnan S, et al. India State-Level Disease Burden Initiative CVD Collaborators. The changing patterns of cardiovascular diseases and their risk factors in the states of India: the Global Burden of Disease Study 1990-2016. Lancet Glob Health. 2018; 6: e1339-e1351.
95. Prabhu SD, Frangogiannis NG. The biological basis for cardiac repair after myocardial infarction: from inflammation to fibrosis. *Circ. Res.* 2016; 119: 91-112.
96. Raposeiras-Roubín S, Rodiño-Janeiro BK, Paradela-Dobarro B, Grigorian-Shamagian L, García-Acuña JM, Aguiar-Souto P, et al. Predictive value of advanced glycation end products for the development of post-infarction heart failure: a preliminary report. *Cardiovasc. Diabetol. 2012;* 11: 102.
97. Reddy K, Shah B, Varghese C, Ramadoss A. Responding to the threat of chronic diseases in India. Lancet. 2005; 366: 1744-1749.
98. Ren J, Pulakat L, Whaley-Connell A, Sowers JR. Mitochondrial biogenesis in the metabolic syndrome and cardiovascular disease. J. Mol. Med. (Berl). 2010; 88: 993-1001.
99. Rousset S, Alves-Guerra MC, Mozo J, Miroux B, Cassard-Doulcier AM, Bouillaud F, Ricquier D. The biology of mitochondrial uncoupling proteins. Diabetes. 2004; 53 1: S130-S135.
100. Samuel VT, Shulman GI. The pathogenesis of insulin resistance: integrating signaling pathways and substrate flux. *J. Clin. Invest.* 2016; 126: 12-22.
101. Sasaki K, Oki T, Kai Y, Nishiba Y, Okuno S. Effect of repeated harvesting on the content of caffeic acid and seven species of caffeoylquinic acids in sweet potato leaves. Biosci. Biotechnol. Biochem. 2015; 79: 1308-1314.
102. Schilling JD. The mitochondria in diabetic heart failure: from pathogenesis to therapeutic promise. Antioxid. Redox Signal. 2015; 22: 1515-1526.
103. Schroder K, Zhou R, Tschopp J. The NLRP3 inflammasome: a sensor for metabolic danger? Science. 2010; 327: 296-300.
104. Severson D. Diabetic cardiomyopathy: recent evidence from mouse models of type 1 and type 2 diabetes. *Can. J. Physiol. Pharmacol. 2004;* 82: 813-823.

105. Shalini S, Dorstyn L, Dawar S, Kumar S. Old, new and emerging functions of caspases. *Cell Death Differ.* 2015; 22: 526-539.
106. Sheedy FJ, Grebe A, Rayner KJ, Kalantari P, Ramkhelawon B, Carpenter SB, et al. CD36 coordinates NLRP3 inflammasome activation by facilitating the intracellular nucleation from soluble to particulate ligands in sterile inflammation. *Nat. Immunol.* 2013; 14: 812-820.
107. Sivitz WI, Yorek MA. Mitochondrial dysfunction in diabetes: from molecular mechanisms to functional significance and therapeutic opportunities. *Antioxid. Redox Signal.* 2010; 12: 537-577.
108. Smail MMA, Howarth CF, Singh J, Ismail AM. Inflammation and diabetic cardiomyopathy. *inTechopen*. doi: 10.5772.
109. Sova, M. Antioxidant and antimicrobial activities of cinnamic acid derivatives. *Mini Rev. Med. Chem.* 2012; 12: 749-767.
110. Stenlöf K, Cefalu WT, Kim KA, Alba M, Usiskin K, Tong C, et al. Efficacy and safety of canagliflozin monotherapy in subjects with type 2 diabetes mellitus inadequately controlled with diet and exercise. Diabetes Obes. Metab. 2013; 15: 372-382.
111. Sun M, Dawood F, Wen WH, Chen M, Dixon I, Kirshenbaum LA, et al. Excessive tumor necrosis factor activation after infarction contributes to susceptibility of myocardial rupture and left ventricular dysfunction. *Circulation.* 2004; 110: 3221-3228.
112. Suroowan, S., Mahomoodally, F. Common phyto-remedies used against cardiovascular diseases and their potential to induce adverse events in cardiovascular patients. *Clin. Phytosci. 2015;* **1,** 1.
113. Tan Y, Zhang Z, Zheng C, Wintergerst KA, Keller BB, Cai L. Mechanisms of diabetic cardiomyopathy and potential therapeutic strategies: preclinical and clinical evidence. Nat. Rev. Cardiol. 2020; 17: 585-607.
114. Tate M, Deo M, Cao AH, Hood SG, Huynh K, Kiriazis H, et al. Insulin replacement limits progression of diabetic cardiomyopathy in the low-dose streptozotocin-induced diabetic rat. Diab. Vasc. Dis. Res. 2017; 14: 423-433.
115. Terashima M, Goto Y. Diabetic cardiomyopathy. Nihon Rinsho. 2002; 60 Suppl 10: 347-353.
116. Teshima Y, Takahashi N, Saikawa T, Hara M, Yasunaga S, Hidaka S, et al.

Diminished expression of sarcoplasmic reticulum Ca(2+)-ATPase and ryanodine sensitive Ca(2+)Channel mRNA in streptozotocin-induced diabetic rat heart. J. Mol. Cell Cardiol. 2000; 32: 655-664.

117. Tohge T, Fernie AR. An overview of compounds derived from the shikimate and phenylpropanoid pathways and their medicinal importance. Mini Rev. Med. Chem. 2017; 17: 1013-1027.
118. Tomita M, Mukae S, Geshi E, Umetsu K, Nakatani M, Katagiri T. Mitochondrial respiratory impairment in streptozotocin-induced diabetic rat heart. Jpn. Circ. J. 1996; 60: 673-682.
119. Trost SU, Belke DD, Bluhm WF, Meyer M, Swanson E, Dillmann WH. Overexpression of the sarcoplasmic reticulum Ca(2+)-ATPase improves myocardial contractility in diabetic cardiomyopathy. Diabetes. 2002; 51: 1166-1171.
120. Turan B, Dhalla NS. Diabetic cardiomyopathy biochemical and molecular mechanisms. New York: Springer New York Heidelberg Dordrecht London. 2014.
121. UKPDS. Intensive blood-glucose control with sulphonylureas or insulin compared with conventional treatment and risk of complications in patients with type 2 diabetes (UKPDS 33). UK Prospective Diabetes Study (UKPDS) Group. Lancet. 1998; 352: 837-853.
122. von Lewinski D, Kolesnik E, Wallner M, Resl M, Sourij H. New antihyperglycemic drugs and heart failure: synopsis of basic and clinical data. Biomed. Res. Int.2017; 1253425.
123. Waldman M, Arad M, Abraham NG, Hochhauser E. The peroxisome proliferator-activated receptor-gamma coactivator-1α-heme oxygenase 1 axis, a powerful antioxidative pathway with potential to attenuate diabetic cardiomyopathy. Antioxid. Redox Signal. 2020; 32: 1273-1290.
124. Westermeier F, Riquelme JA, Pavez M, Garrido V, Díaz A, Verdejo HE, et al. New molecular insights of insulin in diabetic cardiomyopathy. Front Physiol. 2016; 7:125.
125. White JR Jr. Empagliflozin, an SGLT2 inhibitor for the treatment of type 2 diabetes mellitus: a review of the evidence. Ann. Pharmacother. 2015; 49: 582-598.
126. Wilding JP, Norwood P, T'joen C, Bastien A, List JF, Fiedorek FT. A study of dapagliflozin in patients with type 2 diabetes receiving high doses of insulin plus

insulin sensitizers: applicability of a novel insulin-independent treatment. Diabetes Care. 2009; 32: 1656-1662.

127. Williamson EM. Drug interactions between herbal and prescription medicines. *Drug Safety.* 2003; 26: 1075-1092.
128. Wolffram S, Weber T, Grenacher B, Scharrer E. A Na(+)-dependent mechanism is involved in mucosal uptake of cinnamic acid across the jejunal brush border in rats. J. Nutr. 1995; 125: 1300-1308.
129. World Health Organization: Cardiovascular Disease. 2017: 1-6.
130. World Health Organization: Diabetes. 2020.
131. Wu B, Huang XY, Li L, Fan XH, Li PC, Huang CQ, et al. Attenuation of diabetic cardiomyopathy by relying on kirenol to suppress inflammation in a diabetic rat model. J. Cell. Mol. Med. 2019; 23: 7651-7663.
132. Xiao H, Ma X, Feng W, Fu Y, Lu Z, Xu M, et al. Metformin attenuates cardiac fibrosis by inhibiting the TGFbeta1-Smad3 signalling pathway. Cardiovasc. Res. 2010; 87: 504-513.
133. Yamagishi S, Maeda S, Matsui T, Ueda S, Fukami K, Okuda S. Role of advanced glycation end products (AGEs) and oxidative stress in vascular complications in diabetes. Biochim Biophys Acta. 2012; 1820: 663-671.
134. Yang J, Sambandam N, Han X, Gross RW, Courtois M, Kovacs A, et al. CD36 deficiency rescues lipotoxic cardiomyopathy. Circ. Res. 2007; 100: 1208-1217.
135. Younce CW, Wang K, Kolattukudy PE. Hyperglycemia-induced cardiomyocyte death is mediated via MCP-1 production and induction of a novel zinc-finger protein MCPIP. *Cardiovas. Res.* 2010; 87: 665-674.
136. Young ME, Patil S, Ying J, Depre C, Ahuja HS, Shipley GL et al. Uncoupling protein 3 transcription is regulated by peroxisome proliferator-activated receptor (alpha) in the adult rodent heart. *FASEB J.* 15: 833-845.
137. Zhang CX, Pan SN, Meng RS, Peng CQ, Xiong ZJ, Chen BL, et al. Metformin attenuates ventricular hypertrophy by activating the AMP-activated protein kinase-endothelial nitric oxide synthase pathway in rats. Clin. Exp. Pharmacol. Physiol. 2011; 38: 55-62.
138. Zhou R, Tardivel A, Thorens B, Choi I, Tschopp J. Thioredoxin-interacting protein links oxidative stress to inflammasome activation. Nat. Immunol. 2010; 11: 136-140.

139. Zinman B, Lachin JM, Inzucchi SE. Empagliflozin, cardiovascular outcomes, and mortality in type 2 diabetes. N. Engl. J. Med. 2016; 374: 1094.
140. Zu Y, Wan LJ, Cui SY, Gong YP, Li CL. The mitochondrial Na+/Ca2+ exchanger may reduce high glucose-induced oxidative stress and nucleotide-binding oligomerization domain receptor 3 inflammasome activation in endothelial cells. J. Geriatr. Cardiol. 2015; 12: 270-278.

Chapter 2

Materials and Methods

2.1 Chemicals and cell culture reagents

Cinnamic acid (CiA) was purchased from Natural Remedies Pvt. Ltd, Bangalore, India. Dimethyl sulfoxide (DMSO), 3-(4,5-dimethylthiazol-2-yl)-2,5-diphenyltetrazolium bromide (MTT), metformin hydrochloride, 2, 7 dichloro dihydro fluorescein diacetate (DCFH-DA) and 5,5',6,6'-tetrachloro-1,1',3,3'-tetraethyl- benzimidazol carbocyanine iodide (JC-1), JNK inhibitor SP600125, p38 MAPK inhibitor SB220025 and ERK inhibitor PD98059 were from Sigma Aldrich (St. Louis, USA). Fetal bovine serum (FBS), pencillin-streptomycin antibiotics, trypsin – ethylene diamine tetra acetate (EDTA), phosphate buffered saline (PBS) and Hank's balanced saline solution (HBSS) were from Gibco, USA. MitoSOX™ red, Fura 2-AM, MitoTracker Red and Calcein AM were from Invitrogen (Carlsbad, CA, USA). Kits for biochemical assays like lactate dehydrogenase (LDH), creatinine kinase myocardial B fraction (CK-MB), serum glutamic oxaloacetic transaminase (SGOT), CRP- ultra , total cholesterol (TC), triglyceride (TG), low density lipoprotein (LDL-C) and high density lipoprotein (HDL-C) were from Agappe Diagnostics, Kerala, India. Kit for determining the glycated haemoglobin, insulin levels and atrial natriuretic peptides were obtained from Immunotag, (Geno Technology Inc., USA). BAX and BCL-2 antibodies were from Cell Signaling Technology (USA). OPA1, MFN2, DRP1, FIS1, NFkB, iNOS, BNP, TNNI3K, GATA-4 and β-actin were from Santa Cruz, USA. TLR-4, MyD88, ICAM, NLRP3, Alexa fluor 488 antibodies were from Abcam (USA). O-GlcNAc, pGSK-3β, and troponin were from Cell Signaling Technology (USA). TNF-α, IL-6, IL-1β, MCP-1 and IL-10 were from BD Biosciences, USA and anti-ST2L antibody was from Immunotag (Geno Technology Inc., USA). All other chemicals were of analytical grade.

2.2 *In vitro* cell based assays

2.2.1 Cell culture

H9c2 cardiomyoblasts from American Type Culture Collection (ATCC) were cultured in Dulbecco's modified eagle medium (DMEM) alongwith with 10% fetal bovine serum (FBS), and antibiotics (100 U/ml of penicillin and 100 μg/ml of streptomycin) in a humidified incubator with 95 % air and 5 % CO_2 at 37 °C. Mannitol was used to exclude

the effect of changes in osmolarity. Cells were allowed to attain 60 % confluence and were treated with high glucose (33 mM) for 48 hrs to simulate hyperglycemia. All parameters were determined after 48 hrs of incubation of cells with high glucose in the presence or absence of various doses of CiA in 0.1 % DMSO (100 and 500 nM) or metformin (positive control, 1 mM).

Experimental groups consisted of control (C; 5.5 mM glucose), high glucose (HG; 33 mM glucose), high glucose + metformin - 1 mM (Met;), HG + cinnamic acid - 100 nM (CiA1), HG + cinnamic acid - 500 nM (CiA2), control + cinnamic acid -500 nM (C + CiA2 for toxicity evaluation).

2.2.2 Cell viability was analyzed by MTT assay and LDH release to the medium.

a) MTT assay: The assay was carried out as per method of Wilson, 2000. Briefly, 5 x 10^ 6 cells were seeded in 96 well plates. Cells after 60 - 70% confluence were treated with different concentrations of the compound. CiA was dissolved in DMSO and the final concentration used was lower than 0.1% DMSO. The cells were then incubated for 48 hrs. After incubation, medium was removed and cells were incubated for 4 hrs with 10 mg/ml of MTT, dissolved in serum free medium (DMEM). Then it was washed with 100 µl PBS, and 100 µl of DMSO was added, gently shaken for 10 min so that complete dissolution was achieved and absorbance was recorded at 570 nm using the microplate spectrophotometer (Biotek Synergy 4, USA).

b) **LDH release assay**: LDH release to medium was measured using assay kit (Takara, USA). LDH is a soluble enzyme located in the cytosol that is released into the surrounding culture medium upon cell damage or lysis processes. LDH activity in the culture medium can therefore be used as an indicator of cell membrane integrity and thus a measurement of cytotoxicity. After respective treatments, 100 µl of cell culture medium was collected and transferred to 96 well plates. To this, LDH reaction solution containing NAD+, lactic acid, iodo nitro tetrazolium (INT) and diaphorase, were added. The mixture was incubated with gentle shaking for 30 min at room temperature and the absorbance was taken at 490 nm. LDH release to the culture medium was calculated as the percentage of cytotoxicity of the cell.

2.2.3 Quantification of atrial natriuretic peptide (ANP)

ANP was quantified using the assay kit from Elabscience, USA. Briefly, the trypsinized cells were collected and centrifuged. To 50 µl of samples, 50 µl of antibody solution was added and incubated for 45 min at 37 °C. The solution was aspirated and then it was soaked for 1 min in the wash buffer and 100 µl of HRP conjugate solution was added and incubated for 30 min at 37 °C. The solution was aspirated again and 90 µl of substrate was added and incubated for 15 min at 37 °C. Finally 50 µl of stop solution was added and the absorbance was measured at 450 nm.

2.2.4 Detection of intracellular reactive oxygen species (ROS) generation

Intracellular ROS levels were measured using DCFH-DA (Choi et al., 2008). After respective treatments, cells were washed with PBS and then incubated with DCFH-DA for 20 min at 37 °C in a humidified atmosphere containing 5 % CO_2. After incubation, cells were washed three times with a Krebs-Ringer-phosphate buffer. DCFH-DA upon entering the cells would be deacetylated by cellular esterases which will later be oxidised by ROS to produce fluorescent product. DCF fluorescence imaging was performed with a spinning disk imaging system (BD Pathway™ Bioimager System, BD Biosciences, USA) at excitation wavelength of 488 nm and emission wavelength of 525 nm.

2.2.5 Cell based antioxidant studies

For these H9c2 cells were seeded in 6 well plates at a density of 3×10^5 cells per well. At sub confluence, cells were given HG treatment along with compound and metformin for 48 hrs.

2.2.5.1 SOD activity assay

SOD activity was assayed with a commercial kit from Biovision, USA. Briefly, after protein concentration was determined, samples were treated with 2-(4-iodophenyl)-3-(4-nitrophenyl)-5-(2, 4-disulfophenyl) 2H-tetrazolium, monosodium salt, which produces a water-soluble formazan dye upon reduction with a superoxide anion. After 20 min of incubation at 37 °C, absorbance was measured at 450 nm.

2.2.5.2 Estimation of GSH

GSH content was estimated using a kit from Cayman chemicals (USA). Briefly after respective treatments, cells were collected and homogenized on ice in a cold buffer and centrifuged at 10000 x g for 15 min at 4 °C. The supernatants were collected and deproteinized. To that 50 µl of sample and standard were added. Freshly prepared assay

cocktail mixture was added to the samples and standard in each well and incubated at 37 °C for 25 min. GSH concentration was measured by the end point method at 405 nm.

2.2.5.3 Glutathione peroxidase activity assay

Glutathione peroxidase was estimated as per the protocol of Rotruck (Rotruck et al., 1973). Briefly, 200 µl of tris buffer was mixed with 20 µl EDTA and 100 µl of sodium azide. To this 500 µl of sample along with glutathione and hydrogen peroxide were added and incubated for 10 min. Then the reaction was terminated by adding 500 µl of TCA followed by centrifugation after which 2ml of supernatant was added to phosphate buffer and DTNB reagent and absorbance was measured at 412 nm. Results are expressed as µg glutathione/min/mg protein.

2.2.5.4 Total antioxidant assay

Total antioxidant activity of the samples was assayed using kit from Cayman chemicals (USA). This assay is based on the ability of antioxidants in the sample to inhibit the oxidation of 2, 2-azinobis (3-ethylbenzothiazoline-6-sulfonic acid) (ABTS*) to reduced $ABTS^{**+}$ by metmyoglobin. The amount of $ABTS^{**+}$ produced was monitored by measuring absorbance at 405 nm. After respective treatments cells were collected by centrifugation at 2000 x g for 10 min at 4 °C. The pellets were sonicated on ice in 1-2 ml of cold buffer and further centrifuged at 10000 x g for 15 min at 4 °C. The supernatant was collected. To 10 µl of sample, 10 µl of metmyoglobin and 150 µl of chromogen were added. The reactions were initiated by adding 40 µl of hydrogen peroxide working solution to each wells. The wells were incubated for 5 min at room temperature and the absorbance was measured.

2.2.6 Estimation of thiobarbituric acid reactive substances (TBARS)

Oxidative stress in the cellular environment results in the formation of highly reactive and unstable lipid hydroperoxides. Lipid peroxidation was estimated with TBARS assay kit (Himedia, India). TBARS assay measures malondialdehyde present in the sample. Briefly, cells were collected and sonicated for 5s. 100 µl of sample and standard were added to the labelled tubes. To that 100 µl of sodium dodecyl sulfate (SDS) and 4 ml of coloring reagent were added. The tubes were then kept in a water bath and boiled for 1 h and were then placed on an ice bath for 10 min to stop the reaction. After incubation it was then centrifuged for 10 min at 1600 x g at 4 °C and incubated at room temperature

for 30 min. From this 150 µl of samples were transferred to the plate and the absorbance of the colored product was measured at 530 nm.

2.2.7 Estimation of protein carbonyls

Protein carbonyl content was determined using a kit from Cayman chemicals (USA). After respective treatments, cells were collected and homogenized on ice in cold buffer. Then the homogenized samples were centrifuged and supernatants were collected. To 200 µl of sample, 800 µl of 2, 4 dinitrophenylhydrazine (DNPH) and 800 µl of HCl were added. After incubation in the dark for 1 h, 1 ml of 20 % trichloroacetic acid (TCA) was added followed by centrifugation. The pellet was resuspended in 1 ml of 10 % TCA. After centrifugation again the pellet was collected and resuspended in ethanol / ethyl acetate mixture and centrifuged for 10 min. This step was repeated 2 more times. Finally the protein pellets were resuspended in 500 µl of guanidine hydrochloride and centrifuged to remove any debris. Then absorbance was measured at 360 nm.

2.2.8 Studies on mitochondria

2.2.8.1 Mitochondrial transmembrane potential (ψm)

Alteration in ψm was detected using JC-1 mitochondria staining kit that uses JC-1, a cationic fluorescent dye. Briefly the cells were seeded in 96-well black plates at a density of 5×10^3 for treatment. In normal cells, due to the electrochemical potential gradient, the dye is concentrated in the mitochondrial matrix, where it forms red fluorescent aggregates (JC-1 aggregates). Any event that dissipates the mitochondrial membrane potential prevents the accumulation of JC-1 dye in the mitochondria, and thus the dye is dispersed throughout the entire cell leading to a shift from red (JC-1 aggregates) to green (JC-1 monomers). The cells after respective treatments were incubated with JC-1 stain for 20 min. The stain was washed off with HBSS and examined under a spinning disk imaging system (BD Pathway™ Bioimager System, BD Biosciences, USA). The fluorescence was measured at 490 nm excitation and 530 nm emission wavelengths for JC-1 monomers, and for aggregates, the wavelengths were set at 525 nm for excitation and 590 nm for emission.

2.2.8.2 Mitochondrial superoxide production

Changes in mitochondrial superoxide production were monitored using MitoSOX™ red. The cells were seeded in 96-well plates at a density of 5×10^3 and subjected to treatments. Solution of MitoSOX™ in Hank's buffered saline solution (5 µM

in HBSS) was added to cells and incubated at 37 °C for 15 min. Cells were then washed with HBSS and processed for imaging at excitation/emission range of 514/580 nm.

2.2.8.3 Estimation of mitochondrial content

Mitochondrial content was evaluated using Mitotracker Deep Red FM. Briefly, the cells after treatments were incubated with 5 μM Mitotracker deep red stain in HBSS at 37°C for 30 min. The cells were washed three times and visualised by Nikon Eclipse TS 100 microscope (Nikon, Melville, NY) and the fluorescence intensity was measured at excitation and emission wavelengths of 644 and 665 nm respectively.

2.2.8.4 Expression of mitochondrial fission and fusion proteins

The expression of mitochondrial fission and fusion proteins was determined at protein levels by western blotting (please see section 2.2.13 for details).

2.2.8.5 Complex IV enzyme activity

The mitochondrial complex IV enzyme activity was determined according to the manufacturers' protocol (Abcam, UK). Briefly, 200 μl of diluted sample was loaded into individual wells of a plate followed by 3 hrs incubation at room temperature. The wells were then washed with 300 μl of Solution 1. Then the wells were emptied and added 200 μl of assay solution containing Reagent C and Solution 1. Absorbance was monitored at 550 nm at 30°C for 120 min.

2.2.8.6 Detection of ATP content

The ATP content in the cells was quantitatively determined by using ATP bioluminescent assay kit purchased from Sigma (Sigma-Aldrich, USA). The assay is based on luciferase's requirement for ATP in producing light. Briefly, cells were collected after respective treatments. 100 μl of assay mix working solution was added to a reaction vial and swirled and allowed to stand for 3 min at room temperature. To this a mixture containing 50 μl of sample, 100 μl of somatic cell ATP releasing reagent and 50 μl of ultrapure water was added. The amount of light emitted was measured immediately with a luminometer (Biotek Synergy 4, USA).

2.2.9 Detection of intracellular calcium levels by Fura 2 AM

The cells were seeded in 96 - well plates at a density of 5 x 10^3 cells and subjected t treatments. Intracellular calcium was detected by staining the cells with Fura-2 AM (Robinson et al., 2004) for 20 min at 37 °C. The cells were washed three times with HBSS

and the images were visualized using a spinning disk imaging system (BD Pathway™ Bioimager System, BD Biosciences, USA) at excitation of 340 nm and the emission of 510 nm.

2.2.10 Detection of apoptosis

2.2.10.1 Caspase-3 fluorimetry assay

Analysis of apoptosis was done by caspase-3 fluorimetry assay kit (Biovision, USA). Briefly, the cells were resuspended in a chilled lysis buffer. Cells were incubated on ice for 10 min. 50 µl of reaction buffer was added to each sample and to it 1 mM (Asp-Glu-Val-Asp)- 7-amino-4-trifluoromethylcoumarin (DEVD-AFC) substrate was added and incubated for 1 h. Fluorescence was measured at excitation wavelength of 405 nm and emission of 505 nm.

2.2.10.2 Flow cytometric analysis with annexin V/PI

Apoptotic cells were quantified by flow cytometry using annexin V-FITC apoptosis detection kit from Biovision (USA). For cytometry analysis cells were resuspended in 500 µl of 1X binding buffer and to this 5 µl of annexin V-FITC was added. Then 5 µl of propidium iodide was added and incubated at room temperature for 5 min in dark. Annexin V-FITC binding was analyzed by flow cytometry (Ex = 488 nm; Em = 530 nm) using FITC signal detector {fluorescence 1 (FL1)} and PI staining by the phycoerythrin emission signal detector {fluorescence 2 (FL2)}.

2.2.10.3 Detection of pro-apoptotic and anti-apoptotic protein expression

Expression of pro-apoptotic protein BAX and anti-apoptotic protein BCL-2 was determined by western blot analysis (please see section 2.2.13 for details).

2.2.11 Detection of sorbitol levels

Sorbitol levels were determined as per manufacturer's protocol (Biovision, USA). Initially a working solution of sorbitol standards (1 mM) was prepared using the stock solution provided in the kit. Standards (including reaction blanks) were pipetted into wells of a 96-well plate to generate 0, 2, 4, 6, 8 and 10 nmol/well by dilution in the assay buffer. 50 µl of protein samples was pipetted into the wells. This was followed by addition of 50 µl of reaction mixture (enzyme mixture, developer and probe diluted in assay buffer) to all wells and incubated at 37 °C for 30 min. Then absorbance was read at 560 nm and sorbitol concentration was calculated.

2.2.12 Studies on inflammation

2.2.12.1 Estimation of nitrite levels

Nitrite levels were determined in cell culture supernatant as per the method of Grisham (Grisham et al., 1996). Griess reagent was used in this method. Briefly, 50 µl of samples were coated in 96-well plates. The standard curve was performed with nitrite solution, at various concentrations. 50 µl of Griess reagent were added to the samples and the mixture was incubated for 10 min in dark. Absorbance was measured at 540 nm.

2.2.12.2 Measurements of TNF α, IL-6 and IL-10 by ELISA

The levels of TNF α, IL-6 and IL-10 were estimated in the cell culture supernatant as per the protocol of Engvall (Engvall and Perlmann, 1971). Briefly, 100 µl of serum was coated onto the wells of a 96 well plate for 24 hrs at 37 °C followed by blocking with 5 % skimmed milk or gelatin. The wells were incubated with primary antibody for 2 hrs followed by 1 h incubation with secondary antibody. 100 µl of substrate solution was added to each well to which 3N HCl was added to stop the reaction. Absorbance was measured at 490 nm.

2.2.12.3 Cell nuclear and cytoplasmic extraction

Cytoplasmic extraction was performed according to the manufacturer's instructions (Abcam, UK). Briefly, the cell pellet was resuspended in 100 µl of 1X-pre extraction buffer (containing DTT and PIC at a 1:1000 ratio) per 10^6 cells followed by centrifugation for 1 min at 12000 rpm. The cytoplasmic extract was separated from the nuclear pellet and the same was used for protein analysis.

2.2.12.4 Immunofluorescence

Cells from experimental groups were washed three times with ice cold PBS and fixed with 4 % paraformaldehyde. Then the cells were permeabilized with PBST containing triton-X 100. Again the cells were washed with PBS three times followed by blocking with 3% normal goat serum at room temperature for 30 min. Then after washing, cells were incubated with primary antibody for 2 hrs followed by secondary antibody Alexa fluor 488 for 1 h at room temperature. This was followed by washing and counterstaining with DAPI and was examined under the Nikon Eclipse TS 100 microscope (Nikon, Melville, NY).

2.2.13 Western blot analysis

Protein was extracted from cell lysates using ice-cold radioimmunoprecipitation assay (RIPA) buffer containing protease inhibitor cocktail (Sigma Aldrich, USA). After incubation at 4 °C for 1 h, with constant agitation to ensure complete lysis, the cell suspension was centrifuged at 12000 rpm for 15 min at 4 °C and the supernatant was collected. Protein content in the supernatant was quantified using the bicinchoninic acid (BCA) protein assay kit (Pierce, Rockford, IL, USA) in accordance with the manufacturer's instructions. Proteins extracted using RIPA buffer were separated by sodium dodecyl sulfate polyacrylamide gel electrophoresis (SDS-PAGE), and transferred to polyvinylidene difluoride (PVDF) membranes using turbo trans blot apparatus (BD Bioscience, USA). The membrane was blocked with 5 % skimmed milk in TBST for 1 h at room temperature. Then it was washed thrice in TBST for 10 min each and probed with antibodies against OPA1, MFN2, FIS1, DRP1, BAX, BCL-2, MCUR1, TLR4, MyD88, IkB, iNOS, NLRP3, ICAM, pJNK, pERK, pp38 MAPK, TxNIP, p- GSK3β, GATA-4, TNNI3K, ST2L, OGlcNAc, mTOR, p mTOR, Akt, pAkt, hexokinase, and Raptor followed by incubation with HRP conjugated secondary antibodies. After washing, the membrane was developed using Clarity ™ Western ECL Substrate (BIO-RAD, USA). The immunoblot images were analyzed in the ChemiDocin ChemiDoc XRS system (BIO-RAD, USA) using Image Lab software.

2.3 *In vivo* study

2.3.1 Experimental Design

All animal experiments were approved (No: JMMC & RI SARF/IAEC/RP-02/2017) by the institutional animal ethics committee of Jubilee Mission Medical College and Research Institute, Thrissur, Kerala where we performed our experiments. All procedures conform to the guidelines from International Guiding Principles of Biomedical Research and Committee for the Purpose of Control and Supervision of Experiments on Animals (CPCSEA) formed by Govt. of India. Male Wistar rats of 90-120 g were used in this study and they were obtained from College of Veterinary and Animal Sciences, Thrissur, Kerala. During acclimatization before experiments, the animals were provided with a standard diet and water *ad libitum.* Then rats were divided into two groups. First group (n = 12) were fed normal rat chow throughout the experimental period and they were control groups. Second group (n = 33) were fed with diabetogenic

diet (high fat - high fructose (HF/HF): 46.5 % carbohydrate, 25.7 % fat, and 18.6 % protein- 4.9 kcal/g; TD05482, Teklad, USA). To induce diabetes, after 2 months of diabetogenic diet, 27 animals were fasted for 16 hrs and a single intraperitoneal injection of 25 mg/kg bwt streptozotocin (STZ) (in 0.1 M citrate buffer, pH 4.5) was given. After 72 hrs of STZ injection the animals with blood glucose (fasting) above 300 mg/dl were taken as diabetic and grouped into various experimental groups and continued in a diabetogenic diet for another 2 months. At 121st day the animals under these groups received test material CiA - 5 &10 mg/kg bwt, and metformin (50 mg/kg bwt) through oral gavage for another 60 days. Vehicle (1 % gum acacia in normal saline) was administered to the control and diabetic groups. Duration of the entire study was 180 days. Details of experimental groups are given below with 6 animals in each group.

Group 1 - Control (Normal diet for 180 days)

Group 2 - Diabetogenic diet for 180 days with single dose of STZ

Group 3 - Diabetogenic diet for 180 days with single dose of STZ + Met (50 mg/kg bwt) for 60 days starting from 121 to 180 days

Group 4 - Diabetogenic diet for 180 days with single dose of STZ + CiA1 (5 mg/kg bwt) for 60 days starting from 121 to 180 days

Group 5 - Diabetogenic diet for 180 days with single dose of STZ + CiA2 (10 mg/kg bwt) for 60 days starting from 121 to 180 days

Group 6 - Normal diet + CiA2 (10 mg/kg bwt) for 60 days starting from 121 to 180 days (to check toxicity of CiA)

Group 7 - Sham control (Diabetogenic diet only)

Temperature of the animal laboratory was maintained at 22 ± 2 °C with 12 hrs periods of light and dark. The fasting blood glucose was monitored weekly by tail tip prick using glucose strips. Body weight and food intake were recorded weekly and daily respectively. Blood was collected by cardiac puncture under general anaesthesia at the end of the experiment. General anaesthesia was performed by isoflurane (Forane) inhalation. The proportion used was 30 % isoflurane and 70 % propylene glycol. Serum was separated and stored at -80 °C. Rats were sacrificed by carbon dioxide inhalation. Heart was collected in liquid nitrogen containers for the various biochemical analyses.

2.3.2 Biochemical Assays

2.3.2.1 Determination of biochemical parameters

At the end of the experiment the rats were fasted for 16 hrs and fasting blood glucose levels were determined using test strips by an Accu-Chek® Active blood glucometer (Roche Diabetes Care India, Pvt. Ltd.). Also, the heart weight was determined for estimating cardiac mass index (CMI). CMI was calculated by the following formula:

CMI= Total heart weight / Total body weight. Cardiac mass index was used to determine cardiac hypertrophy.

2.3.2.2 Estimation of glycated haemoglobin (HbA1c) levels of rat serum

The glycated haemoglobin (HbA1c) levels of blood were estimated using rat haemoglobin ELISA kit from ImmunoTag (Geno Technology Inc., USA) according to the manufacturer's instructions. Briefly, 40 µl of samples were added to the wells to which 10 µl anti-HbA1c antibody was added. This was followed by the addition of 50 µl of streptavidin-HRP to sample wells and standard wells. It was then mixed and incubated for 1 h at 37 °C. Then the plate was washed five times with a wash buffer. 50 µl of substrate solution A and 50 µl of substrate solution B were added to each well. Then incubated the plates for another 10 min at 37 °C in the dark. Finally 50 µl stop solution was added and the blue colour was changed to yellow immediately. Absorbance was measured at 450 nm within 10 min after addition of stop solution.

2.3.2.3 Estimation of insulin levels

The fasting serum insulin levels were determined using rat insulin ELISA kit from ImmunoTag (Geno Technology Inc., USA) according to the manufacturer's instructions. Briefly, 40 µl of samples were added to the wells to which 10 µl anti-INS antibody was added. This was followed by the addition of 50 µl of streptavidin-HRP to sample wells and standard wells. It was mixed and incubated for 1h at 37 °C. The plates were washed five times with a wash buffer. 50 µl of substrate solution A and 50 µl of substrate solution B was added to each well. The plates were covered and kept in dark for another 10 min at 37 °C. Finally 50 µl of stop solution was added and the blue colour was changed to yellow immediately. Absorbance was measured at 450 nm within 10 min after addition of stop solution.

2.3.3 Estimation of Cardiac Markers in the serum of rats

2.3.3.1 Lactate Dehydrogenase (LDH) assay

LDH activity was estimated in the serum of rats by using kits from Agappe diagnostics, Mumbai, India as per manufacturer's instruction. LDH was determined by mixing 10 µl of serum with 1000 µl of working reagent containing Tris buffer, pyruvate, NaCl, and NADH, and incubated at 37 °C for 1 min and measured the change in absorbance for 3 min duration at 340 nm (Biotek Synergy 4, USA). The LDH levels were measured by using the formula:

LDH-P activity (U/L) = (delta OD/min) x 16030

2.3.3.2 Creatine Kinase – MB assay (CK-MB)

Serum CK-MB (Agappe diagnostics, Mumbai, India) levels were estimated by adding 40 µl of sample to 1000 µl of working reagent containing Reagent 1 (imidazole, D-Glucose, N-acetyl-L-cysteine, magnesium acetate, NADP, EDTA, hexokinase and anti-human polyclonal CK-M antibodies) and Reagent 2 (creatine phosphate, ADP, AMP, diadenosine pentaphosphate and G6PDH).It was mixed well and incubated at 37 °C for 100 seconds and change in absorbance was measured during 5 min at 340 nm (Biotek Synergy 4, USA). The levels of CKMB was calculated as follows:

CK-MB Activity (U/L) = (delta OD/min) x 8254

2.3.3.3 Determination of CRP-Ultra levels

For CRP estimation (Agappe diagnostics, Mumbai, India), 400 µl of CRP Ultra reagent 1 containing glycine buffer was added to 10 µl of sample followed by the addition of 200 µl CRP Ultra reagent 2 containing anti CRP antibodies. Absorbance (A1) was measured after 2 min (A2) of sample addition at 578 nm (Biotek Synergy 4, USA). The delta absorbance was calculated and a standard curve was constructed from which the CRP-ultra levels of standard and samples were calculated.

2.3.3.4 Determination of serum glutamic-oxaloacetic transaminase (SGOT) levels in the serum of rats

SGOT levels were also estimated by using kits from Agappe diagnostics, Mumbai, India. 100 µl of sample was added to 1000 µl of working reagent containing Reagent 1 (Tris buffer pH 7.8, L- aspartate, LDH and malate dehydrogenase) and Reagent 2 (alpha-

ketoglutarate and NADH) and change in absorbance was measured at 340nm per minute during 3 min (Biotek Synergy 4, USA). The SGOT levels were calculated as follows:

SGOT activity (U/L) = (delta OD/min) x 1745.

2.3.3.5 Determination of atrial natriuretic peptide (ANP) levels in the serum of rats

The serum ANP was estimated by ELISA kit from ImmunoTag (Geno Technology Inc., USA). Briefly, 50 µl of standard, blank, or serum samples were taken into the corresponding labelled wells, and 50 µl of biotin-labelled antibody was added immediately to it. Then it was mixed well and incubated for 45 min at 37 °C, and washed with the wash buffer. After the washing step, 100 µl of SABC working solution (kit reagent) was added to all the wells and incubated for 30 min at 37 °C. It was then washed 5 times, and 90 µl of TMB substrate was added into each well and incubated in the dark at 37 °Cfor 20 min. Then 50 µl of stop solution was added, and the absorbance was read at 450 nm. The standard curve for ANP was constructed, and ANP and BNP concentrations were determined and expressed in pg/ml.

2.3.4 Determination of lipid parameters

a) Total cholesterol levels

The rat serum cholesterol levels were estimated as per the protocol of the kit (Agappe diagnostics, Mumbai, India). Briefly, 10 µl of standard or sample were added to 1000 µl working reagent containing PIPES buffer, phenol, sodium cholate, 4-aminoantipyrine, cholesterol esterase, cholesterol oxidase, and peroxidase. It was mixed and incubated for 5 min at 37 °C. Absorbance was measured at 505 and 630 nm. The cholesterol levels were calculated by using the formula:

Cholesterol Conc. (mg/dL) = (Absorbance of sample/Absorbance of standard)*200

b) Triglyceride levels

The serum triglyceride levels were measured using kit from Agappe diagnostics, Mumbai, India**.** Briefly, 10 µl of standard or sample were added to 1000 µl working reagent containing PIPES buffer, TOPS, potassium ferrocyanate, magnesium salt, 4-aminoantipyrine, ATP, lipoprotein lipase, glycerol kinase, glycerol-3-phosphate oxidase, and peroxidase. It was then mixed and incubated for 5 min at 37 °C. Absorbance was

measured at 546 and 630 nm. The triglyceride levels were calculated by using the formula:

Triglyceride Conc. (mg/dL) = (Absorbance of sample/Absorbance of standard)*200

c) Estimation of low density lipoprotein- cholesterol (LDL-C) levels

The LDL-C levels in the serum of rats were measured according to the protocol of Agappe diagnostics, Mumbai, India. Accordingly, 5 µl of calibrator or sample were added to 450 µl of Reagent 1 containing HSDA and Good's buffer. It was mixed and incubated for 5 min at 37 °C. To this 150 µl of Reagent 2 (cholesterol esterase, cholesterol oxidase and 4- aminoantipyrin) was added. It was then mixed and incubated for 5 min at 37 °C. Absorbance was measured at 578/630 nm. Absorbance of the calibrator and reagent blank was measured at 578/630 nm. LDL-C levels were calculated as follows:

LDL-C Conc. (mg/dL) = (Absorbance of sample/Absorbance of calibrator)*Calibrator conc.

d) Estimation of high density lipoprotein- cholesterol (HDL-C) levels

The HDL-C levels in the serum of rats were measured according to the protocol of Agappe diagnostics, Mumbai, India. To estimate HDL-C levels, 5 µl of calibrator or sample were added to 450 µl of Reagent 1 (N—ethyl-N-(3-methylphenyl)-N'succinylethyenediame (EMSE)). The mixture was incubated for 5 min at 37 °C. To this 150 µl of Reagent 2 (cholesterol oxidase and 4- aminoantipyrin) was added. It was then mixed and incubated for 5 min at 37 °C. Absorbance of the calibrator and reagent blank was measured at 578/630 nm. HDL-C levels were calculated as follows:

HDL-C Conc. (mg/dL) = (Absorbance of sample/Absorbance of calibrator)*Calibrator conc.

2.3.5 Determination of lipid peroxidation levels in heart tissue

TBARs levels were estimated according to the protocol of Okhawa (Okhawa et al., 1979). Briefly, the tissue was homogenized in 2 ml Tris HCl buffer followed by addition of 2 ml TCA-TBA reagent to 1 ml of the homogenate. This was kept in a boiling water bath for 15 min and then cooled and centrifuged at 1000 g for 10 min. The supernatant was collected and the absorbance was read at 535 nm.

2.3.6 Estimation of nitrite levels

Nitrite levels were determined in rat serum as per the method of Grisham et al (Grisham et al., 1996). Griess reagent was used in this method. Briefly, 50 µl of samples were coated in 96-well plates. The standard curve was performed with a nitrite solution, at various concentrations. Griess reagent was added to the samples and the mixture was incubated for 10 min after which the absorbance was measured at 540 nm using a microplate reader.

2.3.7 Measurements of TNF α, IL-6, MCP-1, IL-1β, IL-10 by ELISA

The levels of TNF α IL-6, IL-1β, MCP-1 and IL-10 were estimated in the serum of rats as per the protocol of Engvall (Engvall and Perlmann, 1971)). Briefly, 100 µl of serum was coated onto the wells of a 96 well plate for 24 hrs at 37 °C followed by blocking with 5 % skimmed milk or gelatin. The wells were incubated with primary antibody for 2 hrs followed by 1 h incubation with secondary antibody. 100 µl of substrate solution was added to each well to which 3N HCl was added to stop the reaction. Absorbance was measured at 490 nm.

2.3.8 Real time quantitative PCR

The mRNA levels of TGF - β, β - MHC, and β actin were analysed by real time quantitative PCR. Total RNA was separated using a Trizol reagent (Life Technologies, USA) according to the manufacturer's protocols. RNA concentrations and purity were measured at 260/280 nm. PrimeScript RT reagent kits (Takara, Otsu, Shiga, Japan) were used for reverse transcriptase reactions according to the manufacturer's instruction. Real-time PCR was performed with Quantitative PCR with SYBR Premix Ex Taq TM (Takara), and ABI PRISM 7500 sequence detection PCR system (Applied Biosystems, Foster City, CA, USA). The samples were relatively quantified by normalizing the targeted gene level to that of internal control by the ΔΔCt method.

2.3.9 Histopathology of heart tissue

After sacrifice, the hearts were cut into pieces with sharp razor and immediately fixed in 10 % neutral buffered formalin solution. Tissues were then dehydrated in graded ethanol series, cleared in xylene and embedded in paraffin wax. 5 µm thick sections were prepared using a microtome and stained with hematoxylin and eosin (H&E) and van Geison stain. The stained slides were examined under Nikon Eclipse TS 100 inverted microscope for the examination of collagen deposition.

2.3.10 Western blot analysis

Protein was extracted from tissue homogenate using ice-cold RIPA buffer containing protease inhibitor cocktail (Sigma Aldrich, USA). After incubation at 4°C for 1 h, with constant agitation to ensure complete lysis, the tissue suspension was centrifuged at 12000 rpm for 15 min at 4°C and the supernatant was collected. Protein content in the supernatant was quantified using the bicinchoninic acid (BCA) protein assay kit (Pierce, Rockford, IL, USA) in accordance with the manufacturer's instructions. Proteins extracted (25 μg) using RIPA buffer were separated by SDS-PAGE, and transferred to PVDF membranes using turbo transblot apparatus (BD Bioscience, USA). The membrane was blocked with 5% skimmed milk in TBST for 1 h at room temperature. Then it was washed thrice in TBST for 10 min each and probed with antibodies against troponin, BNP, TNNI3K, CRP, MCP-1, TLR4, MyD88, NLRP3, pJNK, pERK, pp38 MAPK, TxNIP, pGSK-3β and GATA-4 followed by incubation with HRP conjugated secondary antibodies. After washing, the membrane was developed using Clarity ™ Western ECL Substrate (BIO-RAD, USA). The immunoblot images were analyzed in ChemiDoc XRS system (BIO-RAD, USA) using Image Lab software.

2.3.11 Statistical analysis

Data are presented as mean ± standard error of mean (SEM). Data were subjected to one way analysis of variance (ANOVA) and the differences among the means of the groups were assessed using Tukey's multiple range tests using Origin Pro version 8.5 (OriginLab Corporation, Massachusetts, USA). The significance was accepted at $p \leq 0.05$.

References

1. Choi SW, Benzie IF, Ma SW, Strain JJ, Hannigan BM. Acute hyperglycemia and oxidative stress: direct cause and effect? Free Radic. Biol. Med. 2008; 44: 1217-1231.
2. Engvall E, Perlmann P. Enzyme-linked immunosorbent assay (ELISA) Quantitative assay of immunoglobulin G. Immunochemistry. 1971, 8, 871-874.
3. Grisham, M.B., Johnson, G.G., Lancaster, J.R. Jr. Quantitation of nitrate and nitrite in extracellular fluids. Meth. Enzymol. 1996; 268, 237-246.
4. Ohkawa H, Oshishi N, Yag K. Assay of lipid peroxidation in animal tissue by thiobarbituric acid reaction. Anal. Biochem. 1979; 95:351-358.
5. Robinson JA, Jenkins NS, Holman NA, Roberts-Thomson SJ, Monteith GR. Ratiometric and non- ratiometric Ca^{2+} indicators for the assessment of

intracellular free Ca^{2+} in a breast cancer cell line using a fluorescence microplate reader. J Biochem Biophys Methods. 2004; 58: 227-37.

6. Rotruck JT, Pope AL, Ganther HE, Swanson AB, Hafeman DG, Hoekstra WG. Selenium: biochemical role as a component of glutathione peroxidase. Science. 1973; 179: 588-590.
7. Wilson AP. Cytotoxicity and viability assays. In JRW Masters, Animal Cell Culture, 3rd ed., Oxford University, Oxford, 175-219; 2000.

Chapter 3

Investigation on redox status during hyperglycemia and possible beneficial effect of cinnamic acid

3.1 Introduction

Cardiovascular complications are the major risk factors of diabetic patients (Pan et al., 2014; Cai et al., 2002). Patients with diabetes are susceptible to the development of DCM which is characterized in the early stages by diastolic dysfunction followed by systolic dysfunction in later stages (Kain et al., 2011; Liu et al., 2014; Matshela, 2016). Exposure to high glucose has been reported to diminish ischemic injury in isolated perfused hearts (Balteau et al., 2011). However, a more recent and large randomized trial questioned this result and failed to establish any beneficial effect of high glucose on mortality. Several lines of evidence indicate that hyperglycemia results in toxic effects in several cell types including cardiomyocytes (Kawahito et al., 2009). Hyperglycemia is a significant factor in cardiovascular damage, exerting its effects through multiple pathways including activation of oxidative stress, protein kinase C, glycation, hexosamine and polyol pathways (Preetha Rani et al., 2018). These pathways are in association with mitochondrial dysfunction, endoplasmic reticulum stress and ROS generation (Fiorentino et al., 2013). Oxidative stress, a significant cause of diabetic complications (Kain et al., 2011), results when there is an excess production of ROS relative to the levels of antioxidant enzymes and antioxidants (Kayama et al., 2015). The diminished endogenous antioxidant defense mechanisms like superoxide dismutase (SOD), catalase, and glutathione peroxidase or reduced concentrations of endogenous antioxidants like vitamin E, ascorbic acid, and glutathione (GSH) can increase the ROS levels (Kayama et al., 2015).

Excessive amounts of ROS in heart induce contractile dysfunctions and structural alterations (Tsutsui et al., 2011). In response to injury, cardiomyocytes also release certain biomarkers such as natriuretic peptides {atrial natriuretic peptide (ANP) and brain natriuretic peptide}, creatine kinase (Liquori et al., 2014), lactate dehydrogenase (LDH) (Bodor, 2016) etc. These biomarkers are very important as they can be used to monitor heart function.

Mitochondria are energy regulators in cardiac myocytes which play a critical role in energy transduction, signalling and cell death pathways (Verma et al., 2017) and any dysfunction in mitochondria profoundly affects the heart and is considered to be the underlying cause in the pathophysiology of DCM. Mitochondrial dysfunction is associated with the various pathological mechanisms that lead to heart failure (Schilling, 2015). The presence of damaged mitochondria in the diabetic hearts of many human subjects as well as in the animal models adds evidence to the current situation.

Alterations in mitochondrial transmembrane potential, mitochondrial dynamics, permeability transmembrane pore, mitochondrial content and overproduction of mitochondrial superoxides are some of the indicators of mitochondrial dysfunctions. The quality control mechanism in mitochondria is determined by their dynamic nature by which the mitochondria undergo constant fusion and fission. Mitochondrial fusion is mediated by fusion proteins such as mitofusins (MFN1 and 2) and optic atrophy 1 (OPA1). Fission protein 1 (FIS1) and dynamin related protein 1 (DRP1) are main players of mitochondrial fission (Ni et al., 2015). Fusion and fission processes play a very important role in the maintenance of important cellular functions including mitochondrial respiratory activity, apoptosis, and calcium signalling (Rovira-Llopis et al., 2017).

Calcium (Ca^{2+}) plays a very important role in the excitation contraction coupling of the myocardium and a normal calcium homeostasis should be maintained for proper cardiac function (Marín-García, 2010). Depolarisation of the cardiomyocytes results in the influx of a small amount of calcium ions via the L-type calcium channels. This triggers the opening of the ryanodine receptor of the sarcoplasmic reticulum (SR) which results in a massive release of calcium ions into the cytoplasm and thus triggering cardiomyocyte contraction (Orchard and Brette, 2008). Later these Ca^{2+} ions are removed from the cytoplasm by the reuptake of the same into the SR via sarco/ER Ca^{2+}-ATPase 2a (SERCA2a) and release of Ca^{2+} ions into the extracellular space via the Na^{+}/Ca^{2+}exchanger (Kanaporis and Blatter, 2017). In addition cytosolic calcium ions also enter the mitochondria through the mitochondrial calcium uniporter (MCUR1) located in the outer mitochondrial membrane. In the mitochondria calcium is essential for the functioning of the ETC complexes (I, II, and IV) and several enzymes like PDH, α-ketoglutarate dehydrogenase, and isocitrate dehydrogenase (Gollmer et al., 2020). Thus the main role of calcium in mitochondria is to ensure enough ATP for myocardial contraction (Brookes et al., 2004). However in the scenario of increased oxidative stress this balance is

disrupted and there will be an accumulation of cytoplasmic Ca^{2+} (calcium overload) which leads to heart failure.

Polyol pathway is another important mechanism by which hyperglycemia leads to redox status imbalance. It is a two-step process in which excess intracellular glucose is reduced to sorbitol by aldose reductase and sorbitol is further metabolized to fructose by sorbitol dehydrogenase. The conversion of glucose to sorbitol by aldose reductase is the rate limiting step in this reaction (Yan, 2018). This leads to a depletion of NADPH and NAD^+. The products of this pathway include sorbitol, fructose and NADH. Approximately 30 % glucose enters the polyol pathway in diabetes. Thus the polyol pathway is largely responsible for the NADH/NAD^+ redox imbalance and ultimately leads to the impairment of intracellular antioxidant defense mechanisms and causes oxidative stress (Oates, 2002; Safi et al., 2014).

Glucose inside a cell is normally metabolized to glucose - 6 - phosphate and then to fructose-6-phosphate during glycolysis. However in the presence of an enzyme GFAT (glutamine: fructose-6 phosphate amidotransferase) the fructose-6-phosphate is converted into UDP-N-acetyl glucosamine via the hexosamine biosynthetic pathway (HBP). UDP-N-acetyl glucosamine is a precursor of O-GlcNAc. In normal conditions approximately 2 to 5 % glucose flux passes through the HBP. The increase in O-GlcNAc is responsible for the acylation of various downstream proteins like thioredoxin interacting protein (TxNIP). HBP also plays an essential role in promoting cardiac hypertrophy and fibrosis.

One of the major outcomes of hyperglycemic oxidative stress in the heart is cardiomyocyte apoptosis (Das et al., 2009). All the above mentioned pathways ultimately end in inflammation causing upregulation of apoptotic factors. Apoptosis is the programmed cell death (Chen et al., 2020). Caspases are the key inducers of apoptosis (Huang et al., 2019). The two main pathways of apoptosis are intrinsic and the extrinsic pathways. The extrinsic pathway involves multiple ligands like TNF-α and Fas that binds to their respective receptors to trigger cell death. Whereas the intrinsic pathway involves mitochondrial proteins such as cytochrome c. It has been reported in diabetic animals that cardiomyocyte apoptosis leads to the loss of contractile tissue, remodeling and finally dysfunction (Cai et al., 2002). But the exact mechanisms by which hyperglycemia induces apoptosis in cardiomyocytes are not yet fully understood. Since DCM is still an

unmet need for the medical fraternity this information will pave a path for the identification of novel biochemical targets for therapeutic purposes.

Management of cardiovascular dysfunctions linked with diabetes has been a challenge for decades. Nowadays, the recent trend is the prevention of diabetic cardiovascular complications by a nutraceutical approach (Daftardar et al., 2014). India has been a hub for several types of edible spices and medicinal plants. These plants exhibit various beneficial pharmacological properties in addition to their nutritional value. Extensive research and development has produced many drugs against diabetes and associated complications. But none of them is effective for complete recovery. Moreover, some of them have adverse effects restricting their common use. In consideration of the excellent health-promoting effects, natural products have been regarded as important drug resources and served as remedies for thousands of years worldwide. Recent research has revealed the importance of bioactives from edible spices for the treatment of lifestyle-related diseases. Cinnamon is a culinary spice found abundantly in our area. Herein we have selected cinnamic acid (CiA), a bioactive from cinnamon for evaluation against hyperglycemia-induced apoptosis in H9c2 cells. It is reported to have antidiabetic (Lakshmi et al., 2009), cardioprotective (Song et al., 2013), anticancer (Niero and Machado-Santelli, 2013), anti-inflammatory and antioxidant properties (Yang et al., 2015).

3.2 Materials and Methods (please refer Chapter 2 for details)

- Estimation of cell viability by MTT and LDH assay.
- Quantification of ANP and sorbitol levels by ELISA.
- Studies on ROS, mitochondrial integrity (mitochondrial superoxides, transmembrane potential, mitochondrial content) and intracellular calcium levels by fluorescence imaging.
- Studies on apoptosis.
- Estimation of the activity of antioxidant enzymes, bioenergetics (Complex IV and ATP levels) by ELISA.
- Studies on proteins related to calcium homeostasis (MCUR1) and mitochondrial dynamics (OPA1, MFN2, DRP, FIS2).

Experimental groups consist of control (C; 5.5 mM glucose), high glucose (HG; 33 mM glucose), HG + metformin (Met; 1 mM), HG + cinnamic acid-100 nM (CiA1), HG + cinnamic acid-500 nM (CiA2), control + cinnamic acid-500 nM (C + CiA2 for toxicity evaluation).

3.3 Results

3.3.1 Effect of CiA on cell viability

In order to select an ideal dose of CiA, cell viability was checked with 100 nM, 500 nM, 1 μM, 10 μM and 50 μM of the same and we selected 100 nM and 500 nM based on the results (Fig. 3.1A).

3.3.2 Effect of CiA on HG induced cell death

Incubation of H9c2 cells with 33 mM glucose (HG) caused 24% cell death for 48 hrs of incubation. Interestingly CiA of 100 and 500 nM concentrations or metformin (1 mM) significantly ($p \leq 0.05$) improved (16.8 %, 21.4 % and 12.4 % respectively) cell viability compared to HG group (Fig. 3.1B).

3.3.3 LDH release detection

LDH analysis showed significant release ($p \leq 0.05$) of enzyme (44.8 %) to the medium in HG group compared to the control (18 %; Fig. 3.1C). While with CiA, LDH release was found to be lowered by 14.3 % and 20.8 % for 100 and 500 nM respectively compared to HG (Fig.3.1C). Metformin reduced LDH release by 40.5 % compared HG ($p \leq 0.05$; Fig. 3.1C).

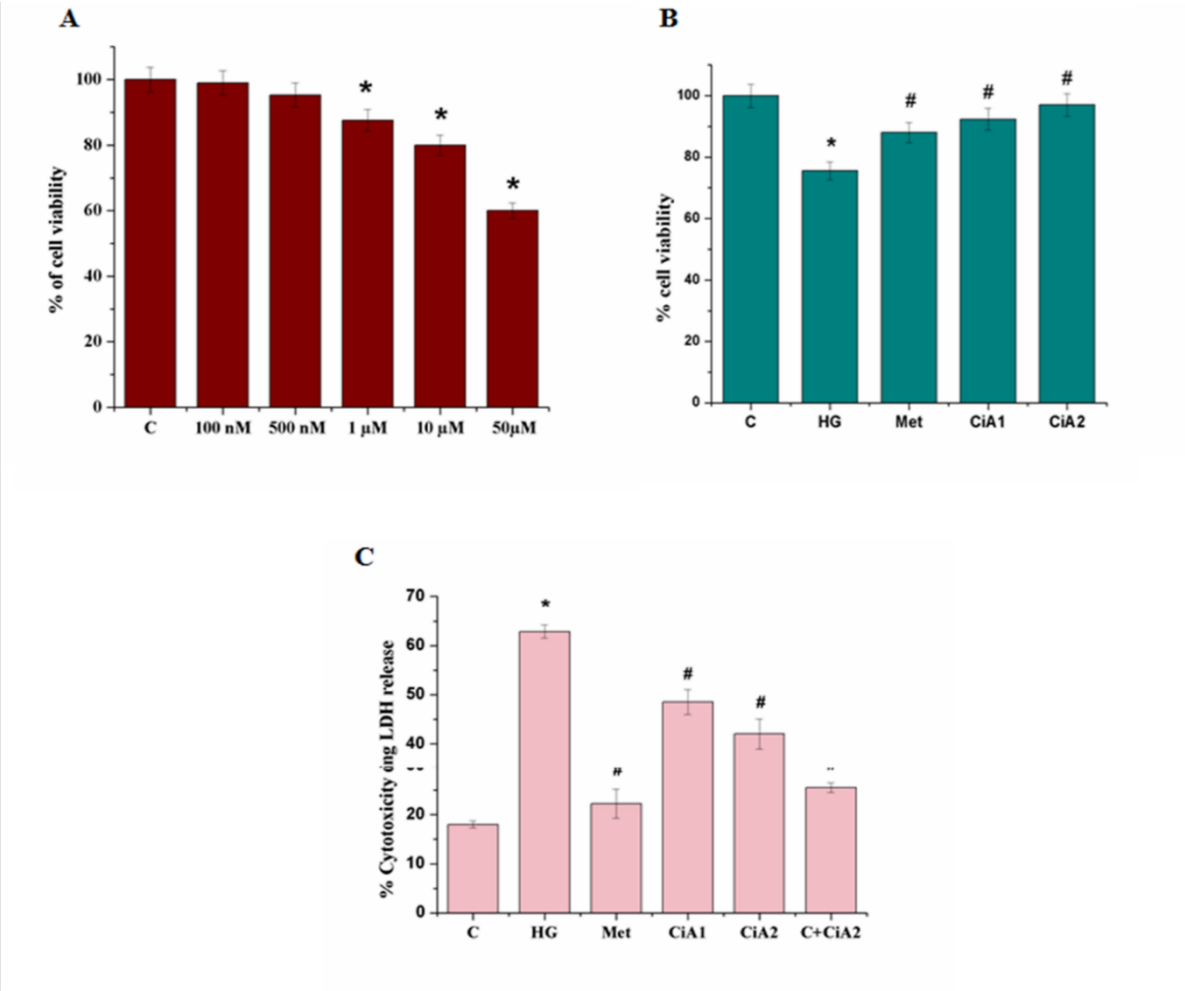

Fig. 3.1 Cell viability assessment. A) H9c2 cells were treated with different concentrations of cinnamic acid (100 nM, 500 nM, 1 µM, 10 µM, 50 µM) and viability was assessed by MTT assay. B) Cytotoxicity in H9c2 cells following treatment with 33 mM glucose and amelioration with cinnamic acid or metformin. C) Lactate dehydrogenase release during hyperglycemia with H9c2 cells and the effect of cinnamic acid or metformin. C - control, HG - high glucose treated group, Met - HG + metformin, CiA1 - HG + cinnamic acid (100 nM), CiA2 - HG + cinnamic acid (500 nM), C + CiA2 - control + cinnamic acid (500 nM). Values are expressed as mean ± SEM where n = 6. * $p \leq 0.05$ significantly different from the control group. # $p \leq 0.05$ significantly different from the HG treated group.

3.3.4 Detection of ANP

There was a significant increase ($p \leq 0.05$) in ANP levels in HG treated group (230 %; Fig. 3.2). Cotreatment with CiA at 100 nM and 500 nM reduced ANP levels significantly ($p \leq 0.05$) by 102.8 % and 212 % respectively compared to HG. Treatment with metformin also significantly ($p \leq 0.05$) reduced ANP levels by 210 % compared to HG treated groups (Fig. 3.2).

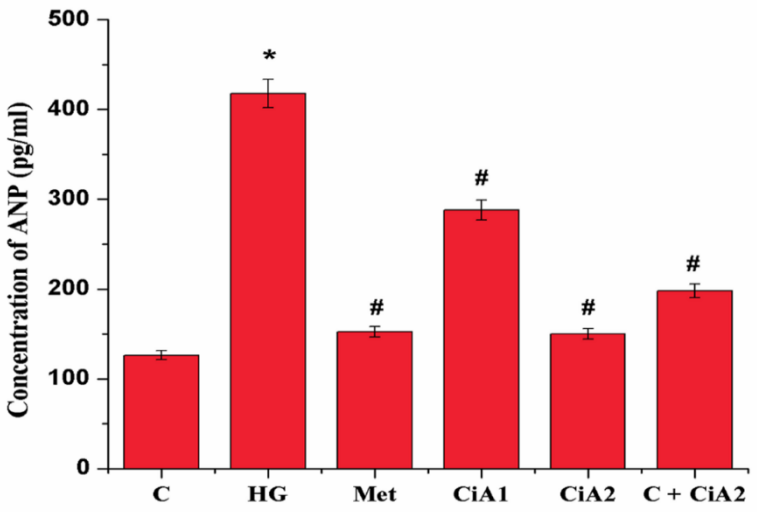

Fig. 3.2 Quantification of atrial natriuretic peptide during hyperglycemia. H9c2 cells were treated with high glucose (33 mM) for 48 hrs in the presence or absence of different doses of cinnamic acid or metformin. C - control, HG - high glucose treated group, Met - HG + metformin, CiA1 - HG + cinnamic acid (100 nM), CiA2 - HG + cinnamic acid (500 nM), C + CiA2 - control + cinnamic acid (500 nM). Values are expressed as mean ± SEM where n = 6. * $p \leq 0.05$ significantly different from the control group. # $p \leq 0.05$ significantly different from the HG treated group.

3.3.5 CiA reduces intracellular ROS generation

Significant generation of ROS ($p \leq 0.05$) was observed in cells treated with HG. Fluorimetry analysis showed 224% increase of fluorescence in HG treated cells compared to control (Fig. 3.3). CiA cotreatment at both concentrations (100 and 500 nM) showed a considerable decrease ($p \leq 0.05$) in the ROS generation (117 % and 128.8 %) respectively (Fig. 3.3). Treatment with metformin also significantly reduced ($p \leq 0.05$) ROS generation by 145.7 %. (Fig. 3.3).

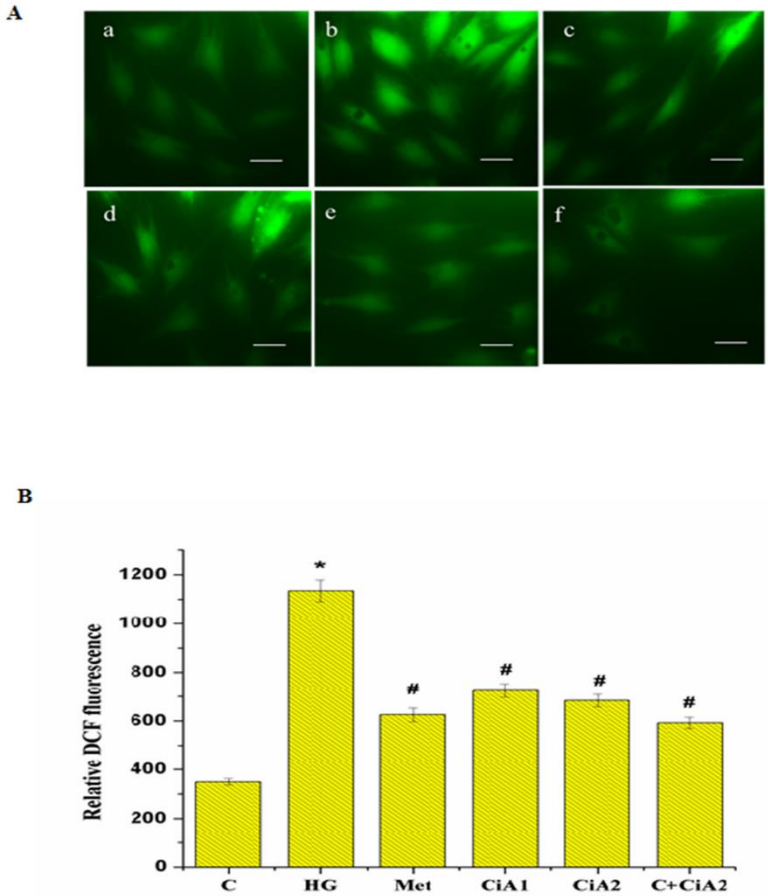

Fig. 3.3 Effect of cinnamic acid on reactive oxygen species generation in H9c2 cells. H9c2 cells were treated with high glucose (33 mM) for 48 hrs in the presence or absence of different doses of cinnamic acid or metformin. A) Reactive oxygen species accumulation in various groups determined by DCFH-DA staining; the representative images of ROS- induced fluorescence. (a) control, (b) high glucose treated group (HG), (c) HG + metformin, (d) HG + cinnamic acid (100 nM), (e) HG + cinnamic acid (500 nM), (f) control + cinnamic acid (500 nM). Scale bar corresponds to 100 μm. B) Relative fluorescent intensity of the fluorescent images. C - control, HG - high glucose treated group, Met - HG + metformin, CiA1 - HG + cinnamic acid (100 nM), CiA2 - HG + cinnamic acid (500 nM), C + CiA2 - control + cinnamic acid (500 nM). Values are expressed as mean ± SEM where n = 6. * $p \leq 0.05$ significantly different from the control group. # $p \leq 0.05$ significantly different from the HG treated group.

3.3.6 CiA restored antioxidant enzyme activity altered by HG

HG caused a significant decrease ($p \leq 0.05$) in SOD activity by 25.3% and cotreatment with CiA increased SOD activity by 8.74 % at 100 nM (not significant) and by 14.7 % ($p \leq 0.05$) at 500 nM compared with HG (Fig. 3.4A). Treatment with metformin also caused a significant increase (17.4 %) compared to HG (Fig. 3.4A). The total antioxidant capacity of the cells was also found to be significantly reduced ($p \leq 0.05$) in

HG (23.7%; Fig. 3.4B). While cotreatment with CiA (100 and 500 nM) or metformin (1 mM) prevented the depletion of total antioxidant status by 12.1 %, 17.6 % and 17.7 % respectively compared to HG (Fig. 3.4B).

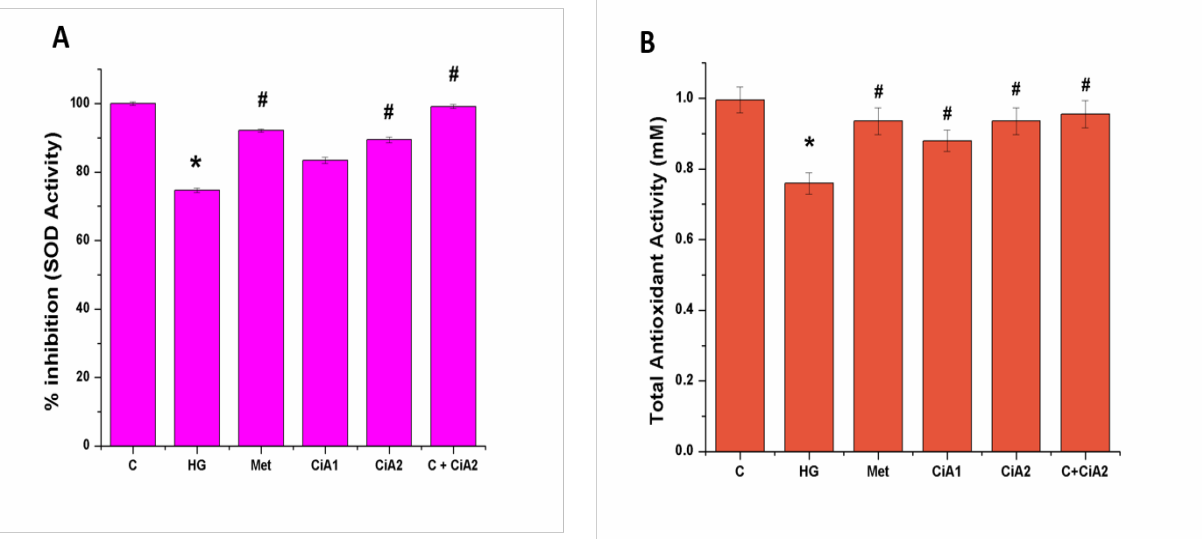

Fig. 3.4 High glucose depleted general innate antioxidant status and cinnamic acid reversed the alterations in endogenous antioxidant status in H9c2 cells. H9c2 cells were treated with high glucose (33 mM) for 48 hrs in the presence or absence of different doses of cinnamic acid or metformin. A) SOD activity B) Total antioxidant capacity. C - control, HG - high glucose treated group, Met - HG + metformin, CiA1 - HG + cinnamic acid (100 nM), CiA2 - HG + cinnamic acid (500 nM), C + CiA2 - control + cinnamic acid (500 nM). Values are expressed as mean ± SEM where n = 6. * $p \leq 0.05$ significantly different from the control group. # $p \leq 0.05$ significantly different from the HG treated group.

3.3.7 Estimation of total glutathione content and glutathione peroxidase activity

There was a significant decrease ($p \leq 0.05$) in total glutathione in HG group by 87.9 % (Fig. 3.5A). Here also treatment with CiA (100 and 500 nM) or metformin (1 mM) significantly ($p \leq 0.05$) increased glutathione content by 32.9 %, 65.9 % and 43.9 % respectively (Fig. 3.5A). Also the glutathione peroxidase activity was lowered ($p \leq 0.05$) by 49.9 % in HG group (Fig. 3.5B). Treatment with CiA at both concentrations increased the activity by 39.2 % and 32.1 % at 100 and 500 nM respectively (Fig. 3.5B). Treatment with metformin at 1 mM also increased the GPx activity by 46.3 % compared to the HG group (Fig. 3.5B).

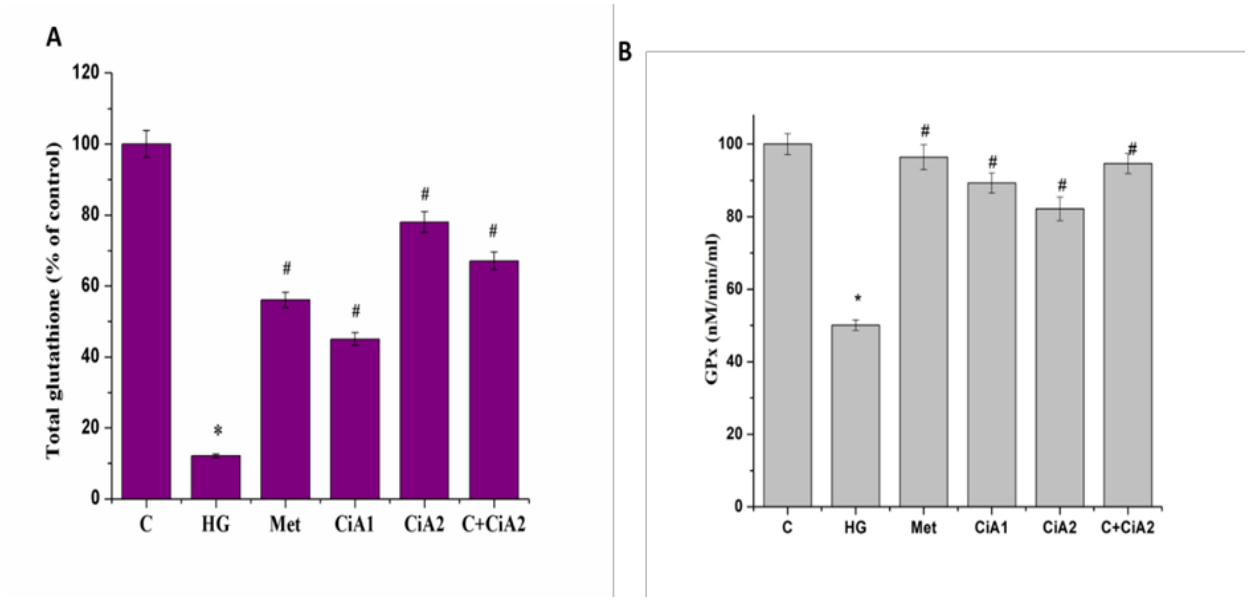

Fig. 3.5 High glucose lowered the total glutathione content and glutathione peroxidase activity. H9c2 cells were treated with high glucose (33 mM) for 48 hrs in the presence or absence of different doses of cinnamic acid or metformin. A) Total glutathione content B) Glutathione peroxidase activity. C - control, HG - high glucose treated group, Met - HG + metformin, CiA1 - HG + cinnamic acid (100 nM), CiA2 - HG + cinnamic acid (500 nM), C + CiA2 - control + cinnamic acid (500 nM). Values are expressed as mean ± SEM where n = 6. * $p \leq 0.05$ significantly different from the control group. # $p \leq 0.05$ significantly different from the HG treated group.

3.3.8 CiA prevented lipid peroxidation and reduced protein carbonyls in H9c2 cells

High glucose induction significantly increased ($p \leq 0.05$) lipid peroxidation (MDA level) by 554% compared to control (Fig. 3.6A). Cotreatment with CiA during hyperglycemia significantly reduced ($p \leq 0.05$) the MDA levels by 407 % (100 nM) and 554 % (500 nM) compared to HG (Fig. 3.6A). There was also a significant reduction ($p \leq 0.05$) of lipid peroxidation in metformin treated group (549 %) (Fig. 3.6A). Protein carbonyl formation was also significantly higher ($p \leq 0.05$) in HG (434.9 %) compared to control (Fig. 3.6B). Treatment with CiA at 100 and 500 nM or metformin lowered protein carbonyls by 264. 7 %, 412.1 % and 404.6 % respectively compared to HG (Fig. 3.6B)

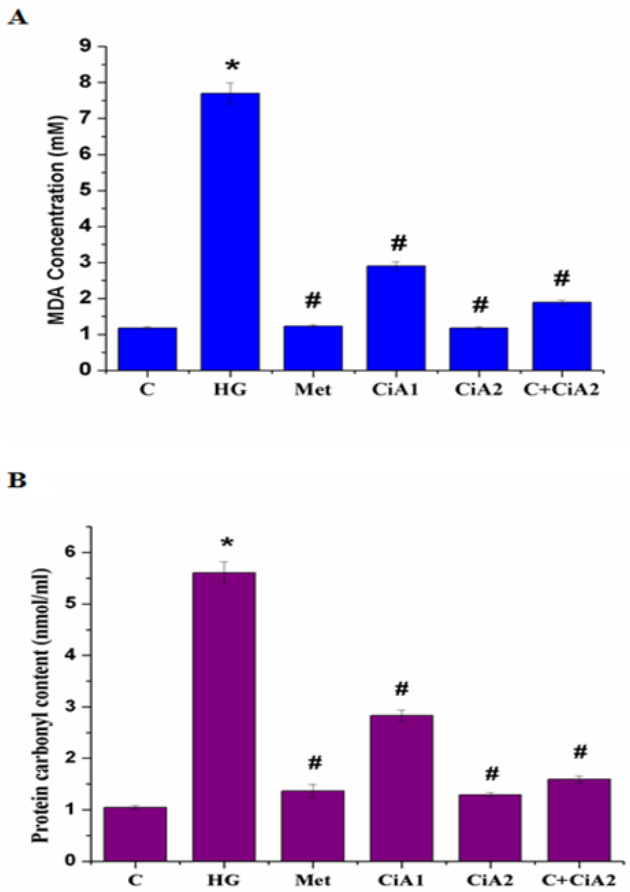

Fig. 3.6 Quantification of oxidative stress markers during hyperglycemia and reversal with cinnamic acid or metformin. H9c2 cells were treated with high glucose (33 mM) for 48 hrs in the presence or absence of different doses of cinnamic acid or metformin. A) Lipid peroxidation in H9c2 cells with high glucose and effect of cinnamic acid and metformin. B) Protein carbonyl content in cells treated with high glucose and cinnamic acid. C - control, HG - high glucose treated group, Met - HG + metformin, CiA1 - HG + cinnamic acid (100 nM), CiA2 - HG + cinnamic acid (500 nM), C + CiA2 - control + cinnamic acid (500 nM). Values are expressed as mean ± SEM where n = 6. * $p \leq 0.05$ significantly different from the control group. # $p \leq 0.05$ significantly different from the HG treated group.

3.3.9 Mitochondrial dysfunction during hyperglycemia and amelioration with CiA

3.3.9.1 Mitochondrial transmembrane potential

With HG, JC-1 green monomers were significantly increased ($p \leq 0.05$; 394.4 %; Fig. 3.7) compared to the control indicating a dissipation of ψm. Treatment with CiA prevented the dissipation of ψm which was evident with visibility of red fluorescence compared to HG (Fig. 3.7). Quantitatively, green fluorescence was decreased significantly ($p \leq 0.05$) by 378.5 % and 392.8 % for 100 and 500 nM compared to HG (Fig. 3.7). The

trend was the same with metformin too (Fig. 3.7) where intensity of green fluorescence (monomers) was reduced by 361.1 % ($p \leq 0.05$) and a shift to red fluorescence (aggregates) was observed (Fig. 3.7).

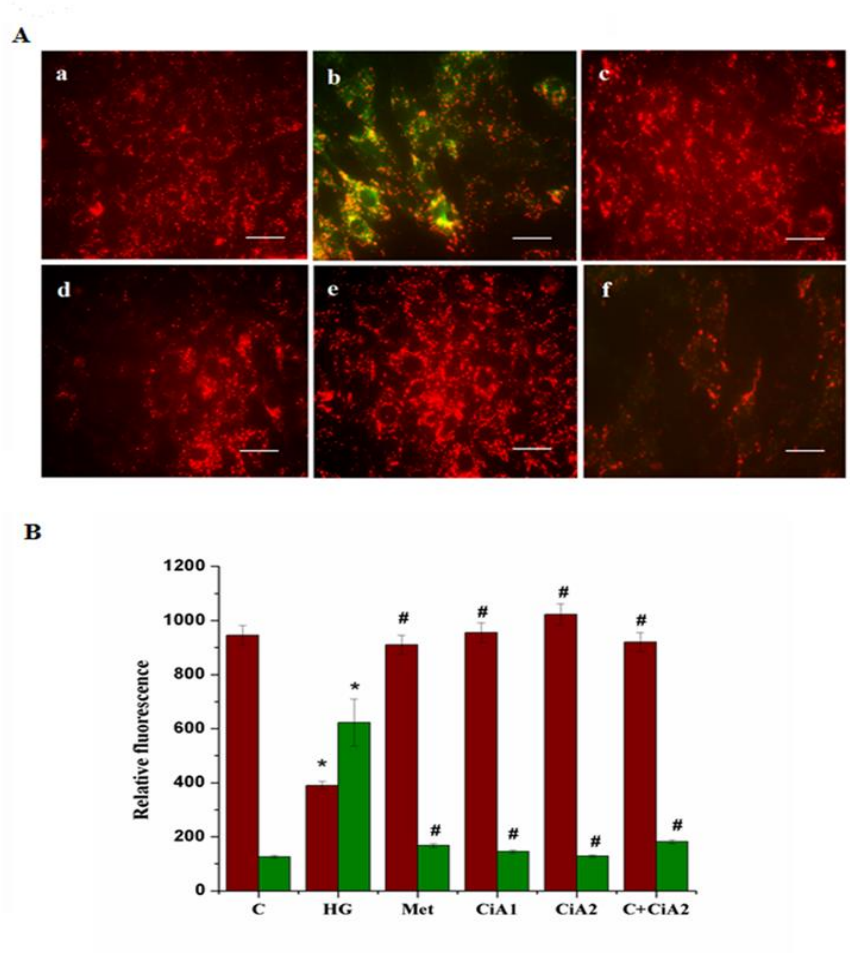

Fig. 3.7 Mitochondrial transmembrane potential changes determined by JC-1 staining. H9c2 cells were treated with high glucose (33 mM) for 48 hrs in the presence or absence of different doses of cinnamic acid or metformin. A) Fluorescent microscopic merged images of H9c2 cells. (a) control, (b) high glucose treated group (HG), (c) HG + metformin, (d) HG + cinnamic acid (100 nM), (e) HG + cinnamic acid (500 nM), (f) control + cinnamic acid (500 nM). Scale bar corresponds to 100 µm. B) Relative fluorescence intensities of mitochondrial transmembrane potential changes. C - control, HG - high glucose treated group, Met - HG + metformin, CiA1 - HG + cinnamic acid (100 nM), CiA2 - HG + cinnamic acid (500 nM), C + CiA2 - control + cinnamic acid (500 nM). Values are expressed as mean ± SEM where n = 6. * $p \leq 0.05$ significantly different from the control group. # $p \leq 0.05$ significantly different from the HG treated group.

3.3.9.2 Mitochondrial superoxide production

Alteration in superoxide generation was detected with Mitosox red. HG caused significant (481.6 %) generation of superoxides while CiA prevented the abnormal superoxide generation (Fig. 3.8). CiA (100 and 500 nM) prevented superoxide generation

significantly ($p \leq 0.05$) by 290 % and 330 % respectively (Fig. 3.8). Metformin treatment also significantly ($p \leq 0.05$) reduced the generation of superoxide radicals (409.3 %; Fig. 3.8).

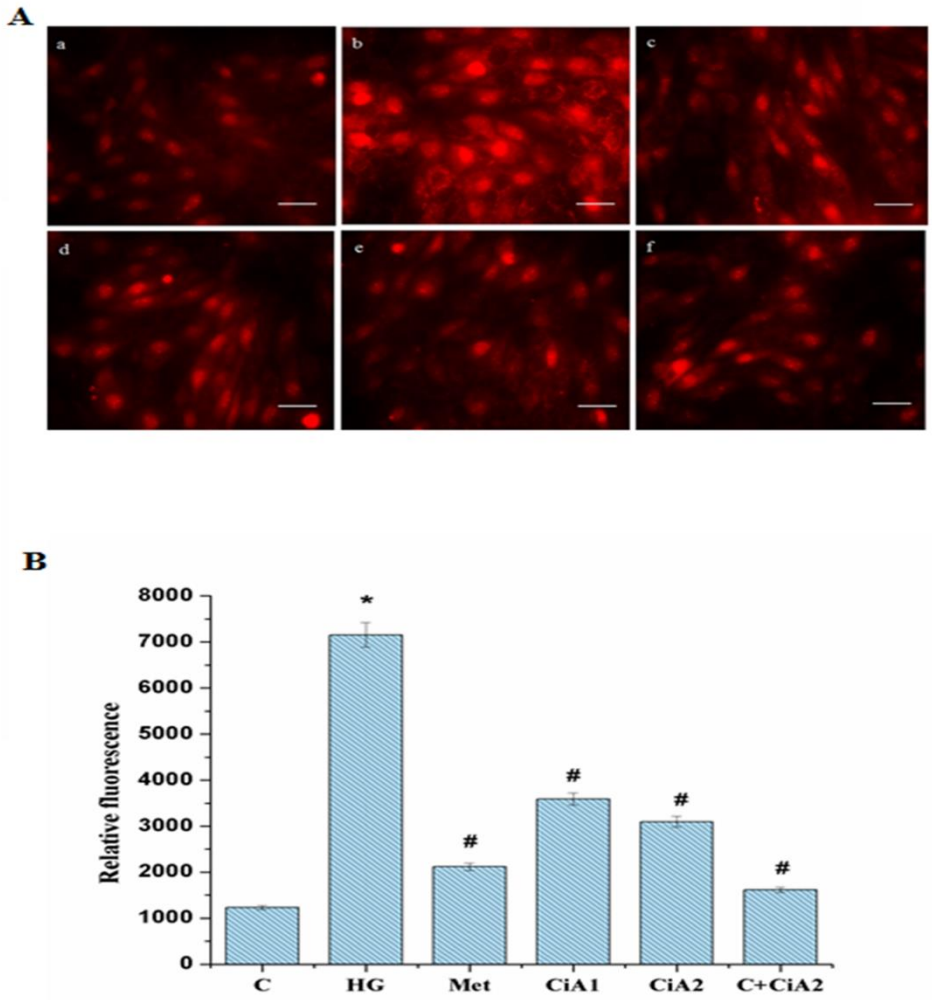

Fig. 3.8 Mitochondrial superoxide generation during hyperglycemia and amelioration with cinnamic acid and metformin. H9c2 cells were treated with high glucose (33 mM) for 48 hrs in the presence or absence of different doses of cinnamic acid or metformin. A) Representative images of mitochondrial superoxide generation in control and treated cells. (a) control, (b) high glucose treated group (HG), (c) HG + metformin, (d) HG + cinnamic acid (100 nM), (e) HG + cinnamic acid (500 nM), (f) control + cinnamic acid (500 nM). Scale bar corresponds to 100 μm. B) Relative fluorescent intensity of the fluorescent images. C - control, HG - high glucose treated group, Met - HG + metformin, CiA1 - HG + cinnamic acid (100 nM), CiA2 - HG + cinnamic acid (500 nM), C + CiA2 - control + cinnamic acid (500 nM). Values are expressed as mean ± SEM where n = 6. * $p \leq 0.05$ significantly different from the control group. # $p \leq 0.05$ significantly different from the HG treated group.

3.3.9.3 Mitochondrial Content

Mitochondrial content was assessed using mitotracker red. In HG treated H9c2 cells, the mitochondrial content was found to be significantly ($p \leq 0.05$) lowered by 50.9 % when compared to the control group (Fig. 3.9). In CiA treated cells the mitochondrial content was significantly ($p \leq 0.05$) restored by 31 % and 34.4 % respectively at 100 and 500 nM respectively (Fig. 3.9). Metformin treatment also increased ($p \leq 0.05$) the mitochondrial content by 49.4 % when compared to the HG treated group (Fig. 3.9).

A

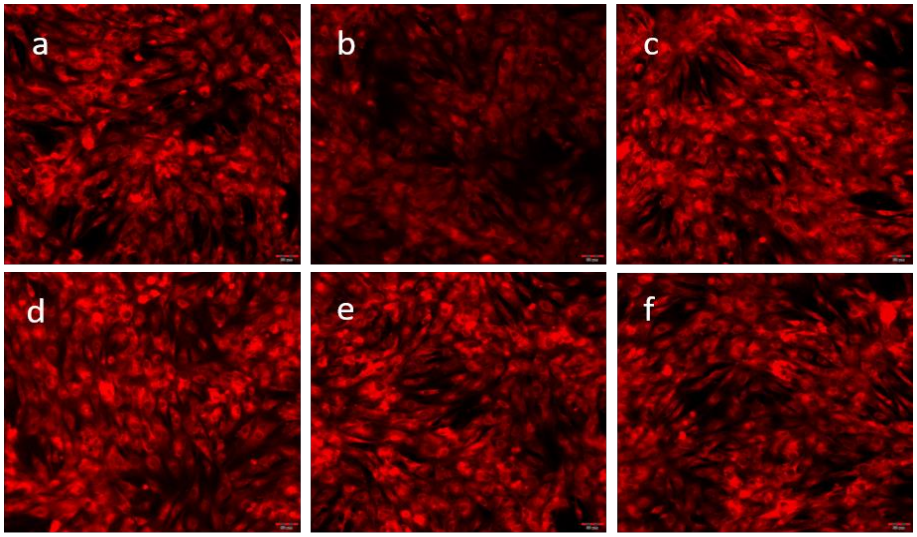

B

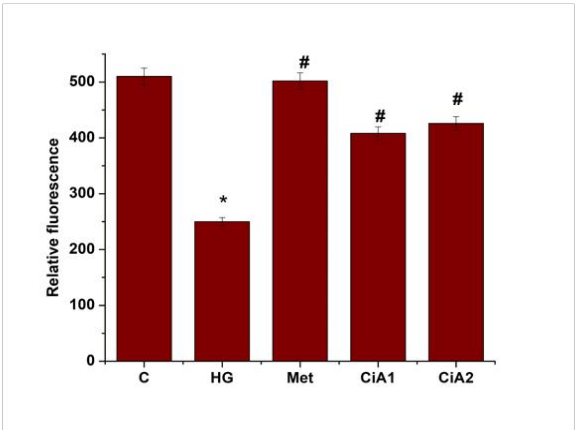

Fig. 3.9 Mitochondrial content during hyperglycemia and restoration of the same with cinnamic acid and metformin. H9c2 cells were treated with high glucose (33 mM) for 48 hrs in the presence or absence of different doses of cinnamic acid or metformin. A) Representative images of mitochondrial content in control and treated cells. (a) control, (b) high glucose treated group (HG), (c) HG + metformin, (d) HG + cinnamic acid (100 nM), (e) HG + cinnamic acid (500 nM), (f) control + cinnamic acid (500 nM). Scale bar corresponds to 50 μm. B) Relative fluorescent intensity of the fluorescent images. C - control, HG - high glucose treated group, Met - HG + metformin, CiA1 - HG + cinnamic acid (100 nM), CiA2 - HG + cinnamic acid (500 nM), C + CiA2 - control + cinnamic acid (500 nM). Values are expressed as mean ± SEM where n = 6. * $p \leq 0.05$ significantly different from the control group. # $p \leq 0.05$ significantly different from the HG treated group.

3.3.9.4 Expression of mitochondrial fission and fusion proteins by western blot analysis

There was also a significant decrease in the expression of mitochondrial fusion proteins OPA1 and MFN2 by 32.8 % and 38.9 % ($p \leq 0.05$; Fig. 3.10) and increased expression of fission proteins DRP1 and FIS1 by 35.2 % and 19.5% in HG treated group (Fig. 3.10). Treatment with CiA at both concentrations (100 and 500 nM) significantly ($p \leq 0.05$) increased the expression of OPA1 by 32.26 % and 26.9 % which is not dose dependent; and MFN2 by 22.7 % and 25.2 % (Fig. 3.10). Also CiA significantly ($p \leq 0.05$) reduced the expression of DRP1 by 29.5 % and 32.9 %; and FIS1 by 16.1 % and 21.7 % respectively compared to the HG treated groups (Fig. 3.10). Treatment with metformin also significantly ($p \leq 0.05$) increased the expression of OPA1 and MFN2 by 32.7 % and 17.9 % respectively and decreased the expression of DRP1 and FIS1 by 15.5 % and 10.3 % compared to HG treated group (Fig. 3.10).

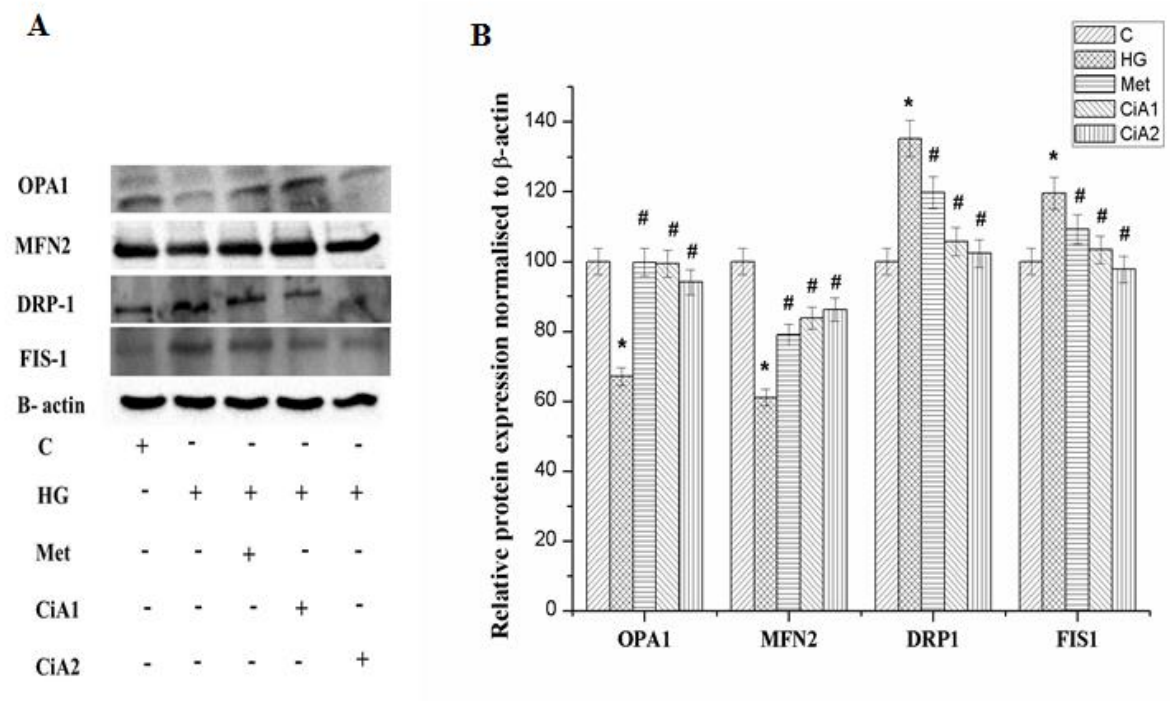

Fig. 3.10 Effect of cinnamic acid on high glucose induced alterations in mitochondrial dynamics in H9c2 cells. H9c2 cells were treated with high glucose (33 mM) for 48 h in the presence or absence of different doses of cinnamic acid or metformin. A) Representative immunoblot of OPA1, MFN2, DRP1 and FIS1 B) Densitometric quantification of western blot of protein level normalized to β actin. * $p \leq 0.05$ significantly different from the control group. # $p \leq 0.05$ significantly different from the HG treated group.

3.3.9.5 Complex IV activity

The activity of complex IV of the electron transport chain was found to be significantly ($p \leq 0.05$) lowered in the HG treated H9c2 cells by 54.5 % when compared to the control (Fig. 3.11). Cotreatment with CiA at 100 and 500 nM significantly ($p \leq 0.05$) increased their activity by 27.2 % and 45.4 % respectively and metformin at 1 mM also significantly ($p \leq 0.05$) increased the activity of the enzyme by 9 % when compared to the diabetic group (Fig. 3.11).

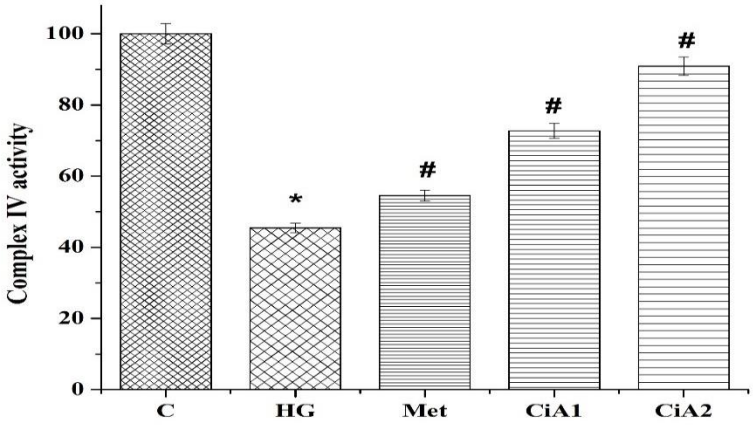

Fig. 3.11 Effect of cinnamic acid on high glucose induced alterations in oxidative phosphorylation. H9c2 cells were treated with high glucose (33 mM) for 48 hrs in the presence or absence of different doses of cinnamic acid or metformin. C - control, HG - high glucose treated group, Met - HG + metformin, CiA1 - HG + cinnamic acid (100 nM), CiA2 - HG + cinnamic acid (500 nM). Values are expressed as mean ± SEM where n = 6. * $p \leq 0.05$ significantly different from the control group. # $p \leq 0.05$ significantly different from the HG treated group.

3.3.9.6 Determination of ATP content in the HG treated H9c2 cells

ATP production was found to be significantly ($p \leq 0.05$) lowered by 45.4 % compared to control group (Fig. 3.12). Cotreatment with CiA at 100 and 500 nm increased the ATP levels significantly ($p \leq 0.05$) by 14.8 % and 25.3 % respectively when compared to the HG treated group (Fig. 3.12). Similarly metformin treatment also significantly ($p \leq 0.05$) increased ATP production by 26.9 % when compared to the HG treated group (Fig. 3.12).

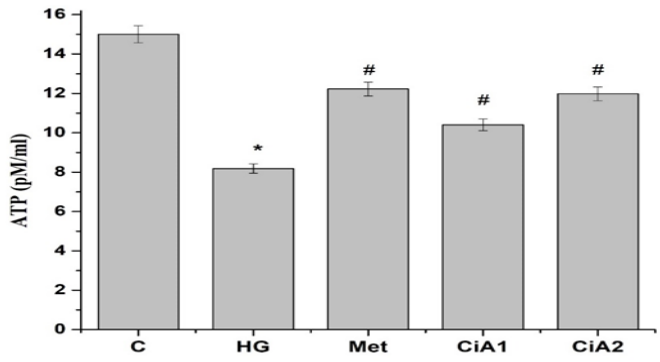

Fig. 3.12 ATP content in H9c2 cells during hyperglycemia. H9c2 cells were treated with high glucose (33 mM) for 48 hrs in the presence or absence of different doses of cinnamic acid or metformin. C - control, HG - high glucose treated group, Met - HG + metformin, CiA1 - HG + cinnamic acid (100 nM), CiA2 - HG + cinnamic acid (500 nM). Values are expressed as mean ± SEM where n = 6. * $p \leq 0.05$ significantly different from the control group. # $p \leq 0.05$ significantly different from the HG treated group.

3.3.10 Ca^{2+} overload

Hyperglycemia induced intracellular calcium overload significantly ($p \leq 0.05$) in H9c2 cells, which was evident from increased blue fluorescence of Fura-2AM (212.7 %) compared to control group (Fig. 3.13A & B). Cotreatment with CiA (100 and 500 nM) or metformin significantly ($p \leq 0.05$) reduced calcium overload by 159.8 %, 172.5 % and 183.3 % respectively compared to HG (Fig. 3.13A & B). Similarly the expression of MCUR1 was found to be significantly ($p \leq 0.05$) downregulated in HG treated H9c2 cells by 39.8% compared to the control group (Fig. 3.13C). Cotreatment with CiA and metformin restored their levels significantly ($p \leq 0.05$) by 26.2%, 30.6 % and 32.7 % at 100 nM, 500 nM, and 1 mM respectively (Fig. 3.13C).

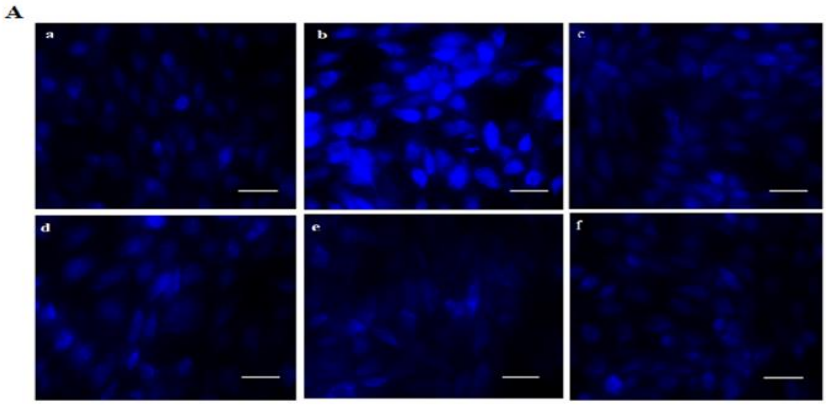

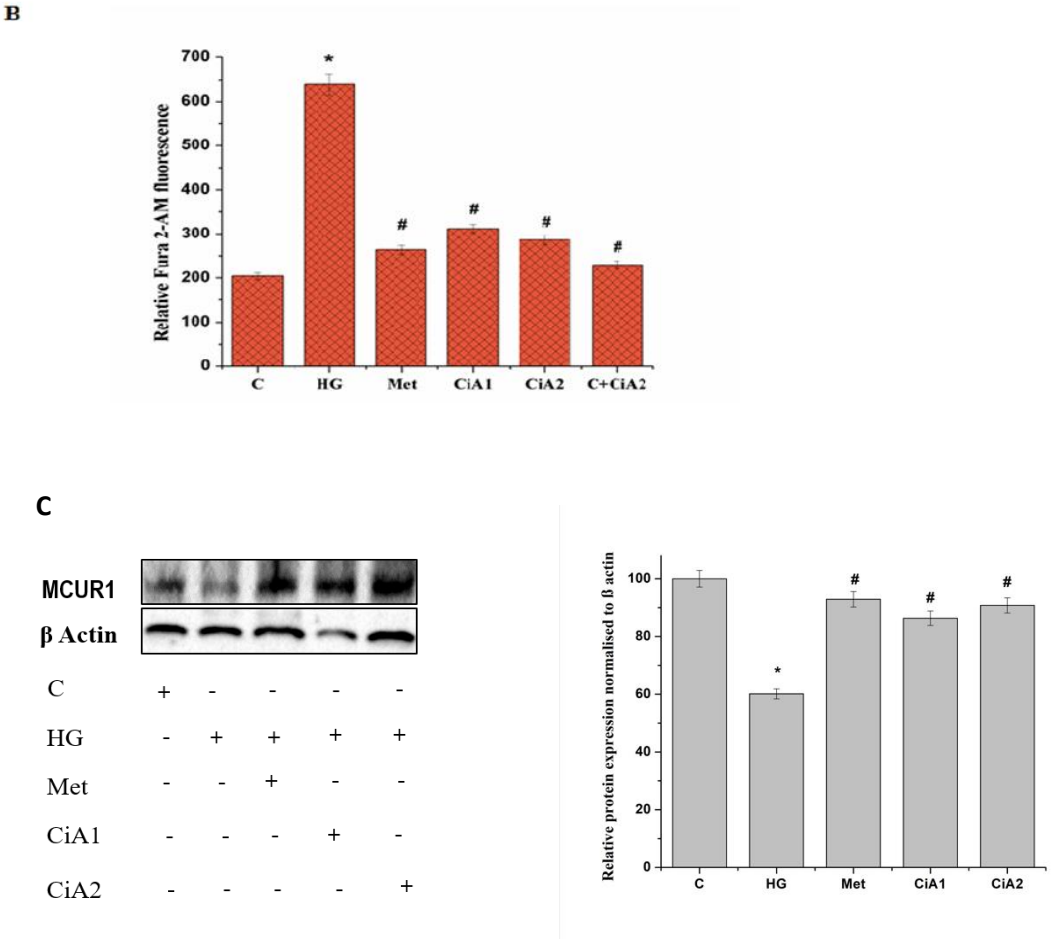

Fig. 3.13 Intracellular calcium overload during hyperglycemia with H9c2 cells determined by Fura 2AM staining. H9c2 cells were treated with high glucose (33 mM) for 48 hrs in the presence or absence of different doses of cinnamic acid or metformin. A) Representative images of intracellular calcium ion accumulation in control and treated cells. (a) control, (b) high glucose treated group (HG), (c) HG + metformin, (d) HG + cinnamic acid (100 nM), (e) HG + cinnamic acid (500 nM), (f) control + cinnamic acid (500 nM). Scale bar corresponds to 100 µm. B) Relative fluorescent intensity of the fluorescent images. C) Representative immunoblot of MCUR1 and its densitometric quantification. C - control, HG - high glucose treated group, Met - HG + metformin, CiA1 - HG + cinnamic acid (100 nM), CiA2 - HG + cinnamic acid (500 nM), C + CiA2 - control + cinnamic acid (500 nM). Values are expressed as mean ± SEM where n = 6. * $p \leq 0.05$ significantly different from the control group. # $p \leq 0.05$ significantly different from the HG treated group.

3.3.11 Sorbitol production during hyperglycemia

There was a significant increase ($p \leq 0.05$, 31.9%; Fig. 3.14) in sorbitol levels with HG compared to control. Treatment with CiA at both concentrations (100 and 500 nM) lowered sorbitol levels significantly ($p \leq 0.05$) by 29.7 % and 42.5 % respectively

compared to HG (Fig. 3.14). Metformin also significantly ($p \leq 0.05$) reduced sorbitol levels by 27.6 % from HG treated group (Fig. 3.14).

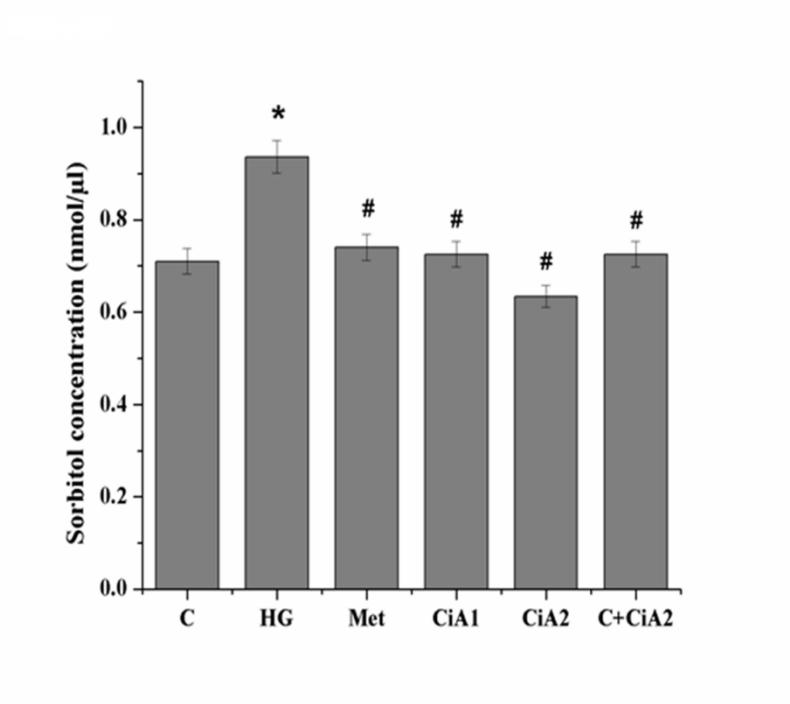

Fig. 3.14 Sorbitol levels in high glucose treated H9c2 cells and amelioration with cinnamic acid. H9c2 cells were treated with high glucose (33 mM) for 48 hrs in the presence or absence of different doses of cinnamic acid or metformin. C - control, HG - high glucose treated group, Met - HG + metformin, CiA1 - HG + cinnamic acid (100 nM), CiA2 - HG + cinnamic acid (500 nM), C + CiA2 - control + cinnamic acid (500 nM). Values are expressed as mean ± SEM where n = 6. * $p \leq 0.05$ significantly different from the control group. # $p \leq 0.05$ significantly different from the HG treated group.

3.3.12 Hyperglycemia increases the hexosamine biosynthetic pathway flux

The end product of hexosamine biosynthetic pathway, O-GlcNAc was found to be significantly ($p \leq 0.05$) upregulated in HG treated H9c2 cells by 62.9 % when compared to the control group (Fig. 3.15). While treatment with CiA downregulated the levels of O-GlcNAc significantly ($p \leq 0.05$) by 27.2 % and 100 % at 100 and 500 nM respectively (Fig. 3.15). Metformin treated cells also showed a significant ($p \leq 0.05$) decrease in the levels of O-GlcNAc significantly by 106.1 % at 1 mM (Fig. 3.15).

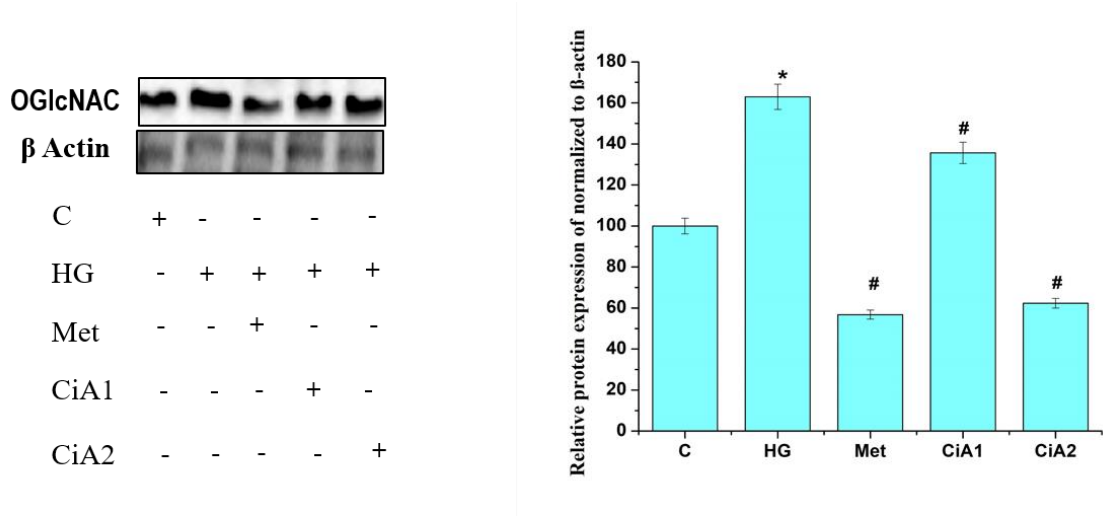

Fig. 3.15 O-GlcNAc levels in high glucose treated H9c2 cells and amelioration with cinnamic acid. H9c2 cells were treated with high glucose (33 mM) for 48 hrs in the presence or absence of different doses of cinnamic acid or metformin. Representative immunoblot of O-GlcNAc and their densitometric quantification. C - control, HG - high glucose treated group, Met - HG + metformin, CiA1 - HG + cinnamic acid (100 nM), CiA2 - HG + cinnamic acid (500 nM), C + CiA2 - control + cinnamic acid (500 nM). Values are expressed as mean ± SEM where n = 6. * $p \leq 0.05$ significantly different from the control group. # $p \leq 0.05$ significantly different from the HG treated group.

3.3.13 Caspase-3 activity assay

Apoptosis was detected by fluorimetric assay of caspase-3. The activity of caspase-3 under high glucose conditions was found to be enhanced ($p \leq 0.05$) by 137% (Fig. 3.16A) whereas cotreatment with CiA was effective in reducing the activity significantly ($p \leq 0.05$) by 108.2 % and 132.4 % for 100 and 500 nM respectively (Fig. 3.16A) and 136.8 % for 1 mM metformin (Fig. 3.16A). In addition protein expression revealed that HG induction caused a significant increase ($p \leq 0.05$) in pro-apoptotic marker protein - Bax (93.6 %) and decreased anti-apoptotic marker protein Bcl-2 by 62.4 % (Fig. 3.16B & C). Cotreatment with CiA prevented the increase of pro-apoptotic protein Bax significantly ($p \leq 0.05$) by 37.1 % and 52.3 % for 100 and 500 nM respectively and decrease ($p \leq 0.05$) of anti-apoptotic protein Bcl-2 by 20.4 % and 21.1 % for 100 and 500 nM respectively (Fig. 3.16B & C). Treatment with metformin also significantly prevented the increase of Bax (28 %) and decrease of Bcl-2 (37.9 %) compared to HG (Fig. 3.16B & C).

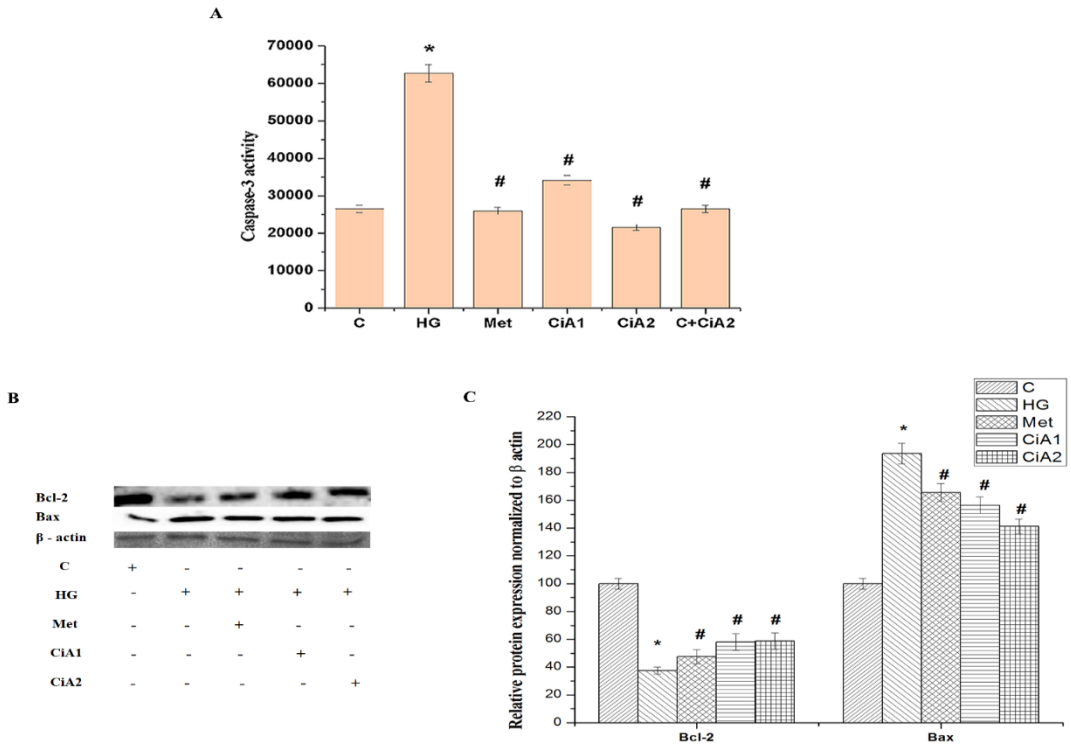

Fig. 3.16 Evaluation of apoptosis in H9c2 cells during hyperglycemia. H9c2 cells were treated with high glucose (33 mM) for 48 hrs in the presence or absence of different doses of cinnamic acid or metformin. A) Caspase-3 activity during hyperglycemia. B) Representative immunoblots of Bax and Bcl-2. C) Densitometric quantification of western blot of protein level normalized to beta actin. C - control, HG - high glucose treated group, Met - HG + metformin, CiA1 - HG + cinnamic acid (100 nM), CiA2 - HG + cinnamic acid (500 nM), C + CiA2 - control + cinnamic acid (500 nM). Values are expressed as mean ± SEM where n = 6. * $p \leq 0.05$ significantly different from the control group. # $p \leq 0.05$ significantly different from the HG treated group.

3.3.14 Flow cytometric analysis with annexin / PI

Flow cytometry results of double staining with annexin V-FITC and PI was interpreted as follows: the upper left quadrant - primary necrotic cells, the upper right - late apoptotic or secondary necrotic cells, the lower left quadrant - viable or live cells and the lower right quadrant - cells with early apoptosis. The results showed that in control cells, 90.5 % of the cells were viable, and 1.8 % was in late apoptosis or dead cells (Fig. 3.17). In cells treated with HG only 47.4 % cells were viable and 44 % cells were in late apoptosis (Fig. 3.17). Treatment with CiA (100 and 500 nM) or metformin increased the

percentage of viable cells by 54.6 %, 54.9 % and 56 % respectively compared to the HG treated group (Fig. 3.17). Also, the percentage of cells undergoing late apoptosis were reduced by 39 %, 38.6 % and 36 % respectively compared to the HG treated group for CiA at both concentrations and metformin (Fig. 3.17).

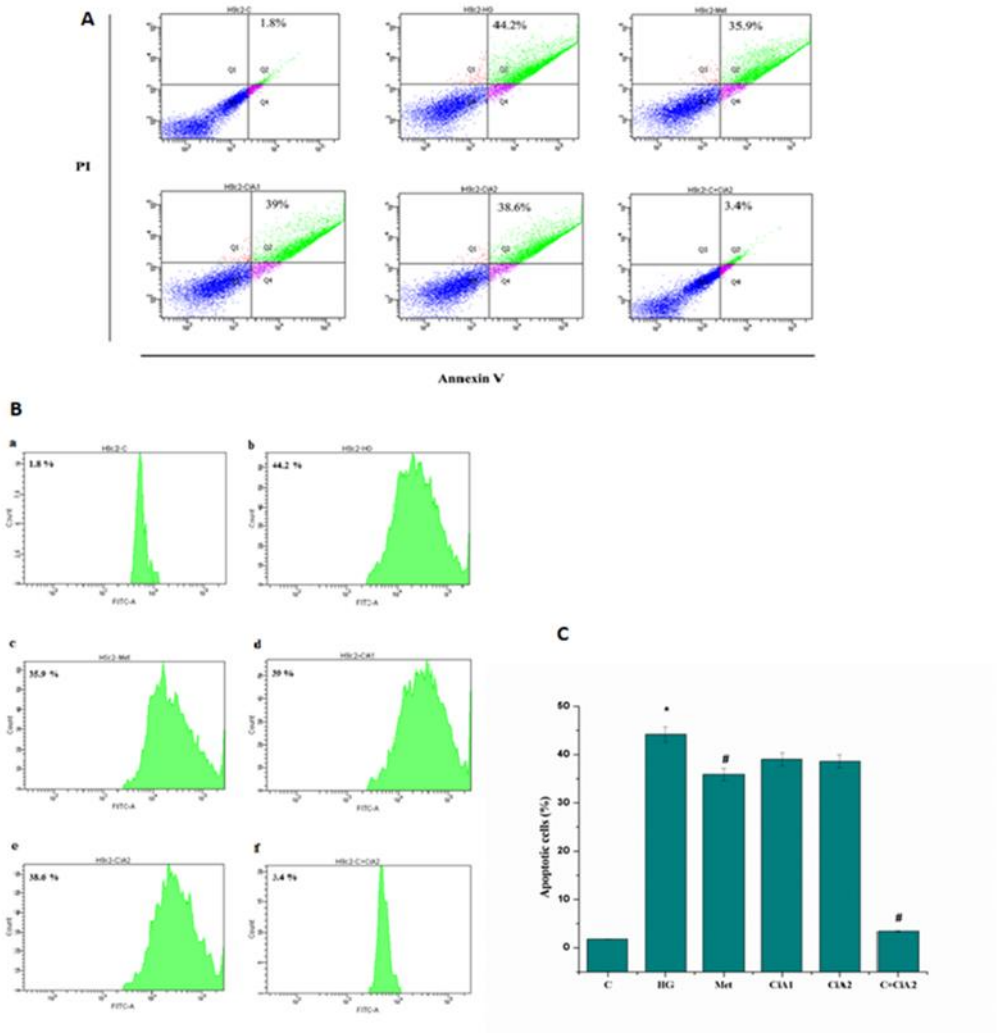

Fig. 3.17 Detection of apoptosis by annexin V-FITC/ PI double staining. H9c2 cells were treated with high glucose (33 mM) for 48 hrs in the presence or absence of different doses of cinnamic acid or metformin. A) Flow cytometric scatter graph showing different quadrants: the upper left quadrant represents primary necrotic cells, the upper right quadrant represents late apoptotic or secondary necrotic cells, the lower left quadrant represents viable or live cells and the lower right quadrant represents cells with early apoptosis. B) The representative histogram showing cells stained with Annexin V-FITC (a) control, (b) high glucose treated group (HG), (c) HG + metformin, (d) HG + cinnamic acid (100 nM), (e) HG + cinnamic acid (500 nM), (f) control + cinnamic acid (500 nM). C) Statistical analysis of flow cytometry results. Values are expressed as mean ± SEM where n = 6. * $p \leq 0.05$ significantly different from the control group. # $p \leq 0.05$ significantly different from the HG treated group.

3.4 Discussion

Cardiovascular diseases are the leading cause of morbidity and mortality in diabetic patients. Emerging evidence from experimental, pathological, epidemiological and clinical studies has shown that diabetes mellitus causes cardiac functional and structural changes leading to heart failure (Spector, 1998). Hyperglycemic shock in H9c2 cells is visible with a decrease in cell viability and increase in LDH release. LDH is a soluble enzyme found in the cytoplasm of many cells. It is released into the bloodstream upon plasma membrane damage thus an indicator of cytotoxicity. Various isoforms of LDH are present. Among them LDH-1 and 2 are present in the heart, kidneys, brain and erythrocytes. LDH-3 & 4 are found in the liver and skeletal muscles (Aydin et al., 2019; Heinova et al., 1999; Patibandla et al., 2020). In addition the LDH-3 is an isoform in the lungs. Natriuretic peptides have emerged as potential biomarkers of cardiovascular diseases. Natriuretic peptides increase the excretion of sodium by the kidneys. ANP and BNP are the two important natriuretic peptides with respect to the heart function. ANP is produced by the atrial muscles of the heart in response to stretch (Baba et al., 2019). DCM was confirmed with up-regulation of LDH and ANP and cotreatment with CiA and metformin reduced their levels significantly.

Oxidative stress occurs when there is an imbalance between the reactive oxygen species generation and innate antioxidant defense mechanism. They are known to play an essential role in the progression of diabetes and related complications. There are many ways by which ROS exerts its detrimental effects. ROS oxidises the cellular proteins and lipids thus generating protein carbonyls and lipid peroxides respectively (Bugger and Abel, 2014). They also react with nitric oxide to form reactive nitrogen species. Another major target of ROS is mitochondrial DNA. Thus, the products of oxidative stress can damage cellular molecules, DNA, proteins, and lipids leading to cell dysfunctions (Matteucci and Giampietro, 2000). The endogenous antioxidant defense systems include enzymes like SOD, glutathione peroxidase, glutathione reductase, catalase and other non-enzymatic antioxidants (Giacco and Brownlee, 2010). There was a surplus generation of ROS as well as depletion of innate antioxidant enzymes like SOD, glutathione peroxidase and a decrease in total antioxidant activity and reduced glutathione levels in the hyperglycemic group. Furthermore, oxidative stress markers like MDA and protein carbonyl content were also found to be increased. These results reveal that hyperglycemia alters the redox status of H9c2 cells. CiA was found to be effective in

suppressing the ROS generation and restoring the antioxidant status in HG-treated cardiomyocytes.

The presence of high blood glucose level activates all the possible pathways required for glucose removal. Polyol pathway is one such pathway (Chung and Chung, 2005). It has been reported that aldose reductase enzyme exhibits certain cardioprotective properties in hypertrophied hearts by facilitating the removal of reactive aldehydes (Tran and Wang, 2019). In the absence of diabetes, polyol pathway remains inactive (Fantus, 2002). The excess NADH produced as a result of the polyol pathway disrupts the redox balance between NADH and NAD+ and overloads the mitochondrial electron transport chain and results in the overproduction of ROS (Luo et al., 2015). Surplus mitochondrial superoxide observed in the present study is most probably via NADH mediated oxidative stress. Besides, NADPH plays a significant role in maintaining the intracellular antioxidant defense by facilitating generation of GSH from GSSG (Yan et al., 2002). Overconsumption of NADPH by the polyol pathway during hyperglycemia impairs the function of glutathione reductase further intensifying cellular redox imbalance (De Mattia et al., 1994). The significant increase in the levels of sorbitol and depletion of GSH observed in the present study is expected to amplify the redox status alteration with hyperglycemia. However, CiA cotreatment effectively reduced the sorbitol accumulation.

Cardiomyocytes are enriched with 30 to 40 % mitochondria in order to meet their energy demand. Approximately 8 % of the total ATP of the body is consumed by the heart (Gollmer et al.,2020). Under normal situations the bulk of ATP in the heart is obtained from the beta oxidation of fatty acids taking place in mitochondria and the remaining contributed by glucose, amino acids, lactate and ketone bodies. The substrate shift from fatty acids to glucose is a major factor responsible for the development of pathogenesis of DCM. Mitochondrial dysfunction is also responsible for inducing insulin resistance in skeletal muscle, adipose tissue and pancreatic β cells (Morino et al., 2006). It is the major source of ROS in most cells. Besides, mitochondria are essential for numerous cellular functions including repair, revival, and apoptosis. The mitochondrial membrane potential is an indicator of mitochondrial membrane integrity. The membrane potential is highly negative due to the chemiosmotic gradient of protons across the inner mitochondrial membrane. The maintenance of the transmembrane potential is essential for functions like ATP synthesis and calcium uptake into mitochondria by the Ca^{2+} uniporter (Skarka

and Ostadal, 2002). Fluorescence imaging revealed dissipation of transmembrane potential with hyperglycemia (Flarsheim et al., 1996; Bugger and Abel, 2010). This is a relevant biomarker for oxidative stress (Korshunov et al, 1997). Cotreatment with CiA or metformin was effective in preventing the dissipation of membrane potential.

Mitochondria are dynamic organelles with the ability to fuse (fusion) and divide (fission), continuously undergoing a change in the tubular networks in most eukaryotic cells for its optimum metabolic function (Fig. 18). This is essential for the proper distribution and localisation of mitochondria within cells (Rovira-Llopis et al., 2017). In addition, the balance between fission and fusion is required for maintaining various functions of mitochondria like mitochondrial respiratory activity, cell survival and calcium signalling. Fission generates small individual mitochondria while fusion results in the formation of large interconnected networks of mitochondria (Ferree and Shirihai, 2012). There are two forms of fusion: transient and complete fusion. Transient fusion involves fusion of outer mitochondrial membranes and complete fusion involves fusion of both the outer and inner membranes (Twig et al., 2006). The proteins that are involved in fission/fusion processes are mainly dynamin related GTPases. The outer mitochondrial membrane fusion is mediated by MFN1/2 whereas OPA1 regulates the inner mitochondrial membrane fusion and also maintains mitochondrial cristae structure (Otera and Mihara, 2011). There are reports in mice suggesting that genetic ablation of fusion proteins results in alterations in glucose homeostasis and induced insulin resistance and obesity (Quirós et al., 2012). There was an overexpression of fission proteins FIS1 and DRP1 aggravating fission and downregulation of fusion proteins OPA1 and MFN2. Oxidative stress has been reported to induce imbalance in mitochondrial dynamics (Ong and Hausenloy, 2010; Yoon et al., 2011). Alterations in mitochondrial dynamics is a major focus recently due to their involvement in cell death (Karbowski and Youle, 2003). It has also been reported that elevated levels of ROS during hyperglycemia also induces mitochondrial fragmentation (Rovira-Llopis et al., 2017; Wang et al., 2012) via mitochondrial fission. Inhibition of mitochondrial fragmentation has been shown to block the release of mitochondrial apoptotic factors, advocating that fission may engage in permeabilization of mitochondrial transition pore during the beginning of apoptosis (Lee et al., 2004).

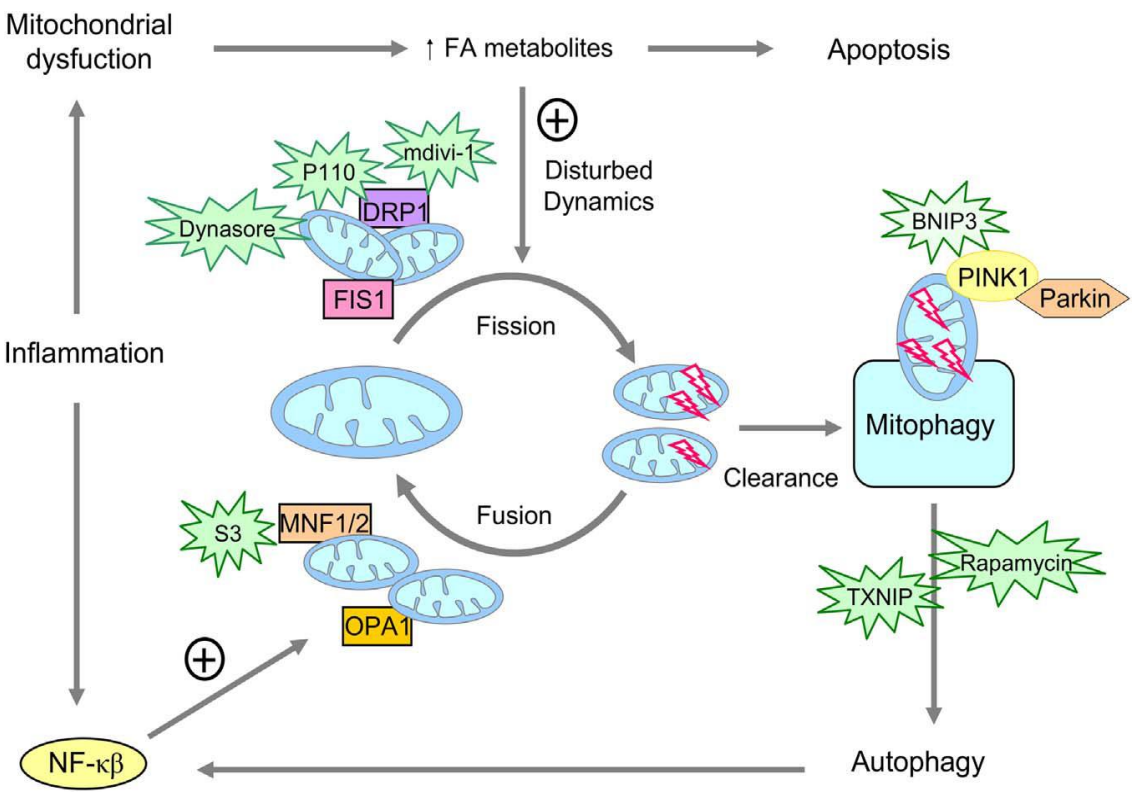

Fig. 3.18 Schematic representation of mitochondrial dynamics (Rovira-Llopis et al., 2017)

Another significant consequence of hyperglycemia is the increased formation of mitochondrial superoxides (Schulze et al., 2004). Mitochondria is the major source of ROS in cardiomyocytes. This can be attributed mainly to the defective antioxidant enzyme activity in the mitochondria. The cristae of mitochondria houses the electron transport complex which is responsible for the synthesis of 90 percent of the body's cellular ATP (Bhatti et al., 2017). The electrons that pass through the mitochondrial complexes ultimately reach the oxygen, the terminal electron acceptor, thus reducing oxygen to water. During this process, 0.4 to 4 % of oxygen is incompletely reduced and this results in the production of ROS, such as superoxide anion. The surplus superoxides are scavenged by mitochondrial superoxide dismutase (MnSOD) enzyme in normal conditions. However under pathological situations due to the defect in the activity of MnSOD the excess superoxides accumulate and interact with many other compounds within and generate secondary ROS (Droge, 2002; Valko et al., 2006). Increase in the mitochondrial superoxides is also related to the activation of polyol pathway (Brownlee, 2001). In the present study also the polyol pathway was upregulated and there was an

increase in the mitochondrial superoxides. This phenomenon has been previously reported by Nishikawa and his group in endothelial cells (Nishikawa et al., 2000). Also the activity of the complex IV of the electron transport chain is reduced in the HG treated H9c2 cells and treatment with CiA and metformin restored their activity when compared to the HG treated group. In addition the efficiency of ATP synthesis also was found to be lowered in the hyperglycemic cells while cotreatment with CiA and metformin maintained the ATP levels. Our results indicate that treatment with CiA improved mitochondrial functions by preserving the transmembrane potential, reducing superoxide generation and mitochondrial fission and preserving the mitochondrial complex 1V activity and maintaining the ATP levels.

Intracellular Ca^{2+} is also an essential factor for cardiac function. An adequate levels of both Ca^{2+} and ATP are required for cardiomyocyte contraction (Balaban, 2002; Isenberg et al., 1993). Hyperglycemia alters the components of calcium homeostasis leading to diastolic dysfunction (Dobrin and Lebeche, 2010). Overproduction of ROS in the hyperglycemic scenario is the main culprit leading to the accumulation of intracellular Ca^{2+} (Wagner et al., 2013). Ca^{2+} gain entry into the mitochondria via the MCUR proteins (Suarez et al., 2018). Although Ca^{2+} is essential for ATP synthesis, prolonged mitochondrial oxidative stress results in the mitochondrial calcium overload which leads to opening of permeability transition pore leading to cytosolic Ca^{2+} accumulation. There was a significant alteration in calcium homeostasis in the hyperglycemic H9c2 cells. The alterations were manifested as an increase in cytoplasmic calcium levels as visualised by Fura 2-AM staining and a decrease in the expression of MCUR1 levels in the HG treated group. Dissipation of mitochondrial membrane potential during hyperglycemia is reported to affect calcium uptake into mitochondria (Skarka and Ostadal, 2002). CiA or metformin cotreatment lowered the intracellular Ca^{2+} accumulation and also upregulated the levels of MCUR1 in H9c2 cells.

Increased cell death and apoptosis are some of the major outcomes of DCM. Different types of cardiomyocyte death have been reported (Chen et al., 2020). They include type 1 or apoptosis, type II or autophagy, type III or necrosis and type IV or entosis (Martins et al., 2017). Apoptosis is characterised by plasma membrane blebbing, cytoplasmic shrinkage and nuclear pyknosis. Formation of autophagosome and lysosomal degradation are the features of autophagy. Necrosis is an unprogrammed cell death which is characterised by loss of plasma membrane integrity and subsequent

release of contents into the extracellular space. Finally entosis is a cell in cell invasion mechanism wherein one cell invades and engulfs the other cell. In the current study also there is an increased apoptosis in the HG treated H9c2 cells as evidenced by the western blot and flow cytometric analysis. Oxidative stress activates the cysteine aspartate protease-3 (caspase-3), which is the executioner caspase that mediates apoptosis. Stressful stimuli activate certain pro-apoptotic members like BAX which leads to its translocation from the cytosol to the outer mitochondrial membrane while BCL-2, an anti-apoptotic protein has been considered as an essential marker of myocardial cell survival (Rovira-Llopis et al., 2017). In the present study caspase-3 activity and the expression of pro-apoptotic protein Bax were found to be elevated and anti-apoptotic protein Bcl-2 found to be lowered during hyperglycemia. In addition, this is supported from the results of flow cytometric analysis. In addition, the alterations in transmembrane potential contribute to apoptosis (Lee et al., 2004). However, the expression of the proapoptotic protein BAX was downregulated and BCL-2 levels were upregulated in the hyperglycemic cardiomyocytes by cotreatment with CiA. It is of paramount importance to identify the cellular and molecular mechanisms responsible for the pathology to design a proper treatment regimen.

In the present study, CiA (100 nM and 500 nM) was applied simultaneously with HG to assess its beneficial property. Although CiA has been evaluated for its potential against diabetes and cardiovascular diseases (Song et al., 2013; Hafizur et al., 2015), the mechanism by which it protects the cardiomyocytes from the adverse effects of HG has not been evaluated. In this study, it is observed that CiA protected the cardiomyocytes by maintaining the antioxidant status and calcium homeostasis, protecting the mitochondria, reducing sorbitol and O-GlcNAc accumulation. Since there is high demand for natural products derived from nutraceuticals, this is highly promising in the area of development of nutraceuticals against diabetes-associated heart problems.

From the overall results, it can be concluded that apoptosis results from the exposure of HG to H9c2 cells via alteration in redox status linked mitochondrial dynamics, polyol pathway and hexosamine biosynthetic pathway. Further CiA is also expected to be a potent phytochemical that protects the myocardium from the hyperglycemic insult.

References

1. Aydin S, Ugur K, Aydin S, Sahin İ, Yardim M. Biomarkers in acute myocardial infarction: current perspectives. Vasc. Health Risk Manag. 2019; 15: 1-10.
2. Baba M, Yoshida K, Ieda M. Clinical applications of natriuretic peptides in heart failure and atrial fibrillation. Int. J. Mol. Sci. 2019; 20: 2824.
3. Balaban RS. Cardiac energy metabolism homeostasis: role of cytosolic calcium. J. Mol. Cell Cardiol. 2002; 34: 1259-1271.
4. Balteau M, Tajeddine N, de Meester C, Ginion A, Des Rosiers C, Brady NR, et al. NADPH oxidase activation by hyperglycaemia in cardiomyocytes is independent of glucose metabolism but requires SGLT1. Cardiovasc. Res. 2011; 92: 237-246.
5. Bhatti JS, Bhatti GK, Reddy PH. Mitochondrial dysfunction and oxidative stress in metabolic disorders - a step towards mitochondria based therapeutic strategies. Biophys. Acta Mol. Basis Dis. 2017; 1863: 1066-1077.
6. Bodor GS. Biochemical markers of myocardial damage. EJIFCC. 2016; 27: 95-111.
7. Brookes PS, Yoon Y, Robotham JL, Anders MW, Shey-Shing S. Calcium, ATP, and ROS: A mitochondrial love-hate triangle. Am. J. Physiol. Cell Physiol. 2004; 287: C817-C833.
8. Brownlee M. Biochemistry and molecular cell biology of diabetic complications. Nature. 2001; 414: 813-820.
9. Bugger H, Abel ED. Mitochondria in the diabetic heart. Cardiovasc. Res. 2010; 8: 229-240.
10. Bugger H, Abel ED. Molecular mechanisms of diabetic cardiomyopathy. Diabetologia. 2014; 57: 660-671.
11. Cai L, Li W, Wang G, Guo L, Jiang Y, Kang YJ. Hyperglycemia-induced apoptosis in mouse myocardium mitochondrial cytochrome c–mediated caspase-3 activation pathway. Diabetes. 2002; 51: 1938-1948.
12. Chen Y, Hua Y, Li X, Arslan IM, Zhang W, Meng G. Distinct types of cell death and the implication in diabetic cardiomyopathy. Front. Pharmacol. 2020;11: 42.
13. Chung SS, Chung SK. Aldose reductase in diabetic microvascular complications. Curr. Drug Targets. 2005; 6: 475-486.
14. Daftardar S, Kaur G, Addepalli V. Diabetic cardiomyopathy. advances in biochemistry in health and disease. Ed. Turan B and Dhalla NS. Springer, New York. 2014.

15. Das J, Ghosh J, Manna P, Sinha M, Sil PC. Taurine protects rat testes against naaso(2)-induced oxidative stress and apoptosis via mitochondrial dependent and independent pathways. Toxicol. Lett. 2009;187: 201-210.
16. De Mattia G, Laurenti O, Bravi C, Ghiselli A, Iuliano L, Balsano F. Effect of aldose reductase inhibition on glutathione redox status in erythrocytes of diabetic patients. Metabolism. 1994; 43: 965-968.
17. Dobrin JS, Lebeche D. Diabetic cardiomyopathy: signaling defects and therapeutic approaches. Expert Rev. Cardiovasc. Ther. 2010; 8: 373-391.
18. Droge W. Free radicals in the physiological control of cell function. Physiol. Rev. 2002; 82: 47-95.
19. Fantus IG. The pathogenesis of the chronic complications of the diabetes mellitus. Endocrinol. Rounds 2002; 2: 1-8.
20. Ferree A, Shirihai O. Mitochondrial dynamics: the intersection of form and function. Adv. Exp. Med. Biol. 2012; 748: 13-40.
21. Fiorentino TV, Prioletta A, Zuo P, Folli F. Hyperglycemia-induced oxidative stress and its role in diabetes mellitus related cardiovascular diseases. Curr. Pharm. Des. 2013; 19: 5695-5703.
22. Flarsheim CE, Grupp IL, Matlib MA. Mitochondrial dysfunction accompanies diastolic dysfunction in diabetic rat heart. Am. J. Physiol. 1996; 271: H192-H202.
23. Giacco F, Brownlee M. Oxidative stress and diabetic complications. Circ. Res. 2010; 107: 1058-1070.
24. Gollmer J, Zirlik A, Bugger H. "Mitochondrial Mechanisms in Diabetic Cardiomyopathy." Diabetes Metab. J. 2020; 44: 33-53.
25. Hafizur RM, Hameed A, Shukrana M, Raza SA, Chishti S, Kabir N, et al. Cinnamic acid exerts anti-diabetic activity by improving glucose tolerance in vivo and by stimulating insulin secretion in vitro. Phytomedicine. 2015; 22: 297-300.
26. Heinova D, Rosival I, Avidar Y, Bogin E. Lactate dehydrogenase isoenzyme distribution and patterns in chicken organs. Res.Vet. Sci. 1999; 67: 309-312.
27. Huang ML, Chiang S, Kalinowski DS, Bae DH, Sahni S, Richardson DR. The role of the antioxidant response in mitochondrial dysfunction in degenerative diseases: cross-talk between antioxidant defense, autophagy, and apoptosis. Oxid. Med. Cell. Longev. 2019; 2019: 6392763.
28. Isenberg G, Han S, Schiefer A, Wendt-Gallitelli MF. Changes in mitochondrial

calcium concentration during the cardiac contraction cycle. Cardiovasc. Res. 1993; 27: 1800-1809.

29. Kain V, Kumar S, Sitasawad SL. Azelnidipine prevents cardiac dysfunction in streptozotocin-diabetic rats by reducing intracellular calcium accumulation, oxidative stress and apoptosis. Cardiovasc. Diabetol. 2011; 10: 97.
30. Kanaporis G, Blatter LA. Membrane potential determines calcium alternans through modulation of SR Ca2+ load and L-type Ca2+ current. J. Mol. Cell Cardiol. 2017; 105: 49-58.
31. Karbowski M, Youle RJ. Dynamics of mitochondrial morphology in healthy cells and during apoptosis. Cell Death Differ. 2003; 10: 870-880.
32. Kawahito S, Kitahata H, Oshita S. Problems associated with glucose toxicity: role of hyperglycemia-induced oxidative stress. World J. Gastroenterol. 2009; 15: 4137-4142.
33. Kayama Y, Raaz U, Jagger A, Adam M, Schellinger IN, Sakamoto M, et al. Diabetic cardiovascular disease induced by oxidative stress. Int. J. Mol. Sci. 2015; 16: 25234-25263.
34. Lakshmi BS, Sujatha S, Anand S, Sangeetha KN, Narayanan RB, Katiyar C, et al. Cinnamic acid, from the bark of cinnamomum cassia, regulates glucose transport via activation of GLUT4 on L6 myotubes in a phosphatidylinositol 3-kinase-independent manner. J. Diabetes. 2009; 1: 99-106.
35. Lee YJ, Jeong SY, Karbowski M, Smith CL, Youle RJ. Roles of the mammalian mitochondrial fission and fusion mediators fis1, drp1, and opa1 in apoptosis. Mol. Biol. Cell. 2004; 15: 5001-5011.
36. Liquori ME, Christenson RH, Collinson PO, deFilippi CR. Cardiac biomarkers in heart failure. Clin. Biochem. 2014; 47: 327-337.
37. Liu Q, Wang S, Cai L. Diabetic cardiomyopathy and its mechanisms : role of oxidative stress and damage. J. Diabetes Investig. 2014; 5:623-634.
38. Luo X, Li R, Yan LJ. Roles of pyruvate, nadh, and mitochondrial complex i in redox balance and imbalance in β cell function and dysfunction. J. Diabetes Res. 2015; 2015: 512618.
39. Marín-García J. Cardiac function in heart failure: the role of calcium cycling. heart failure: bench to bedside, Contemporary Cardiology. Springer, New York, 2010; pp. 15-22.

40. Martins I, Raza SQ, Voisin L, Dakhli H, Law F, De Jong D, et al. Entosis: the emerging face of non-cell-autonomous type iv programmed death. Biomed. J. 2017; 40: 133-140.
41. Matshela RM. Second in a series on diabetes and the heart: diabetic cardiomyopathy-mechanisms and mode of diagnosis. European society of cardiology. 2016; 14: 15-28.
42. Matteucci E, Giampietro O. Oxidative stress in families of type 1 diabetic patients. Diabet. Care. 2000; 23: 1182-1186.
43. Morino K, Petersen KF, Shulman GI. Molecular mechanisms of insulin resistance in humans and their potential links with mitochondrial dysfunction. Diabetes. 2006; 55: S9-S15.
44. Ni HM, Williams JA, Ding WX. Mitochondrial dynamics and mitochondrial quality control. Redox Biol. 2015; 4: 6-13.
45. Niero EL, Machado-Santelli GM. Cinnamic acid induces apoptotic cell death and cytoskeleton disruption in human melanoma cells. J. Exp. Clin. Cancer Res. 2013; 32: 1.
46. Nishikawa T, Edelstein D, Du XL, Yamagishi S, Matsumura T, Kaneda Y et al. Normalizing mitochondrial superoxide production blocks three pathways of hyperglycaemic damage. Nature. 2000; 404: 787-790.
47. Oates PJ. Polyol pathway and diabetic peripheral neuropathy. Int. Rev. Neurobiol. 2002; 50: 325-392.
48. Ong SB, Hausenloy DJ. Mitochondrial morphology and cardiovascular disease. Cardiovasc. Res. 2010; 88: 16-29.
49. Orchard C, Brette F. T-tubules and sarcoplasmic reticulum function in cardiac ventricular myocytes. Cardiovasc. Res. 2008; 77: 237-244.
50. Otera H, Mihara K. Molecular mechanisms and physiologic functions of mitochondrial dynamics. J. Biochem. 2011; 149: 241-251.
51. Pan Y, Wang Y, Zhao Y, Peng K, Li W, Wang Y, et al. Inhibition of JNK phosphorylation by a novel curcumin analog prevents high glucose–induced inflammation and apoptosis in cardiomyocytes and the development of diabetic cardiomyopathy. Diabetes. 2014; 63: 3497-3511.
52. Patibandla S, Gupta K, Alsayouri K. Cardiac enzymes. In: StatPearls [Internet]. Treasure Island (FL): StatPearls Publishing. 2020; PMID: 31424800.

53. Preetha Rani MR, Anupama N, Sreelekshmi M, Raghu KG. Chlorogenic acid attenuates glucotoxicity in H9c2 cells via inhibition of glycation and pkc α upregulation and safeguarding innate antioxidant status. Biomed. Pharmacother. 2018; 100: 467-477.
54. Quirós PM, Ramsay AJ, Sala D, Fernández-Vizarra E, Rodríguez F, Peinado JR, et al. Loss of mitochondrial protease oma1 alters processing of the gtpase opa1 and causes obesity and defective thermogenesis in mice. EMBO J. 2012; 31: 2117-2133.
55. Rajesh M, Bátkai S, Kechrid M, Mukhopadhyay P, Lee WS, Horváth B, et al. Cannabinoid 1 receptor promotes cardiac dysfunction, oxidative stress, inflammation, and fibrosis in diabetic cardiomyopathy. Diabetes. 2012; 61: 716-727.
56. Rovira-Llopis S, Bañuls C, Diaz-Morales N, Hernandez-Mijares A, Rocha M, Victor VM. Mitochondrial dynamics in type 2 diabetes: pathophysiological implications. Redox Biol. 2017; 11: 637-645.
57. Safi SZ, Qvist R, Kumar S, Batumalaie K, Ismail ISB. Molecular mechanisms of diabetic retinopathy, general preventive strategies, and novel therapeutic targets. Biomed. Res. Int. 2014; 2014: 801269.
58. Schilling JD. The mitochondria in diabetic heart failure: from pathogenesis to therapeutic promise. Antioxid. Redox Signal. 2015; 22: 1515-1526.
59. Schulze PC, Yoshioka J, Takahashi T, He Z, King GL, Lee RT. Hyperglycemia promotes oxidative stress through inhibition of thioredoxin function by thioredoxin-interacting protein. J. Biol. Chem. 2004; 279: 30369-30374.
60. Skarka L, Ostadal B. Mitochondrial membrane potential in cardiac myocytes. Physiol. Res. 2002; 51: 425-434.
61. Song F, Li H, Sun J, Wang S. Protective effects of cinnamic acid and cinnamic aldehyde on isoproterenol-induced acute myocardial ischemia in rats. J. Ethnopharmacol. 2013; 150: 125-130.
62. Spector KS. Diabetic cardiomyopathy. Clin. Cardiol. 1998; 21: 885-887.
63. Suarez J, Cividini F, Scott BT, Lehmann K, Diaz-Juarez J, Diemer T. Restoring mitochondrial calcium uniporter expression in diabetic mouse heart improves mitochondrial calcium handling and cardiac function. J. Biol. Chem. 2018; 293: 8182-8195.

64. Tran DH, Wang ZV. Glucose metabolism in cardiac hypertrophy and heart failure. J Am. Heart Assoc.2019; 8: e012673.
65. Tsutsui H, Kinugawa S, Matsushima S. Oxidative stress and heart failure. Am. J. Physiol. Heart Circ. Physiol. 2011; 301: H2181-H2190.
66. Twig G, Graf SA, Wikstrom JD, Mohamed H, Haigh SE, Elorza A, Deutsch M, et al. Tagging and tracking individual networks within a complex mitochondrial web with photoactivatable GFP. Am. J. Physiol. Cell Physiol. 2006; 291: C176-C184.
67. Valko M, Rhodes CJ, Moncol J, Izakovic M, Mazur M. Free Radicals, Metals and antioxidants in oxidative stress-induced cancer. Chem. Biol. Interact. 2006; 160: 1-40.
68. Verma SK, Garikipati VNS, Kishore R. Mitochondrial dysfunction and its impact on diabetic heart. Biochim. Biophys. Acta Mol. Basis Dis. 2017; 1863: 1098-1105.
69. Wang W, Wang Y, Long J, Wang J, Haudek SB, Overbeek P etal. Mitochondrial fission triggered by hyperglycemia is mediated by rock1 activation in podocytes and endothelial cells. Cell Metab. 2012; 15: 186-200.
70. Yan LJ. Redox imbalance stress in diabetes mellitus: role of the polyol pathway. Animal Model Exp. Med. 2018; 1: 7-13.
71. Yan LJ, Christians ES, Liu L, Xiao X, Sohal RS, Benjamin IJ. Mouse heat shock transcription factor 1 deficiency alters cardiac redox homeostasis and increases mitochondrial oxidative damage. EMBO J. 2002; 21: 5164-5172.
72. Yang L, Wu QQ, Liu Y, Hu ZF, Bian ZY, Tang QZ. Cinnamaldehyde attenuates pressure overload-induced cardiac hypertrophy. Int. J. Clin. Exp. Pathol. 2015; 8: 14345-14354.
73. Yoon Y, Galloway CA, Jhun BS, Yu T. Mitochondrial Dynamics in Diabetes.Antioxi.Red Sig.. 2011; 14: 439-457.

Chapter 4

Upregulation of inflammatory pathways in diabetic cardiomyopathy (*In vivo study*).

4.1 Introduction

DCM is recently considered to be one among the major CVD worldwide which is usually associated with structural and functional changes in the myocardium. The early stages of DCM are usually asymptomatic and occur independently of other cardiac risk factors like coronary artery disease and hypertension (Voulgari et al., 2010). Hyperglycemia that emerge during diabetes mellitus leads to oxidative stress (Tan et al., 2020) which then paves a pathway for inflammation, extracellular matrix remodeling and ultimately cardiomyocyte death (Tan et al., 2020; Hölscher et al., 2016).

Several animal models have been used recently to mimic human diabetic scenarios in the lab. Rodents are the most commonly used models due to their natural resistance to atherosclerosis (Severson, 2004), shorter generation times and economic (Zhang et al., 2008). Although the administration of toxins like streptozotocin or alloxan and certain genetic modifications can induce T1DM, the induction of T2DM can be effected only through feeding the animals a high fat diet (Fuentes-Antras et al., 2015; Lorenzo-Almorós et al., 2017). However studies have reported that the high fat diet fed animals develop only insulin resistance but no hyperglycemia (Tanaka et al., 2007; Zhao et al., 2008). In order to overcome this situation scientists nowadays also administer a low dose of streptozotocin along with the high fat diet. Low dose of streptozotocin injection is reported to trigger a mild deficiency in insulin secretion which is similar to what is happening in the later stages of T2DM (Srinivasan et al., 2005; Reed et al., 2000). Thus, rats fed with a high fat diet followed by injection of a small dose of streptozotocin would be an ideal model of T2DM mimicking all the events from insulin resistance to β cell dysfunction and the simultaneously occurring metabolic derangements. Such an experimental model is cheaper, easily accessible and also can be used for testing of the effects of various compounds for the treatment of T2DM.

There are many challenges in the clinical setup to diagnose DCM accurately. DCM is currently identified when the condition has advanced so far such that it has already reached the systolic dysfunction stage and heart failure has already been established.

This creates a situation whereby a proper treatment strategy cannot be elucidated (Tillquist and Maddox, 2012). Different methods are employed to diagnose DCM which include invasive methods such as endomyocardial biopsy sampling, cardiac catheterization, and non-invasive techniques like echocardiography, magnetic resonance imaging, multislice computed tomography and nuclear imaging techniques like positron emission tomography. Echocardiography is considered to be a gold standard method to study disorders in cardiac structure (Aneja et al., 2008). Through echocardiography, it is easy to detect left ventricular hypertrophy and impaired diastolic filling but it is expensive and time consuming.

Recently, efforts have been put into developing minimally invasive blood sampling methods like the determination of plasma biomarkers exclusive for DCM. These biomarkers are thought to give more stable results (Lorenzo-Almorós et al., 2017). Damaged myocardium is thought to secrete many factors in response to chronic diabetes. Detection of markers related to hypertrophy, contractility and fibrosis might be essential in the early diagnosis of DCM. Cardiac troponin is one such marker that is related to myocardial contraction (Gomes et al., 2002). The common pro-hypertrophic markers include natriuretic peptides like ANP, BNP and NT-pro BNP (Dahlström, 2004). Other factors secreted by the myocardium in response to inflammation and apoptosis are CRP and creatinine kinase phosphate (CK). They are secreted under chronic and irreversible pathological situations (Lorenzo-Almorós et al., 2017). But these are identified only after a prolonged period of diabetes. However early diagnosis of DCM is very essential and research has been focussed in developing therapeutic strategies.

Recently myocardial inflammation is thought to contribute to the development of pathogenesis related to DCM (Frieler and Mortenson, 2015). Inflammation is the body's defence mechanism which is generally considered as an adaptive early response to short term stress in the myocardium to restore homeostasis (Mann, 2015; Prabhu and Frangogiannis, 2016). But under prolonged stress this response changes into a maladaptive one. Inflammatory response usually involves a cascade of pathways well organized by the immune system (Smail et al., 2019) in order to eliminate the causative factor. Many studies have revealed the occurrence of myocardial inflammation in human subjects and experimental models of T1DM and T2DM (Vasanji et al., 2006; Zhou et al., 2000).

Nutraceuticals have gained more importance in preventing many degenerative diseases like cardiovascular diseases and cancer. In the present study, a phenolic acid called cinnamic acid (CiA) has been selected. Polyphenols usually exist in food in the form of esters and glycosides which cannot be absorbed by the small intestine (Manach et al., 2004). Hence, they are initially hydrolysed to digestible forms by the intestinal enzymes and gut microflora. Since it showed beneficial properties *in vitro* we determined the cardioprotective properties of CiA *in vivo.*

4.2 Materials and Methods (Please refer Chapter 2 for details)

- Estimation of blood glucose levels, glycated haemoglobin, insulin levels and insulin resistance.
- Evaluation of biochemical parameters and lipid profile.
- Studies on various cardiac injury markers by western blot analysis.
- Investigation on the inflammatory pathways during diabetes by western blot analysis in the heart.
- Analysis of mRNA expression of TGF-β and β-MHC by RT-PCR.
- Histopathology of cardiac tissue.

4.3 Results

4.3.1 CiA treatment reduced the blood glucose levels, glycated haemoglobin (HbA1c) and cardiac mass index

The blood glucose levels of diabetic rats reached 406.5 mg/dl after 6 months. It was found that two months of treatment with CiA reduced the blood glucose levels of diabetic rats (Fig. 4.1A). In addition the cardiac mass index was also significantly lowered ($p \leq 0.05$) in CiA treated rats by 27.7 % and 39.1 % for 5 and 10 mg/kg bwt respectively. Similarly metformin also reduced the cardiac mass index by 24.4% (Fig. 4.1B).The levels of glycated haemoglobin were found to be high in the diabetic group (15.7 %; Fig. 4.1C) when compared to the control group while treatment with CiA at 5 and 10 mg/kg reduced the HbA1c levels to 6 % and 5.3 % respectively. Metformin at 50 mg/kg also lowered the

HbA1c levels to 5.8 % (Fig. 4.1C). The toxicity group did not show any significant change in the HbA1c levels when compared to the control group.

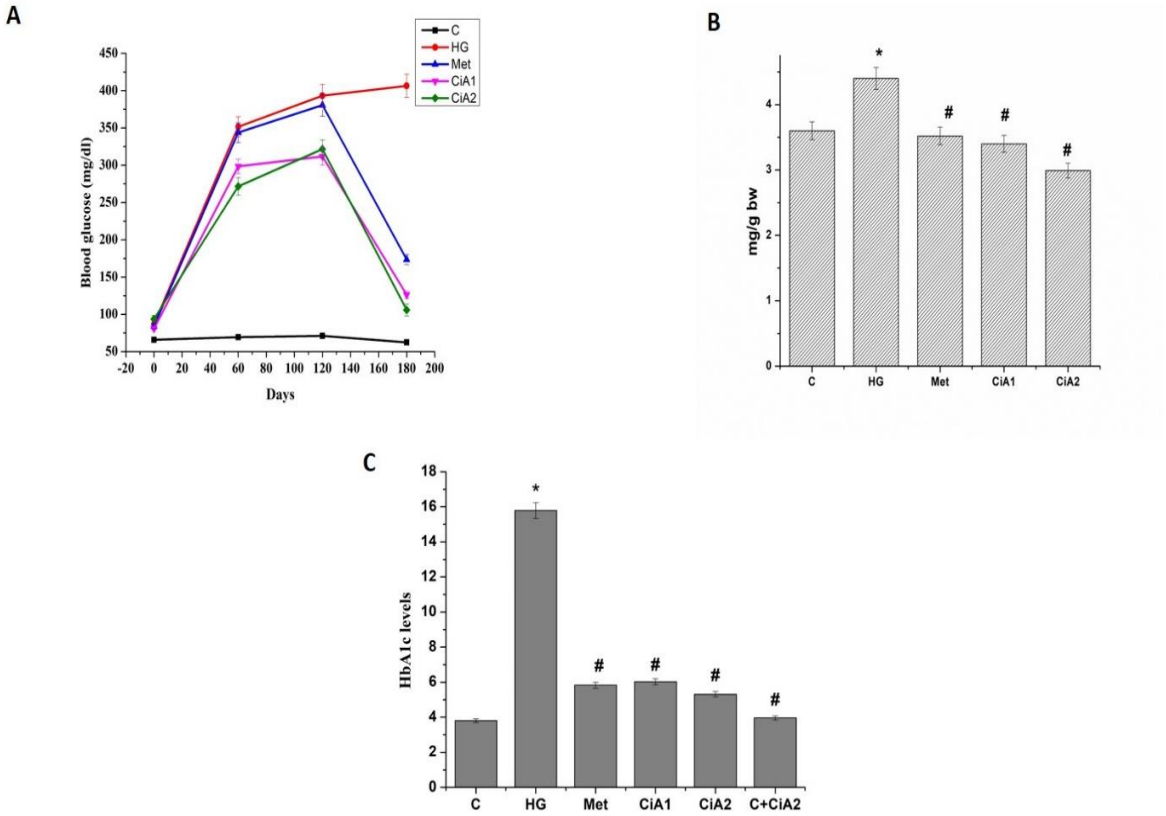

Fig. 4.1 Cinnamic acid reduced the blood glucose, cardiac mass index and glycated hemoglobin levels. C- control, HG- diabetic, Met- HG + metformin (50 mg/kg bwt), CiA1- HG + cinnamic acid (5 mg/kg bwt), CiA2- HG + cinnamic acid (10 mg/kg bwt), C + CiA2- control + cinnamic acid (10 mg/kg bwt). A) Blood glucose levels, B) Cardiac mass index, C) Glycated hemoglobin levels. Values are expressed as mean ± SEM where n = 6. * $p \leq 0.05$ significantly different from the control group. # $p \leq 0.05$ significantly different from the diabetic group.

4.3.2 CiA increased plasma insulin levels and lowered insulin resistance

Insulin levels were found to be significantly ($p \leq 0.05$) lowered in the diabetic group (12.5 mIU/L) when compared to the control animals (27.78 mIU/L; Fig. 4.2A). CiA treatment at 5 and 10 mg/kg and metformin at 50 mg/kg increased the insulin levels significantly ($p \leq 0.05$) by 16.12 mIU/L, 20.35 mIU/L and 16.99 mIU/L respectively (Fig. 4.2A). Similarly the insulin resistance (HOMA-IR) was increased ($p \leq 0.05$) in the diabetic group (12.5 AU) when compared to the control rats (4.28 AU) (Fig. 4.2B). CiA and metformin treatment both reduced insulin resistance significantly (Fig. 4.2B). Again the toxicity group did not show any significant change in the levels of insulin and HOMA-IR.

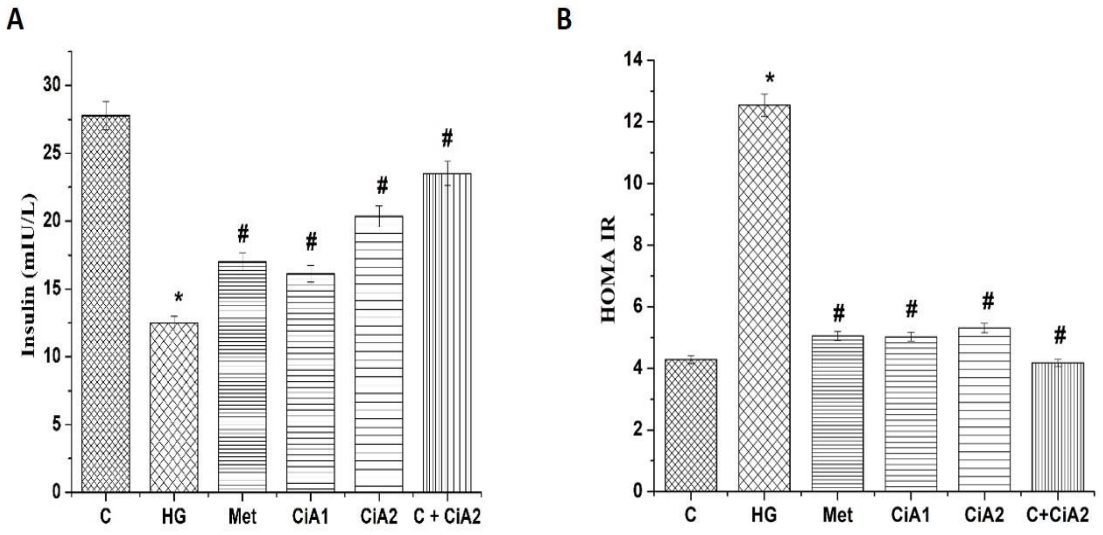

Fig. 4.2 Effect of cinnamic acid on insulin resistance. C- control, HG- diabetic, Met- HG + metformin (50 mg/kg bwt), CiA1- HG + cinnamic acid (5 mg/kg bwt), CiA2- HG + cinnamic acid (10 mg/kg bwt), C + CiA2- control + cinnamic acid (10 mg/kg bwt). A) Plasma insulin levels, B) HOMA-IR. Values are expressed as mean ± SEM where n = 6. * $p \leq 0.05$ significantly different from the control group. # $p \leq 0.05$ significantly different from the diabetic group.

4.3.3 Estimation of biochemical parameters in the serum of diabetic rats

The levels of LDH, CKMB, CRP, SGOT and ANP were found to be significantly increased in the serum of diabetic rats while treatment with CiA or metformin lowered their levels (Table 1).

Groups	I	II	III	IV	V	VI
LDH (U/L)	51.29±1.96	758.22±28.95*	232.43±8.88#	432.8±16.5#	408.7±15.6#	90.6±3.45#
CRP(mg/L)	2.45±0.09	15.09±0.57*	1.36±0.05#	0.91±0.03#	1.36±0.05#	1.45±0.05#
CKMB(U/L)	16.8±0.64	188.7±7.2*	51.7±1.97#	145.7±5.56#	70.1±2.68#	49.1±1.88#
SGOT (U/L)	6.98±0.27	68±2.6*	29.7±1.13#	13.9±0.53#	7.68±0.27#	8.72±0.33#
ANP (pg/ml)	2.08±0.08	2.87±0.11*	2.58±0.09	2.09±0.08	2.56±0.1#	2.43±0.09#

Table 1. Estimation of serum biochemical parameters LDH, CRP, CKMB, SGOT and ANP in wistar rats. Groups: I- Control; II- Diabetic (HG); III- HG + metformin (50 mg/kg bwt); IV- HG + CiA1 (5 mg/kg bwt); V – HG + CiA2 (10 mg/kg bwt); VI- C + CiA2 (10 mg/kg bwt). Values are expressed as mean ± SEM where n =

6. * p ≤ 0.05 significantly different from the control group. # p ≤ 0.05 significantly different from the HG treated group

4.3.4 CiA improved the lipid profile in diabetic rats

Diabetic rats showed an altered lipid profile characterized by significant increase ($p \leq 0.05$) in serum triglycerides, total cholesterol and LDL cholesterol when compared with normal control rats (Table 2). Serum levels of HDL cholesterol were significantly ($p \leq 0.05$) lowered in the diabetic rats. Cotreatment with CiA or metformin significantly ($p \leq 0.05$) reversed these lipid profile derangements (Table 2).

Groups (mg/dL)	I	II	III	IV	V	VI
TG	122.2±4.67	195.7±7.47*	142.2±5.43#	73.26±2.8#	129.9±4.97#	94.12±3.6#
TC	75.5±2.88	196.2±7.49*	81.43±3.11#	41.2±1.6#	164.4±6.3#	141.3±5.4#
LDL	26.3±1.01	199.8±7.63*	33.1±1.27#	24±0.91#	41.8±1.59#	48.4±1.85#
HDL	66.5±2.54	14.9±0.57*	22.06±0.84#	25.6±0.98#	66.48±2.54#	70.3±2.68#

Table 2. Alterations in lipid profile in wistar rats and amelioration with cinnamic acid. Groups: I- Control; II- Diabetic (HG); III- HG + metformin (50 mg/kg bwt); IV- HG + CiA1 (5 mg/kg bwt); V – HG + CiA2 (10 mg/kg bwt); VI- C + CiA2 (10 mg/kg bwt). Values are expressed as mean ± SEM where n = 6. * p ≤ 0.05 significantly different from the control group. # p ≤ 0.05 significantly different from the HG treated group.

4.3.5 Estimation of lipid peroxidation in diabetic rats and the effect of CiA.

The levels of MDA, byproduct of lipid peroxidation was elevated in the serum of diabetic rats by 64.6 % when compared to the control group (Fig. 4.3). Cotreatment with CiA at 5 and 10 mg/kg bwt reduced the levels of MDA by 89.3 % and 69. 8 % respectively when compared to the diabetic group. Treatment with metformin also showed a significant reduction in MDA levels by 41.9 % (Fig. 4.3). CiA alone treated group did not show any significant change in the levels of MDA.

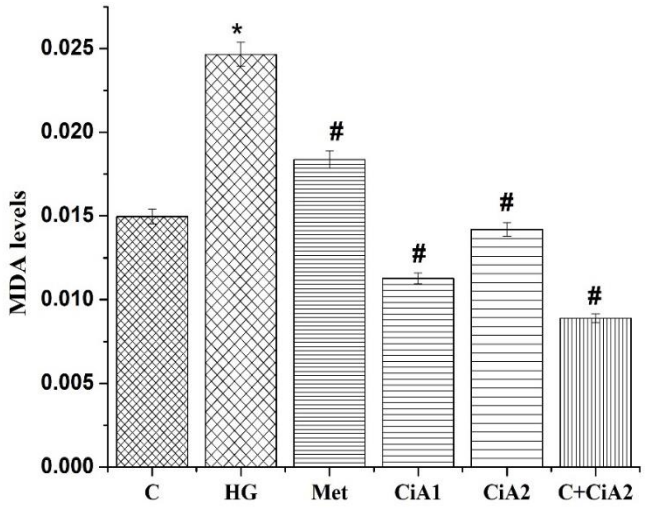

Fig. 4.3 Quantification of lipid peroxidation in diabetic rats and the possible amelioration with cinnamic acid. Malondialdehyde levels in the serum of wistar rats. C- control, HG - diabetic, Met- HG + metformin (50 mg/kg bwt), CiA1- HG + cinnamic acid (5 mg/kg bwt), CiA2- HG + cinnamic acid (10 mg/kg bwt), C+ CiA2- control + cinnamic acid (10 mg/kg bwt). Values are expressed as mean ± SEM where n = 6.

In order to rule out the toxicity of CiA we included group 6 (Refer Chapter 2; Materials and Methods). As observed by the evaluation of biochemical parameters (LDH, CRP, CKMB, SGOT and ANP Table 1), lipid profile and oxidative stress marker (MDA) the toxicity group did not show any significant changes after 180 days of administration of high dose of CiA. So this group was omitted in the further experiments.

4.3.6 Estimation of the levels of cardiac injury markers in diabetic rats

BNP, a clinical marker of hypertrophy showed 259.6 % increase in the serum of diabetic rats while administration of CiA significantly reduced the same (38.7 % and 160.6 % at 5 and 10 mg/kg bwt respectively (Fig. 4.4). However metformin didn't show any effect. The levels of TNNI3K, emerging markers of cardiac disease, and troponin were significantly ($p \leq 0.05$) upregulated by 47.4 % and 71.35 % respectively in the serum of diabetic animals compared to the control group (Fig. 4.4). CiA treatment with both concentrations reduced significantly ($p \leq 0.05$) the levels of both markers indicating the cardioprotective property of CiA (Fig. 4.4).

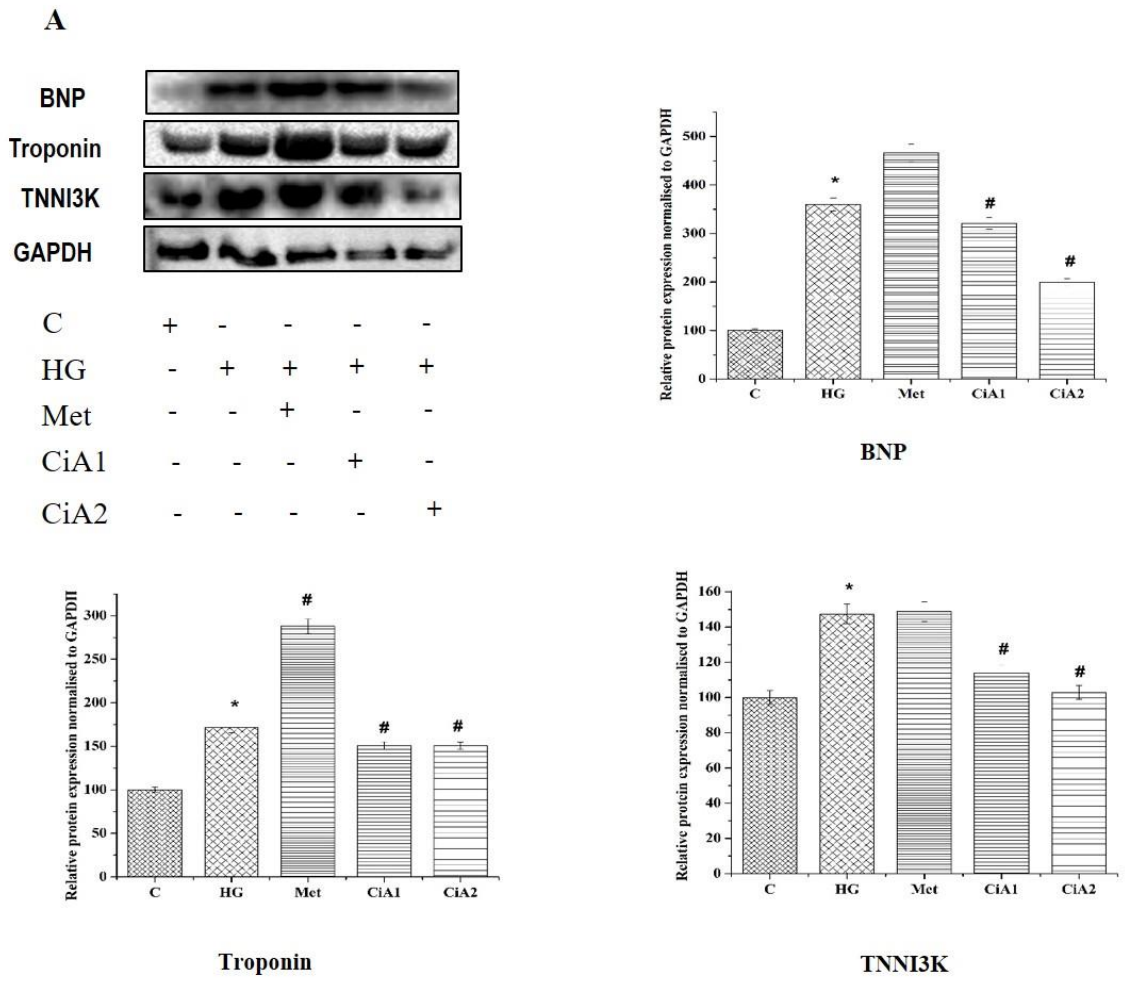

Fig. 4.4 Assessment of cardiomyopathy markers in the serum of diabetic rats. C - control, HG - diabetic, Met- HG + metformin (50 mg/kg bwt), CiA1- HG + cinnamic acid (5 mg/kg bwt), CiA2 - HG + cinnamic acid (10 mg/kg bwt). Representative immunoblots of BNP, troponin and TNNI3K in the serum of male wistar rats and their respective densitometric quantifications normalised to GAPDH. Values are expressed as mean ± SEM where n = 3. * $p \leq 0.05$ significantly different from the control group. # $p \leq 0.05$ significantly different from the diabetic group.

4.3.7 The increased levels of nitrite, CRP and MCP-1 in diabetic rats

There was a significant increase ($p \leq 0.05$) in nitrite production in the serum of diabetic rats (314 %) when compared to the normal group while treatment with CiA or metformin significantly reduced their levels by 290.9 %, 314.3 % and 377.8 % at 5, 10 and 50 mg/kg bwt respectively compared to the diabetic group (Fig. 4.5A). CRP, an indicator of inflammation has been significantly ($p \leq 0.05$) increased in the heart tissue of diabetic rats by 119.8 % whereas in CiA treated rats the CRP levels were lowered in a dose dependent manner by 116.5 % and 155 % respectively compared to the diabetic group (Fig. 4.5B). Metformin treatment also reduced their levels by 40.8 % (Fig. 4.5B).

Likewise MCP-1, an inflammatory chemokine, was also found to be upregulated in the serum of diabetic rats by 17.39 % while CiA treatment at both concentrations (5 and 10 mg) and metformin significantly downregulated their levels by 46.4 %, 53.3 % and 25.2 % respectively (Fig. 4.5B).

A

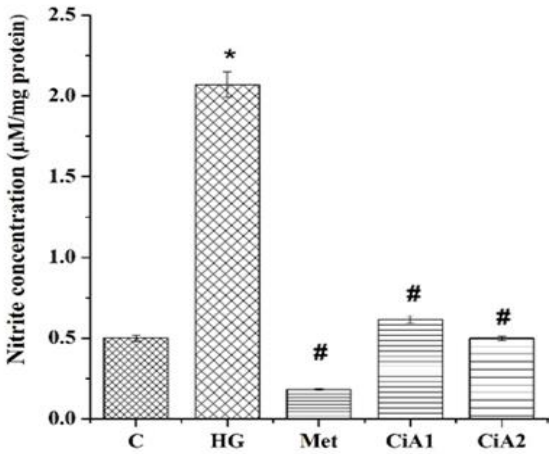

B

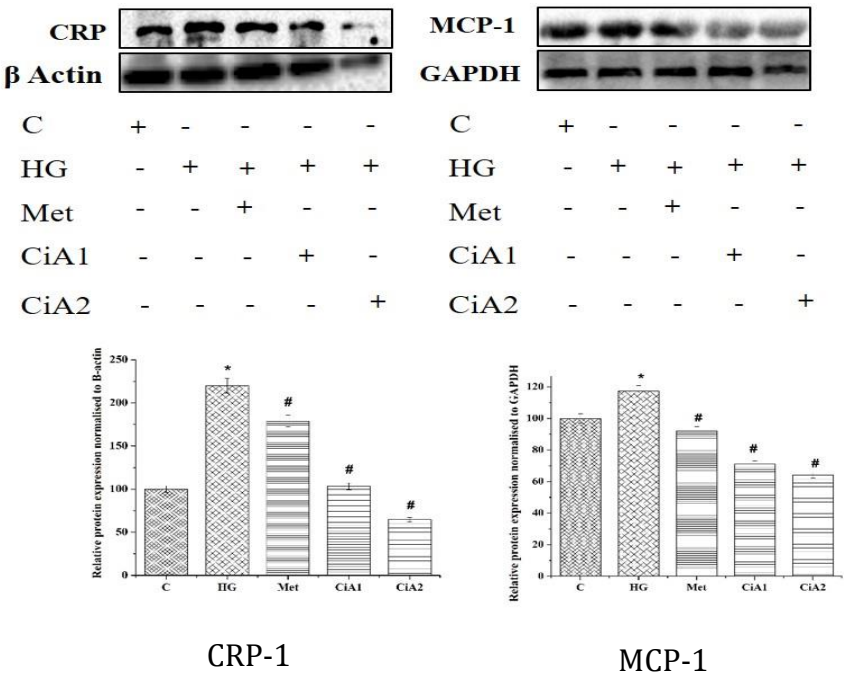

Fig.4.5 Overexpression of inflammatory markers in diabetic rats and amelioration of the same with cinnamic acid. C- control, HG - diabetic, Met- HG + metformin (50 mg/kg bwt), CiA1- HG + cinnamic acid (5 mg/kg bwt), CiA2- HG+ cinnamic acid (10 mg/kg bwt). A) Nitrite levels in the serum of wistar rats. Values are expressed as mean ± SEM where n = 6. B) Representative immunoblots of CRP in the heart and MCP-1 in the serum of wistar rats and their respective densitometric quantifications normalised to β-actin and

GAPDH respectively. Values are expressed as mean ± SEM where n = 3. * $p \leq 0.05$ significantly different from the control group. # $p \leq 0.05$ significantly different from the diabetic group.

4.3.8 Release of pro-inflammatory cytokines during diabetes

The levels of proinflammatory cytokines TNF-α, IL-6, IL-1β and MCP-1 were upregulated significantly ($p \leq 0.05$) by 30 %, 39.6 %, 26.5 % and 46.9 % respectively and the level of the anti-inflammatory cytokine IL-10 was downregulated significantly by 17.24 % in the serum of diabetic rats compared to the control group (Fig. 4.6). Treatment with CiA lowered the levels significantly ($p \leq 0.05$) by 18.3 % and 25 % (TNF-α); 13.2 % and 16.9 % (IL-6); 13.4 % and 16.1 % (IL-1β); 17.3 % and 36.5 % (MCP-1) and upregulated the levels of IL-10 significantly by 10.3 % and 15.5 % at 5 and 10 mg/kg of CiA (Fig. 4.6). Metformin also significantly ($p \leq 0.05$) reduced the levels of the proinflammatory cytokines by 10 %, 11.3 %, 11.06 %, 36.73 % and increased the levels of anti-inflammatory cytokine IL-10 by 3.44 % (not significant) at 50 mg/kg compared to the diabetic group (Fig. 4.6).

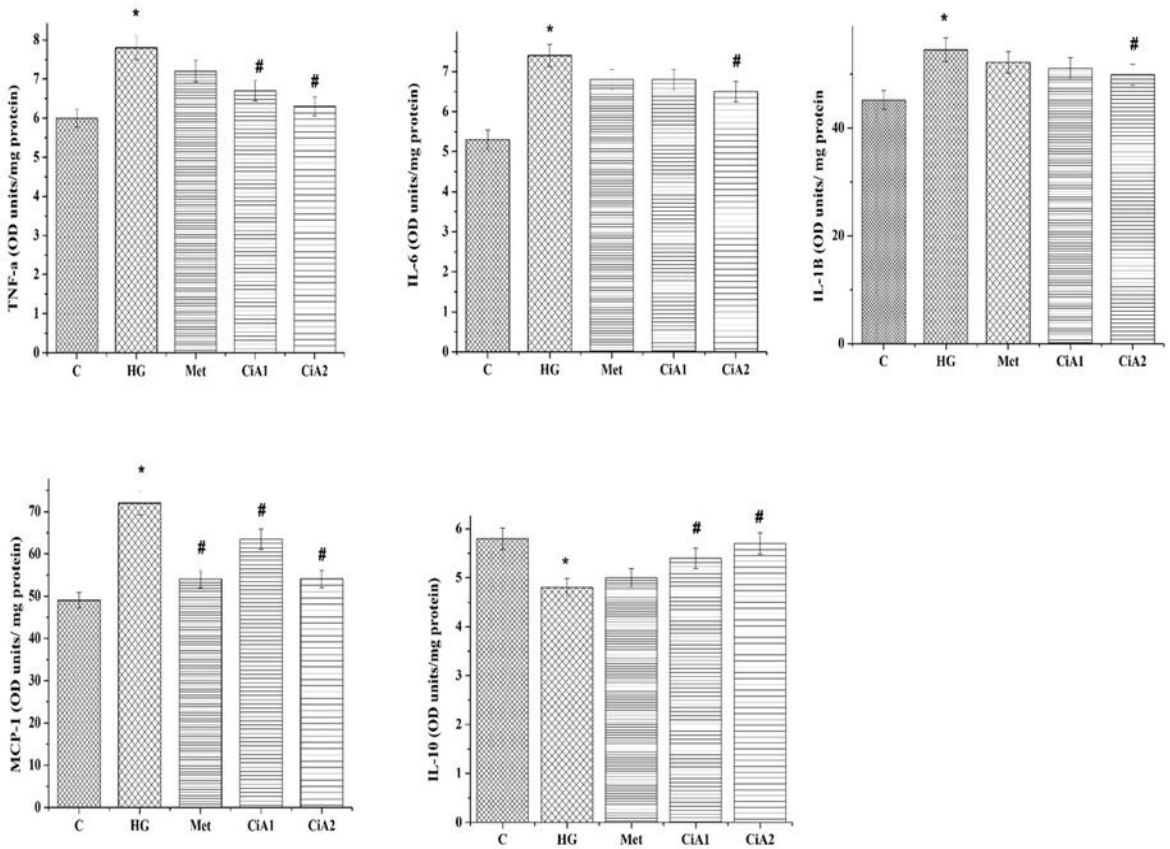

Fig. 4.6 Cinnamic acid reduced the levels of proinflammatory cytokines. C- control, HG - diabetic, Met- HG + metformin (50 mg/kg bwt), CiA1- HG + cinnamic acid (5 mg/kg bwt), CiA2- HG + cinnamic acid (10

mg/kg bwt). The levels of proinflammatory cytokines (TNF-α, IL-6, IL-1β, MCP-1) and anti-inflammatory cytokine IL-10 in the serum of wistar rats. Values are expressed as mean ± SEM where n = 6. * $p \leq 0.05$ significantly different from the control group. # $p \leq 0.05$ significantly different from the diabetic group.

4.3.9 The upregulation of MAPK pathways during hyperglycemia.

The pJNK, pERK and pp38 MAPK levels were found to be upregulated in the hearts of diabetic rats by 18.3 %, 45.4 % and 106.5 %, respectively compared to the normal rats (Fig. 4.7). Treatment with CiA downregulated the expression levels of pJNK by 4.4 % (5 mg) and 11.8 % (10 mg), pERK by 57.5 % (5 mg) and 95.9 % (10 mg) ($p \leq 0.05$) and pp38 MAPK by 7.7 % (5 mg) and 153. 8 % (10 mg; ($p \leq 0.05$) compared to the diabetic group.Treatment with metformin reduced the levels of pJNK, pERK and pp38 MAPK by 78.2 %, 68.7 % and 49.1 % respectively at 50 mg/kg (Fig. 4.7).

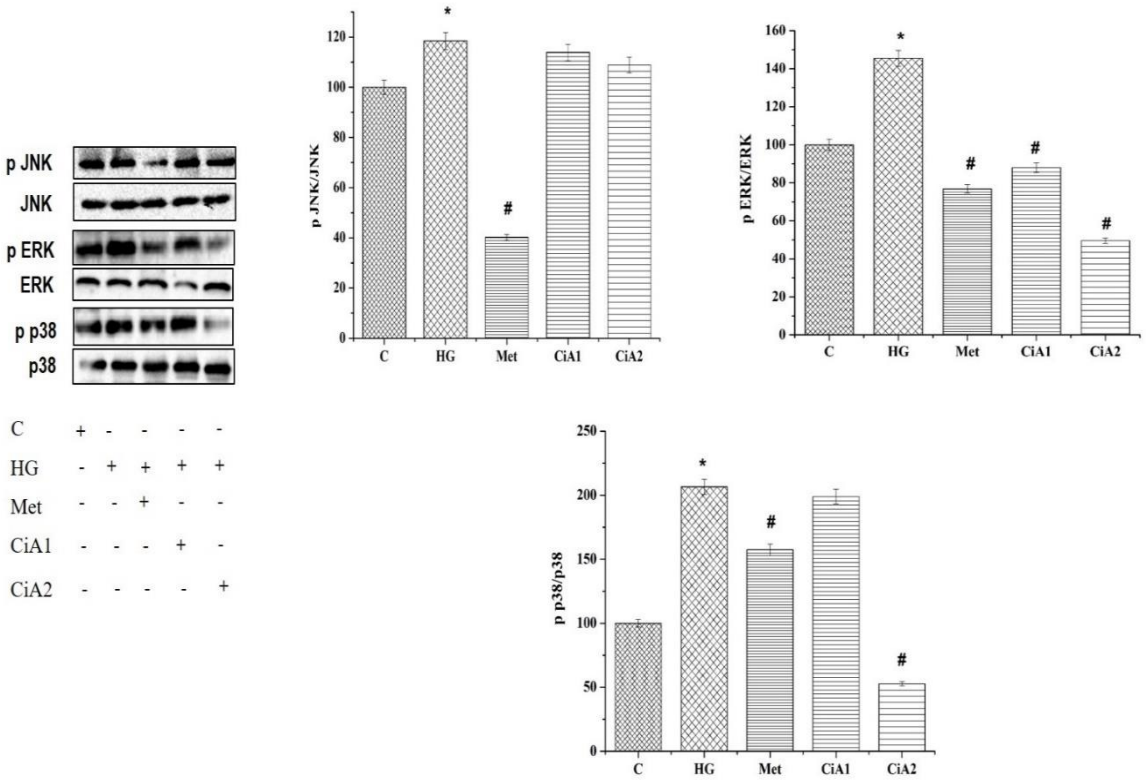

Fig. 4.7 Activation of the MAPK pathways (JNK, ERK and p38 MAPK) in diabetic rats. C- control, HG - diabetic, Met- HG + metformin (50 mg/kg bwt), CiA1- HG + cinnamic acid (5 mg/kg bwt), CiA2- HG + cinnamic acid (10 mg/kg bwt). A) Representative immunoblots of pJNK, pERK and pp38 MAPK and their respective densitometric quantifications. Values are expressed as mean ± SEM where n = 3.* $p \leq 0.05$ significantly different from the control group. # $p \leq 0.05$ significantly different from the diabetic group.

4.3.10 TLR4/Myd88 upregulation in the heart during diabetes

There was a significant ($p \leq 0.05$) upregulation of TLR4 (14.3 %) and MyD88 (42.7 %) protein levels in the heart of diabetic rats (Fig. 4.8). TLR4 level was reduced by 36.3 % significantly ($p \leq 0.05$) with 10 mg of CiA compared to the diabetic group. Myd88 levels were downregulated significantly ($p \leq 0.05$) by 35.2 % and 31.4 % for 5 and 10 mg CiA and metformin treatment reduced the expression of TLR4 and MyD88 by 26.2 % and 42.71 % respectively compared to the diabetic group (Fig. 4.8).

4.3.11 Upregulation of NLRP3 and TxNIP levels in diabetic rats

The level of NLRP3 in diabetic rats was found to be significantly ($p \leq 0.05$) high in diabetic rats by 131.7 % when compared to the control (Fig. 4.8). However cotreatment with CiA caused a significant reduction compared to the diabetic groups (26.8 % and 42.4 % for 5 and 10 mg/kg bwt respectively). Metformin treatment also decreased their levels by 47.7 % at 50 mg (Fig. 8). Similarly TxNIP levels were upregulated significantly in the hearts of diabetic rats by 112.5 % (Fig. 4.8). Cotreatment with CiA reduced their levels significantly by 124.6 % and 138.5 % at 5 and 10 mg/kg respectively. Treatment with metformin also drastically reduced their levels by 186.9 % compared to the diabetic group (Fig. 4.8).

4.3.12 pGSK-3β / GATA-4 axis upregulated during diabetes

Both pGSK-3β and GATA-4 levels were found significantly ($p \leq 0.05$) upregulated by 14.65 % and 22.45 % in the diabetic group compared to the control group (Fig. 4.8). CiA treated rats showed a decrease in the levels of pGSK-3β by 72.3 % (5 mg/kg) and 101.2 % (10 mg/kg) and GATA-4 by 43.2% (5 mg/kg) and 32.4 % (10 mg/kg) compared to the diabetic group (Fig. 4.8). Metformin treatment reduced the levels of pGSK-3β and GATA-4 significantly ($p \leq 0.05$) by 62.6 and 56.2 % respectively compared to the diabetic group (Fig.4.8).

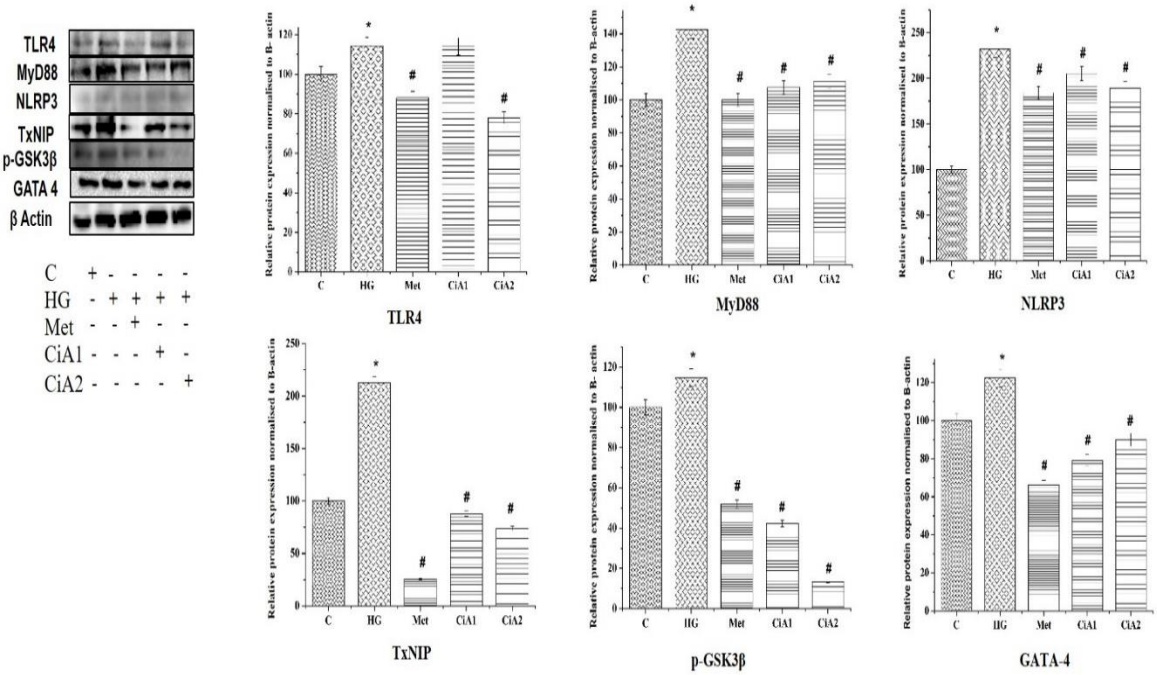

Fig. 4.8 Activation of the toll like receptor mediated inflammatory pathway in diabetic rats and the effect of cinnamic acid. C- control, HG - diabetic, Met- HG + metformin (50 mg/kg bwt), CiA1- HG + cinnamic acid (5 mg/kg bwt), CiA2- HG + cinnamic acid (10 mg/kg bwt). Representative immunoblots of TLR4, MyD88, NLRP3, TxNIP, pGSK-3β and GATA-4 and their respective densitometric quantifications normalised to β-actin. Values are expressed as mean ± SEM where n = 3. * $p \leq 0.05$ significantly different from the control group. # $p \leq 0.05$ significantly different from the diabetic group.

4.3.13 Diabetes increased relative gene expression of TGF-β and β-MHC

TGF - β and β - MHC was found to be significantly ($p \leq 0.05$) upregulated by 2.43 F and 2.18 F respectively in the diabetic group compared to the control (Fig. 4.9). Treatment with CiA at both concentrations (5 & 10 mg/kg) and metformin (50 mg/kg) prevented the upregulation of TGF - β and β - MHC gene expression significantly by 0. 48, 1.5, 1.6 F and 0.48, 0.75 and 1.2 F respectively compared to the diabetic group (Fig.4.9).

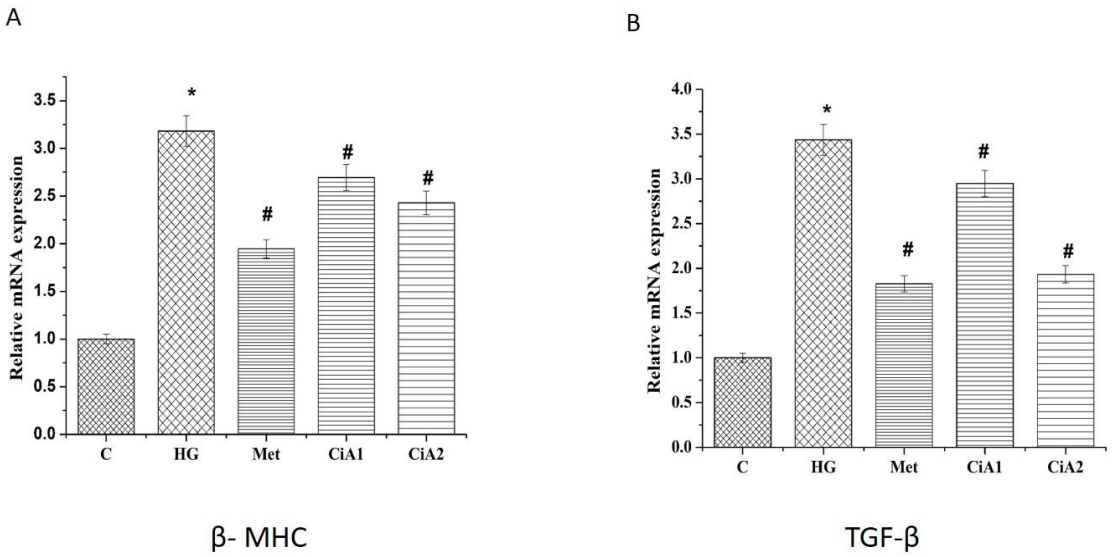

Fig. 4.9 Diabetes increased mRNA expression of β- MHC and TGF-β in rats. A) Representative mRNA levels of β- MHC normalised to β-actin; B) Representative mRNA levels of TGF-β normalised to β-actin. C- control, HG - diabetic, Met- HG + metformin (50 mg/kg bwt), CiA1- HG + cinnamic acid (5 mg/kg bwt), CiA2- HG + cinnamic acid (10 mg/kg bwt). Values are expressed as mean ± SEM where n = 3. * $p \leq 0.05$ significantly different from the control group. # $p \leq 0.05$ significantly different from the diabetic group.

4.3.14 Diabetes induced fibrosis and necrosis in the heart

Hematoxylin and eosin staining of the diabetic heart tissue showed inflammatory infiltration, edema, swollen capillaries and necrosis (Fig. 4.10A). Van gieson staining of the heart section showed severe collagen deposition compared to the control group (Fig. 4.10 B, arrowmark). The yellow colour represents erythrocytes and cytoplasm, and red colour represents collagen. However, the rats treated with CiA or metformin showed reduced levels of inflammation and normal myocardial fibres and also reduced collagen deposition and thus attenuated cardiac fibrosis (Fig. 4.10A&B).

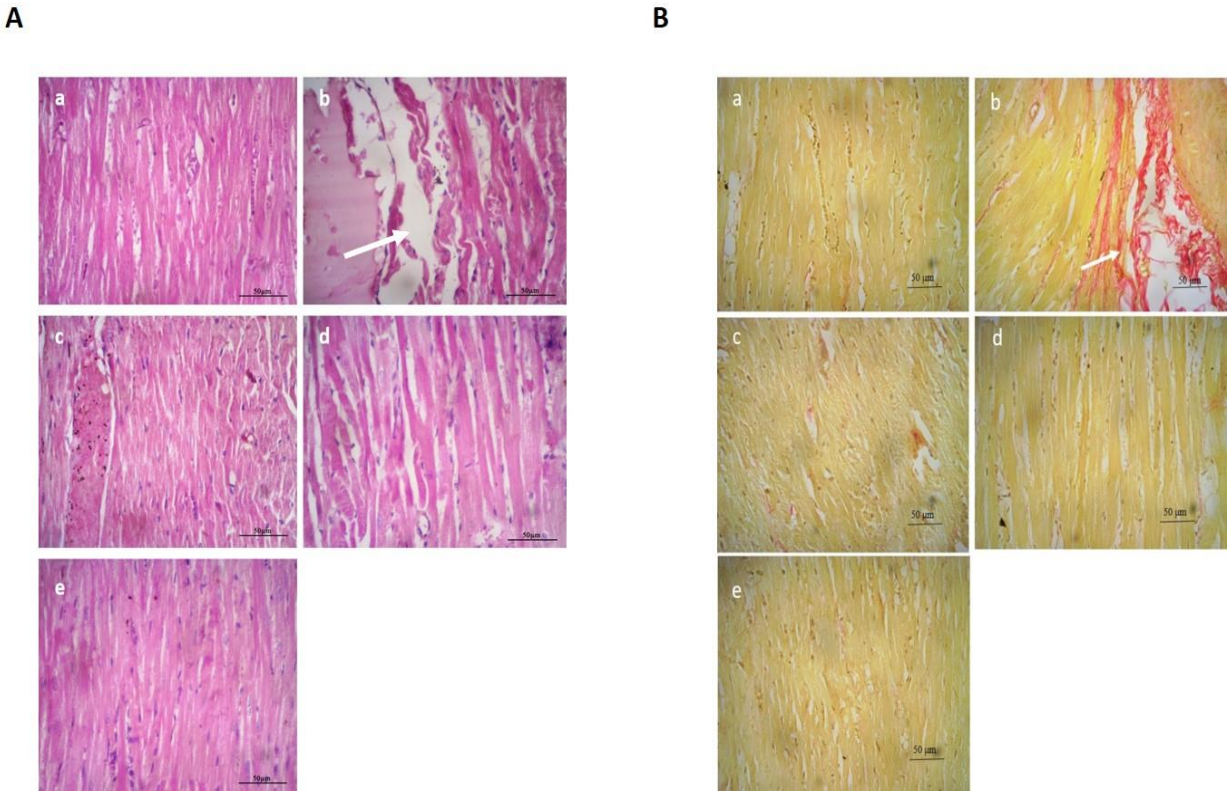

Fig. 4.10 Diabetes induced inflammatory infiltration and collagen deposition. Histopathological analysis of heart tissues. A) Hematoxylin and eosin staining; B) Van Geison staining a) control, b) diabetic (HG), c) HG + metformin (50 mg/kg bwt), d) HG + cinnamic acid (5 mg/kg bwt), e) HG + cinnamic acid (10 mg/kg bwt).

4.4 Discussion

The importance of biomarkers in diagnosing DCM is gaining popularity among researchers. Moreover the differences between the clinical manifestations of DCM due to T1DM and T2DM is still undistinguishable. Herein we have conducted an animal study in order to see whether the *in vitro* results are translated into *in vivo models*. For this a single low dose streptozotocin along with a high fat high fructose diet induced diabetic model (Zhao et al., 2017) of wistar rats were used to elucidate the role of various inflammatory pathways and their crosstalk in the genesis of DCM, to study the role of various markers of DCM and to assess the potential of CiA.

In order to curb the severe complications of a chronic disease like diabetes, early diagnosis particularly by non-invasive tools is necessary. Recently, research is

progressing towards the development of biomarkers for the easy and early diagnosis of the disease. The present study also began with determination of parameters that confirmed DCM. Glycated haemoglobin (HbA1c) is formed by the non-enzymatic glycation between glucose and N-terminal amino acids of beta chains of haemoglobin (Welsh et al., 2016). It is a well-known stable biomarker of long term glycemic control (Ewid et al., 2019). Since 2010 it has been an established diagnostic test for diabetic patients which is also used for the prediction of microvascular and macrovascular complications (Jovanovic et al., 2011). According to recent studies a correlation between high levels of HbA1c and increased risks of cardiovascular events in diabetic patients without a history of coronary artery disease has been found out (Wang et al., 2015). Also, American Heart Association and American Diabetes Association emphasized on the advantage of proper glycemic control in order to prevent the risk of cardiovascular diseases (Buse et al., 2007). In this study also there was an increase in the HbA1c level in the high fat high fructose fed rats. This indicates that the hyperglycemic condition prevails in these rats. Cotreatment with CiA and metformin significantly reduced the levels of HbA1c. However, according to certain reports it has been stated that intensive glycemic control alone has failed to protect the myocardium (Mazzone, 2010). Hence, several ongoing researches focus on the importance of correcting the metabolic imbalance that takes place in the diabetic myocardium.

The most distinctive feature of T2DM is insulin resistance (IR) (DeFronzo, 1988). The existence of insulin resistance is closely associated with certain risk factors of CVDs like hyperglycemia, dyslipidemia and increased blood pressure. Thus, IR can be considered to go hand in hand with CVDs in T2DM. This strongly implicates the necessity of drugs that are capable of enhancing insulin sensitivity. The drug metformin, which improves insulin sensitivity, was reported to reduce the prevalence of myocardial infarction according to UK Prospective Diabetes Study (UKPDS, 1998). The insulin resistance can be accurately predicted by the values of homeostasis model assessment (HOMA-IR) (Bonora et al., 2002). The existence of T2DM was confirmed in the current study by estimating HOMA-IR. Accordingly the diabetic rats showed higher HOMA-IR values than the control group. However, cotreatment with CiA lowered the HOMA-IR values significantly confirming the anti-diabetic property of CiA.

In addition to the HbA1c levels there are many other biomarkers used routinely to assess cardiovascular health. After confirming insulin resistance, we then analysed the

presence of cardiac injury markers. One such marker is troponin. Troponin levels were found to be significantly upregulated in the serum of diabetic rats while treatment with CiA at both concentrations reduced the levels of troponin. Troponin was first discovered by Ebashi and Kodama in 1965 (Park et al., 2017). The discovery of the distinct subunits of troponin by Greaser and Gergely in 1973 has led to the understanding of molecular physiology behind cardiac contraction (Greaser and Gergely, 1973). These findings paved the way for the development of one of the most successful diagnostic investigations to date i.e. cardiac troponin (cTn) assays (Park et al., 2017). Troponin is present in all forms of striated muscle including skeletal and cardiac muscle. But the cardiac specific troponin is distinguished by regions of different amino acid sequences. It has been considered as a gold standard biomarker for detecting acute myocardial infarction. There are three subunits for troponin: troponin I for '*inhibitory*' since it prevents the actin myosin interactions and cross bridge formation in the absence of Ca^{2+}, troponin T for '*tropomyosin*' which serves as the link between tropomyosin and troponin and troponin C for '*calcium*' which is the calcium binding subunit and regulates the activity of thin filament (Park et al., 2017). Generally, troponin is released in response to myocardial necrosis. The heart being a post-mitotic organ and because the cardiomyocyte is unable to repair injured cells, any protein that is released from the myocardium is considered to be a sign of necrosis (Mair et al., 2018). The three myocardial enzymes that facilitate the proteolytic degradation and release of troponin from the myofibril are calpain, caspase and matrix metalloproteinase 2 (Park et al., 2017). Cardiac troponin is usually released into circulation within a few hours after the onset of myocardial ischemia followed by the clearance of the interstitial fluid from the infarct zone by the cardiac lymphatic system.

Zhao et al found a strong interaction between cTnI and a protein kinase called cardiac troponin I interacting kinase (TNNI3K) by using a yeast two hybrid screen (Tang et al., 2013; Zhao et al., 2003). TNNI3K also known as cardiac ankyrin repeat kinase (CARK) is known to play a very important role in cardiac functions like cardiac growth, contractility and repair. It is a cardiac specific tyrosine kinase that belongs to the MAP3K family (Vagnozzi et al., 2013; Lai and Chen, 2012). It consists of three structural domains: ten copies of seven ankyrin repeat near the N terminal region, a protein (Ser/ Thr and Tyr) kinase domain, and a C-terminal Ser rich domain. Not much is known about the biology of TNNI3K. It was known to induce cardiac hypertrophy in neonatal rat ventricular cardiomyocytes (Wang et al., 2011). In a calsequestrin transgenic mouse

model of dilated cardiomyopathy, TNNI3K overexpression led to premature heart failure and death (Wheeler et al., 2009). Similarly the TNNI3K expressed mouse model of left ventricular pressure overload induced by transverse aortic constriction also showed significant disease progression (Wheeler et al., 2009). Some studies have also reported that TNNI3K overexpression induces ventricular remodeling (Vagnozzi et al., 2013). According to a recent study, TNNI3K expression was observed to be high in the heart tissue from patients with end stage dilated cardiomyopathy when compared with the healthy controls (Colak et al., 2009). In the present study also, TNNI3K levels were upregulated in the serum of diabetic rats and treatment with CiA at both concentrations reduced their levels significantly. However, another group also showed that TNNI3K has some protective functions whereby the overexpression of TNNI3K increased the beating mass and induced cardiac myogenesis in P19CL6 cells (Lai et al., 2008). According to them TNNI3K promoted cardiac differentiation by increasing the number of cardiac α actinin cells, enhanced beating frequency and contractility, improved overall cardiac performance and attenuates ventricular remodeling induced by myocardial infarction (Lai et al., 2008). But the high profile studies with genetically modified animals strongly suggested that the overexpression of this particular protein is mostly associated with detrimental phenotype (Lal et al., 2014). These results indicate that the biology of TNNI3K including its downstream targets needs to be elucidated more. Thus TNNI3K can be considered as a potential therapeutic target of kinase inhibitors in heart disease.

Since hypertrophy is one of the major outcome of DCM, the levels of a prohypertrophic factor called BNP were also determined. Natriuretic peptides are another major indicator of cardiac hypertrophy. They are known to induce natriuresis i.e. excretion of sodium by the kidneys. ANP, BNP and C-type natriuretic peptides are some of the examples of natriuretic peptides. These peptides are mainly secreted in response to myocardial strain (Iqbal et al., 2012). BNP is mainly synthesised and secreted by the left ventricular myocytes in response to stretch due to pressure overload and expansion of the ventricle by volume. It is a well-known diagnostic biomarker of heart failure. A prohormone called pre-proBNP, a 134 amino acid molecule, is cleaved to form pro BNP (108 amino acid molecule). The proBNP precursor is split by the convertases corin and furin to form active BNP and inactive NT proBNP (Cao et al., 2019) which are released into the plasma. The plasma BNP then binds to a receptor called NP receptor A that triggers a signalling cascade that leads to natriuresis, diuresis and arterial vasodilation

(Gaggin and Januzzi, 2013; Iqbal et al., 2012). The half-life of BNP is 20 min while that of NT-proBNP is 90-120 min (Cao et al., 2019; Iqbal et al., 2012) making latter a better prognostic marker of heart failure. BNP is usually cleared from the plasma by receptor mediated endocytic mechanism or renal filtration (Gaggin and Januzzi, 2013). In the present study, the serum of diabetic group showed elevated levels of both ANP and BNP and treatment with CiA lowered their levels significantly. However, metformin did not show any change in the levels of BNP levels.

Various other non-specific protein markers also exist that help the diagnosis of myocardial injury. One of the first biomarker used to diagnose myocardial infarction was serum glutamate transaminase (SGOT). Later it was found that SGOT is not a specific marker for heart and its levels in the blood also increases due to hepatic disease and other conditions. This initiated the discovery of other cytoplasmic enzymes like lactate dehydrogenase and creatine kinase (Bodor, 2016). LDH is a soluble enzyme expressed in organs like heart, skeletal muscle, kidney, liver, and erythrocytes. It has five isoenzymes out of which LDH 1 is expressed in the heart (Aydin et al., 2019). Nowadays, LDH is mainly used to distinguish between acute MI and subacute MI and also for detecting erythrocyte hemolysis (Aydin et al., 2019; Jialal and Sokoll, 2015). Another biomarker used to detect cardiac injury is creatine kinase -MB (CK-MB). After the advent of radioimmunoassay in 1970 CK was considered to be a better predictor for cardiac injury (Walsh et al., 1970). CK is an enzyme that catalyses the reversible conversion of creatine and ATP to creatine phosphate and ADP. It is a dimeric enzyme which consists of two subunits: M and B. It has three isoenzymes: CK-BB, CK-MB and CK-MM. Among these CK-MB is found in the heart and skeletal muscle. However, a higher proportion of CK-MB is found in the heart compared to the skeletal muscle. CK-MB elevations in the plasma is a specific evidence of myocardial cell death and also helps in distinguishing non ST elevations from unstable angina (Bodor, 2016). It is a predictor of acute myocardial infarction. Their levels start to increase after 4-9 hours after infarction which reaches peak at 24 hrs and reaches the normal range after 48-72 hrs. However, in the presence of a concurrent liver and skeletal muscle disease and even after a strenuous exercise these enzymes were found to be released into the bloodstream making them unsuitable as an ideal biomarker for heart disease alone. In the present study, estimation of the levels of these non-specific markers in the serum of diabetic groups also confirmed myocardial injury and treatment with

metformin at 50 mg/kg bwt and CiA at 5 and 10 mg/kg bwt reduced the levels of injury markers. This indicates the therapeutic potential of CiA against cardiovascular diseases.

Dyslipidemia is one of the characteristic features of DCM. The principal reason behind abnormal lipid profile in diabetics is due to the alterations taking place in the plasma lipoproteins (Goldberg, 2001). Lipoproteins are those that help in the transport of insoluble lipids through plasma. They are mainly seen circulating in the blood as low density lipoprotein (LDL), high density lipoprotein (HDL), very low density lipoproteins (VLDL), chylomicrons etc. Increased lipolysis due to insulin resistance causes the release of more fatty acids from the adipocytes (Goldberg, 2001). Fatty acids are thus transported to the liver which further initiates VLDL secretion. VLDL secretion contributes to elevations in serum triglyceride levels. Increased triglyceride levels prevents the degradation of Apo-B which further accounts for the increased VLDL formation and secretion. Increased triglyceride and reduced HDL levels are common to both T1DM and T2DM. However, in T2DM the LDL proteins are further converted to more atherogenic lipoproteins termed small dense LDL. Moreover, the lipoprotein abnormality in T1DM can be corrected with glycemic control. However, it has been reported that prediabetic patients with pronounced insulin resistance and normal plasma glucose levels show dyslipidemia (Haffner et al., 2000). Thus it is insulin resistance responsible for the dyslipidemic condition in T2DM and not hyperglycemia. According to a recent study low HDL cholesterol is an independent factor for both cardiovascular disease and diabetes (Abbasi et al., 2013). Several epidemiological studies have reported the association of higher levels of LDL cholesterol and low HDL cholesterol with high incidence of cardiovascular diseases even in nondiabetic patients (Feingold and Siperstein, 1986; Fox et al., 2015). The increase in serum triglyceride levels are also found to be associated with cardiovascular disease in diabetic patients (Martin-Timon et al., 2014) In our diabetic model also there was an increase in total cholesterol, triglycerides and LDL cholesterol and treatment with CiA and metformin significantly reduced the same. Similarly, HDL levels were significantly lowered in the diabetic group and treatment with compound and positive control enhanced their levels. It has been noted that with proper lipid and blood pressure control the risk of developing cardiovascular diseases has reduced recently even in patients with diabetes (Low et al., 2016). Thus maintaining a healthy lipid profile is essential for proper cardiac health.

As observed in the study, there was a release of cardiac injury markers and alterations in lipid profile in the diabetic group which was attenuated by CiA treatment. However, the reason behind the myocardial injury and dyslipidemia may be residing at the molecular level. Hence emphasis was given to inflammation. Myocardial inflammation plays an important role in the development of various pathophysiological processes like cardiac hypertrophy, fibrosis and ventricular remodeling (Frieler and Mortenson, 2015; Prabhu and Frangogiannis, 2016). The visceral adipocytes are known to secrete cytokines and chemokines in subjects with metabolic syndrome and diabetes (Grundy, 2016). This results in the occurrence of a subclinical low grade systemic inflammation also called para-inflammation. The circulating proinflammatory mediators like TNF-α and IL-6 are the main factors responsible for aggravating insulin resistance. Previous studies have reported that higher levels of inflammatory mediators are responsible for the development of heart failure associated with metabolic syndrome (Bahrami et al., 2008). Excess glucose, lipids and various other stressors within cardiomyocytes are responsible for the secretion of cytokines, chemokines (MCP-1) and adhesion molecules (VCAM, ICAM) which in turn promote infiltration of monocytes and lymphocytes to the myocardium (Mann, 2015). The major difference between chronic myocardial inflammation due to metabolic syndrome and inflammation due to viral myocarditis is that the chronic myocardial inflammation is subclinical and associated with development of cardiac abnormalities in the long term whereas the heart failure due to latter occurs in a rapid manner (Frati et al., 2017). Leukocyte infiltration results in the production of reactive oxygen species and also causes the release of profibrotic factors leading to cardiac fibrosis. One of the main factors responsible for leukocyte infiltration is the presence of chemokine monocyte chemoattractant protein-1 (MCP-1). According to many recent reports, it was found that chronic remodeling is reduced by preventing the recruitment of monocytes in the heart. Also neutralisation of ICAM by antibodies reduced macrophage infiltration, cardiac fibrosis and preserved cardiac structure and function (Kuwahara et al., 2003). Another independent risk factor for cardiovascular disease is CRP which is an important marker of systemic inflammation (Ridker et al., 2001). High CRP levels have been linked to an increased risk of thrombotic events including myocardial infarction (Kervinen et al., 2001). Inflammation was confirmed in the present study by the increased levels of MCP-1, CRP and nitrite. CiA and metformin treated groups showed significant reduction in their levels.

In the diabetic heart, inflammation is mainly mediated by the action of damage associated with molecular pattern molecules on toll like receptors (TLRs) like TLR2 and TLR4 (Sciarretta et al., 2009; Yan et al., 2003). This initiates a signalling cascade that includes the MAPK pathways which ultimately converge towards the activation of nuclear factor kappa-light-chain-enhancer of activated B cells (NF-Kb) (Prabhu and Frangogiannis, 2016). Mediators resulting from this inflammatory cascade in turn modulate specific intracellular signalling mechanisms in cardiac cells causing cardiomyocyte hypertrophy, mitochondrial dysfunction, endoplasmic reticulum (ER) stress and cell death, fibroblast proliferation, and collagen production. Activation of MAPK pathways is known to stimulate TNF-α and IL-6 secretion (Volz et al., 2010). Also, studies using TNF- α antagonists lowered myocardial inflammation, leukocyte infiltration and fibrosis in streptozotocin-induced diabetic rats. Similarly genetic ablation of IL-6 in mice also reduced cardiac inflammation and fibrosis and preserved cardiac function (González et al., 2015). Recent reports also emphasizes the role of nucleotide-binding oligomerization domain-like receptor protein 3 (NLRP3)-dependent inflammasome in the development of DCM (Luo et al., 2014) because the inflammasomes serve as a link between inflammation and metabolic disorders (Nagashima et al., 2011). There is evidence for reduced type 2 diabetes-induced cardiac inflammation, pyroptosis and fibrosis in diabetic rat models in which NLRP3 inflammasome complex has been inhibited (Luo et al., 2014). Several downstream inflammatory events occurring due to glycotoxicity and lipotoxicity during the pathogenesis of T2DM are also known to be initiated by the activation of NLRP3 inflammasomes (Vandanmagsar et al., 2011). In obese mice and also in human subjects the expression of cardiac NLRP3, caspase 1 and IL-1β was found to be substantially increased (Vandanmagsar et al., 2011). NLRP3 inflammasome complex assembly is mediated by a protein known as thioredoxin interacting protein (TxNIP) (Zhou et al., 2010). In summary during diabetes high glucose activates the TLRs which triggers ROS production in the heart which in turn leads to the translocation of NFkB and activation of the inflammasome complex. NLRP3 signalling is also known to affect glycolysis and enhance local myocardial cytokine levels and aggravate macrophage infiltration (Wen et al., 2012). Diabetes also exerts its detrimental effects in the heart through the activation of GSK-3β/GATA-4, JNK/ERK/p38 MAPK pathway and by the upregulation of OGlcNAc (Frati et al., 2017) (refer chapter 5 for detailed explanation). In our study also there was an activation of the TLR4 mediated

inflammatory pathway in the diabetic group. This triggered a cascade of intracellular signalling pathways involving MAPK (JNK, ERK and p38 MAPK) which led to the activation of the inflammasome complex. Parallel to this the GSK-3β/GATA-4 axis and the hexosamine signalling pathway was also activated in the diabetic model. CiA and metformin treated rats prevented the activation of the inflammatory pathway.

Hypertrophy and fibrosis are the two important consequences of DCM (Hölscher et al., 2016). Cardiac fibrosis is primarily due to the deposition of stiff collagen and its crosslinking. Fibrosis was confirmed in the heart of diabetic animals in this study with histopathology (Van Gieson) of the heart. Hematoxylin-eosin staining showed a complete disarray of myofibrils, with inflammatory infiltration, edema and necrosis. CiA or metformin treatment however reduced cardiac fibrosis, lowered the levels of infiltration, necrosis and prevented the disarray of myofibrils. Moreover, hypertrophy was further confirmed with high cardiac mass index, elevated gene expression of TGF-β and β –MHC in the heart tissue of diabetic rats which was again reversed by treatment with CiA and metformin. TGF-β and β-MHC are proteins involved in the pathogeneisis of cardiac hypertrophy. TGF-β induces the extracellular matrix protein deposition and thus mediates cardiac hypertrophy and ventricular remodeling (Rosenkranz, 2004).

CiA and its derivatives have gained much attention recently due to its beneficial health properties. Oral administration of cinnamic acid in mice has shown rapid absorption and distribution with 96 % bioavailability (Chen et al., 2009). Hippuric acid is the major excretory product of cinnamic acid metabolism. Several pharmacokinetic studies have shown that cinnamic acid can easily be absorbed by small intestine by passive diffusion, monocarboxylic acid transporters (Konishi et al., 2004; Zhao and Moghadasian ,2008) and is actively transported by a Na^+ dependent transport mechanism in rat jejunum (Ader et al., 1996). In our study we have observed a decrease in the cardiac injury markers like BNP, troponin and TNNI3K, inflammatory markers (CRP, MCP-1) in the rats treated with CiA at both concentrations (5 & 10 mg/kg bwt). Similarly it reduced the blood glucose and the glycated Hb levels after two months treatment. We have also found that the inflammatory pathway involving TLR4, NLRP3 inflammasome and GSK-3β/GATA-4 axis is downregulated following treatment of rats with CiA at 5 and 10 mg/kg bwt validating its anti-inflammatory property.

References

1. Abbasi A, Corpeleijn E, Gansevoort RT, Gans RO, Hillege HL, Stolk RP, et al. Role of HDL cholesterol and estimates of hdl particle composition in future development of Type 2 diabetes in the general population: The PREVEND Study. J. Clin. Endocrinol. Metab. 2013; 98: E1352-E1359.
2. Ader P, Grenacher B, Langguth P, Scharrer E, Wolffram S. Cinnamate uptake by rat small intestine: transport kinetics and transepithelial transfer. Exp. Physiol. 1996; 81: 943-955.
3. Aneja A, Tang WHW, Bansilal S, Garcia MJ, Farkouh ME. Diabetic cardiomyopathy: insights into pathogenesis, diagnostic challenges, and therapeutic options. Am. J. Med. 2008; 121: 748-757.
4. Aydin S, Ugur K, Aydin S, Sahin İ, Yardim M. Biomarkers in acute myocardial infarction: current perspectives. Vasc. Health Risk Manag. 2019; 15: 1-10.
5. Bahrami H, Bluemke DA, Kronmal R, Bertoni AG, Lloyd-Jones DM, Shahar E, et al. Novel metabolic risk factors for incident heart failure and their relationship with obesity: The MESA (Multi-Ethnic Study of Atherosclerosis) Study. J. Am. Coll. Cardiol. 2008; 51: 1775-1783.
6. Bodor GS. Biochemical markers of myocardial damage. EJIFCC. 2016; 27: 95-111.
7. Bonora E, Formentini G, Calcaterra F, Lombardi S, Marini F, Zenari L, et al. HOMA-estimated insulin resistance is an independent predictor of cardiovascular disease in type 2 diabetic subjects: prospective data from the Verona diabetes complications study. Diabetes Care, 2002; 25: 1135-1141.
8. Buse JB, Ginsberg HN, Bakris GL, Clark NG, Costa F, Eckel R et al. Primary prevention of cardiovascular diseases in people with diabetes mellitus: a scientific statement from the American Heart Association and the American Diabetes Association. Circulation. 2007; 115: 114-126.
9. Cao Z, Jia Y, Zhu B. BNP and NT-ProBNP as diagnostic biomarkers for cardiac dysfunction in both clinical and forensic medicine. Int. J. Mol. Sci. 2019; 20: 1820.
10. Chen Y, Ma Y, Ma W. Pharmacokinetics and bioavailability of cinnamic acid after oral administration of ramulus cinnamomi in rats. Eur.J. Drug Metab. Pharmacokinet. 2009; 34: 51-56.
11. Colak D, Kaya N, Al-Zahrani J, Al Bakheet A, Muiya P, Andres E, et al. Left ventricular global transcriptional profiling in human end-stage dilated

cardiomyopathy. Genomics. 2009; 94: 20-31.

12. Dahlström U. Can natriuretic peptides be used for the diagnosis of diastolic heart failure? Eur. J. Heart Fail. 2004; 6: 281-287.
13. DeFronzo RA. "The triumvirate: B-cell, muscle, liver: a collusion responsible for NIDDM." Diabetes. 1988; 37: 667-687.
14. Ewid M, Sherif H, Billah SMB, Saquib N, AlEnazy W, Ragab O, et al. "Glycated hemoglobin predicts coronary artery disease in non-diabetic adults." BMC Cardiovasc. Disord. 2019; 19: 309.
15. Feingold KR, Siperstein MD. Diabetic vascular disease." Adv. Intern. Med . 1986; 31: 309-340.
16. Fox CS, Golden SH, Anderson C, Bray GA, Burke LE, de Boer IH, et al. "Update on prevention of cardiovascular disease in adults with type 2 diabetes mellitus in light of recent evidence: a scientific statement from the American Heart Association and the American Diabetes Association." Diabetes Care. 2015; 38: 1777-1803.
17. Frati G, Schirone L, Chimenti I, Yee D, Biondi-Zoccai G, Volpe M, et al. An overview of the inflammatory signalling mechanisms in the myocardium underlying the development of diabetic cardiomyopathy. Cardiovas. Res. 2017; 113: 378-388.
18. Frieler RA, Mortensen RM. Immune cell and other noncardiomyocyte regulation of cardiac hypertrophy and remodeling. Circulation. 2015; 131: 1019-1030.
19. Fuentes-Antras J, Picatoste B, Gomez-Hernandez A, Egido J, Tunon J, Lorenzo O. Updating experimental models of diabetic cardiomyopathy. J. Diabetes Res. 2015; 2015: 656795.
20. Gaggin HK, Januzzi JL Jr. Biomarkers and diagnostics in heart failure. Biochim. Biophys. Acta. 2013; 1832: 2442-2450.
21. Goldberg IJ. Diabetic dyslipidemia: causes and consequences. J. Clin. Endocrinol. Metab. 2001; 86: 965-971.
22. Gomes AV, Potter JD, Szczesna-Cordary D. The role of troponins in muscle contraction. IUBMB Life. 2002; 54: 323-333.
23. González GE, Rhaleb NE, D'Ambrosio MA, Nakagawa P, Liu Y, Leung P, et al. Deletion of interleukin-6 prevents cardiac inflammation, fibrosis and dysfunction without affecting blood pressure in angiotensin II-high salt-induced hypertension. J. Hypertens. 2015; 33: 144-152.

24. Greaser ML, Gergely J. Purification and properties of the components from troponin. J. Biol. Chem. 1973; 248: 2125-2133.
25. Grundy SM. Metabolic syndrome update. Trends Cardiovasc. Med. 2016; 26: 364-373.
26. Haffner SM, Mykkanen L, Festa A, Burke JP, Stern MP. Insulin-resistant prediabetic subjects have more atherogenic risk factors than insulin-sensitive prediabetic subjects: implications for preventing coronary heart disease during the prediabetic state. Circulation. 2000; 101: 975-980.
27. Hölscher ME, Bode C, Bugger H. Diabetic cardiomyopathy: does the type of diabetes matter? Int. J. Mol. Sci. 2016; 17: 2136.
28. Iqbal N, Wentworth B, Choudhary R, Landa Ade L, Kipper B, Fard A, et al. Cardiac biomarkers: new tools for heart failure management. Cardiovasc. Diagn. Ther. 2012; 2: 147-164.
29. Jialal I, Sokoll LJ. Clinical utility of lactate dehydrogenase: a historical perspective. Am. J. Clin. Pathol. 2015; 143: 158-159.
30. Jovanovic L, Savas H, Mehta M, Trujillo A, Pettitt DJ. Frequent monitoring of A1C during pregnancy as a treatment tool to guide therapy. Diabetes Care. 2011; 34: 53-54.
31. Kervinen H, Palosuo T, Manninen V, Tenkanen, Manttari M L, Vaarala O. Joint effects of c-reactive protein and other risk factors on acute coronary events. Am. Heart J . 2001; 141: 580-585.
32. Konishi Y, Hitomi Y, Yoshioka E. Intestinal absorption of p-coumaric and gallic acids in rats after oral administration. J. Agric. Food Chem. 2004; 52: 2527-2532.
33. Kuwahara F, Kai H, Tokuda K, Niiyama H, Tahara N, Kusaba K, et al. Roles of intercellular adhesion molecule-1 in hypertensive cardiac remodeling. Hypertension. 2003; 41: 819-823.
34. Lai ZF, Chen YZ. Evidence, hypotheses and significance of MAP Kinase TNNI3K Interacting with Its Partners. World J. Hypertens. 2012; 2: 22-28.
35. Lai ZF, Chen YZ, Feng LP, Meng XM, Ding JF, Wang LY, et al. Overexpression of TNNI3K, a cardiac- specific map kinase, promotes p19cl6-derived cardiac myogenesis and prevents myocardial infarction-induced injury. Am. J. Physiol. Heart Circ. Physiol. 2008; 295: H708-H716.
36. Lal H, Ahmad F, Parikh S, Force T. Troponin I-interacting protein kinase: a novel

cardiac-specific kinase, emerging as a molecular target for the treatment of cardiac disease. Circ. J. 2014; 78: 1514-1519.

37. Lorenzo-Almorós A, Tuñón J, Orejas M, Cortés M, Egido J, Lorenzo Ó. Diagnostic approaches for diabetic cardiomyopathy. Cardiovasc. Diabetol. 2017; 16: 28.
38. Low Wang CC, Hess CN, Hiatt WR, Goldfine AB. Clinical Update: Cardiovascular disease in diabetes mellitus: atherosclerotic cardiovascular disease and heart failure in type 2 diabetes mellitus - mechanisms, management, and clinical considerations. Circulation. 2016; 133: 2459-2502.
39. Luo B, Li B, Wang W, Liu X, Xia Y, Zhang C, et al. NLRP3 gene silencing ameliorates diabetic cardiomyopathy in a type 2 diabetes rat model. PloS One. 2014; 9: e104771.
40. Manach C, Scalbert A, Morand C, Rémésy C, Jiménez L. Polyphenols: food sources and bioavailability. Am. J. Clin. Nutr. 2004; 79: 727-747.
41. Mair J, Lindahl B, Hammarsten O, Müller C, Giannitsis E, Huber K, et al. How is cardiac troponin released from injured myocardium? Eur. Heart J. Acute Cardiovasc. Care. 2018; 7: 553-560.
42. Mann DL. Innate immunity and the failing heart: the cytokine hypothesis revisited. Circ. Res. 2015; 116: 1254-1268.
43. Martin-Timon I, Sevillano-Collantes C, Segura-Galindo A, Del Canizo-Gomez FJ. Type 2 diabetes and cardiovascular disease: have all risk factors the same strength? World J. Diabetes. 2014; 5: 444-470.
44. Mazzone T. Intensive glucose lowering and cardiovascular disease prevention in diabetes reconciling the recent clinical trial data. Circulation. 2010; 122: 2201-2211.
45. Nagashima M, Watanabe T, Terasaki M, Tomoyasu M, Nohtomi K, Kim-Kaneyama J, et al. Native incretins prevent the development of atherosclerotic lesions in apolipoprotein e knockout mice. Diabetologia. 2011; 54: 2649-2659.
46. Park KC, Gaze DC, Collinson PO, Marber MS. Cardiac troponins: from myocardial infarction to chronic disease. Cardiovasc. Res. 2017; 113: 1708-1718.
47. Prabhu SD, Frangogiannis NG. The biological basis for cardiac repair after myocardial infarction: from inflammation to fibrosis. Circ. Res. 2016; 119: 91-112.
48. Reed MJ, Meszaros K, Entes LJ, Claypool MD, Pinkett JG, Gadbois TM et al. A new rat model of type 2 diabetes: the fat-fed, streptozotocin-treated rat metabolism.

2000; 49: 1390-1394.

49. Ridker PM, Rifai N, Lowenthal SP. Rapid reduction of c-reactive protein with cerivastatin among 785 patients with primary hypercholesterolemia. Circulation. 2001; 103: 1191-1193.
50. Rosenkranz S. TGF-beta1 and angiotensin networking in cardiac remodeling. Cardiovasc. Res. 2004, 63: 423-432.
51. Smail MMA, Howarth CF, Singh J, Ismail AM. Inflammation and diabetic cardiomyopathy. inTechopen. doi: 10.5772/intechopen.88149.
52. Sciarretta S, Paneni F, Palano F, Chin D, Tocci G, Rubattu S, et al. Role of the renin-angiotensin-aldosterone system and inflammatory processes in the development and progression of diastolic dysfunction. Clin. Sci. (Lond). 2009; 116: 467-477.
53. Severson D. Diabetic cardiomyopathy: recent evidence from mouse models of type 1 and type 2 diabetes. Can. J. Physiol. Pharmacol. 82: 813-823.
54. Srinivasan K, Viswanad B, Asrat L, Kaul CL, Ramarao P. Combination of high-fat diet-fed and low-dose streptozotocin-treated rat: a model for type 2 diabetes and pharmacological screening. Pharmacol. Res. 2005; 52: 313-320.
55. Tan Y, Zhang Z, Zheng C, Wintergerst KA, Keller BB, Cai L. Mechanisms of diabetic cardiomyopathy and potential therapeutic strategies: preclinical and clinical evidence. Nat. Rev. Cardiol. 2020; 17: 585-607.
56. Tanaka S, Hayashi T, Toyoda T, Hamada T, Shimizu Y, Hirata M, et al. High-fat diet impairs the effects of a single bout of endurance exercise on glucose transport and insulin sensitivity in rat skeletal muscle. Metabolism. 2007; 56: 1719-1728.
57. Tang H, Xiao K, Mao L, Rockman HA, Marchuk DA. Overexpression of TNNI3K, a cardiac-specific MAPKKK, promotes cardiac dysfunction. J. Mol. Cell. Cardiol. 2013; 54: 101-111.
58. Tillquist MN, Maddox TM. Update on diabetic cardiomyopathy: inches forward, miles to go. Curr. Diab. Rep. 2012; 12: 305-313.
59. UK Prospective Diabetes Study (UKPDS) Group: Effect of intensive blood glucose control with metformin on complications in overweight patients with type 2 diabetes (UKPDS 34). Lancet. 1998; 352:854-865,
60. Vagnozzi RJ, Gatto GJ Jr, Kallander LS, Hoffman NE, Mallilankaraman K, Ballard VL, et al. Inhibition of the cardiomyocyte-specific kinase tnni3k limits oxidative stress, injury, and adverse remodeling in the ischemic heart. Sci. Transl. Med. 2013; 5:

207.

61. Vandanmagsar B, Youm YH, Ravussin A, Galgani JE, Stadler K, Mynatt RL, et al. The NLRP3 inflammasome instigates obesity-induced inflammation and insulin resistance. Nat. Med. 2011; 17: 179-188.
62. Vasanji Z, Cantor EJ, Juric D, Moyen M, Netticadan T. Alterations in cardiac contractile performance and sarcoplasmic reticulum function in sucrose-fed rats is associated with insulin resistance. Am. J. Physiol. Cell Physiol. 2006; 291: C772-C780.
63. Volz HC, Seidel C, Laohachewin D, Kaya Z, Muller OJ, Pleger ST, et al. HMGB1: The missing link between diabetes mellitus and heart failure. Basic Res. Cardiol. 2010; 105: 805-820.
64. Voulgari C, Papadogiannis D, Tentolouris N. Diabetic cardiomyopathy: from the pathophysiology of the cardiac myocytes to current diagnosis and management strategies. Vasc. Health Risk. Manag. 2010; 6: 883-903.
65. Walsh JH, Yalow R, Berson SA. Detection of australia antigen and antibody by means of radioimmunoassay techniques. J. Infect. Dis. 1970; 121: 550-554.
66. Wang L, Wang H, Ye J, Xu RX, Song L, Shi N, et al. Adenovirus-mediated overexpression of cardiac troponin i-interacting kinase promotes cardiomyocyte Hypertrophy. Clin. Exp. Pharmacol. Physiol. 2011; 38: 278-284.
67. Wang P, Huang R, Lu S, Xia W, Sun H, Sun J, et al. HbA1c below 7% as the goal of glucose control fails to maximize the cardiovascular benefits: A Meta-Analysis. Cardiovasc. Diabetol. 2015; 14: 1241-1251.
68. Welsh KJ, Kirkman MS, Sacks DB. Role of glycated proteins in the diagnosis and management of diabetes: research gaps and future directions. Diabetes Care. 2016; 39: 1299-1306.
69. Wen H, Ting JP, O'Neill LA. A role for the nlrp3 inflammasome in metabolic diseases—did Warburg miss inflammation? Nat. Immunol. 2012; 13: 352-357.
70. Wheeler FC, Tang H, Marks OA, Hadnott TN, Chu PL, Mao L, et al. Tnni3k modifies disease progression in murine models of cardiomyopathy. PLoS Genet. 2009; 5: e1000647.
71. Yan SF, Ramasamy R, Naka Y, Schmidt AM. Glycation, inflammation, and RAGE: A scaffold for the macrovascular complications of diabetes and beyond. Circ. Res. 2003; 93: 1159-1169.

72. Zhang M, Lv XY, Li J, Xu ZG, Chen L. The characterization of high-fat diet and multiple low-dose streptozotocin induced type 2 diabetes rat model. Exp. Diabetes Res. 2008; 2008: 704045.
73. Zhao MX, Zhou B, Ling L, Xiong XQ, Zhang F, Chen Q, et al. Salusin-β contributes to oxidative stress and inflammation in diabetic cardiomyopathy. Cell Death Dis. 2017; 8(3): e2690.
74. Zhou R, Tardivel A, Thorens B, Choi I, Tschopp J. Thioredoxin-interacting protein links oxidative stress to inflammasome activation. Nature Immunology. 2010; 11: 136-140.
75. Zhao S, Chu Y, Zhang C, Lin Y, Xu K, Yang P, et al. Diet-induced central obesity and insulin resistance in rabbits. J. Anim. Physiol. Anim. Nutr. (Berl). 2008, 92: 105-111.
76. Zhao Y, Meng XM, Wei YJ, Zhao XW, Liu DQ, Cao HQ. Cloning and characterization of a novel cardiac-specific kinase that interacts specifically with cardiac troponin I. J. Mol. Med. 2003; 81: 297-304.
77. Zhou YT, Grayburn P, Karim A, Shimabukuro M, Higa M, Baetens D, et al. Lipotoxic heart disease in obese rats: implications for human obesity. Proc. Natl. Acad. Sci .U S A. 2000; 97: 1784-1789.
78. Zhao Z, Moghadasian MH. Chemistry, natural sources, dietary intake and pharmacokinetic properties of ferulic acid: a review. Food Chem. 2008; 109: 691-702.

Chapter 5

Elucidation of mechanisms involved in the upregulation of inflammation during diabetic cardiomyopathy

5.1 Introduction

Recently myocardial inflammation is thought to be a responsible factor for the development of pathogenesis related to DCM (Frati et al., 2017; Frieler and Mortensen, 2015). Multiple inflammatory signalling pathways which are closely linked to insulin resistance are triggered during diabetes (Frieler and Mortensen, 2015). Most of these pathways focus towards stimulation of NFkB (Baker et al., 2011) which results in the production of various proinflammatory mediators like cytokines, chemokines and adhesion molecules in cardiac cells (Kaminska, 2005). A study has reported that overexpression of IkB protein prevented DCM in streptozotocin induced transgenic mouse (Thomas et al., 2014) indicating the importance of NFkB activation in the progression of DCM.

In the diabetic myocardium, the inflammatory mechanisms are known to act via the TLRs. TLR-2 and TLR-4 expression is found to be increased in dilated cardiomyopathy (Ma et al., 2012). TLR-4 gene deletion in streptozotocin induced mice improved cardiac function and prevented myocardial steatosis (Dong et al., 2012). IL-6 secretion is mainly attributed to TLR4 activation according to Boyd et al (Boyd et al., 2006). The TLRs are responsible for the activation of the downstream mitogen- activated protein kinase (MAPK) cascade (Aggarwal, 2003). Three major MAPK pathways include the JNK, ERK, and p38 MAPK pathways (Kaminska, 2005; Pearson et al., 2001; Jia et al., 2018). The outcome of this inflammatory burst is increased reactive oxygen species production, mitochondrial dysfunction, endoplasmic reticulum stress, collagen production and cardiomyocyte hypertrophy (Frieler and Mortensen, 2015; Prabhu and Frangogiannis, 2016). Also, the generation of the inflammatory mediators might interfere with the contractile properties of the myocardium (Prabhu and Frangogiannis, 2016). All these factors cumulatively contribute to the development of DCM.

The role of MAPK pathways in regulating cardiac hypertrophy and remodeling during DCM has not been elucidated in detail (Nunes et al., 2012; Jia et al., 2016). The

importance of p38 MAPK in the development of LV dysfunction during DCM has been reported by Westermann et al. (Westermann et al., 2006). Also, recent study showed that inhibition of TGF-β/ERK pathway by PPARγ attenuates DCM in vitro and in vivo (Yan et al., 2018). Similarly, inhibition of JNK phosphorylation prevents high glucose induced inflammation and DCM in diabetic mice (Pan et al., 2014). In spite of this we do not have optimum therapeutic strategy to mitigate inflammation in the heart. This demands the need for detailed research in the inflammation during DCM.

GATA-4 is a sequence of DNA of the proximal region of the cardiac troponin I gene to which binds the GATA-4 transcriptional factor (Murphy et al., 1997) followed by the transcriptional activation of the gene in vitro (Du et al., 2008). The nuclear translocation of GATA-4 reduces myocardial contractility (Ku et al., 2011). Phosphorylation of GATA-4 at Ser105 by ERK1/2 increases its transcriptional activity (Liang et al., 2001). The GATA-4 is prevented from nuclear accumulation by GSK-3β protein (Morisco et al., 2001). Lithium chloride inhibition of GSK-3β led to the translocation of GATA-4 into the nucleus (Morisco et al., 2001). Another novel marker in DCM is the NLRP3 inflammasome. The inflammasome is a complex consisting of an adaptor protein called apoptosis-associated specklike protein, caspase-1 (a proinflammatory factor), and NLRP3 (Nod like receptor family) (Schroder et al., 2010. Once active, NLRP3 leads to the activation of procaspase-1 to caspase-1 (Schroder et al., 2010). Activated caspase-1 transforms the inactive forms of pro IL-1β and pro IL-18 to their active forms which then activates inflammation mediated apoptotic and fibrotic processes. In addition post translational modification of NLRP3 by potential ligands like TxNIP has emerged as a novel target in DCM since TxNIP triggers the NLRP3 inflammasome complex assembly (Luo et al., 2017). Here we have studied the network between the NLRP3, TxNIP, GATA-4, pGSK-3β and the MAPK pathways in the genesis of DCM which is found to be essential for better understanding of molecular mechanisms of inflammation during DCM.

Roles of TLRs and NLRP3 inflammasome complexes in the amplification of cardiac inflammation during DCM have not been elucidated much. The discovery of novel pathways of inflammation in cardiomyocytes in response to diabetes has become a necessity to design drugs for DCM. In addition to the aforesaid pathways two important targets have been studied in the present study: Troponin I- interacting kinase (TNNI3K) and ST2L. The former is a MAP3K which is expressed exclusively in the heart (Tang et al., 2013) and the latter is essentially a marker of inflammation and is thought to signal the

presence of adverse cardiac remodeling and tissue fibrosis (Kakkar and Lee, 2008). Fibrosis is also instigated by increased O-GlcNAcylation of proteins by hexosamine signalling. Although transient activation of hexosamine signalling is cytoprotective the sustained activation of the same exerts detrimental effects like mitochondrial dysfunction and apoptosis (Ducheix et al., 2018). The role of OGlcNAcylation has also been investigated in this study.

Plant derived compounds have been found to be attractive therapeutic agents. This is found to be the case with cardiovascular diseases too. Herein cinnamic acid (CiA), a phenolic acid present in a wide variety of fruits and vegetables has been selected to assess its potential against DCM. It is a potent antioxidant (Sova, 2012) and anti-inflammatory agent (De Cássia et al., 2014). The beneficial properties of CiA have been found in our previous study in the in vitro model of hyperglycemia with H9c2 cells (Anupama et al., 2018). The present study intends to check the mechanism by which CiA is an attractive bioactive against various inflammatory pathways responsible for DCM.

This study is an attempt to elucidate the role of inflammation to unlock the mystery behind DCM. The questions that are putting forward here are 1) whether TLR mediated inflammatory mechanism is upregulated during DCM in vitro, 2) whether MAPK pathways are involved in the genesis of cardiac hypertrophy via hexosamine biosynthetic pathway and p-GSK3β/GATA-4 axis, 3) whether cinnamic acid could be a potential nutraceutical against DCM.

5.2 Materials and Methods (Please refer chapter 2 for details)

- Estimation of nitrite levels and proinflammatory markers by indirect ELISA.
- Investigation on TLR4 mediated inflammatory pathways and Akt/mTOR pathway by western blot analysis.
- Studies on PPAR α by immunofluorescence.

Experimental groups consist of control (C; 5.5 mM glucose), high glucose (HG; 33 mM glucose), HG + metformin (Met; 1 mM), HG + cinnamic acid-100 nM (CiA1), HG + cinnamic acid-500 nM (CiA2), control + cinnamic acid-500 nM (C + CiA2 for toxicity evaluation), HG + JNK inhibitor (SP; 10 μM), HG + ERK inhibitor (PD; 20 μM), HG + pp38 MAPK inhibitor (SB; 20 μM).

5.3 Results

5.3.1 HG increased the nitrite levels and inducible NOS levels in H9c2 cells

There was a significant increase ($p \leq 0.05$) in nitrite content in HG treated cells (186.32 %) compared to the control. While treatment with CiA (100 nM and 500 nM) or positive control metformin (1mM) significantly prevented the increase by 155 %, 165.3 % and 167. 23 % respectively in hyperglycemic H9c2 cells (Fig. 5.1A). Similarly iNOS expression in HG treated cells was also found to be significantly upregulated by 137.9 % compared to the control group and CiA cotreatment reversed their levels by 77 % and 98 % respectively in a dose dependent manner. Metformin also prevented upregulation of iNOS significantly by 195.9 %. (Fig. 5.1B)

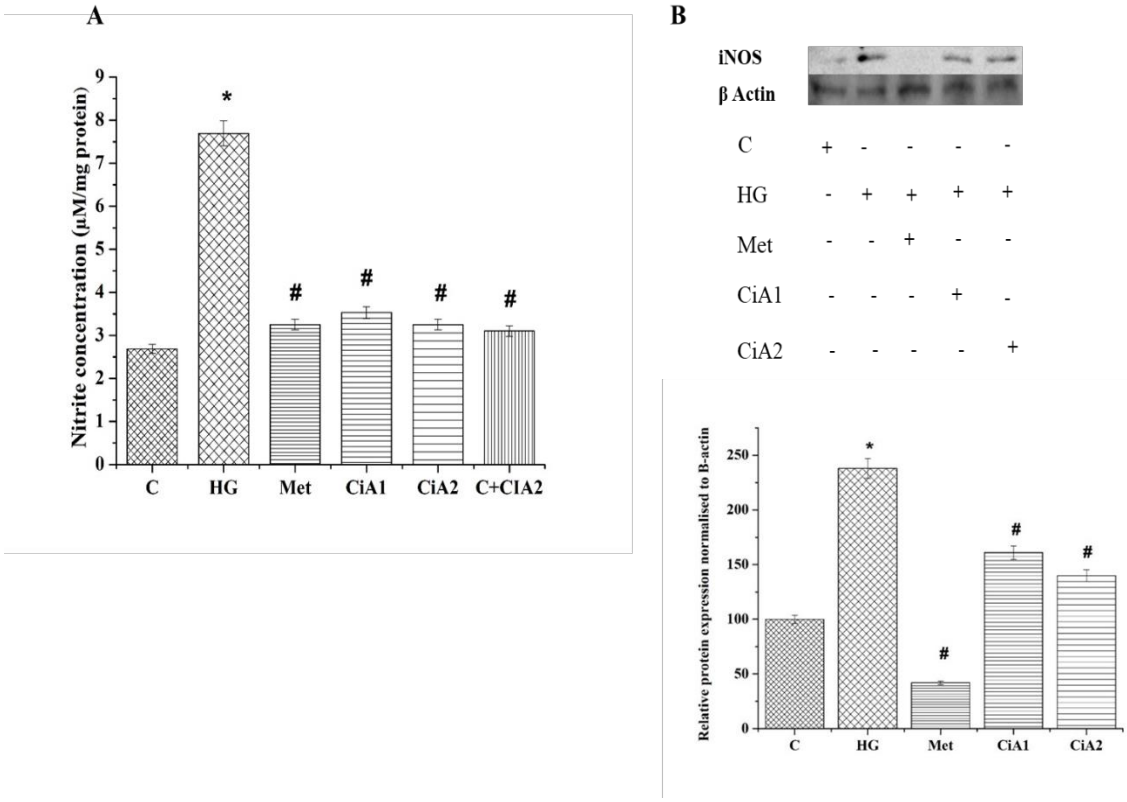

Fig. 5.1 Expression of inflammatory markers in high glucose treated H9c2 cells and attenuation of the same by cinnamic acid. H9c2 cells were treated with high glucose (33 mM) for 48 hrs in the presence or absence of different doses of cinnamic acid or metformin. C - control, HG - high glucose treated group, Met - HG + metformin, CiA1 - HG + cinnamic acid (100 nM), CiA2 - HG + cinnamic acid (500 nM), C + CiA2 - control + cinnamic acid (500 nM). A) Quantification of nitrite levels. Values are expressed as mean ± SEM where n = 6. B) Representative immunoblot of iNOS and densitometric quantification normalised to β-actin. Values are expressed as mean ± SEM where n = 3. * $p \leq 0.05$ significantly different from the control group. #$p \leq 0.05$ significantly different from the HG treated group.

5.3.2 Release of pro-inflammatory cytokines during hyperglycemia in H9c2 cells.

The levels of proinflammatory cytokines TNF-α and IL-6 were upregulated significantly ($p \leq 0.05$) by 501 % and 42 % respectively (Fig. 5.2 A & B) and the level of the anti-inflammatory cytokine IL-10 was downregulated significantly by 63.9 % in HG treated H9c2 cells (Fig. 5.2 C) compared to the control group. Treatment with CiA lowered the levels significantly ($p \leq 0.05$) by 286.9 % and 314.1 % (TNF-α); 30 % and 44 % (IL-6) (Fig. 5.2 A & B) and upregulated the levels of IL-10 significantly by 44.2 % and 37.1 % (Fig. 5.2 C) at 100 and 500 nM of CiA. Metformin also significantly ($p \leq 0.05$) reduced the levels of the proinflammatory cytokines by 223.9 % and 48 % for TNF-α and IL-6 respectively and increased the levels of anti-inflammatory cytokine IL-10 by 59.7 % compared to the diabetic group (Fig. 5.2).

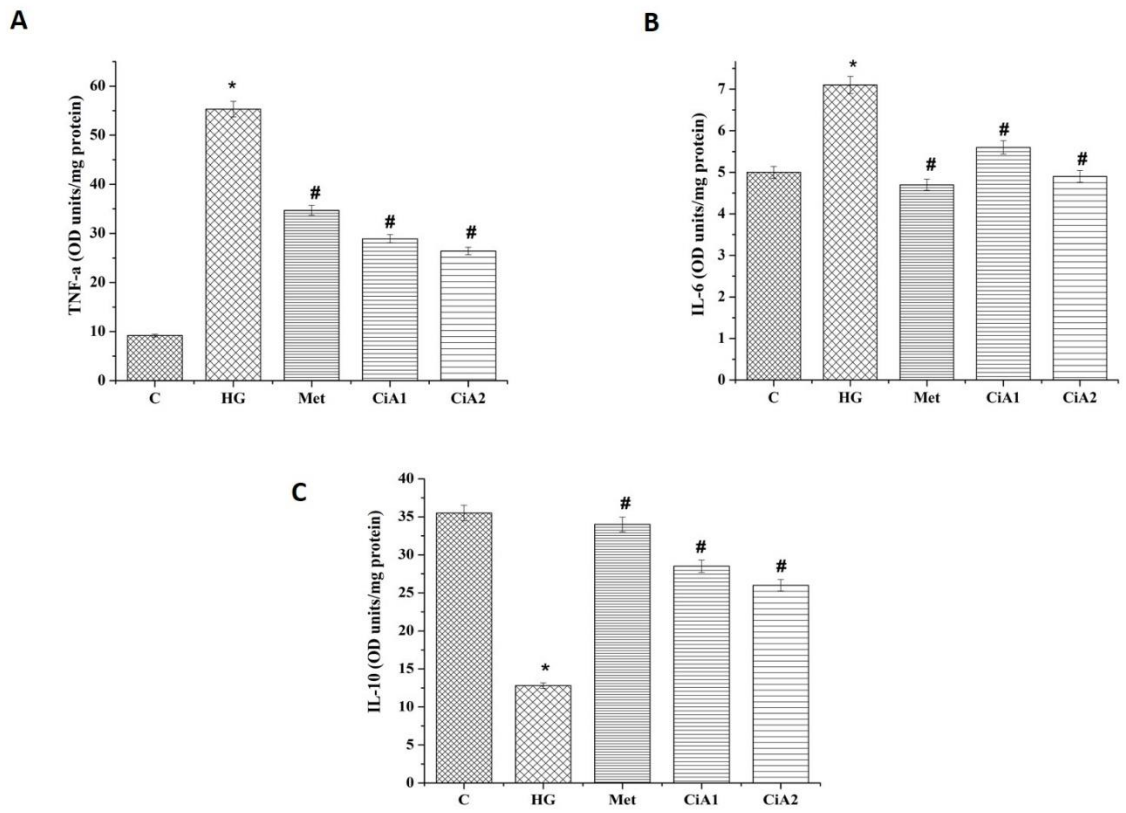

Fig. 5.2 Cinnamic acid reduced the levels of proinflammatory cytokines. H9c2 cells were treated with high glucose (33 mM) for 48 hrs in the presence or absence of different doses of cinnamic acid or metformin. C - control, HG - high glucose treated group, Met - HG + metformin, CiA1 - HG + cinnamic acid (100 nM), CiA2 - HG + cinnamic acid (500 nM). A & B). The levels of proinflammatory cytokines (TNF-α, IL-6) and C) anti-inflammatory cytokine IL-10 in cell culture supernatant of respective groups. Values are expressed as mean ± SEM where n = 6. * $p \leq 0.05$ significantly different from the control group. # $p \leq 0.05$ significantly different from the diabetic group.

5.3.3 Investigation on TLR4/MyD88 pathway

5.3.3.1 TLR4/MyD88 was activated during hyperglycemia

There was a significant ($p \leq 0.05$) upregulation of TLR4 (134.1%) and MyD88 (45 %) levels in the hyperglycemic H9c2 cells (Fig. 5.3). CiA treatment prevented the upregulation of TLR4 significantly (36.6 % by 100 nM, 84.2 % by 500 nM) in a dose dependent manner. Metformin also protected the cells (25.4 %) from hyperglycemia

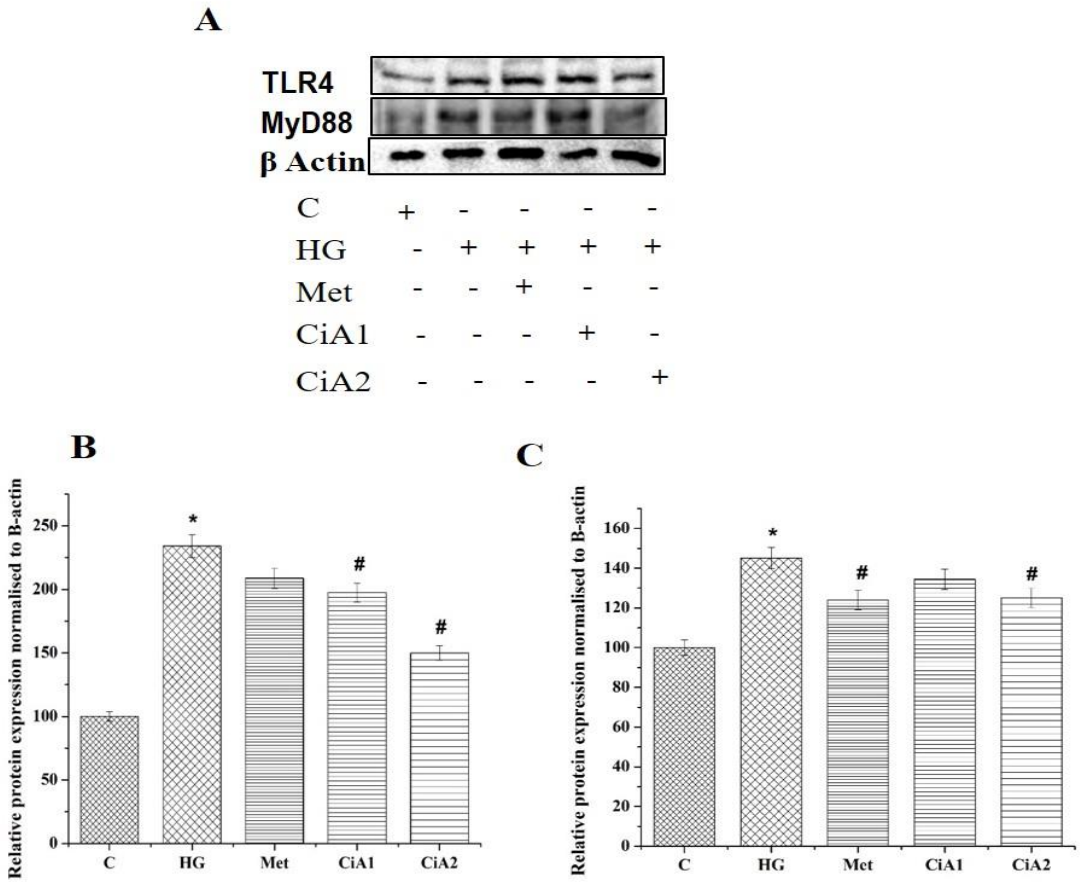

induced overexpression of TLR4 (Fig. 5.3). Similarly the MyD88 overexpression levels were reduced by 10.6 % and 19.9 % ($p \leq 0.05$) with 100 and 500 nM of CiA respectively and treatment with metformin also reduced the levels of MyD88 significantly by 21.06 %in hyperglycemic cells (Fig 5.3).

Fig. 5.3 Activation of the toll like receptor pathway in high glucose treated H9c2 cells. H9c2 cells were treated with high glucose (33 mM) for 48 hrs in the presence or absence of different doses of cinnamic acid or metformin. C - control, HG - high glucose treated group, Met - HG + metformin, CiA1 - HG + cinnamic acid (100 nM), CiA2 - HG + cinnamic acid (500 nM). A) Representative immunoblots of TLR4 and MyD88 and their respective densitometric quantifications normalised to β-actin. Values are expressed as mean ± SEM

where n = 3. *p ≤ 0.05 significantly different from the control group. #p ≤ 0.05 significantly different from the HG treated group.

5.3.3.2 Upregulation of JNK, ERK and p 38 MAPK during hyperglycemia

There was a significant (p ≤ 0.05) upregulation of pJNK, pERK and pp38 MAPK in HG treated H9c2 cells by 37.5 %, 66.8 % and 92 % respectively (Fig. 5.4). Cotreatment with CiA at both concentrations (100 and 500 nM) and metformin reduced the levels of pJNK by 14 %, 64 %, 43 % (p ≤ 0.05) and 48.7 % (p ≤ 0.05); pERK by 44 %, 61.1 %, and 63.3% and pp38 MAPK by 37.7 %, 38.3 % and 73.4 % respectively (Fig. 5.4).

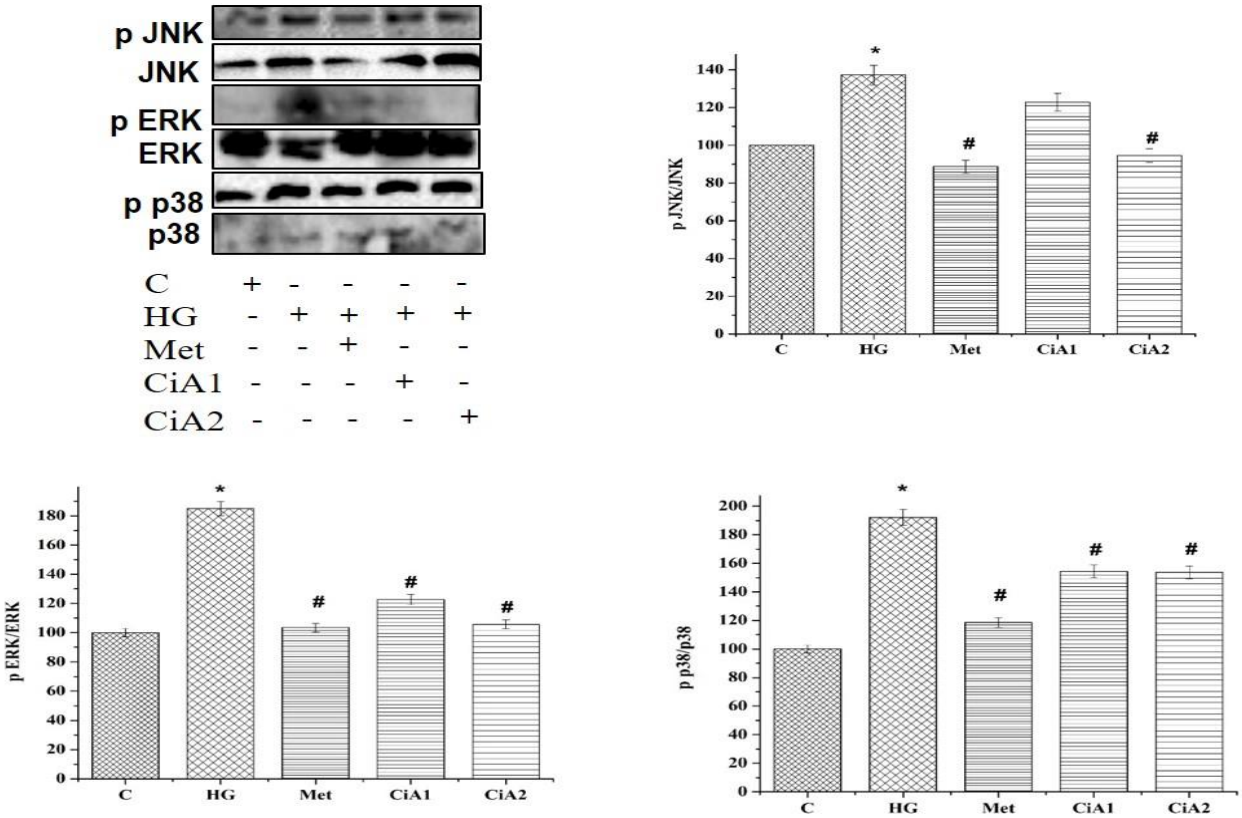

Fig. 5.4 Activation of the MAPK pathways (JNK, ERK, p38 MAPK) in high glucose treated H9c2 cells. H9c2 cells were treated with high glucose (33 mM) for 48 hrs in the presence or absence of different doses of cinnamic acid or metformin. C - control, HG - high glucose treated group, Met - HG + metformin, CiA1 - HG + cinnamic acid (100 nM), CiA2 - HG + cinnamic acid (500 nM). Representative immunoblots of pJNK, pERK and pp38 MAPK and their respective densitometric quantifications. Values are expressed as mean ± SEM where n = 3. *p ≤ 0.05 significantly different from the control group. #p ≤ 0.05 significantly different from the HG treated group.

5.3.3.3 Hyperglycemia induced translocation of NFKB, increased pIKB and ICAM

The expression of pIKB and ICAM were significantly upregulated in HG treated cells by 155 % and 404.1 % respectively (Fig. 5.5 A). Cotreatment with CiA prevented the

upregulation of pIKB by 30.9 % (100 nM) and 109.3 % (500 nM) (Fig. 5.5 A). Similarly the increased level of ICAM was also reduced significantly by 378.7 % and 400. 2 % with 100 nM and 500 nM of CiA respectively. Also metformin protected the levels of both pIKB and ICAM significantly by 123 % and 248.7 % respectively (Fig. 5.5 A). There was an increased translocation of NFKB into the nucleus in HG treated H9c2 cells and the same was found to be reduced in the CiA and metformin treated group (Fig. 5.5 B).

A

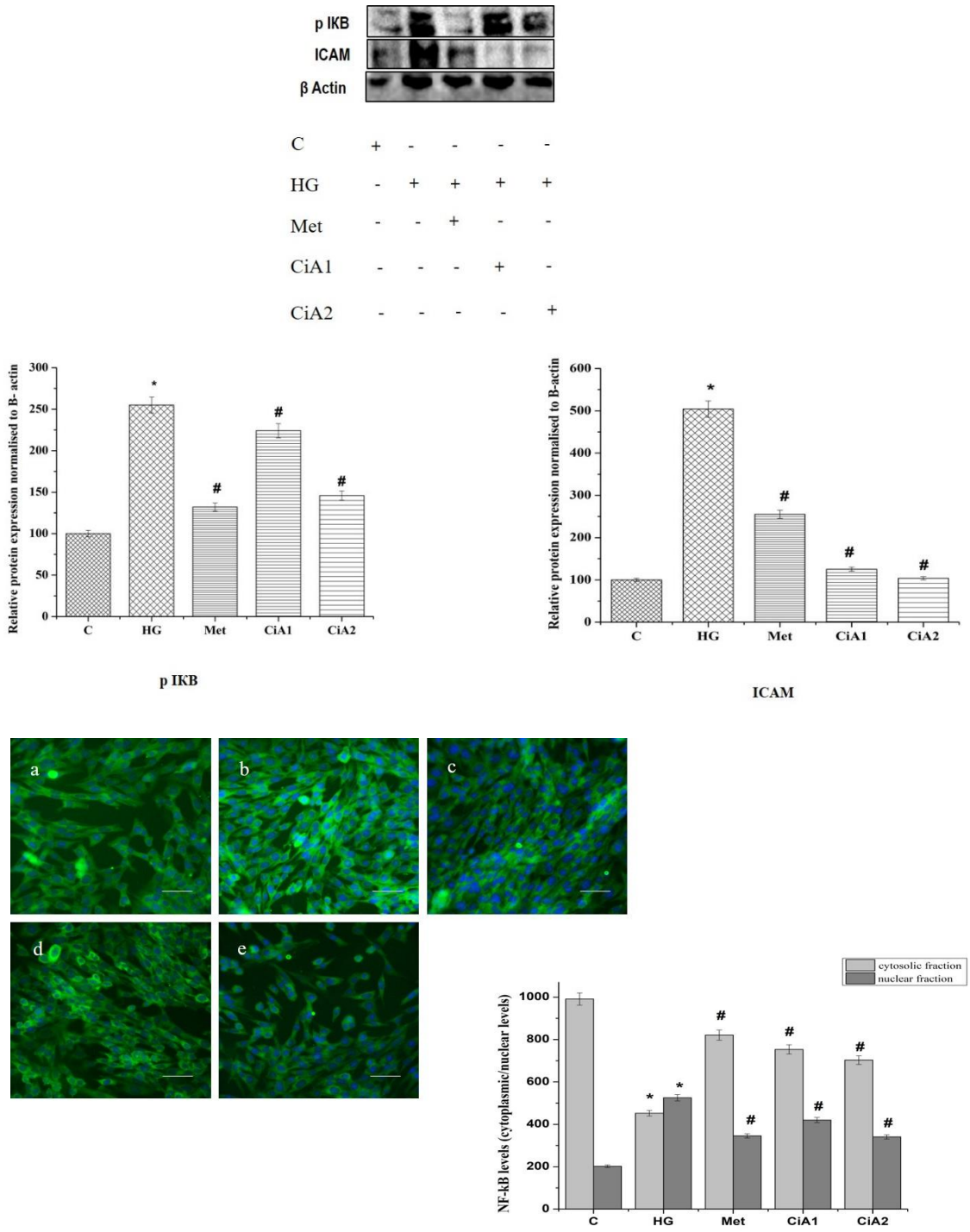

Fig. 5.5 Effect of high glucose on NFKB translocation and protective effect of cinnamic acid. H9c2 cells were treated with high glucose (33 mM) for 48 hrs in the presence or absence of different doses of cinnamic acid or metformin. C - control, HG - high glucose treated group, Met - HG + metformin, CiA1 - HG + cinnamic acid (100 nM), CiA2 - HG + cinnamic acid (500 nM). A) Representative immunoblots of pIKB and ICAM and their respective densitometric quantifications normalised to β-actin. B) NFKB translocation during hyperglycemia. a - control, b - high glucose treated group (HG), Met - HG + metformin, CiA1 - HG + cinnamic acid (100 nM), CiA2 - HG + cinnamic acid (500 nM). Scale bar corresponds to 50 µm. Values are expressed as mean ± SEM where n = 3. *p ≤ 0.05 significantly different from the control group. #p ≤ 0.05 significantly different from the HG treated group.

5.3.3.4 Estimation of TNNI3K levels during hyperglycemia and the effect of MAPK inhibition on the same.

The expression of TNNI3K was upregulated significantly ($p \leq 0.05$) in the HG treated group by 24.6 % compared to the control group (Fig. 5.6). While cotreatment with CiA or metformin downregulated their levels significantly ($p \leq 0.05$) by 41.8 % (100 nM), 45.5 % (500 nM) and 46.9 % (1 mM) respectively compared to the hyperglycemic group (Fig. 5.6). However, treatment with MAPK inhibitors did not show any significant change.

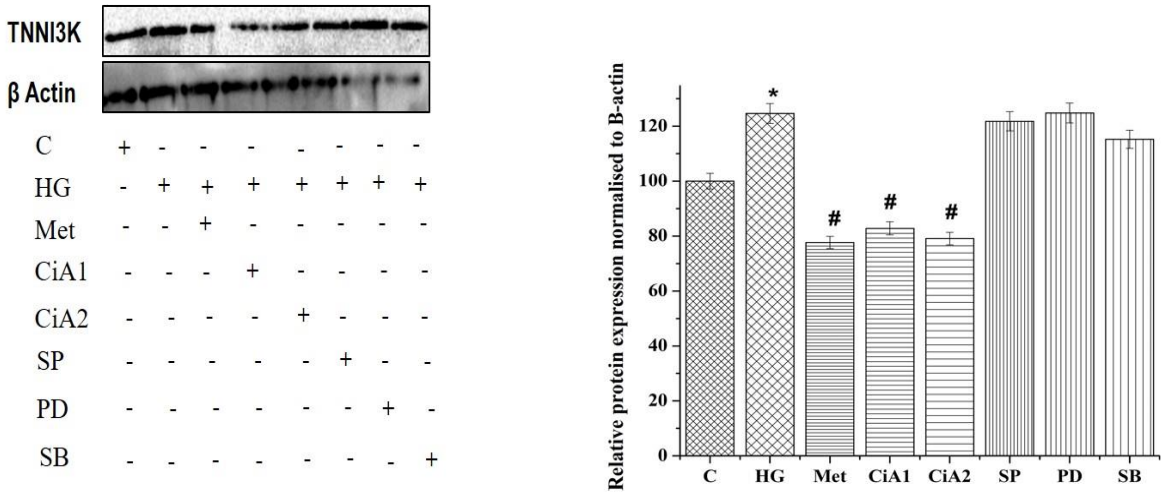

Fig. 5.6 Estimation of TNNI3K during hyperglycemia and effect of MAPK or cinnamic acid. H9c2 cells were treated with high glucose (33 mM) for 48 hrs in the presence or absence of different doses of cinnamic acid, metformin or inhibitors of JNK (SP600125), ERK (PD98059) and p p38 MAPK (SB220025). C - control, HG - high glucose treated group, Met - HG + metformin, CiA1 - HG + cinnamic acid (100 nM), CiA2 - HG + cinnamic acid (500 nM). A) Representative immunoblot of TNNI3K and the densitometric quantification normalised to β-actin. Values are expressed as mean ± SEM where n = 3. * p ≤ 0.05 significantly different from the control group. # p ≤ 0.05 significantly different from the HG treated group.

5.3.3.5 Phosphorylation of GSK-3β and activation of GATA-4 during hyperglycemia and MAPK inactivation.

There was a significant ($p \leq 0.05$) increase in the phosphorylation of GSK-3β in the hyperglycemic group by 39.9 % compared to the control group (Fig. 5.7A). CiA treatment reduced the expression of pGSK-3β by 0.8 % and 7.1 % for 100 and 500 nM respectively (not significant) and by 6.1 % for 1 mM metformin (Fig. 5.7A). Similarly GATA-4 levels were downregulated significantly in the cytoplasmic fraction of HG treated cardiomyocytes by 11.9 % when compared with the control group (Fig. 5.7B). CiA (100 and 500 nM) or metformin (1 mM) cotreatment significantly ($p \leq 0.05$) increased their levels by 19.7 %, 18.4 % and 16.1% respectively (Fig. 5.7 B). Upon inhibition of JNK, ERK and p38 MAPK there was a downregulation of pGSK-3β by 8.2 %, 40.05 % and 22.1 % respectively (Fig. 5.7 A). Also cytoplasmic GATA-4 levels were significantly upregulated upon MAPK inhibition by 30.5 %, 29.3% and 51.8 % respectively for JNK, ERK and p38 MAPK (Fig. 5.7 B).

5.3.3.6 NLRP3 and TxNIP protein activation during hyperglycemia and the role played by MAPK in inhibiting their levels.

There was a significant ($p \leq 0.05$) increase in the level of NLRP3 in HG treated H9c2 cells by 15.17 % compared to the normal group (Fig. 5.7 A). Treatment with high dose of CiA (500 nM) or metformin reduced their levels significantly by 21.5 % and 14.6 % respectively (Fig. 5.7 A). While in the MAPK inhibitors treated groups there was a significant reduction by 28.9 %, 28.4 % and 26.4 % respectively for JNK, ERK and p 38 MAPK (Fig. 5.7 A). Similarly the TxNIP levels were also upregulated significantly in the hyperglycemic group by 82.8 % from the control cells (Fig. 5.7 A). While CiA and metformin treatment reduced their levels significantly by 133. 2 %, 91.8 % and 81.8 % for 100 nM, 500 nM, and 1 mM respectively (Fig. 5.7 A). TxNIP levels were drastically reduced in the MAPK inhibitor group by 81.5 %, 94.1 % and 107 % for JNK, ERK and p 38 MAPK (Fig. 5.7 A).

5.3.3.7 MAPK inhibition suppressed the expression of OGlcNAc in H9c2 cells

The levels of O-GlcNAc were significantly ($p \leq 0.05$) upregulated in HG treated H9c2 cells by 66 % compared to the normal (Fig. 5.7 A). Cotreatment with CiA or metformin reduced their levels by 13.6 %, 18.2 % and 52.29 % respectively when compared with the HG group (Fig. 5.7 A). MAPK inhibition reduced their levels

significantly by 59 %, 62.2 % and 62.6 % for JNK, ERK and p 38 MAPK respectively when compared with hyperglycemic cells (Fig. 5.7 A).

5.3.3.8 MAPK inhibition did not influence the expression of ST2 levels

ST2L expression was significantly ($p \leq 0.05$) downregulated in HG treated H9c2 cells by 40.8 % and CiA cotreatment at 500 nM upregulated their levels significantly ($p \leq 0.05$) by 24.8 % (Fig. 5.7A). Metformin also increased the levels of ST2L significantly by 22.8 % (Fig. 5.7A). However there was no change in the expression of ST2L upon inhibition with JNK, ERK and p38 MAPK inhibitors (Fig. 5.7A). The expression was found to be downregulated similar to that of the diabetic group. This indicates that the reduced ST2L expression in the diabetic group is neither due to the upregulation of the MAPK pathways nor due to its downstream regulators.

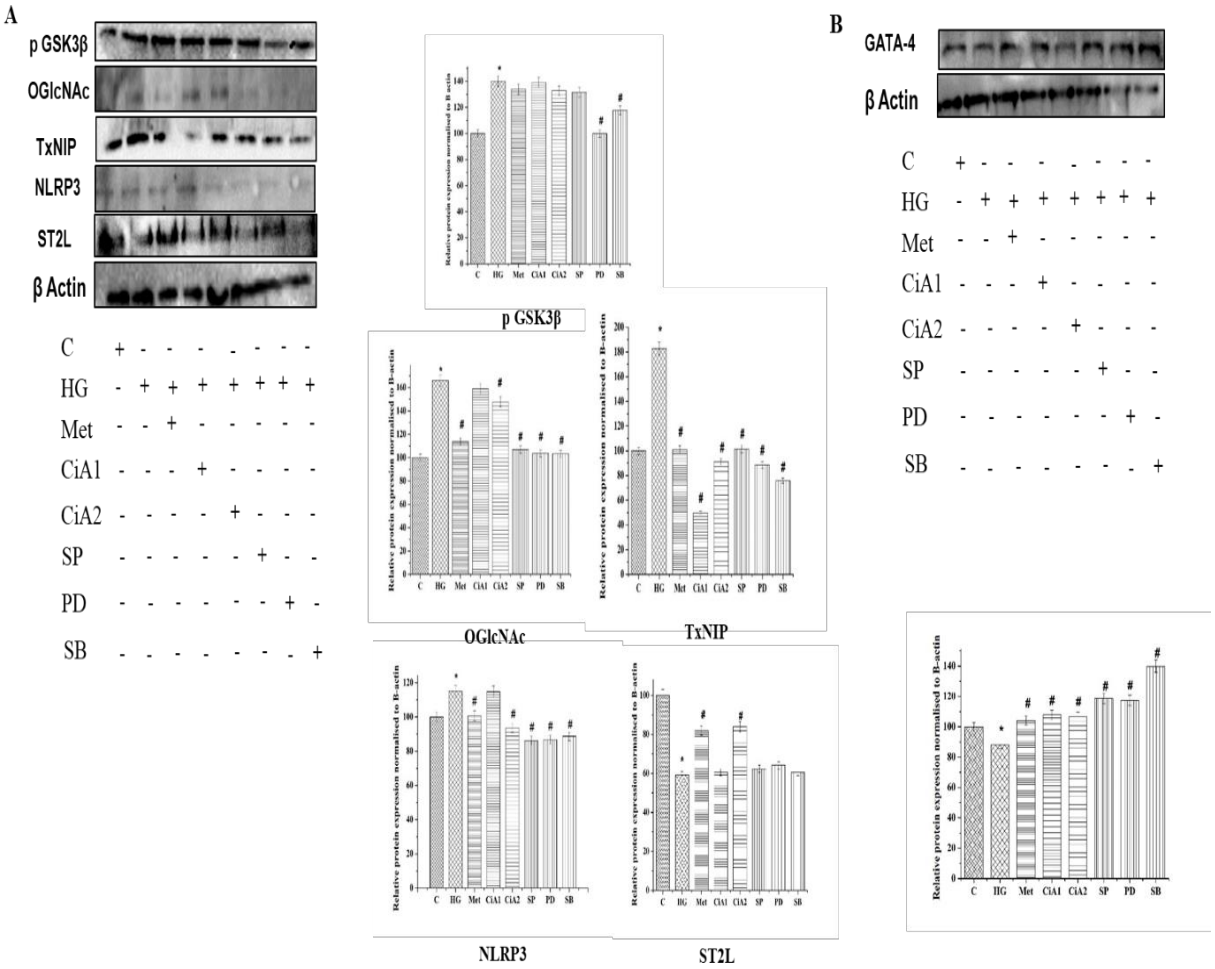

Fig. 5.7 Effect of MAPK (JNK, ERK and p38 MAPK) pathways inhibition on the expression levels of proteins like pGSK-3β, GATA-4, O-GlcNAc, TxNIP, NLRP3 and ST2L. H9c2 cells were treated with high glucose (33 mM) for 48 hrs in the presence or absence of different doses of cinnamic acid, metformin or

inhibitors of JNK (SP600125), ERK (PD98059) and p p38 MAPK (SB220025). C - control, HG - high glucose treated group, Met - HG + metformin, CiA1 - HG + cinnamic acid (100 nM), CiA2 - HG + cinnamic acid (500 nM). A) Representative immunoblots of pGSK-3β, O-GlcNAc, TxNIP, NLRP3 and ST2L and their respective densitometric quantifications normalised to β-actin. B) Representative immunoblot of GATA-4 in the cytoplasmic fraction. Values are expressed as mean ± SEM where n = 3. * $p \leq 0.05$ significantly different from the control group. # $p \leq 0.05$ significantly different from the HG treated group.

5.3.4 Hyperglycemia inhibited the Akt pathway

Akt pathway was inhibited in HG treated H9c2 cells. The pAkt levels were downregulated significantly ($p \leq 0.05$) by 16.9 % in the hyperglycemic group when compared to the control (Fig. 5.8). Treatment with CiA at 100 and 500 nM significantly ($p \leq 0.05$) increased their levels by 44.8 % and 51 % respectively. Similarly treatment with metformin also significantly ($p \leq 0.05$) elevated their levels by 19.9 % (Fig. 5.8).

The inhibitor of Akt pathway called pPTEN was also found to be significantly ($p \leq 0.05$) upregulated in the HG treated H9c2 cells by 23.3 % compared to the control group (Fig. 5.8). However treatment with CiA at 100 and 500 nM and metformin at 1 mM significantly ($p \leq 0.05$) reduced their levels by 42.6 %, 41 % and 51.8 % respectively (Fig. 5.8) compared to the hyperglycemic group.

Hexokinase (HKII) is an enzyme of the glycolytic pathway. However the levels of hexokinase were found to be upregulated significantly ($p \leq 0.05$) in the HG treated H9c2 cells by 99 % (Fig. 5.8). Cotreatment with CiA at 100 and 500 nM and metformin at 1 mM significantly ($p \leq 0.05$) reduced their levels by 80.5 %, 94.6 % and 125.7 % respectively (Fig. 5.8).

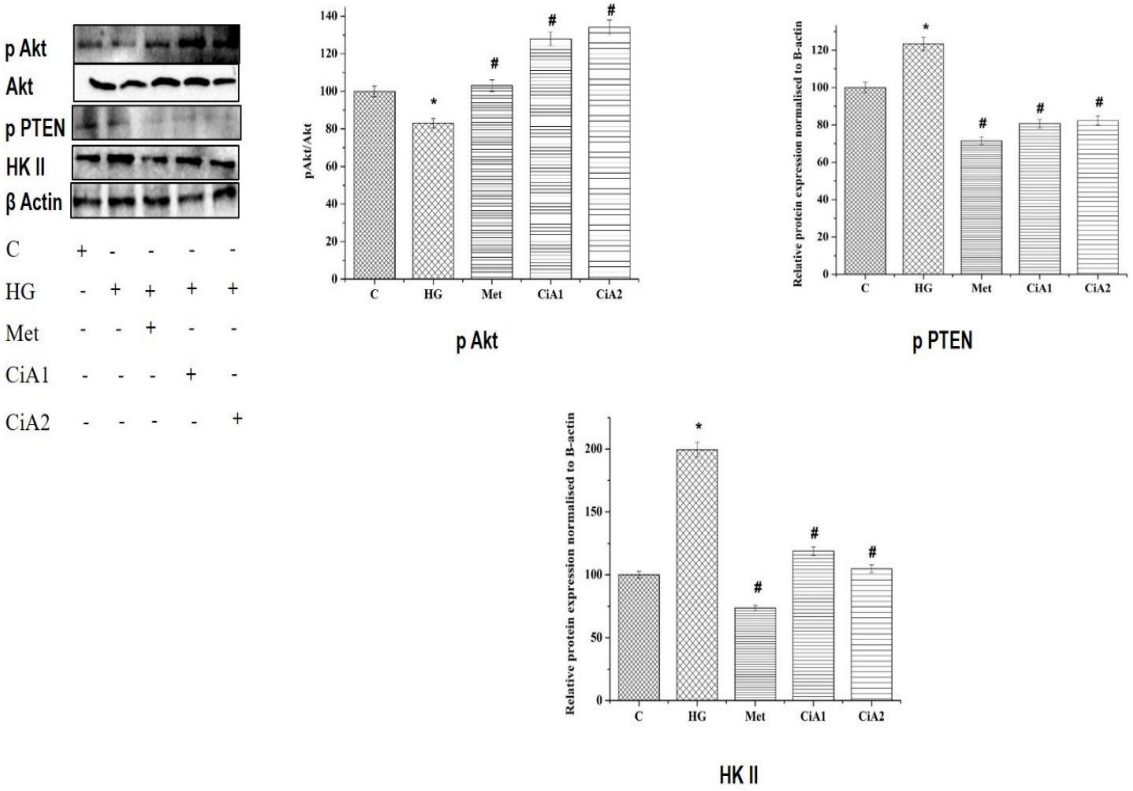

Fig. 5.8 Effect of high glucose on Akt signalling and the effect of cinnamic acid. H9c2 cells were treated with high glucose (33 mM) for 48 hrs in the presence or absence of different doses of cinnamic acid or metformin C - control, HG - high glucose treated group, Met - HG + metformin, CiA1 - HG + cinnamic acid (100 nM), CiA2 - HG + cinnamic acid (500 nM). Representative immunoblots of p Akt, p PTEN and hexokinase II and their respective densitometric quantifications normalised to β-actin. Values are expressed as mean ± SEM where n = 3. * $p \leq 0.05$ significantly different from the control group. # $p \leq 0.05$ significantly different from the HG treated group.

5.3.5 Effect of HG on mTOR signalling

HG treatment activated the mTOR pathway. The levels of p mTOR were found to be significantly ($p \leq 0.05$) upregulated by 50 % in HG treated H9c2 cells compared to the control group (Fig. 5.9). CiA treatment reduced the levels of p mTOR by 6 % (not significant) at 100 nM and 19.9 % ($p \leq 0.05$) at 500 nM (Fig. 5.9). Similarly treatment with metformin also reduced the levels of p m TOR significantly ($p \leq 0.05$) by 32.1 % compared to the HG treated group (Fig. 5.9).

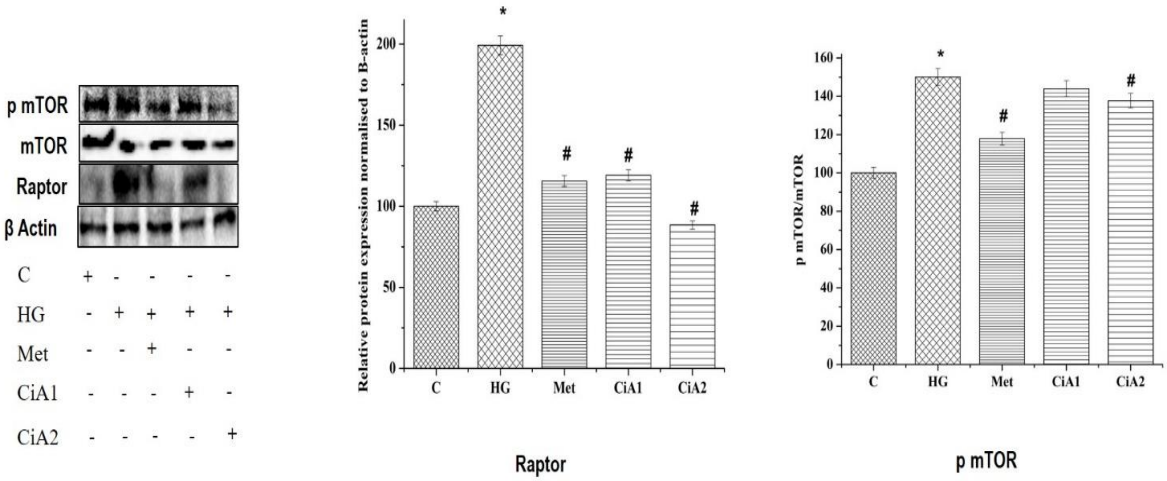

Fig. 5.9 mTOR signalling during diabetes and effect of cinnamic acid on the same. H9c2 cells were treated with high glucose (33 mM) for 48 hrs in the presence or absence of different doses of cinnamic acid or metformin C - control, HG - high glucose treated group, Met - HG + metformin, CiA1 - HG + cinnamic acid (100 nM), CiA2 - HG + cinnamic acid (500 nM). Representative immunoblots of p mTOR and Raptor and their respective densitometric quantifications normalised to β-actin. Values are expressed as mean ± SEM where n = 3. * $p \leq 0.05$ significantly different from the control group. # $p \leq 0.05$ significantly different from the HG treated group.

5.3.6 PPAR α translocation during hyperglycemia

PPAR α translocation indicates increased fatty acid oxidation. Here, there was a significant translocation of PPAR alpha into the nucleus in the HG treated H9c2 cells and treatment with CiA at both concentrations and metformin at 1 mM prevented the translocation of PPAR alpha compared to the HG treated group (Fig. 5.10).

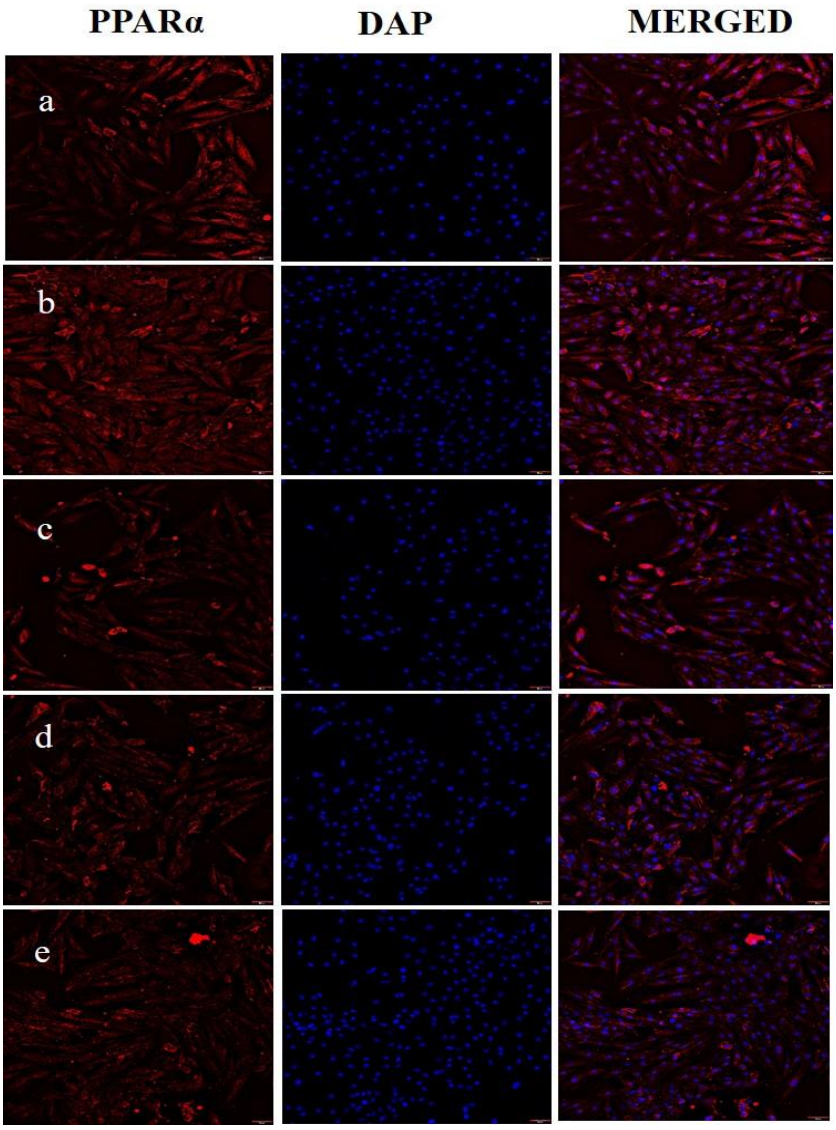

Fig. 5.10 Effect of high glucose on PPARα translocation and protective effect of cinnamic acid. H9c2 cells were treated with high glucose (33 mM) for 48 hrs in the presence or absence of different doses of cinnamic acid or metformin. a - control, b - high glucose treated group (HG), Met - HG + metformin, CiA1 - HG + cinnamic acid (100 nM), CiA2 - HG + cinnamic acid (500 nM). Scale bar corresponds to 50 µm. Values are expressed as mean ± SEM where n = 3.

5.4 Discussion

We found here that TLR4 mediated Myd88 inflammatory pathway is being activated during diabetes in heart; MAPK upregulation leads to the activation of hexosamine biosynthetic pathway and NLRP3 inflammasome; increase in the cardiac injury marker troponin might be attributed to the MAPK pathway mediated inactivation of GSK-3β and nuclear translocation of GATA-4; the cardioprotective role exhibited by ST2L receptor is diminished during DCM which is occurring independent of MAPK activation; and finally CiA is found a potent molecule against DCM *in vitro*.

The *in vitro* model of hyperglycemia was created by incubating H9c2 rat cardiomyoblasts with HG for 48 hrs (Anupama et al., 2018; Preetha Rani et al., 2018; Salin Raj et al., 2019). Sustained hyperglycemic condition leads to an outburst of complex and intertwined inflammatory responses (Chen et al., 2017). Nitric oxide, a marker of inflammation and an essential intercellular signalling molecule, has a significant influence on the function of the cardiovascular system (Bøtker and Møller, 2013; Menaka et al., 2009). NO is usually estimated in *in vitro* studies by quantifying its metabolite, nitrite (NO^{2-}) levels. The presence of iNOS (inducible nitric oxide synthase) which is a calcium insensitive enzyme produces excess nitric oxides which eventually reacts with superoxides to form peroxynitrite, a free radical (Förstermann and Sessa, 2012). Here we have investigated the levels of nitrite during hyperglycemia to confirm inflammation in H9c2 cells. The nitrite level was found to be very high in the H9c2 cells treated with HG. Genesis of inflammation was also confirmed with the upregulation of iNOS and adhesion molecule (ICAM) and the release of various proinflammatory cytokines (TNF α, IL-6, IL-1β), chemokine (MCP-1) and decrease in the levels of anti-inflammatory cytokine (IL-10) in the HG treated group. However, there are multiple mechanisms by which these proinflammatory mediators are released (Westermann et al., 2006; Zhao et al., 2017) and thus elicit a detrimental inflammatory response in the myocardium.

We focussed on the TLR4/MyD88/MAPK/NLRP3 pathway to elucidate in detail the cascade of inflammatory processes. TLRs are membrane anchored protein receptors that are present in a wide range of cells including cardiomyocytes (Mohammad et al., 2006). They are the members of pattern recognition receptors which play an essential role in initiating cardiac innate immune response (Yu and Feng, 2018). TLRs are capable of responding to both pathogen associated molecular patterns and damage associated molecular patterns (Satoh et al., 2006). Some of the ligands of TLRs include high mobility

group B1, advanced glycation end products, necrotic cells and extracellular matrix components (Tsan and Gao, 2004). Since TLR4 is the most widely expressed TLRs in the myocardium, we analysed whether the TLR4 pathway had any role in triggering inflammation during DCM. The exact and the precise role of TLR4 in the diabetic scenario is scanty except their role in the regulation of lipid accumulation in the heart of type 1 diabetic mice (Dong et al., 2012) and TLR4/MyD88 upregulation in high fat diet induced obese mice (Ko et al., 2009). Also it was found that absence of TLR4 reduced atherosclerosis in mice deficient in apolipoprotein B (Michelson et al., 2004). The TLR4 is known to mediate the downstream signalling events via two routes depending on the adapter proteins MyD88 or TRIF (Premkumar et al., 2010). A significant upregulation of TLR4/MyD88 pathway in H9c2 cells has been observed in this study suggesting that during diabetes MyD88 mediated TLR4 activation is occurring. Further, MyD88 facilitates the recruitment of IL-1R associated kinase (IRAK1) and TNFR-associated factor (TRAF) (Kawai and Akira, 2006). This induces the proteasomal degradation of NFkB inhibitors like IkB thus leading to the translocation of NFkB to the nucleus (Kawai and Akira, 2006). It can thus be proposed that excess glucose can act as a ligand for these receptors during diabetes.

Activation of TLR4 stimulates the major intracellular signalling pathways: MAPK pathways. MAPKs include ERK1/2 (extracellular signal regulated kinase, JNK (c-Jun N-terminal protein kinase) and p38 MAPK. Interestingly all the three MAPK pathways were found to be simultaneously upregulated in HG treated H9c2 cells also. It has been reported that any one of the MAPK pathways are activated during insulin resistance and heart failure (Zhao et al., 2015; Thandavarayan et al., 2015, Pan et al., 2014). Out of the three MAPKinases the p38 MAPK has been known to play an essential role in the pathophysiology of diabetes (Westermann et al., 2006; Thandavarayan et al., 2009). In particular, the p38 MAPKα inhibition has prevented the detrimental effects of inflammation in the heart (O'Keefe et al., 2007). Whereas another isoform of p38 MAPK .i.e. p38 MAPKβ is antiapoptotic for cardiomyocytes (Zhao et al., 2015). The consequence of the persistent activation of p38 MAPK is cardiomyocyte apoptosis (Oh et al., 2014) and hypertrophy (Maillet et al., 2013). The JNK pathway is seen to be activated in cardiac myocyte apoptosis and DCM according to certain reports (Vaishnav et al., 2011). The potent inducers of JNK signalling include oxidative stress and various proinflammatory cytokines. Activation of the JNK pathway results in increased ROS production, ER stress,

interstitial fibrosis and apoptosis (Jia et al., 2018). Similarly many others have reported that elevated ERK1/2 signalling is associated with obesity and insulin resistance associated cardiac dysfunction (Jia et al., 2018; Zhang et al., 2001)). However, the activation of ERK1/2 signalling is generally associated with growth, proliferation, and survival of cells (Mutlak and Kehat, 2015). Activation of MAPK causes phosphorylation and activation of various transcription factors like GATA-4 and NFKB thereby eliciting adverse biological responses.

As mentioned earlier left ventricular hypertrophy and myocardial fibrosis are the two prominent manifestations of DCM (Jia et al., 2018). Fibrosis was earlier confirmed in the cardiomyopathic heart in male wistar rats (Refer Chapter 4 for details). Hypertrophy was confirmed by the release of surplus ANP (Anupama et al., 2018) and low levels of ST2L in the *in vitro* model.

But the detailed molecular mechanisms leading to these pathological events during diabetes need to be elucidated. Various pathways were investigated in this study. First we began with TNNI3K. It was already seen that the levels of TNNI3K were increased in the diabetic rats. So here we checked the levels of the same in the in vitro model and it was observed that the expression was higher in HG treated H9c2 cells also. TNNI3K is a protein whose overexpression in neonatal rat ventricular myocytes (Wang et al., 2011) is known to induce cardiac hypertrophy (Tang et al., 2013). However, the function of this protein is poorly understood and needs to be studied in detail. However by inhibition with MAPK their levels were found to be unchanged. Based on this we have hypothesized that this protein being a MAPKKK might be acting upstream of the MAPK (JNK, ERK and p38 MAPK) and phosphorylating any of the MAPKs. But whether they have any direct role in phosphorylating the MAPK or activating any of the downstream targets studied here need to be further investigated in detail. This is the first report suggesting a link between TNNI3K and the various downstream proteins like GATA-4, TxNIP, and NLRP3. Since the increased activity of TNNI3K is associated with cardiac hypertrophy, this can be considered as a potential target for exploration in DCM.

In order to conduct a detailed investigation on the role of MAPK in the genesis of cardiac hypertrophy and fibrosis during DCM, we checked the expression levels of various proteins (OGlcNAc, ST2L, TxNIP, NLRP3, GATA-4 and pGSK-3β) from different pathways using MAPK inhibitors. GATA-4 which is expressed in the adult heart belongs to a zinc finger family of highly conserved group of transcription factors with an essential

role in cardiac hypertrophy (Jia et al., 2018). Also the ERK signalling cascade is known to induce myocardial hypertrophy via the phosphorylation of GATA-4 at Ser 105 (Liang et al., 2001). The target genes of the GATA-4 transcription factor include genes that induce hypertrophy like myosin light chains, ANP, BNP, cardiac troponin C, cardiac troponin I and TNNI3K (Molkentin, 2000). The GATA-4 levels are upregulated in the heart in response to stress like pressure overload (Morimoto et al., 2000). The total GATA -4 levels were found to be upregulated in heart of diabetic rats in the present study (please refer chapter 4 for details). To confirm this in vitro, we checked the GATA-4 expression levels with and without MAPK inhibitors in the cytosolic fraction of H9c2 cells. The GATA-4 levels were found to be downregulated in the cytosolic fraction of HG treated H9c2 cells suggesting that most of the GATA-4 has translocated into the nucleus. But during inhibition the same was found to be upregulated. It is known that GATA-4 levels are negatively regulated by GSK-3β. Phosphorylation of GSK-3β results in the nuclear import of GATA-4 protein (Jia et al., 2018). GSK-3β inhibition by alpha adrenergic stimulation results in translocation of GATA-4 into the nucleus (Ku et al., 2011). In the hyperglycemic cells there was an increased phosphorylation of pGSK-3β. Interestingly upon inhibition of MAPK pathways the levels of pGSK-3β were found to be downregulated. This shows that MAPKinases have direct influence on pGSK-3β/GATA-4 axis. Cardiac troponin is one of the target genes of GATA-4. It has been reported that hypertrophic cardiomyopathy occurs as a result of mutations in cardiac troponin I gene (Murakami et al., 2010). In our study also, troponin levels were found to be very high. The high amount of troponin in serum is an indicator of cardiac contractile dysfunction. Thus the reduced myocardial contractility during diabetes might be attributed to the phosphorylation of the troponin gene by GATA-4 transcription factor. The behaviour of GATA-4 and pGSK -3β reveal they are dependent on MAPK during diabetic cardiomyopathy.

The hexosamine biosynthetic pathway is another well-known inducer of fibrosis and hypertrophy (Jia et al., 2018). The protective effect of hexosamine pathway lies in its ability to reduce calcium entry into the cytoplasm post-ischemia (Champattanachai et al., 2007). UDP-N acetylglucosamine (UDP-GlcNAc), the end product of this pathway serves as a precursor of O-GlcNAc (β-O-linkage of N-acetylglucosamine). O-GlcNAc is a carbohydrate which modifies the serine and threonine residues on many nuclear and cytoplasmic proteins. Proteins like calmodulin dependent protein kinase II and phospholamban are modified by O-GlcNAc which causes alterations in myocardial

contractility (Ducheix et al., 2018). In this study also, the expression of O-GlcNAc was found to be significantly higher in HG treated H9c2 cells. Surprisingly the inhibition of the MAP kinases significantly downregulated the levels of OGlcNAc in hyperglycemic H9c2 cells. This further implicates the relationship between the MAPK and hexosamine biosynthetic pathway with cardiac fibrosis and hypertrophy. The critical role played by OGlcNAc in the inflammation induced DCM remains largely unexplored.

NLRP3 plays an important role in eliciting an inflammatory response through an inflammasome complex in the heart. NLRP3 inflammasome complex formation leads to apoptosis in the cardiomyocytes and conversion of inactive forms of pro-IL1β and pro - IL18 to their active forms (Luo et al., 2014). Our study also observed an upregulation of NLRP3 expression levels in HG treated H9c2 cells. The inhibition of all the three MAPK pathways showed a downregulation of NLRP3 protein. In addition, many molecules have been recently identified to act as potential direct ligands of NLRP3 in addition to high glucose and fatty acids (Fuentes-Antrás et al., 2014). One among them is the TxNIP that is involved in the oligomerization of NLRP3 inflammasome complex. TxNIP levels were found to be upregulated in the HG treated cardiomyocytes. Also, the MAPK inhibitor groups showed a decreased expression of TxNIP suggesting the role of the MAPK pathways in activating the inflammasome complex.

Another novel biomarker of cardiac stress mediated hypertrophy and fibrosis is the ST2 receptor (ST2L). ST2L belongs to the toll like receptor superfamily (Kakkar and Lee, 2008). ST2 isoforms undergo alternative splicing to form different variants including a transmembrane form (ST2L) and a soluble form (sST2). The soluble form has recently been considered as a valuable biomarker of heart failure (Bayés-Genis et al., 2018). The ST2L serves as a receptor for the ligand interleukin-33 (IL-33) and the IL-33/ST2L axis is thought to have a cardioprotective role that reduces cardiac hypertrophy, fibrosis and remodeling. But sST2 acts as a decoy receptor for IL-33 under pathological situations (Iwahana et al., 1999). This prevents the binding of IL-33 to ST2L. Studies on sST2 and ST2L are very limited. Hence we have investigated the status of ST2L during diabetic cardiomyopathy and whether the inhibition of either the JNK / ERK / p 38 MAPK had any effect on the expression of this particular receptor which is considered to be a promising molecular target. In the HG group there was a significant downregulation of this receptor and inhibition of MAPK also showed a downregulation indicating that MAPKinases have no role in activating the IL-33/ST2L axis.

The liberation of pro-inflammatory cytokines converge towards the activation of the transcription factor NFKB (Zhao et al., 2017). Once activated, NFKB is translocated into the nucleus and triggers gene expression that causes the release of proinflammatory mediators like TNF-α, IL-6 and ICAM. However in the present investigation during DCM the NFKB was found to translocate into the nucleus of HG treated H9c2 cells. Moreover the canonical pathway involving the phosphorylation of IKB is activated during hyperglycemia as evidenced by the increased levels of the same in our *in vitro* model. All these events are expected to amplify the various processes of inflammation during DCM.

mTOR is a serine threonine kinase belonging to the phosphoinositide kinase-related kinase (PIKK) family. mTOR makes contact with specific adaptor proteins and forms two distinct macromolecular complexes, called mTOR complex 1 (mTORC1) and mTOR complex 2 (mTORC2). The regulatory subunits of mTORC1 are Raptor and mLST8 (Kim et al., 2002). mTORC1 activation is involved mainly in regulating cell growth by increasing protein, lipid and nucleotide synthesis. mTOR activation under chronic stress conditions leads to many detrimental effects leading to pathological hypertrophy, unfolded protein accumulation and energy stress (Sciaretta et al., 2018). It is now known that the mTOR pathway also controls other important cellular processes, like mitochondrial biogenesis and autophagy (Cunningham et al., 2007). However, complete deregulation of mTOR signalling can lead to the development of several pathologies, such as cancer, metabolic syndrome and cardiovascular diseases. It has been reported that ERK pathway leads to the activation of the m TOR (Du et al., 2016). In our study we have obtained an increased levels of pmTOR and Raptor levels indicating that the mTORC1 complex is activated. The ERK pathway activated in the heart during the diabetic condition might be responsible for the upregulation of the mTORC1 complex. Moreover the elevated levels of PPAR α which is responsible for increased fatty acid synthesis in the myocardium might also be the consequence of mTORC1 activation. Thus during DCM another pathway involving ERK/m TORC1/ PPAR α is triggered.

Studies indicate that mTOR has both adaptive and maladaptive functions in the heart. The heart fails to develop compensatory cardiac hypertrophy in response to stress in studies involving genetic ablation of both mTORC1 and mTORC2 (Sciaretta et al., 2014). In addition many studies conducted on mouse models have proved that mTOR signalling plays an essential role in regulating the development of the cardiovascular system and in maintaining cardiovascular integrity under normal conditions (Ramos et al., 2012).

Hence it has been found that cardioprotection is enabled by partially inhibiting mTORC1 in the heart. Partial inhibition reduced accumulation of misfolded proteins, and activated autophagy (Sciaretta et al., 2018). This highlights the importance of partially inhibiting mTORC1 and which may be considered as a potential therapeutic target against cardiovascular diseases.

The major upstream regulators of the mTORC1 pathway are the Akt and AMPK pathways. Akt is another serine threonine kinase which plays an essential role in glucose homeostasis and cell proliferation (Xie et al., 2019). Nutrient rich conditions favour the activation of the Akt pathway under normal conditions. There are three isoforms of Akt: Akt1, Akt2, and Akt3. Akt1 is the isoform that is present in the heart (Xie et al., 2019). The phosphorylation of Akt at Ser 473 is required for the complete activation of Akt. Usually mTORC1 activation is mediated by Akt. However in our study due to insulin resistance there is an inhibition of Akt signalling pathway. The levels of pAkt were lowered and the levels of pPTEN, an inhibitor of Akt pathway were increased in the HG treated group. This suggests an overall deactivation of the Akt pathway. The stress induced kinases like ERK and JNK phosphorylate the insulin receptor substrate (IRS) at serine residue thereby blocking tyrosine phosphorylation and insulin signalling. The cause of insulin resistance in our study also might be due to the low grade inflammatory state created by the activation of MAPK which might then inhibit Akt signalling in the diabetic myocardium. However one of the glycolytic enzyme hexokinase was upregulated in the diabetic group. This might be attributed to the increased mTORC1 complex activation which has the capability to induce glycolysis.

Several anti-inflammatory compounds like cannabidol (Westermann et al., 2006), caffeic acid and rosuvastatin (Luo et al., 2014) were proved to be beneficial for the treatment of DCM. In spite of many efforts taken to develop treatment against DCM none of them have found to be effective in clinical set up. So nowadays research is targeted towards identifying new anti-inflammatory molecules for DCM. CiA which is already reported to have anti-inflammatory activity in various systems also showed the same here also. CiA prevented the activation of the TLR4/MyD88 pathway and also inhibited the MAPKinases in H9c2 cells. It also lowered the levels of pGSK-3β, GATA-4 and upregulated the levels of ST2L ensuring cardioprotection. The levels of O-GlcNAc are also lowered with CiA treatment suggesting its anti-fibrotic and anti-hypertrophic property. In addition, CiA inhibited the NLRP3 inflammasome activation and NFKB translocation.

Also, CiA improved the insulin signalling by Akt and inhibited the mTORC1 complex. From the analysis of these results we strongly believe that the non-toxic nature and the anti-inflammatory potential of CiA contribute immensely to its beneficial effects in addition to its antioxidant activity reported in our previous study (Anupama et al., 2018).

Overall results conclude that the inflammatory response in DCM might be elicited by MyD88 dependent TLR4 mediated NLRP3 inflammasome activation via the MAPK pathway. The results of this research reveal the importance of MAPK inhibitors in the development of drugs against DCM. The efficacy of CiA and metformin against DCM is also visible in this study and could be evaluated further in appropriate models for development of nutraceuticals or drugs.

References

1. Aggarwal BB. Signalling pathways of the TNF superfamily: A double-edged sword. Nat. Rev. Immunol. 2003; 3: 745-756.
2. Anupama N, Preetha Rani MR, Shyni GL, Raghu KG. Glucotoxicity results in apoptosis in H9c2 cells via alteration in redox homeostasis linked mitochondrial dynamics and polyol pathway and possible reversal with cinnamic acid. Toxicol. In Vitro. 2018; 53: 178-192.
3. Baker RG, Hayden MS, Ghosh S. NF-kappaB, inflammation, and metabolic disease. Cell Metab. 2011; 13: 11-22.
4. Bayés-Genis A, González A, Lupón J. ST2 in Heart Failure. Circ. Heart Fail. 2018; 11: e005582.
5. Bøtker HE, Møller N. On NO-The continuing story of nitric oxide, diabetes, and cardiovascular disease. Diabetes. 2013; 62: 2645-2647.
6. Boyd JH, Mathur S, Wang Y, Bateman RM, Walley KR. Toll-like receptor stimulation in cardiomyoctes decreases contractility and initiates an NF-kappaB dependent inflammatory response. Cardiovasc. Res. 2006; 72: 384-393.
7. Champattanachai V, Marchase RB, Chatham JC. Glucosamine protects neonatal cardiomyocytes from ischemia-reperfusion injury via increased protein-associated O-GlcNAc. Am. J. Physiol. Cell Physiol. 2007; 292: C178-187.
8. Chen YL, Qiao YC, Xu Y, Ling W, Pan YH, Huang YC et al. Serum TNF-alpha concentrations in type 2 diabetes mellitus patients and diabetic nephropathy patients: a systematic review and meta-analysis. Immunol. Lett. 2017; 186: 52-58.

9. Cunningham JT, Rodgers JT, Arlow DH, Vazquez F, Mootha VK, Puigserver P. mTOR controls mitochondrial oxidative function through a YY1-PGC-1alpha transcriptional complex. Nature. 2007; 450: 736-740.
10. De Cássia da Silveira e Sá R, Andrade LN, Dos Reis Barreto de Oliveira R, de Sousa DP. A review on anti-inflammatory activity of phenylpropanoids found in essential oils. Molecules. 2014; 19: 1459-1480.
11. Dong B, Qi D, Yang L, Huang Y, Xiao X, Tai N, et al.. TLR4 regulates cardiac lipid accumulation and diabetic heart disease in the nonobese diabetic mouse model of type 1 diabetes. Am. J. Physiol. Heart Circ. Physiol. 2012; 303: H732-H742.
12. Du J, Tong A, Wang F, Cui Y, Li C, Zhang Y, et al. The Roles of PI3K/AKT/mTOR and MAPK/ERK signaling pathways in human pheochromocytomas. Int. J. Endocrinol. 2016; 2016: 5286972.
13. Ducheix S, Magré J, Cariou B, Prieur X. chronic o-glcnacylation and diabetic cardiomyopathy: the bitterness of glucose. Front. Endocrinol. (Lausanne). 2018; 9: 642.
14. Du J, Nan C, Huang JJ, Zhang C, Liu J, Jia P et al. Functional characterization of mouse fetal TnI gene promoters in myocardial cells. J. Biomed. Sci. 2008; 15: 605-613.
15. Frati G, Schirone L, Chimenti I, Yee D, Biondi-Zoccai G, Volpe M et al.. An overview of the inflammatory signalling mechanisms in the myocardium underlying the development of diabetic cardiomyopathy. Cardiovasc. Res. 2017; 113: 378-388.
16. Förstermann U, Sessa WC. Nitric oxide synthases: regulation and function. Eur. Heart J. 2012; 33: 829-837.
17. Frieler RA, Mortensen RM. Immune cell and other noncardiomyocyte regulation of cardiac hypertrophy and remodeling. Circulation. 2015; 131: 1019-1030.
18. Fuentes-Antrás J, Ioan AM, Tuñón J, Egido J, Lorenzo O. Activation of toll-like receptors and inflammasome complexes in the diabetic cardiomyopathy-associated inflammation. Int. J. Endocrinol. 2014; 2014: 847827.
19. Hölscher ME, Bode C, Bugger H. Diabetic cardiomyopathy: does the type of diabetes matter? Int. J. Mol. Sci. 2016; 17: 2136.
20. Iwahana H, Yanagisawa K, Ito-Kosaka A, Kuroiwa K, Tago K, Komatsu N, et al. Different promoter usage and multiple transcription initiation sites of the interleukin-1 receptor-related human ST2 gene in UT-7 and TM12 cells. FEBS J.

1999; 264: 397-406.

21. Jia G, DeMarco VG, Sowers JR. Insulin resistance and hyperinsulinaemia in diabetic cardiomyopathy. Nat. Rev. Endocrinol. 2016; 12: 144-153.
22. Jia G, Hill MA, Sowers JR. Diabetic cardiomyopathy: An update of mechanisms contributing to this clinical entity. Circ. Res. 2018; 122: 624-638.
23. Kakkar R, Lee RT. The IL-33/ST2 pathway: therapeutic target and novel biomarker. Nat Rev Drug Discov. 2008; 7: 827-840.
24. Kaminska B. MAPK signalling pathways as molecular targets for anti-inflammatory therapy - From molecular mechanisms to therapeutic benefits. Biochim. Biophys. Acta. 2005; 1754: 253-262.
25. Kawai T, Akira S. TLR signaling. Cell Death Differ. 2006; 13: 816-825.
26. Kim DH, Sarbassov DD, Ali SM, King JE, Latek RR, Erdjument-Bromage H, et al. mTOR interacts with raptor to form a nutrient-sensitive complex that signals to the cell growth machinery. Cell. 2002; 110: 163-175.
27. Ko HJ, Zhang Z, Jung DY, Jun JY, Ma Z, Jones KE et al. Nutrient stress activates inflammation and reduces glucose metabolism by suppressing AMP-activated protein kinase in the heart. Diabetes. 2009; 58: 2536-2546.
28. Ku PM, Chen LJ, Liang JR, Cheng KC, Li YX, Cheng JT. Molecular role of GATA binding protein 4 (GATA-4) in hyperglycemia-induced reduction of cardiac contractility. Cardiovasc. Diabetol. 2011; 10: 1-15.
29. Liang Q, Wiese RJ, Bueno OF, Dai YS, Markham BE, Molkentin JD. The transcription factor GATA4 is activated by extracellular signal-regulated kinase 1- and 2-mediated phosphorylation of serine 105 in cardiomyocytes. Mol. Cell Biol. 2001; 21: 7460-7469.
30. Luo B, Huang F, Liu Y, Liang Y, Wei Z, Ke H, et al. NLRP3 inflammasome as a molecular marker in diabetic cardiomyopathy. Front. Physiol. 2017; 8: 519.
31. Luo B, Li B, Wang W, Liu X, Liu X, Xia Y, et al. Rosuvastatin alleviates diabetic cardiomyopathy by inhibiting NLRP3 inflammasome and MAPK pathways in a type 2 diabetes rat model. Cardiovasc. Drugs Ther. 2014; 28: 33-43.
32. Ma Y, Zhang X, Bao H, Mi S, Cai W, Yan H, et al. Toll-like receptor (TLR) 2 and TLR4 differentially regulate doxorubicin induced cardiomyopathy in mice. PLoS One. 2012; 7: e40763.
33. Maillet M, van Berlo JH, Molkentin JD. Molecular basis of physiological heart

growth: fundamental concepts and new players. Nat. Rev. Mol .Cell. Biol. 2013; 14: 38-48.

34. Menaka KB, Ramesh A, Thomas B, Kumari NS. Estimation of nitric oxide as an inflammatory marker in periodontitis. J. Indian Soc. Periodontol. 2009; 13: 75-78.
35. Michelsen KS, Wong MH, Shah PK, Zhang W, Yano J, Doherty TM, et al. Lack of Toll-like receptor 4 or myeloid differentiation factor 88 reduces atherosclerosis and alters plaque phenotype in mice deficient in apolipoprotein E. Proc. Natl. Acad. Sci. U S A. 2004; 101:10679-10684.
36. Mohammad MK, Morran M, Slotterbeck B, Leaman DW, Sun Y, Grafenstein Hv et al. Dysregulated Toll-like receptor expression and signaling in bone marrow-derived macrophages at the onset of diabetes in the non-obese diabetic mouse. Int. Immunol. 2006; 18: 1101-1113.
37. Molkentin J D. The zinc finger-containing transcription factors GATA-4, -5, and -6: ubiquitously expressed regulators of tissue-specific gene expression. J Biol. Chem. 2000; 275: 38949-38952.
38. Morimoto T, Hasegawa K, Kaburagi S, Kakita T, Wada H, Yanazume T, et al. Phosphorylation of GATA-4 is involved in alpha 1-adrenergic agonist-responsive transcription of the endothelin-1 gene in cardiac myocytes. J. Biol. Chem. 2000; 275: 13721-13726.
39. Morisco C, Seta K, Hardt SE, Lee Y, Vatner SF, Sadoshima J. Glycogen synthase kinase 3beta regulates GATA4 in cardiac myocytes. J. Biol. Chem. 2001; 27; 276: 28586-28597.
40. Murakami C, Nakamura S, Kobayashi M, Maeda K, Irie W, Wada B, et al. Analysis of the sarcomere protein gene mutation on cardiomyopathy - Mutations in the cardiac troponin I gene. Leg. Med. (Tokyo). 2010; 12: 280-283.
41. Murphy AM, Thompson WR, Peng LF, Jones L 2nd. Regulation of the rat cardiac troponin I gene by the transcription factor GATA-4. Biochem J. 1997; 1: 322.
42. Mutlak M, Kehat I. Extracellular signal-regulated kinases 1/2 as regulators of cardiac hypertrophy. Front. Pharmacol. 2015; 6: 149.
43. Nunes S, Soares E, Pereira F, Reis F. The role of inflammation in diabetic cardiomyopathy. Int. J. Interferon Cytokine Mediat. Res. 2012; 4: 59-73.
44. Oh CC, Nguy MQ, Schwenke DC, Migrino RQ, Thornburg K, Reaven P. p38α mitogen-activated kinase mediates cardiomyocyte apoptosis induced by

palmitate. Biochem. Biophys. Res. Commun. 2014; 450: 628-633.

45. O'Keefe SJ, Mudgett JS, Cupo S, Parsons JN, Chartrain NA, Fitzgerald C, et al. Chemical genetics define the roles of p38 alpha and p38 beta in acute and chronic inflammation. J.Biol.Chem. 2007; 282: 34663-34671.
46. Pan Y, Wang Y, Zhao Y, Peng K, Li W, Wang Y, et al. Inhibition of JNK phosphorylation by a novel curcumin analog prevents high glucose-induced inflammation and apoptosis in cardiomyocytes and the development of diabetic cardiomyopathy. Diabetes. 2014; 63: 3497-3511.
47. Pearson G, Robinson F, Beers Gibson T, Xu BE, Karandikar M, Berman K, et al. Mitogen-activated protein (MAP) kinase pathways: Regulation and physiological functions. Endocr. Rev. 2001; 22: 153-183.
48. Prabhu SD, Frangogiannis NG. The biological basis for cardiac repair after myocardial infarction. Circ. Res. 2016; 119: 91-112.
49. Preetha Rani MR, Anupama N, Sreelekshmi M, Raghu KG. Chlorogenic acid attenuates glucotoxicity in H9c2 cells via inhibition of glycation and PKC α upregulation and safeguarding innate antioxidant status. Biomed. Pharmacother. 2018; 100: 467-477.
50. Premkumar V, Dey M, Dorn R, Raskin I. MyD88-dependent and independent pathways of Toll-Like Receptors are engaged in biological activity of Triptolide in ligand-stimulated macrophages. BMC Chem. Biol. 2010; 10: 3.
51. Ramos FJ, Chen SC, Garelick MG, Dai DF, Liao CY, Schreiber KH, et al. Rapamycin reverses elevated mTORC1 signaling in lamin A/C-deficient mice, rescues cardiac and skeletal muscle function, and extends survival. Sci. Transl. Med. 2012; 4: 144ra103.
52. Salin Raj P, Swapna SUS, Raghu KG. High glucose induced calcium overload via impairment of SERCA/PLN pathway and mitochondrial dysfunction leads to oxidative stress in H9c2 cells and amelioration with ferulic acid. Fundam. Clin. Pharmacol. 2019; 33: 412-425.
53. Satoh M, Shimoda Y, Maesawa C, Akatsu T, Ishikawa Y, Minami Y, et al.. Activated toll-like receptor 4 in monocytes is associated with heart failure after acute myocardial infarction. Int. J. Cardiol. 2006; 109: 226-234.
54. Schroder K, Zhou R, Tschopp J. The NLRP3 Inflammasome : A sensor for metabolic danger. Science. 2010; 327: 296-300.

55. Sciarretta S, Forte M, Frati G, Sadoshima J. New insights into the role of mTOR signaling in the cardiovascular system. Circ. Res. 2018; 122: 489-505.
56. Sciarretta S, Volpe M, Sadoshima J. Mammalian target of rapamycin signaling in cardiac physiology and disease. Circ. Res. 2014; 114: 549-564.
57. Sova M. Antioxidant and antimicrobial activities of cinnamic acid derivatives. Mini Rev. Med. Chem. 2012; 12: 749-767.
58. Tan Y, Zhang Z, Zheng C, Wintergerst KA, Keller BB, Cai L. Mechanisms of diabetic cardiomyopathy and potential therapeutic strategies: preclinical and clinical evidence. Nat. Rev. Cardiol. 17: 585-607.
59. Tang H, Xiao K, Mao L, Rockman HA, Marchuk DA. Overexpression of TNNI3K, a cardiac-specific MAPKKK, promotes cardiac dysfunction. J. Mol. Cell Cardiol. 2013; 54: 101-111.
60. Thandavarayan RA, Giridharan VV, Arumugam S, Suzuki K, Ko KM, Krishnamurthy P, et al. Schisandrin B prevents doxorubicin induced cardiac dysfunction by modulation of DNA damage, oxidative stress and inflammation through inhibition of MAPK/p53 signaling. PLoS One. 2015; 10: e0119214.
61. Thandavarayan RA, Watanabe K, Ma M, Gurusamy N, Veeraveedu PT, Konishi T, et al. Dominant-negative p38alpha mitogen-activated protein kinase prevents cardiac apoptosis and remodeling after streptozotocin-induced diabetes mellitus. Am. J. Physiol. Heart Circ. Physiol. 2009; 297: H911-H919.
62. Thomas CM, Yong QC, Rosa RM, Seqqat R, Gopal S, Casarini DE, et al. Cardiac-specific suppression of NF-kappaB signaling prevents diabetic cardiomyopathy via inhibition of the renin-angiotensin system. Am. J. Physiol. Heart Circ. Physiol. 2014; 307: H1036-H1045.
63. Tsan MF, Gao B. Endogenous ligands of toll-like receptors. J. Leukoc. Biol. 2004; 76: 514-519.
64. Vaishnav M, MacFarlane M, Dickens M. Disassembly of the JIP1/JNK molecular scaffold by caspase-3-mediated cleavage of JIP1 during apoptosis. Exp. Cell Res. 2011; 317: 1028-1039.
65. Wang L, Wang H, Ye J, Xu XR, Song L, Shi N et al. Adenovirus-mediated overexpression of cardiac troponin I-interacting kinase promotes cardiomyocyte hypertrophy. Clin. Exp. Pharmacol. Physiol. 2011; 38: 278-284.
66. Westermann D, Rutschow S, Van Linthout S, Linderer A, Bücker-Gärtner C, Sobirey

M et al. Inhibition of p38 mitogen-activated protein kinase attenuates left ventricular dysfunction by mediating pro-inflammatory cardiac cytokine levels in a mouse model of diabetes mellitus. Diabetologia. 2006; 49: 2507-2513.

67. Wu B, Huang XY, Li L, Fan XH, Li PC, Huang CQ et al. Attenuation of diabetic cardiomyopathy by relying on kirenol to suppress inflammation in a diabetic rat model. J. Cell Mol. Med. 2019; 23: 7651-7663.
68. Xie Y, Shi X, Sheng K, Han G, Li W, Zhao Q, et al. PI3K/Akt signaling transduction pathway, erythropoiesis and glycolysis in hypoxia (Review). Mol. Med. Rep. 2019; 19: 783-791.
69. Yan XL, Wang YY, Yu ZF, Tian MM, Li H. Peroxisome proliferator-activated receptor-gamma activation attenuates diabetic cardiomyopathy via regulation of the TGF-β/ERK pathway and epithelial-to-mesenchymal transition. Life Sci. 2018; 213: 269-278.
70. Yu L, Feng Z. The Role of Toll-Like receptor signaling in the progression of heart failure. Mediators Inflamm. 2018; 2018: 9874109.
71. Zhang H, Shi X, Hampong M, Blanis L, Pelech S. Stress-induced inhibition of ERK1 and ERK2 by direct interaction with p38 MAP kinase. J. Biol. Chem. 2001; 276: 6905-6908.
72. Zhao MX, Zhou B, Ling L, Xiong XQ, Zhang F, Chen Q et al. Salusin-β contributes to oxidative stress and inflammation in diabetic cardiomyopathy. Cell Death Dis. 2017; 8, e2690.
73. Zhao Y, Tan Y, Xi S, Li Y, Li C, Cui J, et al. A novel mechanism by which SDF-1β protects cardiac cells from palmitate-induced endoplasmic reticulum stress and apoptosis via CXCR7 and AMPK/p38 MAPK-mediated interleukin-6 generation. Diabetes. 2013; 62: 2545-2558.
74. Zhao Y, Tang Z, Zhu X, Wang X, Wang C, Zhang W, et al. TAB3 involves in hepatic insulin resistance through activation of MAPK pathway. Gen. Comp. Endocrinol. 2015; 224: 228-234.

Chapter 6

Summary and Conclusion

DCM accounts for about 12 % of the total T2DM patients. Since this is a considerably high proportion attention has to be given to find out the exact reasons behind the development of DCM. Two experimental models have been used in this study. In *in vitro* model H9c2 cells were incubated in 33 m M glucose for 48 hrs. High fat high fructose fed male wistar rats were used for *in vivo* study.

In our study we have demonstrated that inflammation plays an essential role in the progression of DCM. Inflammation is an initial response to any injury. Here we have initially observed an upregulation of the Myd88 dependent TLR4 mediated NLRP3 inflammasome activation via MAPKinases (JNK, ERK, p38 MAPK) *in vitro* and *in vivo*. Thus glucose might be acting as a ligand for the TLR. Simultaneously there was an activation of MAPK mediated pGSK-3β/ GATA-4 axis and hexosamine signalling (O-GlcNAc). Various proinflammatory mediators like cytokines (TNF-α, IL-6, IL-1β), chemokines (MCP-1) and adhesion molecules (ICAM) were released in response to activation of inflammatory pathways. Also the levels of anti-inflammatory cytokine IL-10 were found to be reduced during DCM. These inflammatory pathways will lead to apoptosis, hypertrophy and fibrosis. Apoptosis was confirmed by H & E staining of heart tissue, increased levels of caspase-3, Bax which is a pro-apoptotic protein and reduced levels of anti-apoptotic protein Bcl2 in *in vitro* model. Increased levels of ANP, BNP, TNNI3K, TGF-β and β-MHC and diminished levels of ST2L receptor indicate hypertrophy and fibrosis was confirmed with van-Gieson staining of heart tissue and increased levels of O-GlcNAc.

Meanwhile another pathway involving mTOR was also upregulated during hyperglycemia in H9c2 cells. mTORC1 complex activation (mTOR and Raptor) was also associated with detrimental effects like hypertrophy, insulin resistance and increased fatty acid oxidation. The activation of mTORC1 complex might be attributed to the upregulation of ERK pathway which is usually associated with adaptive mechanisms in the heart. Moreover there was an increased translocation of PPAR α into the nucleus which is responsible for fatty acid oxidation. Hence the substrate shift of the myocardium towards fatty acids was also confirmed in this study. Also, the levels of cardiac injury

markers like troponin, TNNI3K, ANP, BNP and CRP were upregulated in the diabetic heart.

The activation of the inflammatory pathways might be responsible for the remaining molecular events happening in the myocardium like alterations in redox homeostasis and mitochondrial dysfunction in our *in vitro* model. In our study oxidative stress was confirmed by increased reactive oxygen species generation, reduction in the activity of antioxidant enzymes like SOD and glutathione peroxidase and reduced levels of glutathione. Further oxidative stress was confirmed with lipid peroxidation and protein carbonyl content. Cardiomyocytes need more energy and hence it is equipped with abundant mitochondria. Any dysfunction in mitochondria would adversely affect the proper functioning of the heart. In the present study also high glucose altered mitochondrial function. It affected mitochondrial dynamics, transmembrane potential, electron transport chain and ATP synthesis. Alterations in mitochondrial dynamics was observed with increased mitochondrial fission and reduced fusion which was confirmed by overexpression of fission proteins like DRP1 and FIS1 and downregulation of fusion proteins like MFN1 and OPA1. Mitochondrial membrane potential which is an indicator of the mitochondrial membrane integrity was found to be dissipated in the high glucose treated group. Any change in the membrane potential would affect the calcium entry into mitochondria that is required for ATP synthesis. Also the activities of complex 4 and ATP synthesis were severely affected in the hyperglycemic group. Mitochondria is a major source of ROS during pathological situation. Increased mitochondrial superoxide production was obeserved in the high glucose treated H9c2 cells. Maintaining a proper calcium homeostasis is essential for cardiac contraction. However in our study altered calcium homeostasis was observed with increased cytosolic calcium levels as well as downregulation of MCUR1 (mitochondrial cacium uniporter). The levels of sorbitol which is an intermediate in the polyol pathway were also found to be elevated in high glucose treated H9c2 cells.

The phytochemical CiA and positive control metformin were also evaluated against the pathophysiology associated with DCM. CiA is a low toxicity compound which exhibited cardioprotective properties according to our study. The antioxidant enzyme status was found to be restored by CiA. There was an increase in the activity of SOD, GPx and total antioxidant enzyme and elevated levels of glutathione in CiA treated group. Other oxidative stress markers like lipid peroxides and protein carbonyl were reduced

by treatment with CiA. It was also effective in preserving the mitochondrial function by increasing mitochondrial fusion, preventing the dissipation of mitochondrial membrane potential and reducing mitochondrial superoxide production. Complex IV activity and ATP synthesis were also improved by treatment with CiA. CiA treatment also reduced the levels of sorbitol (polyol pathway) and downregulated the expression of O-GlcNAc (hexosamine pathway). CiA was also effective in maintaining calcium homeostasis by reducing intracellular calcium levels and upregulating the expression of MCUR1. Finally, CiA also exhibited anti-inflammatory property. It prevented the MyD88 mediated TLR4 activation. It also prevented the activation of NLRP3 inflammasome complex via inhibition of the MAPK pathways. The levels of proinflammatory mediators were also reduced by CiA treatment. Lastly CiA treatment downregulated the m TORC1 complex activation and prevented PPAR a translocation levels. Thus, the overall results reveal the complex mechanisms that contribute to the etiology of DCM. CiA can be considered as a cardioprotective drug.

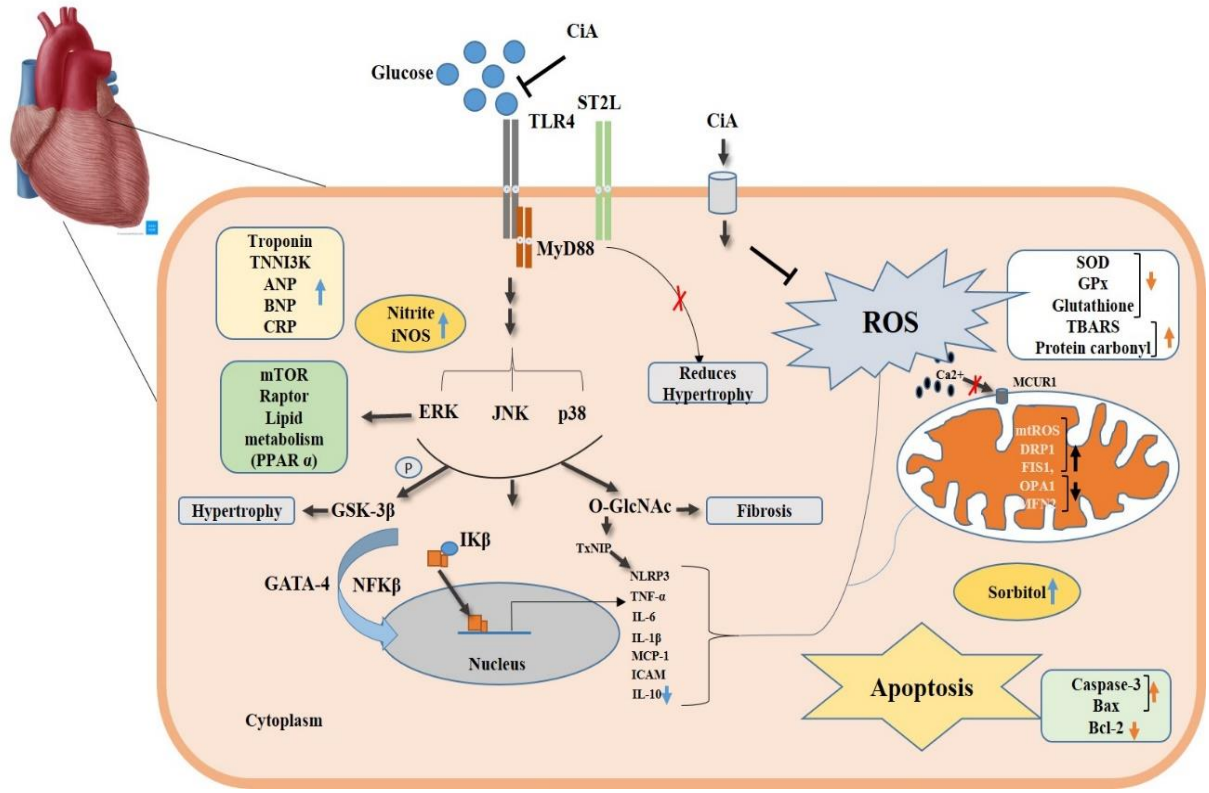

Fig. 6.1 Schematic representation of inflammatory signalling pathways during DCM and proposed mechanism of the action of CiA

ABSTRACT

Name of the Student: **Anupama Nair** Registration No. : 10BB15A39021
Faculty of Study: Biological Sciences Year of Submission: February 2021
AcSIR academic centre/CSIR Lab: NIIST Name of the Supervisor(s):Dr. KG Raghu
Title of the thesis: **Upregulation of inflammatory mediators during diabetic cardiomyopathy and possible amelioration with cinnamic acid**

Diabetic cardiomyopathy (DCM) related health issues are increasing day by day in our public health. So researchers are sharpening their focus to the various molecular mechanisms underlying in this area. The present study aims to elucidate in detail the various inflammatory pathways, mitochondrial dysfunction, alterations in redox homeostasis. We have employed both *in vitro* and *in vivo* models in our study. The H9c2 cells were incubated with 33 mM glucose for 48 hrs to simulate the diabetic condition. Male wistar rats fed with a high energy diet with a single dose of streptozotocin (25 mg/kg bwt) were used as in vivo models. We have observed that the hyperglycemic insult has significantly affected redox homeostasis via depletion of superoxide dismutase, glutathione and enhanced reactive oxygen species generation in high glucose treated H9c2 cells. It also caused dysregulation in mitochondrial dynamics (fusion, fission proteins), dissipation of mitochondrial transmembrane potential, elevated mitochondrial superoxide production and increased sorbitol accumulation. Since myocardial inflammation plays an essential role in the progression of DCM, we have focussed on inflammation in the Chapters 4 and 5. During DCM, there was an upregulation of NLRP3 inflammasome complex via MyD88 dependent TLR4 signalling pathway in both *in vitro* and *in vivo* models. The TLR4 pathway mediated the downstream intracellular signalling mechanisms involving MAPKinases, pGSK-3β, GATA-4 axis and O-GlcNAc. In addition the inhibition of the three MAPKinases (pJNK, pERK and pp38 MAPK) in H9c2 cells attenuated the expression of the pGSK-3β/GATA-4 axis and O-GlcNAc levels suggesting a MAPK dependent inflammatory mechanism. There was an overexpression of TNNI3K and downregulation of ST2L during diabetes. Finally, apoptosis was observed with upregulation of BAX, activation of caspase-3 and downregulation of BCL-2. Cinnamic acid (CiA) and metformin were effective against inflammation, preserved mitochondrial function and maintained redox status during DCM. Thus, CiA was found as a potential bioactive for DCM.

Publications

From thesis

1. Anupama Nair, Preetha Rani MR, Shyni GL, Raghu KG. Glucotoxicity results in apoptosis in H9c2 cells via alteration in redox homeostasis linked mitochondrial dynamics and polyol pathway and possible reversal with cinnamic acid. Toxicol. in Vitro. 2018;53: 178-192.
2. Preetha Rani MR, Anupama Nair, Sreelekshmi Mohan, Raghu KG. Chlorogenic acid attenuates glucotoxicity in H9c2 cells via inhibition of glycation and PKC α upregulation and safeguarding innate antioxidant status. Biomed. Pharmacother. 2018; 100: 467-477.
3. Anupama Nair, Sindhu G, Raghu KG. Significance of mitochondria on cardiometabolic syndromes. Fundam. Clin. Pharmacol. 2018; 32(4): 346-356.

Other than thesis

1. Reshma PL, Binu P, Anupama N, Vineetha RC, Abhilash S, Nair RH, Raghu KG. Pretreatment of Tribulus terrestris L. causes anti-ischemic cardioprotection through MAPK mediated anti-apoptotic pathway in rat. Biomed. Pharmacother. 2019; 111: 1342-1352.
2. Antu KA, Riya MP, **Nair A**, Mishra A, Srivastava AK, Raghu KG. Symplocos cochinchinensis enhances insulin sensitivity via the downregulation of lipogenesis and insulin resistance in high energy diet rat model. J. Ethnopharmacol. 2016; 193: 500-509.
3. Priyanka A., **Anupama Nair**, Anusree S.S., Nisha V.M., Raghu KG. Bilobalide safeguards 3T3-L1 adipocytes from hypoxia through protecting mitochondrial bioenergetics, biogenesis and dynamics. RSC Advances. 2016; 6: 114969-114979.
4. Prathapan A, Mathews V V, Abhilash S, Salin Raj P, **Anupama Nair**, Anil K M, Harikumaran Nair R, Raghu KG. Polyphenol rich ethanolic extract from Boerhavia diffusa L. mitigates angiotensin II induced cardiac hypertrophy and fibrosis in rats. Biomed. Pharmacother. 2017; 87: 427-436.
5. Priyanka A, Shyni GL, **Anupama N**, Raj PS, Anusree SS, Raghu KG. Development of insulin resistance through sprouting of inflammatory markers during hypoxia in 3T3-L1 adipocytes and amelioration with curcumin. Eur. J. Pharmacol. 2017; 812: 73-81.

Scientific Conferences

Oral presentations

1. Cinnamic Acid (CiA) from Cinnamon Ameliorates Hyperglycemia Induced Depletion of Innate Antioxidant Status, Prevent Apoptosis and Safeguard Mitochondria in H9c2 Cells. National Conference on Recent Trends in Biotechnology and Annual Meet of the Society for Biotechnologists (India). National Institute of Ocean Technology, Chennai, 19-21 October 2016.

2. *Boerhavia diffusa*, is a potential nutraceutical for cardiac hypertrophy evident from in vitro and in vivo study. Second International Conference on "Nutraceuticals and Chronic Diseases" (INCD 2017) held at Bogmallo Beach Resort, Bogmalo, Goa, 1-3 September 2017. **Received best oral presentation award.**

3. Evaluation of cinnamic acid against hyperglycemic cardiomyopathy induced alterations in mitochondrial function and calcium homeostasis. International Seminar on Phytochemistry (ISP), Jawaharlal Nehru Tropical Botanical Garden and Research Institute, Palode, Trivandrum, 26 -27 March 2018.

4. Cinnamic acid prevents mitochondrial dysfunction and inflammation during diabetic cardiomyopathy in H9c2 cells. Annual Meet of Society for Biotechnologists (India) & National Conference on Recent Breakthroughs in Biotechnology (NCRBB-2021), virtual conference, January 22-23, 2021.

Poster presentations

1. Modulation of estradiol induced electrophysiological alterations on cardiac action potential by ionic imbalance, gender difference, pacing frequency, ischemia reperfusion insult. Indo-Canadian Symposium on Heart Failure, Progress and Prospects, Rajiv Gandhi Centre for Biotechnology, Kerala, March 12-14, 2015.

2. Abscisic acid acts as a nutraceutical against metabolic syndromes. Annual Meeting of Society for Biotechnologists India (SBTI) 2015 & National Conference on Recent Advances in Biomedical Sciences and Biotechnology. Lakeshore Hospital and Research Centre, Kochi, Kerala, 17-19 December 2015.
3. A novel bioactive from Garcinia sp. improves hepatic steatosis via up-regulation

of PPAR α and AMPK activation. The Ramanbhai Foundation 8th International Symposium on Current Trends in Pharmaceutical Sciences: Advances in New Drug Discovery and Development", Ahmedabad, Gujarat, 2-4 February 2017.

4. Glucotoxicity alters the redox status via mitochondria mediated pathway and cinnamic acid reverses the sameInternational. Congress on Obesity and Metabolic Syndromes (ICOMES 2018), Conrad Hotel, Seoul, South Korea, 6-9 September 2018. **Received travel grant award.**

Toxicology in Vitro xxx (xxxx) xxxx

Contents lists available at ScienceDirect

Toxicology in Vitro

journal homepage: www.elsevier.com/locate/toxinvit

Corrigendum

Corrigendum to < "Glucotoxicity results in apoptosis in H9c2 cells via alteration in redox homeostasis linked mitochondrial dynamics and polyol pathway and possible reversal with cinnamic acid" > < [Toxicology in Vitro 53 (2018) 178–192] >

Nair Anupama[a,b], M.R. Preetha Rani[a,b], G.L. Shyni[a], K.G. Raghu[a,b,*]

[a] Biochemistry and Molecular Mechanism Laboratory, Agro-processing and Technology Division, CSIR- National Institute for Interdisciplinary Science and Technology (NIIST), Thiruvananthapuram 695,019, Kerala, India

[b] Academy of Scientific and Innovative Research (AcSIR), CSIR-HRDC Campus, Ghaziabad, Uttar Pradesh 201,002, India

The authors regret < [b]**Academy of Scientific and Innovative Research (AcSIR), CSIR-HRDC Campus, Ghaziabad, Uttar Pradesh, 201,002, India** > was missing in the affiliation section due to error from them during preparation of manuscript.

The authors would like to apologise for any inconvenience caused.

DOI of original article: https://doi.org/10.1016/j.tiv.2018.08.010

* Corresponding author at: Biochemistry and Molecular mechanism laboratory, Agro-Processing and Technology Division, CSIR - National Institute for Interdisciplinary Science and Technology (NIIST), Industrial Estate P.O., Pappanamcode, Thiruvananthapuram, Kerala, India.

E-mail address: raghukgopal@niist.res.in (K.G. Raghu).

https://doi.org/10.1016/j.tiv.2020.105020

Toxicology in Vitro 53 (2018) 178–192

Contents lists available at ScienceDirect

Toxicology in Vitro

journal homepage: www.elsevier.com/locate/toxinvit

Glucotoxicity results in apoptosis in H9c2 cells via alteration in redox homeostasis linked mitochondrial dynamics and polyol pathway and possible reversal with cinnamic acid

Nair Anupama, Preetha Rani M.R., Shyni G.L., Raghu K.G.*

Biochemistry and Molecular Mechanism Laboratory, Agro-processing and Technology Division, CSIR- National Institute for Interdisciplinary Science and Technology (NIIST), Thiruvananthapuram 695019, Kerala, India

ARTICLE INFO

Keywords:
Hyperglycemia
Mitochondria
Calcium
Cinnamic acid
H9c2 cells

ABSTRACT

Several mechanisms have been proposed for the heart dysfunction during hyperglycemia. The aim of the present *in vitro* study is to elucidate the role of alterations in redox homeostasis in the induction of apoptosis during hyperglycemia in H9c2 cells via dysfunction in mitochondria and polyol pathway and evaluation of the beneficial effect of cinnamic acid against the same. The H9c2 cells were incubated with 33 mM glucose for 48 h to simulate the diabetic condition. Cell injury was confirmed with a significant increase of atrial natriuretic peptide and lactate dehydrogenase release. Alterations in the innate antioxidant system, polyol pathway, mitochondrial integrity, dynamics and apoptosis were investigated. Hyperglycemic insult has significantly affected redox homeostasis via depletion of superoxide dismutase, glutathione and enhanced reactive oxygen species generation. It also caused dysregulation in mitochondrial dynamics (fusion, fission proteins), dissipation of mitochondrial transmembrane potential and increased sorbitol accumulation. Finally, apoptosis was observed with upregulation of Bax, activation of caspase-3 and downregulation of Bcl-2. Cinnamic acid cotreatment increased the innate antioxidant status, improved mitochondrial function and prevented apoptosis in H9c2 cardiomyoblasts. Moreover, this *in vitro* model is found to be ideal for the elucidation of mechanisms at the cellular and molecular level of any physiological, pharmacological and toxicological incidents in H9c2 cells.

1. Introduction

The effect of high-glucose (HG) concentration on heart function is debatable. Exposure to HG has been reported to diminish ischemic injury in isolated perfused hearts (Balteau et al., 2011). However, a more recent and large randomized trial questioned this result and failed to establish any beneficial effect of HG on mortality. Several lines of evidence indicate that hyperglycemia results in toxic effects in several cell types including cardiomyocytes (Kawahito et al., 2009). Hyperglycemia is a significant factor in cardiovascular damage, exerting its effects through multiple pathways including activation of oxidative stress, protein kinase C, glycation, hexosamine and polyol pathways (Preetha Rani et al., 2018). Oxidative stress, a significant cause of diabetic complications (Kain et al., 2011), results when there is an excess production of reactive oxygen species (ROS) relative to the levels of antioxidant enzymes and antioxidants (Kayama et al., 2015). The diminished endogenous antioxidant defense mechanisms like superoxide dismutase (SOD), catalase, and glutathione peroxidase or reduced concentrations of endogenous antioxidants like vitamin E, ascorbic acid, and glutathione (GSH) can increase the ROS levels (Kayama et al., 2015). In response to injury, cardiomyocytes release certain biomarkers such as the natriuretic peptides {atrial natriuretic peptide (ANP) and

Abbreviations: DCM, diabetic cardiomyopathy; ANP, atrial natriuretic peptide; LDH, lactate dehydrogenase; ROS, reactive oxygen species; SOD, superoxide dismutase; GSH, glutathione; CiA, cinnamic acid; FBS, fetal bovine serum; HBSS, Hanks balanced saline solution; DCFH-DA, 2, 7 dichloro dihydro fluorescein diacetate; DMEM, Dulbecco's modified eagle medium; DMSO, dimethyl sulfoxide; ABTS, 2, 2 - azinobis (3-ethylbenzothiazoline-6-sulfonic acid); LDH, lactate dehydrogenase; ANP, atrial natriuretic peptide; EDTA, ethylenediaminetetraacetate; JC-1, 5, 5′, 6, 6′- tetrachloro-1, 1′, 3, 3′- tetraethyl- benzimidazol carbocyanine iodide; TBARS, Thiobarbituric acid reactive substances; DNPH, 2,4-dinitrophenylhydrazine; TCA, trichloroacetic acid; PBS, phosphate buffered saline; MFN2, mitofusin 2; OPA1, optic atrophy 1; FIS1, fission 1 protein; DRP1, dynamin related protein 1; DEVD-AFC, (Asp-Glu-Val-Asp)- 7-amino-4-trifluoromethylcoumarin; FL1, fluorescence 1; HRP, horseradish peroxidase; BCA, bicinchoninic acid; RIPA, radioimmuno precipitation assay; PVDF, polyvinylidene difluoride; SDS-PAGE, sodium dodecyl sulfate - polyacrylamide gel electrophoresis; GSSG, glutathione disulfide

* Corresponding author at: Agro-processing and Technology Division, CSIR - NIIST, Thiruvanathapuram, Kerala 695019, India.
E-mail address: raghukgopal@niist.res.in (K.G. Raghu).

https://doi.org/10.1016/j.tiv.2018.08.010
Received 17 April 2018; Received in revised form 2 August 2018; Accepted 20 August 2018
Available online 23 August 2018
0887-2333/

brain natriuretic peptide}, creatine kinase (Liquori et al., 2014), lactate dehydrogenase (LDH) (Bodor, 2016) etc. These biomarkers are very important as they can be used to monitor heart function.

Mitochondria are energy regulators in cardiac myocytes and any dysfunction in mitochondria profoundly affects the heart. Alterations in mitochondrial transmembrane potential, mitochondrial dynamics, and overproduction of mitochondrial superoxides are some of the indicators of mitochondrial dysfunctions. The quality control mechanism in mitochondria is determined by their dynamic nature by which the mitochondria undergo constant fusion and fission. Mitochondrial fusion is mediated by fusion proteins such as mitofusins (MFN1 and 2) and optic atrophy 1 (OPA1). Fission protein 1 (FIS1) and dynamin related protein 1 (DRP1) are the main players of mitochondrial fission (Ni et al., 2015). Fusion and fission processes play a very important role in the maintenance of important cellular functions including mitochondrial respiratory activity, apoptosis, and calcium signaling (Rovira-Llopis et al., 2017). Calcium (Ca^{2+}) plays a very important role in cardiac function and a normal calcium homeostasis should be maintained for proper myocyte contraction. The interplay between numerous cellular proteins maintains Ca^{2+} cycling in the cell (Marín-García, 2010). Ca^{2+} also enters the mitochondria and their main role is to trigger the oxidative phosphorylation ensuring enough ATP is generated for myocardial contraction (Brookes et al., 2004). However, in the scenario of increased oxidative stress, this balance is disrupted and there will be an accumulation of cytoplasmic Ca^{2+} (calcium overload) which leads to heart failure.

Polyol pathway is another important mechanism by which hyperglycemia induces oxidative stress. It is a two-step process in which excess intracellular glucose is reduced to sorbitol by aldose reductase and sorbitol is further metabolized to fructose by sorbitol dehydrogenase. This leads to a depletion of NADPH and NAD^+ ultimately impairing the intracellular antioxidant defense mechanism and causing oxidative stress (Safi et al., 2014; Oates, 2002).

One of the major outcomes of hyperglycemic oxidative stress in the heart is cardiomyocyte apoptosis (Das et al., 2009). It has been reported in diabetic animals that cardiomyocyte apoptosis leads to loss of contractile tissue, remodeling and finally dysfunction (Cai et al., 2002). But the exact mechanisms by which hyperglycemia induces apoptosis in cardiomyocytes are not yet fully understood. The elucidation of molecular events responsible for cardiac myocyte apoptosis during hyperglycemia will be highly exciting for biomedical scientists and cardiovascular researchers. Since diabetic cardiomyopathy is still an unmet need for medical fraternity this information will pave a path for the identification of novel biochemical targets for therapeutic purpose. Considering the clinical relevance of these data, the identification of critical pathways linked to apoptosis via hyperglycemia in cardiomyoblast is the primary aim of this study. Moreover from this study, a robust *in vitro* model is expected to develop for general cardiac toxicity screening as well as elucidation of mechanisms involved. This will be a fast and cost-effective method and use of precious test materials, animals and associated regulatory issues could be minimized.

Extensive research and development have produced many drugs against diabetes and associated complications. But none of them is effective for complete recovery. Moreover, some of them have adverse effects restricting their common use. This has created a search for much better candidate molecules for diabetes as well as cardiovascular diseases. In consideration of the excellent health-promoting effects, natural products have been regarded as important drug resources and served as remedies for thousands of years worldwide. Recent research has revealed the importance of bioactive from edible spices for the treatment of lifestyle-related diseases. Cinnamon is a culinary spice found abundantly in our area. Herein we have selected cinnamic acid (CiA), a bioactive from cinnamon for evaluation against hyperglycemia-induced apoptosis in H9c2 cells. It is reported to have antidiabetic (Lakshmi et al., 2009), cardioprotective (Song et al., 2013), anticancer (Niero and Machado-Santelli, 2013), anti-inflammatory and antioxidant properties (Yang et al., 2015). In brief, the present investigation is also looking for the possible beneficial effect of CiA against hyperglycemia-induced alterations in H9c2 cells.

2. Materials and methods

2.1. Chemicals and cell culture reagents

Cinnamic acid (CiA) was purchased from Natural Remedies Pvt. Ltd., Bangalore, India. Fetal bovine serum (FBS), pencillin-streptomycin antibiotics, trypsin - ethylenediaminetetraacetate (EDTA) and Hanks balanced saline solution (HBSS) were from Gibco, USA. MitoSOX™ red and Fura 2-AM were from Invitrogen (Carlsbad, CA, USA). Dimethyl sulfoxide (DMSO), 3-(4,5-dimethylthiazol-2-yl)-2,5-diphenyltetrazolium bromide (MTT), 2, 7 dichloro dihydro fluorescein diacetate (DCFH-DA) and 5,5′,6,6′-tetrachloro-1,1′,3,3′-tetraethyl- benzimidazol carbocyanine iodide (JC-1) were from Sigma Aldrich (St. Louis, USA). Bax and Bcl-2 antibodies were from Cell Signaling Technology (USA). OPA1, MFN2, DRP1, FIS1 and β-actin were from Santa Cruz, USA. All other chemicals were of analytical grade.

2.2. Cell culture

H9c2 cardiomyoblasts from American Type Culture Collection (ATCC) were cultured in Dulbecco's modified eagle medium (DMEM) supplemented with 10% fetal bovine serum (FBS), and antibiotics (100 U/ml of penicillin and 100 μg/ml of streptomycin) in a humidified incubator with 95% air and 5% CO_2 at 37 °C. H9c2 cells mimic most of the electrophysiological, biochemical and pharmacological properties of adult primary cardiomyocytes, so this is found to be an ideal model for *in vitro* study (Kuznetsov et al., 2015). In order to rule out the effect of changes in osmolarity, mannitol was used. Cells were allowed to attain 60% confluence and were treated with high glucose (33 mM) for 48 h to simulate hyperglycemia. Cardiac dysfunction was confirmed by the significant increase of ANP and LDH release. All parameters were determined after 48 h of incubation of cells with high glucose in the presence or absence of various doses of CiA in 0.1% DMSO (100 and 500 nM) or metformin (positive control, 1 mM).

2.3. Experimental groups

Experimental groups consist of control (C; 5.5 mM glucose), high glucose (HG; 33 mM glucose), high glucose + metformin (Met; 1 mM), HG + Cinnamic acid-100 nM (CiA1), HG + Cinnamic acid-500 nM (CiA2), control + Cinnamic acid-500 nM (C + CiA2 for toxicity evaluation).

2.4. Cell viability during experiments was analyzed by MTT assay and LDH release to the medium

a) MTT assay: The method was carried out as per method of Wilson, 2000. Briefly, 5×10^3 cells were seeded in 96 well plates. Cells after 60–70% confluence were treated with different concentrations of the compound. CiA was dissolved in DMSO and the final concentration used was < 0.1% DMSO. The cells were then incubated for 48 h. After incubation, the medium was removed and cells were incubated for 4 h with 10 mg/ml of MTT, dissolved in serum free medium (DMEM). Then it was washed with 100 μl phosphate buffered saline (PBS), and 100 μl of DMSO was added, gently shaken for 10 min so that complete dissolution was achieved and absorbance was recorded at 570 nm using the microplate spectrophotometer (Biotek Synergy 4, USA).
b) LDH release assay: LDH release to the medium was measured using assay kit (Takara, USA). LDH is a soluble enzyme located in the cytosol that is released into the surrounding culture medium upon cell damage or lysis processes. LDH activity in the culture medium

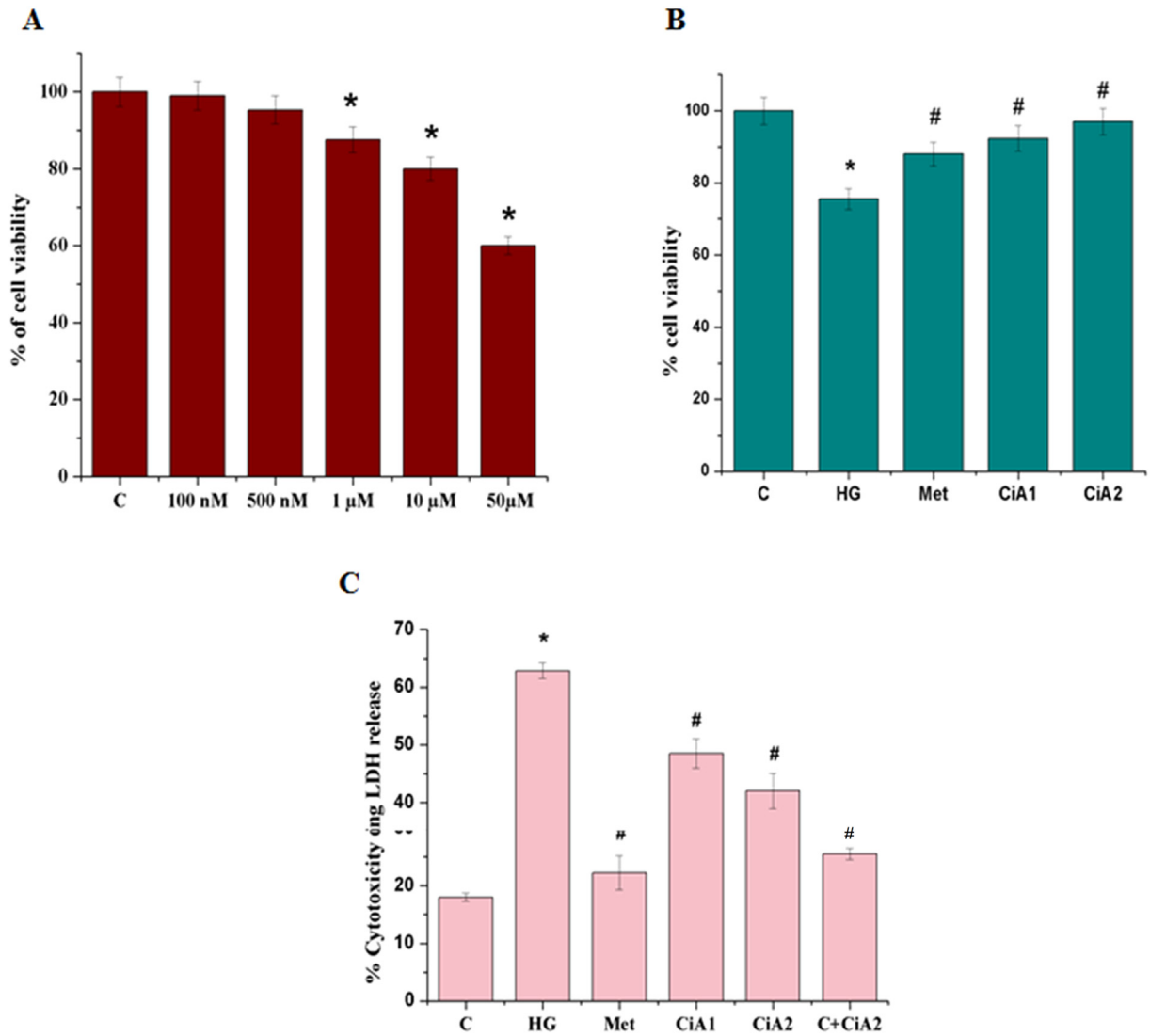

Fig. 1. Cell viability assessment A) H9c2 cells were treated with different concentrations of cinnamic acid (100 nM, 500 nM, 1 µM, 10 µM, 50 µM) and viability was assessed by MTT assay. B) Cell death in H9c2 cells after treatment with 33 mM glucose (high glucose) and amelioration with cinnamic acid or metformin. C) Lactate dehydrogenase (LDH) release during hyperglycemia with H9c2 cells and the effect of cinnamic acid or metformin. C - control, HG - high glucose treated group, Met - HG + metformin, CiA1 - HG + cinnamic acid (100 nM), CiA2 - HG + cinnamic acid (500 nM), C + CiA2 – control + cinnamic acid (500 nM). Values are expressed as mean ± SEM where $n = 6$. * $p \leq 0.05$ significantly different from the control group. # $p \leq 0.05$ significantly different from HG treated group.

can therefore be used as an indicator of cell membrane integrity and thus a measurement of cytotoxicity. After respective treatments, 100 µl of cell culture medium was collected and transferred to 96 well plates. To this LDH reaction solution containing NAD+, lactic acid, iodonitrotetrazolium (INT) and diaphorase, was added. The mixture was incubated with gentle shaking for 30 min at room temperature and the absorbance was taken at 490 nm. LDH release to culture medium was calculated as the percentage of cytotoxicity of cell.

2.5. Quantification of ANP

ANP was quantified using the assay kit from Elabscience, USA. Briefly, the trypsinized cells were collected and centrifuged. To 50 µl of samples, 50 µl of antibody solution was added and incubated for 45 min at 37 °C and washed with buffer. Then it was soaked for 1 min in wash buffer and 100 µl of HRP conjugate solution was added and incubated for 30 min at 37 °C. The solution was aspirated again and 90 µl of substrate was added and incubated for 15 min at 37 °C. Finally 50 µl of stop solution was added and the absorbance was measured at 450 nm.

2.6. Detection of intracellular ROS generation

Intracellular ROS levels were measured using DCFH-DA (Choi et al., 2008). After respective treatments, cells were washed with PBS and then incubated with DCFH-DA for 20 min at 37 °C in a humidified atmosphere containing 5% CO_2. After incubation, cells were washed with Krebs-Ringer phosphate buffer. DCF fluorescence imaging was done (Ex.488 nm; Em. 525 nm) to detect the difference in the intensity of fluorescence.

2.7. Cell based antioxidant studies

For these, H9c2 cells were seeded in 6 well plates at a density of 3×10^5 cells per well. At subconfluence, cells were given HG treatment along with compound and metformin for 48 h.

2.7.1. SOD activity assay

SOD activity was assayed with a commercial kit from Biovision, USA. Briefly, after protein concentration was determined, samples were treated with 2-(4-iodophenyl)-3-(4-nitrophenyl)-5-(2, 4-disulfophenyl)

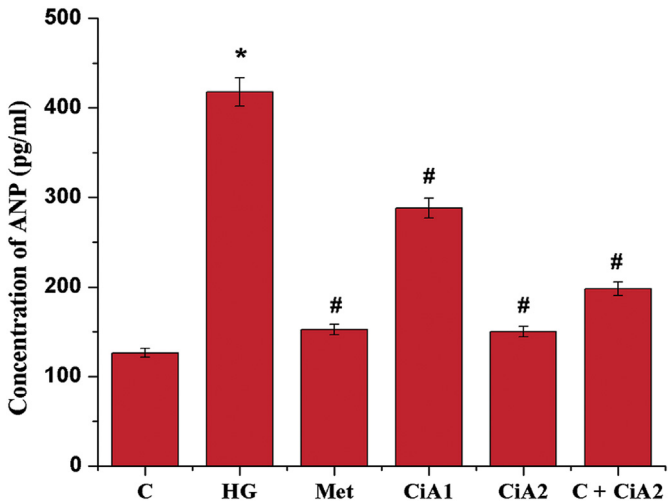

Fig. 2. Quantification of atrial natriuretic peptide (ANP) during hyperglycemia H9c2 cells were treated with high glucose (33 mM) for 48 h in the presence or absence of various concentrations of cinnamic acid or metformin. C - control, HG - high glucose treated group, Met - HG + metformin, CiA1 - HG + cinnamic acid (100 nM), CiA2 - HG + cinnamic acid (500 nM), C + CiA2 – control + cinnamic acid (500 nM). Values are expressed as mean ± SEM where n = 6. * $p \leq 0.05$ significantly different from the control group. # $p \leq 0.05$ significantly different from HG treated group.

2H-tetrazolium, monosodium salt, which produces a water-soluble formazan dye upon reduction with a superoxide anion. After 20 min of incubation at 37 °C, the absorbance was measured at 450 nm.

2.7.2. Estimation of GSH

GSH content was estimated using a kit from Cayman chemicals (USA). Briefly, after respective treatments, cells were collected and homogenized on ice in cold buffer and centrifuged at 10000 x g for 15 min at 4 °C. The supernatants were collected and deproteinized. To that 50 µl of sample and standard were added. Freshly prepared assay cocktail mixture was added to the samples and standard in each well and incubated at 37 °C for 25 min. GSH concentration was measured by end point method at 405 nm.

2.7.3. Total antioxidant assay

Total antioxidant activity of the samples was assayed using kit from Cayman chemicals (USA). This assay is based on the ability of antioxidants in the sample to inhibit the oxidation of 2, 2-azinobis (3-ethylbenzothiazoline-6-sulfonic acid) (ABTS*) to reduced $ABTS^{**+}$ by metmyoglobin. The amount of $ABTS^{**+}$ produced was monitored by measuring absorbance at 405 nm. After respective treatments, cells were collected by centrifugation at 2000 x g for 10 min at 4 °C. The pellets were sonicated on ice in 1–2 ml of cold buffer and further centrifuged at 10000 x g for 15 min at 4 °C. The supernatant was collected. To 10 µl of sample, 10 µl of metmyoglobin and 150 µl of chromogen were added. The reactions were initiated by adding 40 µl of hydrogen peroxide working solution to each wells. The wells were incubated for 5 min at room temperature and the absorbance was measured.

2.7.4. Estimation of thiobarbituric acid reactive substances (TBARS)

Oxidative stress in the cellular environment results in the formation of highly reactive and unstable lipid hydroperoxides. Lipid peroxidation was estimated with TBARS assay kit (Himedia, India). TBARS assay measures the levels of malondialdehyde present in the sample. Briefly, cells were collected and sonicated for 5 s. 100 µl of sample and standard were added to the labeled tubes. To that 100 µl of sodium dodecyl sulfate (SDS) and 4 ml coloring reagent were added. The tubes were then kept in a water bath and boiled for 1 h and were then placed on an ice bath for 10 min to stop the reaction. After incubation, it was then centrifuged for 10 min at 1600 x g at 4 °C and incubated at room temperature for 30 min. From this 150 µl of samples were transferred to the plate and the absorbance of the colored product was measured at 530 nm.

2.7.5. Estimation of protein carbonyls

Protein carbonyl content was determined using a kit from Cayman chemicals (USA). After respective treatments, cells were collected and homogenized on ice in cold buffer. Then the homogenized samples were centrifuged and supernatants were collected. To 200 µl of sample 800 µl of 2, 4 dinitrophenylhydrazine (DNPH) and 800 µl of HCl were added. After incubation in the dark for 1 h 1 ml of 20% trichloroacetic acid (TCA) was added followed by centrifugation. The pellet was resuspended in 1 ml of 10% TCA. After centrifugation again the pellet was collected and resuspended in ethanol/ethyl acetate mixture and centrifuged for 10 min. This step was repeated 2 more times. Finally, the protein pellets were resuspended in 500 µl of guanidine hydrochloride and centrifuged to remove any debris. Then the absorbance was measured at 360 nm.

2.8. Studies on mitochondria

2.8.1. Mitochondrial transmembrane potential (ψm)

Alteration in ψm was detected using JC-1 mitochondria staining kit that uses JC-1, a cationic fluorescent dye. Briefly, the cells were seeded in 96-well black plate at a density of 5×10^3 for treatment. In normal cells, due to the electrochemical potential gradient, the dye is concentrated in the mitochondrial matrix, where it forms red fluorescent aggregates (JC-1 aggregates). Any event that dissipates the mitochondrial membrane potential prevents the accumulation of JC-1 dye in the mitochondria, and thus the dye is dispersed throughout the entire cell leading to a shift from red (JC-1 aggregates) to green (JC-1 monomers). The cells after respective treatments were incubated with JC-1 stain for 20 min. The stain was washed off with HBSS and examined under the spinning disk imaging system (BD, USA). The fluorescence was measured at 490 nm excitation and 530 nm emission wavelengths for JC-1 monomers, and for aggregates, the wavelengths were set at 525 nm for excitation and 590 nm for emission.

2.8.2. Mitochondrial superoxide production

Changes in mitochondrial superoxide production were monitored using MitoSOX™ red. The cells were seeded in 96-well plate at a density of 5×10^3 for experiment and subjected to treatments. The solution of MitoSOX™ in Hanks buffered saline solution (HBSS) was added to cells and incubated at 37 °C for 15 min. Cells were then washed with HBSS and processed for imaging at excitation/emission range of 514/580 nm.

2.8.3. Expression of mitochondrial fission and fusion proteins

The expression of mitochondrial fission and fusion proteins was determined at protein levels by western blotting (please see Section 2.12 for details).

2.9. Detection of intracellular calcium levels by Fura 2 AM

Intracellular calcium was detected by staining the cells with Fura-2 AM (Robinson et al., 2004). For this, cells were washed three times with HBSS and the images were visualized using the spinning disk imaging system at an excitation of 340 nm and emission of 510 nm.

2.10. Detection of apoptosis

2.10.1. Caspase-3 fluorimetry assay

Analysis of apoptosis was done by caspase-3 fluorimetry assay kit (Biovision, USA). Briefly, the cells were resuspended in chilled lysis buffer. Cells were incubated on ice for 10 min. 50 µl of reaction buffer was added to each sample and to it 1 mM (Asp-Glu-Val-Asp)- 7-amino-

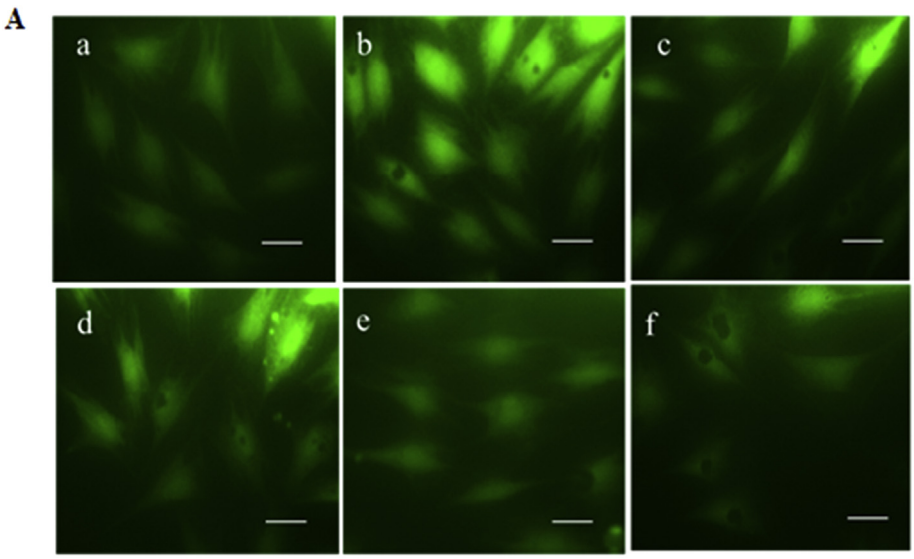

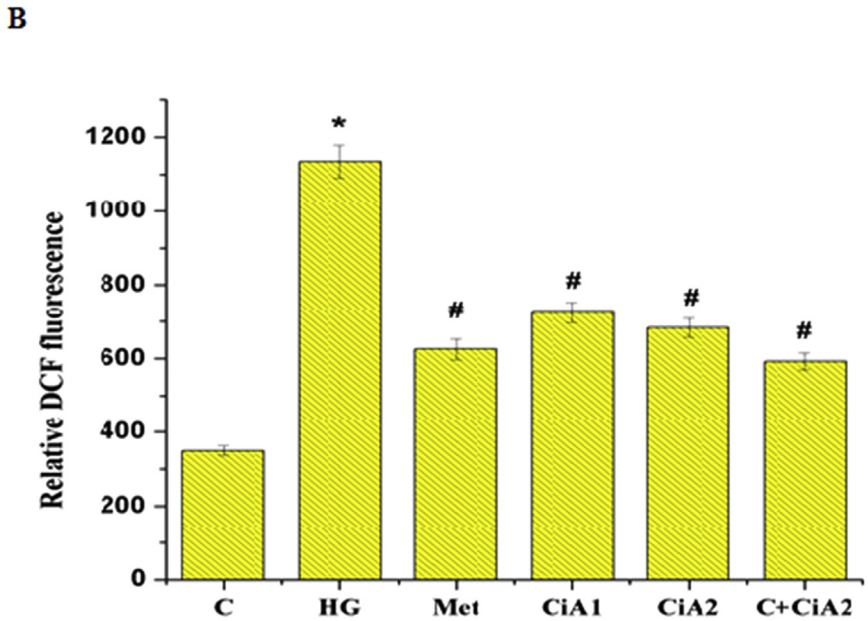

Fig. 3. Effect of cinnamic acid on reactive oxygen species generation in H9c2 cells- H9c2 cells were treated with high glucose (33 mM) for 48 h in the presence or absence of various concentrations of cinnamic acid or metformin. A) Reactive oxygen species accumulation in various groups determined by DCFH-DA staining; the representative images of ROS- induced fluorescence. (a) control, (b) high glucose treated group (HG), (c) HG + metformin, (d) HG + cinnamic acid (100 nM), (e) HG + cinnamic acid (500 nM), (f) control + cinnamic acid (500 nM). Scale bar corresponds to 100 µm. B) Relative fluorescent intensity of the fluorescent images. C - control, HG - high glucose treated group, Met - HG + metformin, CiA1 - HG + cinnamic acid (100 nM), CiA2 - HG + cinnamic acid (500 nM), C + CiA2 – control + cinnamic acid (500 nM). Values are expressed as mean ± SEM where $n = 6$. * $p \leq 0.05$ significantly different from the control group. # $p \leq 0.05$ significantly different from HG treated group.

4-trifluoromethylcoumarin (DEVD-AFC) substrate was added and incubated for 1 h. Fluorescence was measured at excitation wavelength of 405 nm and emission of 505 nm.

2.10.2. Flow cytometric analysis with annexin V/PI

Apoptotic cells were quantified by flow cytometry (BD FACSARIA) using annexin V-FITC apoptosis detection kit from Biovision (USA). For cytometry analysis, the cells were resuspended in 500 µl of 1X binding buffer and to this, 5 µl of annexin V-FITC was added. Then 5 µl of propidium iodide was added and incubated at room temperature for 5 min in dark. Annexin V-FITC binding was analyzed by flow cytometry (Ex = 488 nm; Em = 530 nm) using FITC signal detector {fluorescence 1 (FL1)} and PI staining by the phycoerythrin emission signal detector {fluorescence 2 (FL2)}.

2.10.3. Detection of pro-apoptotic and anti-apoptotic protein expression

Expression of pro-apoptotic protein BAX and anti-apoptotic protein BCL-2 was determined by western blot analysis (please see Section 2.12 for details).

2.11. Detection of sorbitol levels

Sorbitol levels were determined as per manufacturer's protocol (Biovision, USA). Initially, a working solution of sorbitol standards (1 mM) was prepared using the stock solution provided in the kit. Standards (including reaction blanks) were pipetted into wells of a 96-well microtitre plate to generate 0, 2, 4, 6, 8 and 10 nmol/well by dilution in assay buffer. 50 µl of protein samples were pipetted into the wells. This was followed by addition of 50 µl of reaction mixture (enzyme mixture, developer and probe diluted in assay buffer) to all wells and incubated at 37 °C for 30 min. The absorbance was read at 560 nm and sorbitol concentration was calculated.

2.12. Western blotting

Protein was extracted from cell lysates using ice-cold radio-immunoprecipitation assay (RIPA) buffer containing protease inhibitor cocktail (Sigma Aldrich, USA). After incubation at 4 °C for 1 h, with constant agitation to ensure complete lysis, the cell suspension was centrifuged at 12,000 rpm for 15 min at 4 °C and the supernatant was

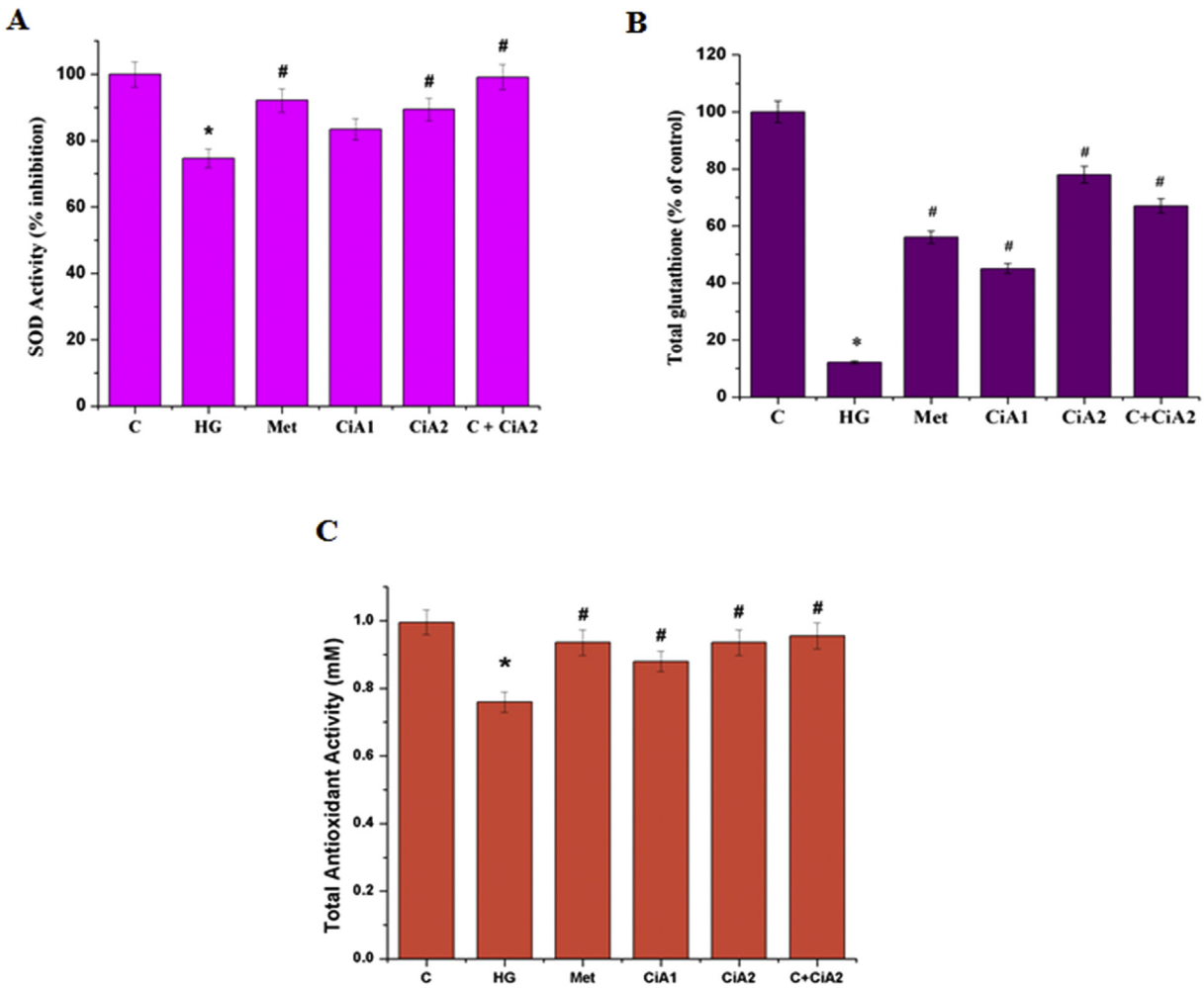

Fig. 4. High glucose depleted general innate antioxidant status and cinnamic acid dose dependently reversed high glucose induced alterations in endogenous antioxidant status in H9c2 cells- H9c2 cells were treated with high glucose (33 mM) for 48 h in the presence or absence of various concentrations of cinnamic acid or metformin. A) SOD activity B) Total glutathione content C) Total antioxidant capacity. C - control, HG - high glucose treated group, Met - HG + metformin, CiA1 - HG + cinnamic acid (100 nM), CiA2 - HG + cinnamic acid (500 nM), C + CiA2 – control + cinnamic acid (500 nM). Values are expressed as mean ± SEM where $n = 6$. * $p \leq 0.05$ significantly different from the control group. # $p \leq 0.05$ significantly different from HG treated group.

collected. Protein content in the supernatant was quantified using the bicinchoninic acid (BCA) protein assay kit (Pierce, Rockford, IL, USA) in accordance with the manufacturer's instructions. Proteins extracted using RIPA buffer were separated by sodium dodecyl sulfate polyacrylamide gel electrophoresis (SDS-PAGE) and transferred to polyvinylidene difluoride (PVDF) membranes using turbo trans blot apparatus (BD Bioscience, USA). The membrane was blocked with 5% skimmed milk in TBST for 1 h at room temperature. The membrane was washed 3 times in TBST for 10 min each. The membranes were probed with antibodies against OPA1, MFN2, FIS1, DRP1, Bax, Bcl-2 and β actin followed by incubation with HRP conjugated secondary antibodies. After washing, the membrane was developed using Clarity ™ Western ECL Substrate (BIO-RAD, USA). The immunoblot images were analyzed in ChemiDoc XRS system (BIO-RAD, USA) using Image Lab software.

2.13. Statistical analysis

Data are presented as mean ± standard error of mean (SEM) for the control and experimental groups ($n = 6$). Data were subjected to one-way analysis of variance (ANOVA) and the differences among the means for the groups were assessed using Duncan's multiple range tests using SPSS for Windows standard version 7.5.1 (SPSS, Inc), to determine which mean values were significantly different at $p \leq 0.05$.

3. Results

3.1. Effect of CiA on cell viability

In order to select an ideal dose of CiA, cell viability was checked with 100 nM, 500 nM, 1 μM, 10 μM and 50 μM of the same and we selected 100 nM and 500 nM based on the results (For data please see Fig. 1a).

3.2. Effect of CiA on HG induced cell death

Incubation of H9c2 cells with 33 mM glucose (HG) caused 24% cell death for 48 h of incubation. Interestingly CiA of 100 and 500 nM concentrations or metformin (1 mM) significantly ($p \leq 0.05$) improved (16.8%, 21.4% and 12.4% respectively) cell viability compared to HG group (Fig. 1b).

3.3. LDH release detection

LDH analysis showed significant release ($p \leq 0.05$) of enzyme (44.8%) to the medium with HG group compared to the control (l8%; Fig. 1c). While with CiA, LDH release was found to be lowered by 14.3% and 20.8% for 100 and 500 nM respectively compared to HG (Fig.1c). Metformin reduced LDH release by 40.5% compared HG

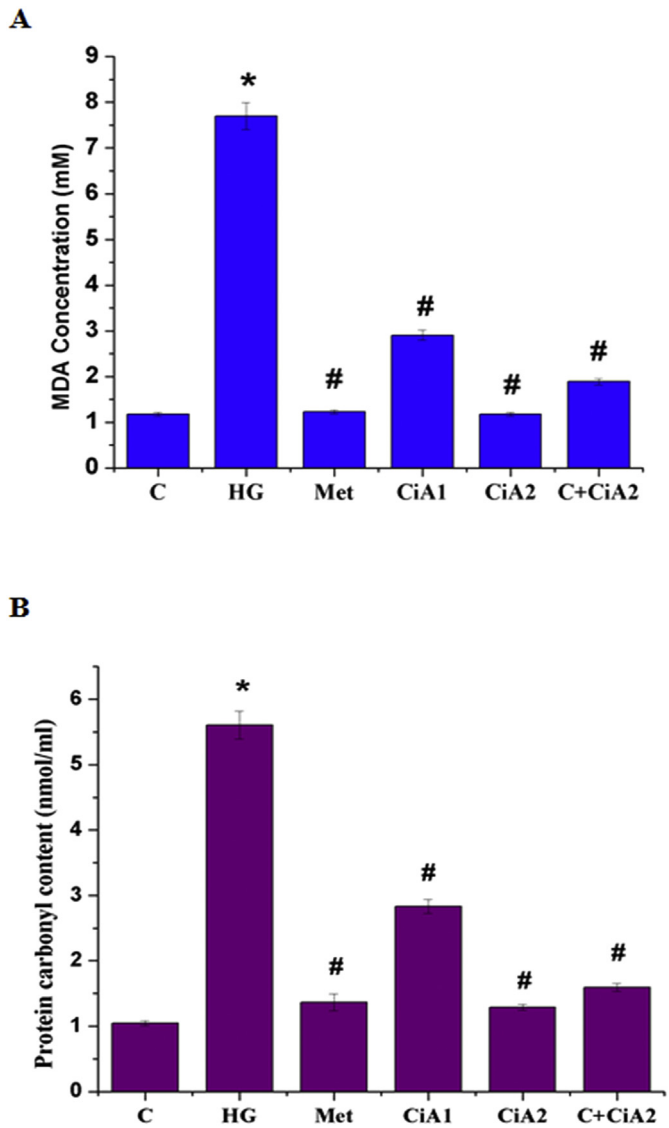

Fig. 5. Quantification of oxidative stress markers during hyperglycemia and reversal with cinnamic acid or metformin- H9c2 cells were treated with high glucose (33 mM) for 48 h in the presence or absence of various concentrations of cinnamic acid or metformin. A) Lipid peroxidation in H9c2 cells with high glucose and effect of cinnamic acid and metformin. B) Protein carbonyl content in cells treated with high glucose and cinnamic acid. C - control, HG - high glucose treated group, Met - HG + metformin, CiA1 - HG + cinnamic acid (100 nM), CiA2 - HG + cinnamic acid (500 nM), C + CiA2 – control + cinnamic acid (500 nM). Values are expressed as mean ± SEM where $n = 6$. * $p \leq 0.05$ significantly different from the control group. # $p \leq 0.05$ significantly different from HG treated group.

($p \leq 0.05$; Fig. 1c).

3.4. Detection of ANP

There was a significant increase ($p \leq 0.05$) in ANP levels in HG treated group (230%; Fig. 2). Cotreatment with CiA at 100 nM and 500 nM reduced ANP levels significantly ($p \leq 0.05$) by 102.8% and 212% respectively compared to HG. Treatment with metformin also significantly ($p \leq 0.05$) reduced ANP levels by 210% compared to HG treated group (Fig. 2).

3.5. CiA reduces intracellular ROS generation

Significant generation of ROS ($p \leq 0.05$) was observed in cells treated with HG. Fluorimetry analysis showed 224% increase of fluorescence in HG treated cells compared to control (Fig. 3). CiA cotreatment at both concentrations (100 and 500 nM) showed a considerable decrease ($p \leq 0.05$) in the ROS generation (117% and 128.8%) respectively (Fig. 3). Treatment with metformin also significantly reduced ($p \leq 0.05$) ROS generation by 145.7%. (Fig. 3).

3.6. CiA restored antioxidant enzyme activity altered by HG

HG caused a significant decrease ($p \leq 0.05$) in SOD activity by 25.3% and cotreatment with CiA increased SOD activity by 8.74% at 100 nM (not significant) and by 14.7% ($p \leq 0.05$) at 500 nM compared with HG (Fig. 4a). Treatment with metformin also caused a significant increase (17.4%) compared to HG (Fig. 4a). There was also a significant decrease ($p \leq 0.05$) in total glutathione in HG group by 87.9% (Fig. 4b). Here also treatment with CiA (100 and 500 nM) or metformin (1 mM) significantly ($p \leq 0.05$) increased glutathione content by 32.9%, 65.9% and 43.9% respectively (Fig. 4b). The total antioxidant capacity of the cells was also found to be significantly reduced ($p \leq 0.05$) in HG (23.7%; Fig. 4c). While cotreatment with CiA (100 and 500 nM) or metformin (1 mM) prevented the depletion of total antioxidant status by 12.1%, 17.6% and 17.7% respectively compared to HG (Fig. 4c).

3.7. CiA prevented lipid peroxidation and reduced protein carbonyls in H9c2 cells

High glucose induction significantly increased ($p \leq 0.05$) lipid peroxidation (MDA level) by 554% compared to control (Fig. 5a). Cotreatment with CiA during hyperglycemia significantly reduced ($p \leq 0.05$) the MDA levels by 407% (100 nM) and 554% (500 nM) compared to HG (Fig. 5a). There was also a significant reduction ($p \leq 0.05$) of lipid peroxidation in metformin treated group (549%) (Fig. 5a). Protein carbonyl formation was also significantly higher ($p \leq 0.05$) in HG (434.9%) compared to control (Fig. 5b). Treatment with CiA at 100 and 500 nM or metformin lowered protein carbonyls by 264. 7%, 412.1% and 404.6% respectively compared to HG (Fig. 5b).

3.8. Mitochondrial dysfunction during hyperglycemia and amelioration with CiA

With HG, JC-1 green monomers were significantly increased ($p \leq 0.05$; 394.4%; Fig. 6) compared to the control indicating a dissipation of ψm. Treatment with CiA prevented the dissipation of ψm which was evident with visibility of red fluorescence compared to HG (Fig. 6). Quantitatively, green fluorescence was decreased significantly ($p \leq 0.05$) by 378.5% and 392.8% for 100 and 500 nM compared to HG (Fig. 6). The trend was the same with metformin too (Fig. 6) where the intensity of green fluorescence (monomers) was reduced by 361.1% ($p \leq 0.05$) and a shift to red fluorescence (aggregates) was observed (Fig. 6). Alteration in superoxide generation was detected with Mitosox red. HG caused significant (481.6%) generation of superoxides while CiA prevented the abnormal superoxide generation (Fig. 7). CiA (100 and 500 nM) prevented superoxide generation significantly ($p \leq 0.05$) by 290% and 330% respectively (Fig. 7). Metformin treatment also significantly ($p \leq 0.05$) reduced the generation of superoxide radicals (409.3%; Fig. 7).

3.9. Expression of mitochondrial fission and fusion proteins by western blot analysis

There was also a significant decrease in the expression of mitochondrial fusion proteins OPA1 and MFN2 by 32.8% and 38.9%

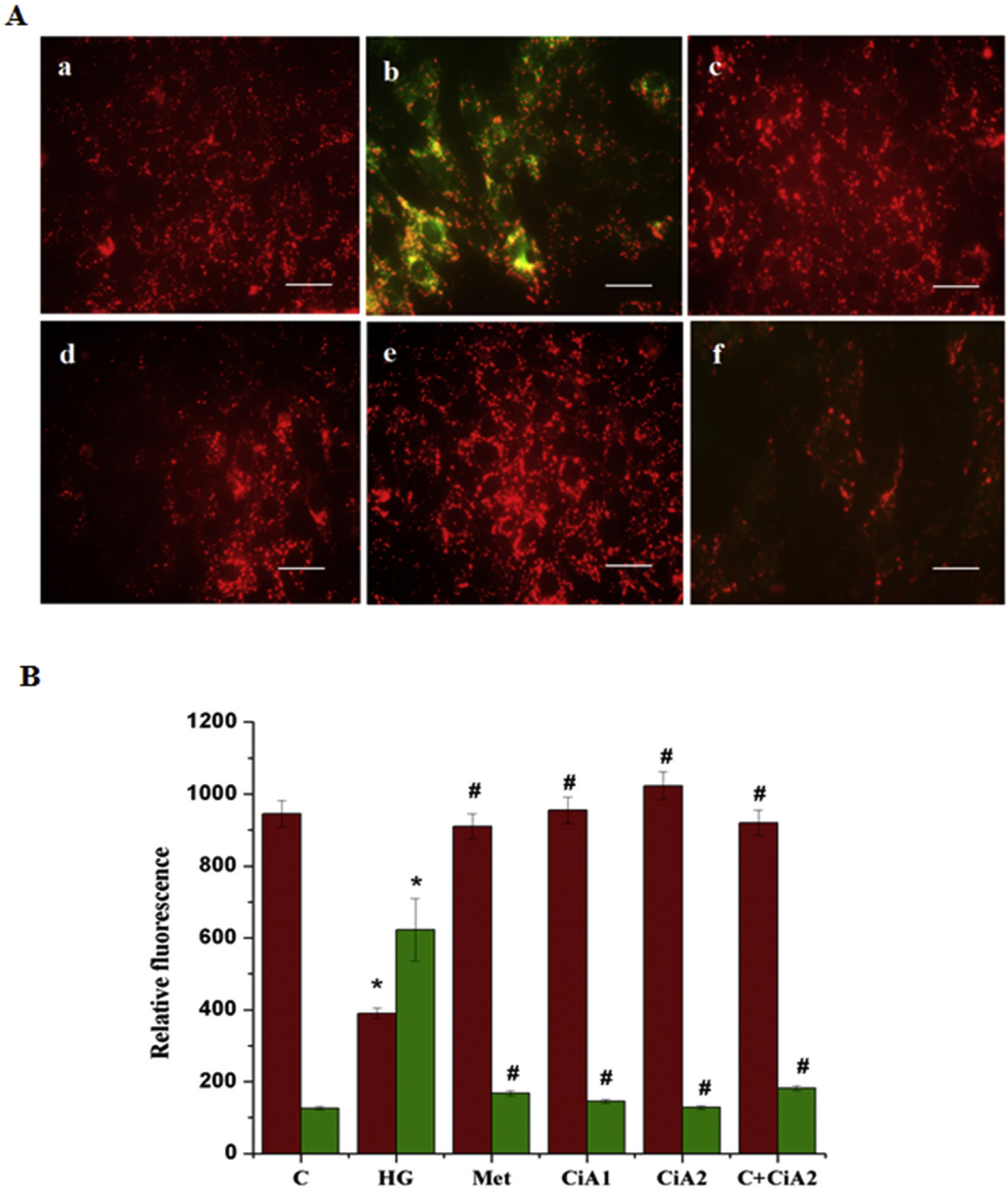

Fig. 6. Mitochondrial transmembrane potential changes in control and high glucose treated groups determined by JC-1 staining- H9c2 cells were treated with high glucose (33 mM) for 48 h in the presence or absence of various concentrations of cinnamic acid or metformin. A) Fluorescent microscopic merged images of H9c2 cells. (a) control, (b) high glucose treated group (HG), (c) HG + metformin, (d) HG + cinnamic acid (100 nM), (e) HG + cinnamic acid (500 nM), (f) control + cinnamic acid (500 nM). Scale bar corresponds to 100 µm. B) Relative fluorescence intensities of mitochondrial transmembrane potential changes. C - control, HG - high glucose treated group, Met - HG + metformin, CiA1 - HG + cinnamic acid (100 nM), CiA2 - HG + cinnamic acid (500 nM), C + CiA2 – control + cinnamic acid (500 nM). Values are expressed as mean ± SEM where $n = 6$. * $p \leq 0.05$ significantly different from the control group. # $p \leq 0.05$ significantly different from HG treated group.

($p \leq 0.05$; Fig. 8) and increased expression of fission proteins DRP1 and FIS1 by 35.2% and 19.5% in HG treated group (Fig. 8). Treatment with CiA at both concentrations (100 and 500 nM) significantly ($p \leq 0.05$) increased the expression of OPA1 by 32.26% and 26.9% which is not dose dependent; and MFN2 by 22.7% and 25.2% (Fig. 8). Also CiA significantly ($p \leq 0.05$) reduced the expression of DRP1 by 29.5% and 32.9% and FIS1 by 16.1% and 21.7% respectively compared to the HG treated groups (Fig. 8). Treatment with metformin also significantly ($p \leq 0.05$) increased the expression of OPA1 and MFN2 by 32.7% and 17.9% respectively and decreased the expression of DRP1 and FIS1 by 15.5% and 10.3% compared to HG treated group (Fig. 8).

3.10. Ca^{2+} overload

Hyperglycemia induced intracellular calcium overload significantly ($p \leq 0.05$) in H9c2 cells, which was evident from increased blue fluorescence of Fura-2 AM (212.7%) compared to control group (Fig. 9). Cotreatment with CiA (100 and 500 nM) or metformin significantly ($p \leq 0.05$) reduced calcium overload by 159.8%, 172.5% and 183.3% respectively compared to HG (Fig. 9).

3.11. Caspase-3 activity assay

Apoptosis was detected by fluorimetric assay of caspase-3. The

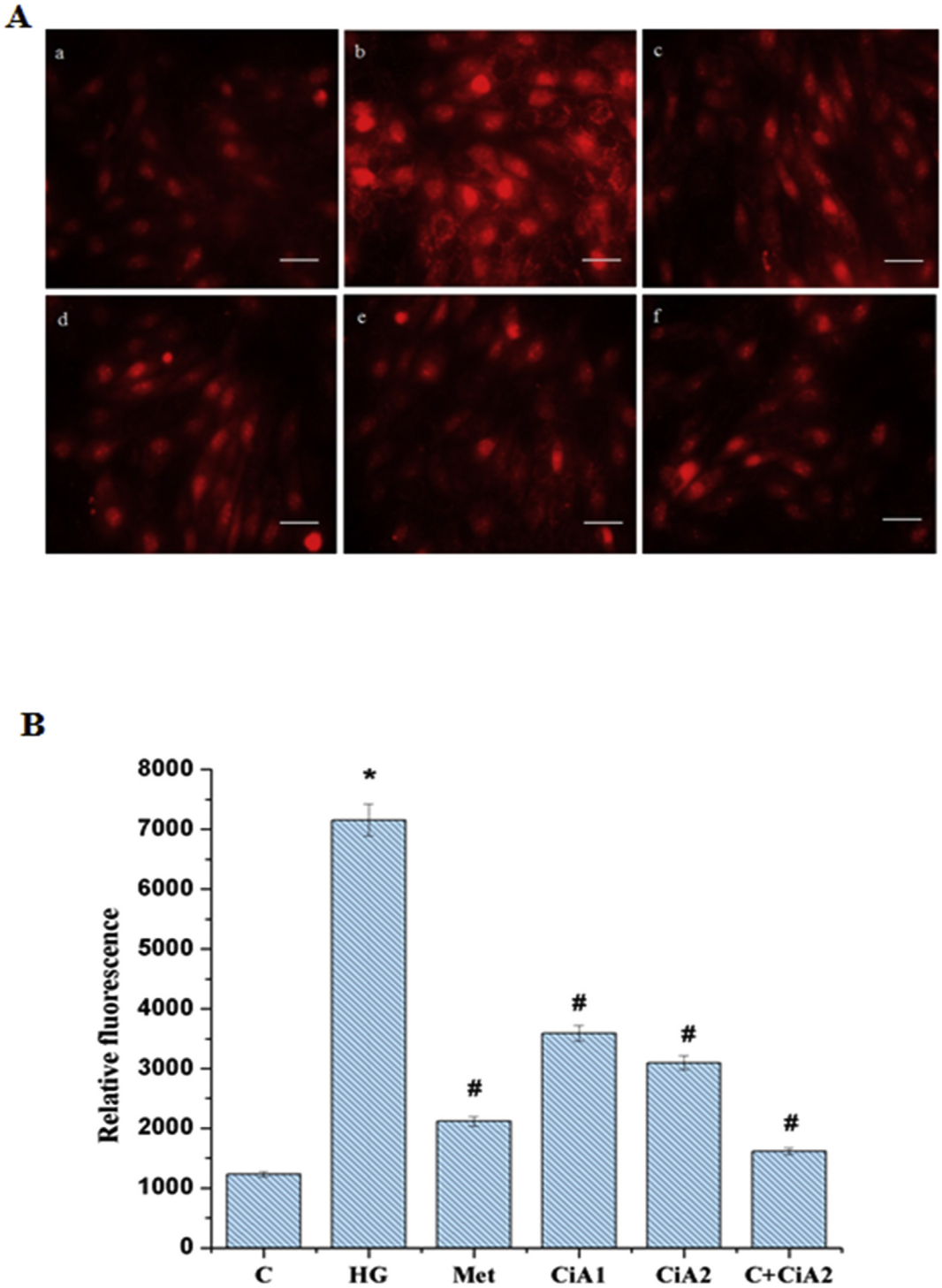

Fig. 7. Mitochondrial superoxide generation during hyperglycemia and amelioration with cinnamic acid and metformin- H9c2 cells were treated with high glucose (33 mM) for 48 h in the presence or absence of various concentrations of cinnamic acid or metformin. A) Representative images of mitochondrial superoxide generation in control and treated cells. (a) control, (b) high glucose treated group (HG), (c) HG + metformin, (d) HG + cinnamic acid (100 nM), (e) HG + cinnamic acid (500 nM), (f) control + cinnamic acid (500 nM). Scale bar corresponds to 100 μm. B) Relative fluorescent intensities of superoxide generation. C - control, HG - high glucose treated group, Met - HG + metformin, CiA1 - HG + cinnamic acid (100 nM), CiA2 - HG + cinnamic acid (500 nM), C + CiA2 – control + cinnamic acid (500 nM). Values are expressed as mean ± SEM where $n = 6$. * $p \leq 0.05$ significantly different from the control group. # $p \leq 0.05$ significantly different from HG treated group.

activity of caspase-3 under high glucose conditions was found enhanced ($p \leq 0.05$) by 137% (Fig.10a) whereas cotreatment with CiA was effective in reducing the activity significantly ($p \leq 0.05$) by 108.2% and 132.4% for 100 and 500 nM respectively (Fig. 10a) and 136.8% for 1 mM metformin (Fig. 10a). In addition protein expression revealed that HG induction caused a significant increase ($p \leq 0.05$) in pro-apoptotic marker protein - Bax (93.6%) and decreased anti-apoptotic marker protein Bcl-2 by 62.4% (Fig. 10b & c). Cotreatment with CiA prevented the increase of pro-apoptotic protein Bax significantly ($p \leq 0.05$) by 37.1% and 52.3% for 100 and 500 nM respectively and

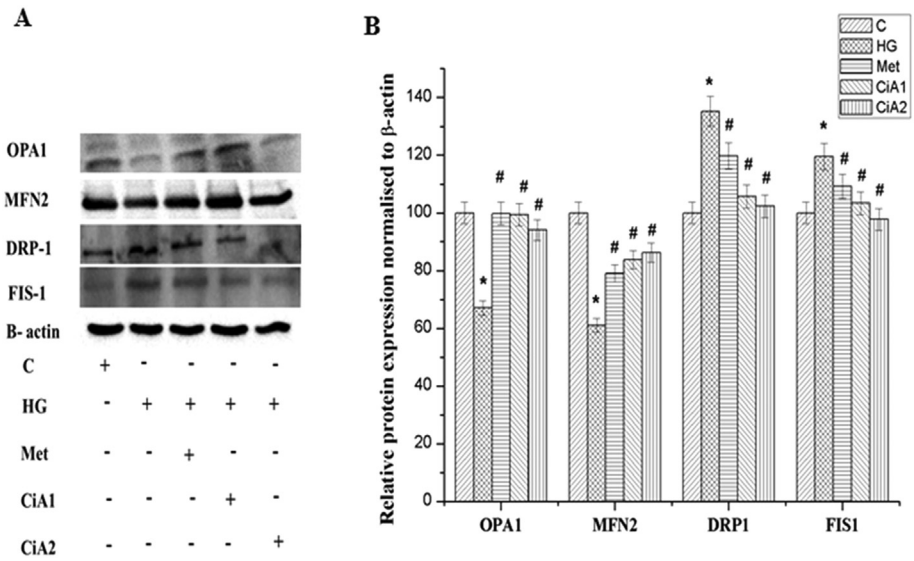

Fig. 8. Effect of cinnamic acid on high glucose induced alterations in mitochondrial dynamics in H9c2 cells- H9c2 cells were treated with high glucose (33 mM) for 48 h in the presence or absence of various concentrations of cinnamic acid or metformin. A) Representative immunoblot of OPA1, MFN2, DRP1 and FIS1 B) Densitometric quantification of western blot of protein level normalized to β actin. * $p \leq 0.05$ significantly different from the control group. # $p \leq 0.05$ significantly different from HG treated group.

decrease ($p \leq 0.05$) of anti-apoptotic protein Bcl-2 by 20.4% and 21.1% for 100 and 500 nM respectively (Fig. 10b & c). Treatment with metformin also significantly prevented the increase of Bax (28%) and decrease of Bcl-2 (37.9%) compared to HG (Fig. 10b & c).

3.12. Flow cytometric analysis with annexin/PI

Flow cytometry results of double staining with annexin V-FITC and PI was interpreted as follows: the upper left quadrant- primary necrotic cells, the upper right- late apoptotic or secondary necrotic cells, the lower left quadrant- viable or live cells and the lower right quadrant- cells with early apoptosis. The results showed that in control cells, 90.5% of the cells were viable, and 1.8% was in late apoptosis or dead cells (Fig. 11). In cells treated with HG only 47.4% cells were viable and 44% cells were in late apoptosis (Fig. 11). Treatment with CiA (100 and 500 nM) or metformin increased the percentage of viable cells by 54.6%, 54.9% and 56% respectively compared to HG treated group (Fig. 11). Also, the percentage of cells undergoing late apoptosis was reduced by 39%, 38.6% and 36% respectively compared to HG treated group for CiA at both concentrations and metformin (Fig. 11).

3.13. Sorbitol production during hyperglycemia

There was a significant increase ($p \leq 0.05$, 31.9%; Fig. 12) in sorbitol levels with HG compared to control. Treatment with CiA at both concentrations (100 and 500 nM) lowered sorbitol levels significantly ($p \leq 0.05$) by 29.7% and 42.5% respectively compared to HG (Fig. 12). Metformin also significantly ($p \leq 0.05$) reduced sorbitol levels by 27.6% from HG treated group (Fig. 12).

4. Discussion

Emerging evidence from experimental, pathological, epidemiological and clinical studies has shown that diabetes mellitus causes cardiac functional and structural changes leading to heart failure (Spector, 1998). In the present study, hyperglycemic shock in H9c2 cells is visible with a decrease in cell viability and an increase in LDH release. This is strengthened with upregulation of ANP, a clinical diagnostic marker for myocardial dysfunction. The products of oxidative stress can damage cellular molecules, DNA, proteins, and lipids leading to cell dysfunctions (Matteucci and Giampietro, 2000). Similarly, lipids are oxidized by free radicals during hyperglycemia leading to lipid peroxidation (Niki, 2008). The redox homeostasis is usually maintained by endogenous antioxidant defense systems like SOD, glutathione peroxidase, catalase and other non-enzymatic antioxidants (Giacco and Brownlee, 2010). We also found a surplus generation of ROS as well as depletion of innate antioxidant enzymes like SOD (total) and a decrease in total antioxidant activity. Furthermore, oxidative stress markers like MDA and protein carbonyl content were also found to be increased. These results reveal that hyperglycemia alters the redox status of H9c2 cells. Similar biochemical alterations have been reported by others too during hyperglycemia with H9c2 cells (Johnson et al., 2017). The present study revealed that CiA treatment suppressed ROS generation and restored the antioxidant status in HG-treated cardiomyocytes.

The presence of high blood glucose level activates all the possible pathways required for glucose removal. Polyol pathway is one such pathway (Chung and Chung, 2005). In the absence of diabetes, polyol pathway remains inactive (Fantus, 2002). The excess NADH produced as a result of the polyol pathway disrupts the redox balance between NADH and NAD+ and overloads the mitochondrial electron transport chain and results in the overproduction of ROS (Luo et al., 2015). Surplus mitochondrial superoxide observed in the present study is most probably via NADH mediated oxidative stress. Besides, NADPH plays a significant role in maintaining the intracellular antioxidant defense by facilitating generation of GSH from its oxidised form, GSSG (Yan et al., 2002). Overconsumption of NADPH by the polyol pathway during hyperglycemia impairs the function of glutathione reductase further intensifying cellular redox imbalance (De Mattia et al., 1994). The significant increase in the levels of sorbitol and depletion of GSH observed in the present study is expected to amplify the redox status alteration with hyperglycemia. However, these parameters were reversed by CiA cotreatment.

Mitochondrial dysfunction constitutes the primary source of ROS in most cells. The primary source of energy in the heart is mitochondria (Nishida and Otsu, 2017). Besides, mitochondria are essential for numerous cellular functions including repair, revival, and apoptosis. The maintenance of mitochondrial transmembrane potential is vital for functions like ATP synthesis and calcium uptake into mitochondria by the Ca^{2+} uniporter (Skarka and Ostadal, 2002). Fluorescence imaging revealed the dissipation of transmembrane potential with hyperglycemia which has been reported by others also (Flarsheim et al., 1996; Bugger and Abel, 2010). This is a relevant biomarker for oxidative stress (Korshunov et al., 1997).

Mitochondria are dynamic organelles with the ability to fuse (fusion) and divide (fission), continuously undergoing a change in the tubular networks in most eukaryotic cells for its optimum metabolic function. The balance between fission and fusion is essential in normal physiology, and any imbalance in these two processes affect the

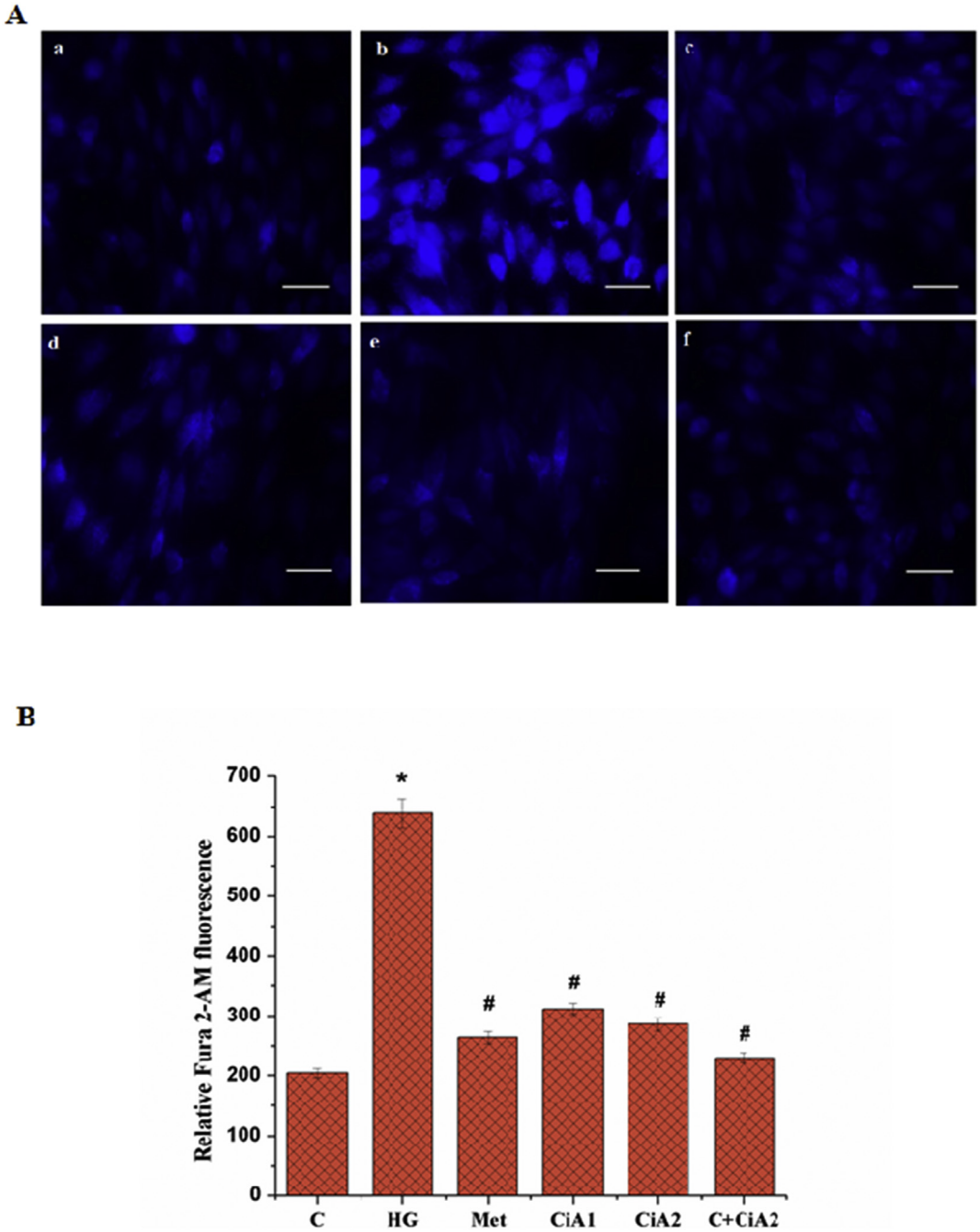

Fig. 9. Intracellular calcium overload during hyperglycemia with H9c2 cells determined by Fura 2 AM staining- H9c2 cells were treated with high glucose (33 mM) for 48 h in the presence or absence of various concentrations of cinnamic acid or metformin. A) Representative images of intracellular calcium ion accumulation in control and treated cells. (a) control, (b) high glucose treated group (HG), (c) HG + metformin, (d) HG + cinnamic acid (100 nM), (e) HG + cinnamic acid (500 nM), (f) control + cinnamic acid (500 nM). Scale bar corresponds to 100 μm. B) Relative fluorescent intensity of the fluorescent images. C - control, HG - high glucose treated group, Met - HG + metformin, CiA1 - HG + cinnamic acid (100 nM), CiA2 - HG + cinnamic acid (500 nM), C + CiA2 – control + cinnamic acid (500 nM). Values are expressed as mean ± SEM where n = 6. * $p \leq 0.05$ significantly different from the control group. # $p \leq 0.05$ significantly different from HG treated group.

function of mitochondria negatively. These networks are maintained by the balance between the opposing processes of mitochondrial fission and fusion (Parra et al., 2011). Hyperglycemia caused overexpression of fission proteins FIS1 and DRP1 accelerating fission and downregulation of fusion proteins OPA1 and MFN2. Oxidative stress, mainly hyperglycemia mediated has been reported to induce an imbalance in mitochondrial dynamics (Ong and Hausenloy, 2010; Yoon and Galloway, 2011). Altered mitochondrial dynamics has become a focus of attention recently due to their involvement in apoptosis (Karbowski and Youle, 2003). It has also been reported that increased levels of ROS during hyperglycemia induces mitochondrial fragmentation (Wang et al., 2012; Rovira-Llopis et al., 2017) via mitochondrial fission. Inhibition of mitochondrial fragmentation has been shown to block the release of mitochondrial apoptotic factors, advocating that fission may engage in permeabilization of mitochondrial transition pore during the beginning of apoptosis (Lee et al., 2004). These alterations in the balance between fusion and fission proteins during hyperglycemia confirm the modifications in redox homeostasis and mitochondrial dynamics.

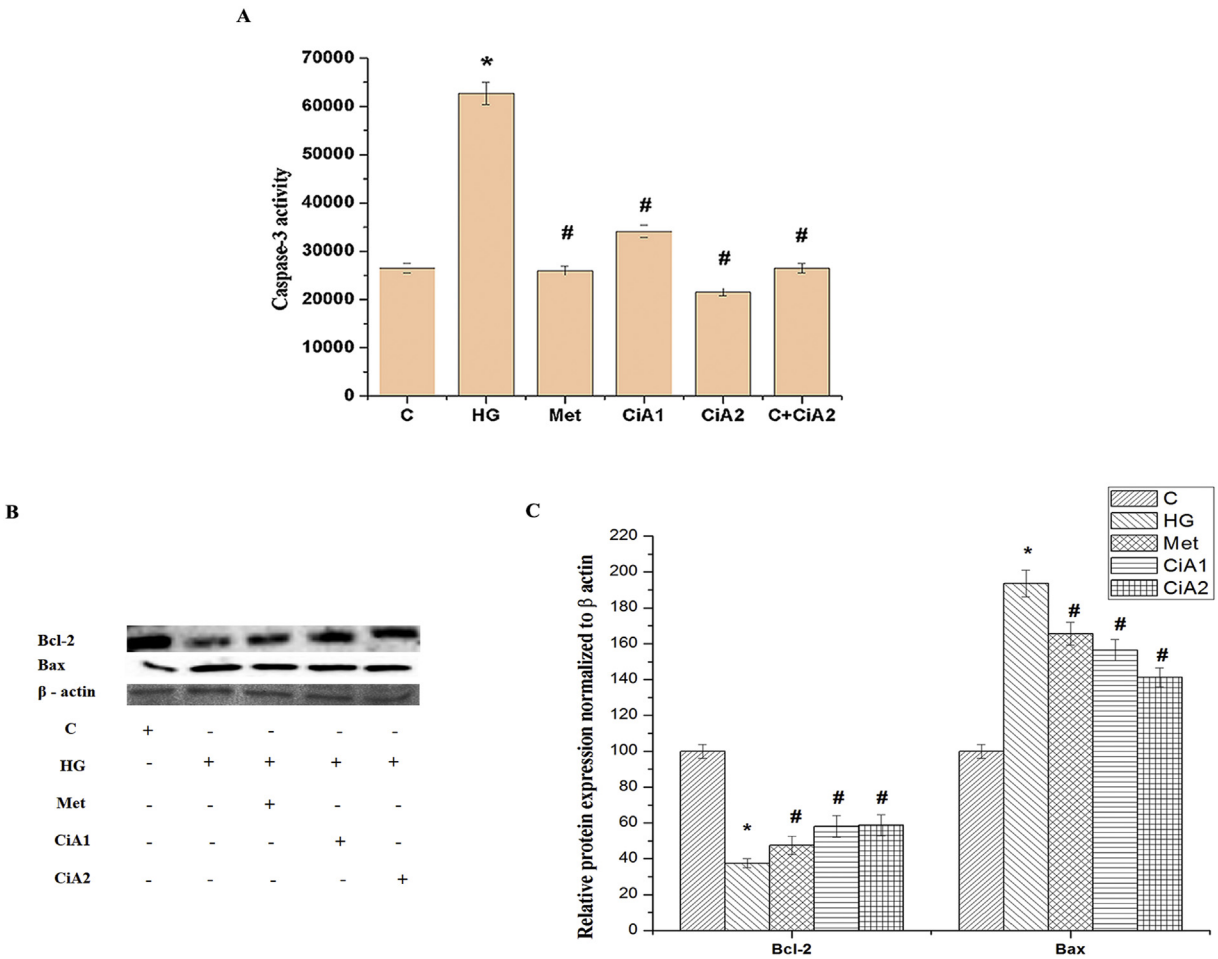

Fig. 10. Evaluation of apoptosis in H9c2 cells during hyperglycemia- H9c2 cells were treated with high glucose (33 mM) for 48 h in the presence or absence of various concentrations of cinnamic acid or metformin. A) Caspase-3 activity during hyperglycemia. B) Representative immunoblot of Bax and Bcl-2. C) Densitometric quantification of western blot of protein level normalized to β actin. C - control, HG - high glucose treated group, Met - HG + metformin, CiA1 - HG + cinnamic acid (100 nM), CiA2 - HG + cinnamic acid (500 nM), C + CiA2 - control + cinnamic acid (500 nM). Values are expressed as mean ± SEM where n = 6. * $p \leq 0.05$ significantly different from the control group. # $p \leq 0.05$ significantly different from HG treated group.

Another significant consequence of hyperglycemia is the increased formation of mitochondrial superoxide anion (Schulze et al., 2004). This activates several major pathways of cellular damage including the previously mentioned polyol pathway (Brownlee, 2001). This has been already observed in the present study and confirms the variation in redox homeostasis in HG in H9c2 cells. This phenomenon has been previously reported by Nishikawa and his group in endothelial cells (Nishikawa et al., 2000). Our results indicate that treatment with CiA improved mitochondrial functions by preserving transmembrane potential, reducing superoxide generation and mitochondrial fission.

Intracellular Ca^{2+} is also an essential factor for cardiac function. Hyperglycemia alters the components of calcium homeostasis leading to diastolic dysfunction (Dobrin and Lebeche, 2010). Increased ROS during hyperglycemia is the main culprit leading to the accumulation of intracellular Ca^{2+} (Wagner et al., 2013). Prolonged mitochondrial oxidative stress results in the opening of permeability transition pore leading to cytosolic Ca^{2+} accumulation. The present study also revealed significant calcium overload in the HG-treated group. Dissipation of mitochondrial membrane potential during hyperglycemia is reported to affect calcium uptake into mitochondria (Skarka and Ostadal, 2002). Our study shows that CiA treatment was able to decrease the intracellular Ca^{2+} accumulation in H9c2 cells via improving mitochondrial functions.

Oxidative stress also leads to the activation of the cysteine aspartate protease-3 (caspase-3), which is the crucial step in the genesis of apoptosis. Pathological stressful stimuli activate certain pro-apoptotic members like Bax which leads to its translocation from the cytosol to the outer mitochondrial membrane while Bcl-2 expression has been proposed as an essential marker of myocardial cell survival (Rovira-Llopis et al., 2017). In the present study. caspase-3 activity and the expression of pro-apoptotic protein Bax were found to have increased and anti-apoptotic protein Bcl-2 was found to have decreased. In addition, this is also supported by visualization of apoptosis. The alteration in transmembrane potential is reported to contribute to apoptosis (Lee et al., 2004) which is already observed in the present study. However, CiA cotreatment downregulated the expression of the proapoptotic protein Bax and increased the expression of Bcl-2 in hyperglycemic cardiomyocytes. This is the first investigation to reveal the role of sorbitol accumulation from polyol pathway with an imbalance in mitochondrial dynamics during hyperglycemia leading to apoptosis in H9c2 cells via alterations in redox status. It is of paramount importance to identify the cellular and molecular mechanisms responsible for the pathology to design a proper treatment regimen.

In the present study, CiA (100 nM and 500 nM) was applied simultaneously with HG to assess its beneficial property. Although CiA has been evaluated for its potential against diabetes and cardiovascular diseases (Song et al., 2013; Hafizur et al., 2015), the mechanism by which it protects the cardiomyocytes from hyperglycemic insult has not been evaluated. In this study, it is observed that CiA prevented cardiomyocyte apoptosis by improving mitochondrial function, calcium

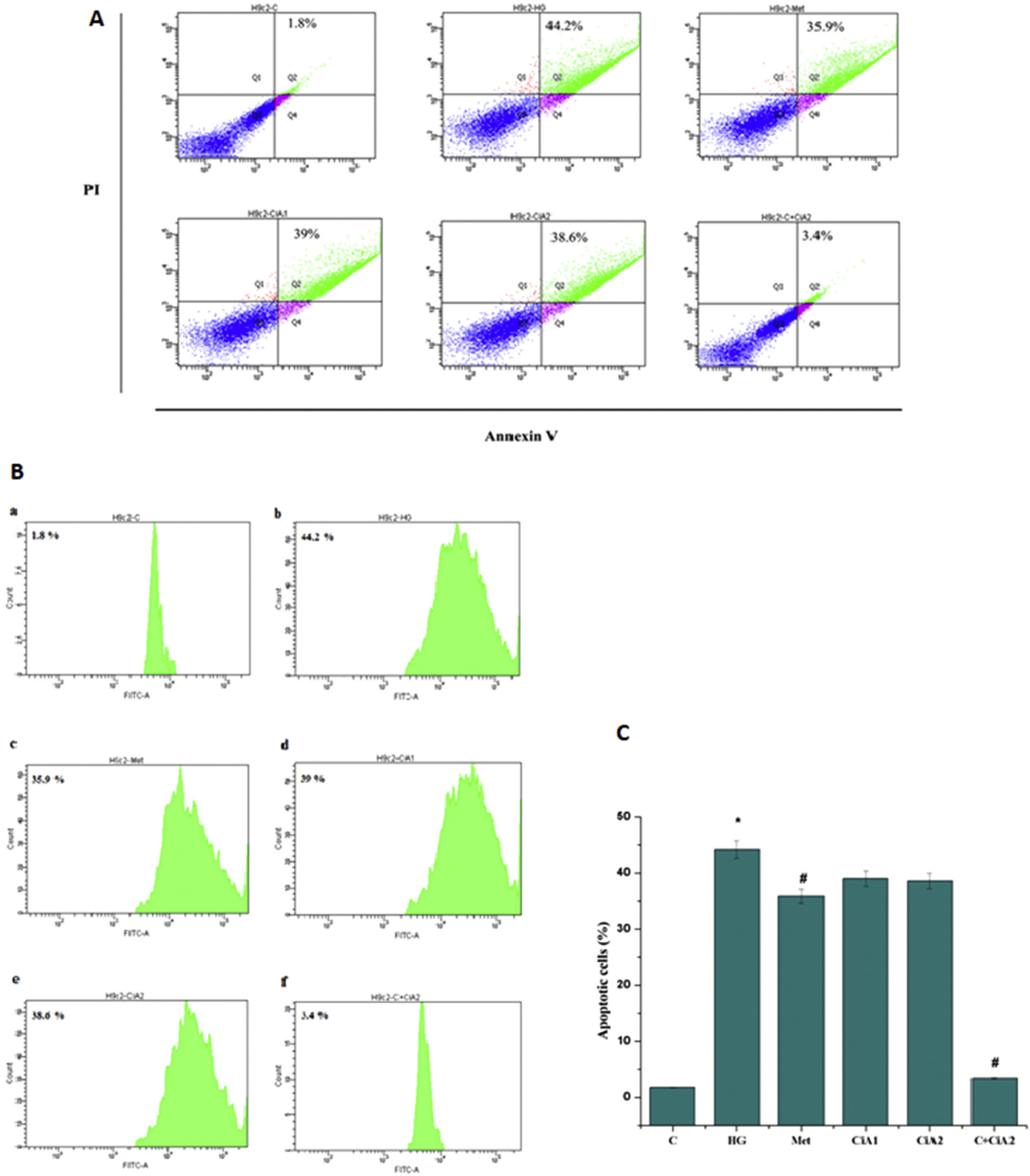

Fig. 11. Detection of apoptosis by annexin V-FITC/PI double staining- H9c2 cells were treated with high glucose (33 mM) for 48 h in the presence or absence of various concentrations of cinnamic acid or metformin. A) Flow cytometric scatter graph showing different quadrants: the upper left quadrant represents primary necrotic cells, the upper right quadrant represents late apoptotic or secondary necrotic cells, the lower left quadrant represents viable or live cells and the lower right quadrant represents cells with early apoptosis. B) The representative histogram showing cells stained with Annexin V-FITC (a) control, (b) high glucose treated group (HG), (c) HG + metformin, (d) HG + cinnamic acid (100 nM), (e) HG + cinnamic acid (500 nM), (f) control + cinnamic acid (500 nM). C) Statistical analysis of flow cytometry results. Values are expressed as mean ± SEM where n = 6. * $p \leq 0.05$ significantly different from the control group. # $p \leq 0.05$ significantly different from HG treated group.

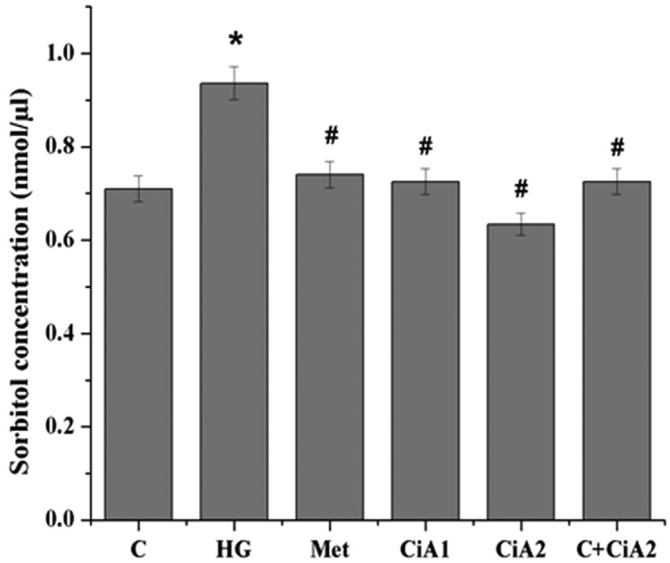

Fig. 12. Sorbitol levels in high glucose treated H9c2 cells and amelioration with cinnamic acid- H9c2 cells were treated with high glucose (33 mM) for 48 h in the presence or absence of various concentrations of cinnamic acid or metformin. C - control, HG - high glucose treated group, Met - HG + metformin, CiA1 - HG + cinnamic acid (100 nM), CiA2 - HG + cinnamic acid (500 nM), C + CiA2 – control + cinnamic acid (500 nM). Values are expressed as mean ± SEM where n = 6. * $p \leq 0.05$ significantly different from the control group. # $p \leq 0.05$ significantly different from HG treated group.

homeostasis and reducing sorbitol accumulation. Since there is high demand for natural products derived nutraceuticals, this study is highly promising in the area of development of nutraceuticals against diabetes-associated heart problems.

5. Conclusion

From the overall results, we conclude that apoptosis results from exposure of HG to H9c2 cells via alteration in redox status linked mitochondrial dynamics and polyol pathway. Further CiA is expected to be a potent phytochemical for the hyperglycemic insult to H9c2 cells. Detailed *in vivo* experiments are required to confirm these *in vitro* study results and to prove beneficial for diabetic cardiomyopathy.

Conflict of interest

Author AN declares that she has no conflict of interest. Author PMR declares that she has no conflict of interest. Author SGL declares that she has no conflict of interest. Author KGR declares that he has no conflict of interest.

Acknowledgement

Anupama Nair thanks Council for Scientific and Industrial Research, Govt. of India, for financial assistance in the form of research fellowship (Grant Id: 31/038(0512)/2015-EMR-I). We thank the Director, CSIR-NIIST for providing necessary facilities.

References

Balteau, M., Tajeddine, N., de Meester, C., et al., 2011. NADPH oxidase activation by hyperglycaemia in cardiomyocytes is independent of glucose metabolism but requires SGLT1. Cardiovasc. Res. 92 (2), 237–246.
Bodor, G.S., 2016. Biochemical markers of myocardial damage. EJIFCC 27, 95–111.
Brookes, P.S., Yoon, Y., Robotham, J.L., Anders, M.W., Shey-Shing, S., 2004. Calcium, ATP, and ROS: a mitochondrial love-hate triangle. Am. J. Phys. Cell Phys. 287, C817–C833.
Brownlee, M., 2001. Biochemistry and molecular cell biology of diabetic complications. Nature 414, 813–820.
Bugger, H., Abel, E.D., 2010. Mitochondria in the diabetic heart. Cardiovasc. Res. 88, 229–240.
Cai, L., Li, W., Wang, G., Guo, L., Jiang, Y., Kang, Y.J., 2002. Hyperglycemia-induced apoptosis in mouse myocardium mitochondrial cytochrome c–mediated caspase-3 activation pathway. Diabetes 51, 1938–1948.
Choi, S.W., Benzie, I.F., Ma, S.W., Strain, J.J., Hannigan, B.M., 2008. Acute hyperglycemia and oxidative stress: direct cause and effect? Free Radic. Biol. Med. 44, 1217–1231.
Chung, S.S., Chung, S.K., 2005. Aldose reductase in diabetic microvascular complications. Curr. Drug Targets 6 (4), 475–486.
Das, J., Ghosh, J., Manna, P., Sinha, M., Sil, P.C., 2009. Taurine protects rat testes against NaAsO(2)-induced oxidative stress and apoptosis via mitochondrial dependent and independent pathways. Toxicol. Lett. 187, 201–210.
De Mattia, G., Laurenti, O., Bravi, C., et al., 1994. Effect of aldose reductase inhibition on glutathione redox status in erythrocytes of diabetic patients. Metabolism 43 (8), 965–968.
Dobrin, J.S., Lebeche, D., 2010. Diabetic cardiomyopathy: signaling defects and therapeutic approaches. Expert. Rev. Cardiovasc. Ther. 8, 373–391.
Fantus, I.G., 2002. The pathogenesis of the chronic complications of the diabetes mellitus. Endocrinol. Rounds 2 (4), 1–8.
Flarsheim, C.E., Grupp, I.L., Matlib, M.A., 1996. Mitochondrial dysfunction accompanies diastolic dysfunction in diabetic rat heart. Am. J. Phys. 271, H192–H202.
Giacco, F., Brownlee, M., 2010. Oxidative stress and diabetic complications. Circ. Res. 107, 1058–1070.
Hafizur, R.M., Hameed, A., Shukrana, M., et al., 2015. Cinnamic acid exerts anti-diabetic activity by improving glucose tolerance in vivo and by stimulating insulin secretion in vitro. Phytomedicine 22, 297–300.
Johnson, R., Dludla, P.V., Muller, C.J., Huisamen, B., Essop, M.F., Louw, J., 2017. The transcription profile unveils the cardio protective effect of aspalathin against lipid toxicity in an in vitro H9c2 model. Molecules 22. https://doi.org/10.3390/molecules22020219.
Kain, V., Kumar, S., Sitasawad, S.L., 2011. Azelnidipine prevents cardiac dysfunction in streptozotocin-diabetic rats by reducing intracellular calcium accumulation, oxidative stress and apoptosis. Cardiovasc. Diabetol. 10, 97. https://doi.org/10.1186/1475-2840-10-97.
Karbowski, M., Youle, R.J., 2003. Dynamics of mitochondrial morphology in healthy cells and during apoptosis. Cell Death Differ. 10, 870–880.
Kawahito, S., Kitahata, H., Oshita, S., 2009. Problems associated with glucose toxicity: Role of hyperglycemia-induced oxidative stress. World J. Gastroenterol. 15 (33), 4137–4142.
Kayama, Y., Raaz, U., Jagger, A., et al., 2015. Diabetic cardiovascular disease induced by oxidative stress. Int. J. Mol. Sci. 16, 25234–25263.
Korshunov, S.S., Skulachev, V.P., Starkov, A.A., 1997. High protonic potential actuates a mechanism of production of reactive oxygen species in mitochondria. FEBS Lett. 416, 15–18.
Kuznetsov, A.V., Javadov, S., Sickinger, S., Frotschnig, S., Grimm, M., 2015. H9c2 and HL-1 cells demonstrate distinct features of energy metabolism, mitochondrial function, and sensitivity to hypoxia-reoxygenation. Biochim. Biophys. Acta 1853 (2), 276–284.
Lakshmi, B.S., Sujatha, S., Anand, S., et al., 2009. Cinnamic acid, from the bark of *Cinnamomum cassia*, regulates glucose transport via activation of GLUT4 on L6 myotubes in a phosphatidylinositol 3-kinase-independent manner. J. Diabetes 1, 99–106.
Lee, Y.J., Jeong, S.Y., Karbowski, M., Smith, C.L., Youle, R.J., 2004. Roles of the mammalian mitochondrial fission and fusion mediators Fis1, Drp1, and Opa1 in apoptosis. Mol. Biol. Cell 15, 5001–5011.
Liquori, M.E., Christenson, R.H., Collinson, P.O., Defilippi, C.R., 2014. Cardiac biomarkers in heart failure. Clin. Biochem. 47, 327–337.
Luo, X., Li, R., Yan, L.J., 2015. Roles of pyruvate, NADH, and mitochondrial complex I in redox balance and imbalance in β cell function and dysfunction. J. Diabetes Res. 2015 (512618). https://doi.org/10.1155/2015/512618.
Marín-García, J., 2010. Cardiac function in heart failure: The role of calcium cycling. Heart failure: Bench to bedside. In: Contemporary Cardiology. Springer, New York, pp. 15–22. https://doi.org/10.1007/978-1-60761-147-9_2.
Matteucci, E., Giampietro, O., 2000. Oxidative stress in families of type 1 diabetic patients. Diabetes Care 23, 1182–1186.
Ni, H.M., Williams, J.A., Ding, W.X., 2015. Mitochondrial dynamics and mitochondrial quality control. Redox Biol. 4, 6–13.
Niero, E.L., Machado-Santelli, G.M., 2013. Cinnamic acid induces apoptotic cell death and cytoskeleton disruption in human melanoma cells. J. Exp. Clin. Cancer Res. 32, 31. https://doi.org/10.1186/1756-9966-32-31.
Niki, E., 2008. Lipid peroxidation products as oxidative stress biomarkers. Biofactors 34, 171–180.
Nishida, K., Otsu, K., 2017. Inflammation and metabolic cardiomyopathy. Cardiovasc. Res. 113, 389–398.
Nishikawa, T., Edelstein, D., Du, X.L., et al., 2000. Normalizing mitochondrial superoxide production blocks three pathways of hyperglycaemic damage. Nature 404, 787–790.
Oates, P.J., 2002. Polyol pathway and diabetic peripheral neuropathy. Int. Rev. Neurobiol. 50, 325–392.
Ong, S.-B., Hausenloy, D.J., 2010. Mitochondrial morphology and cardiovascular disease. Cardiovasc. Res. 88, 16–29.
Parra, V., Verdejo, H., del Campo, A., et al., 2011. The complex interplay between mitochondrial dynamics and cardiac metabolism. J. Bioenerg. Biomembr. 43, 47–51.
Preetha Rani, M.R., Anupama, N., Sreelekshmi, M., Raghu, K.G., 2018. Chlorogenic acid attenuates glucotoxicity in H9c2 cells via inhibition of glycation and PKC α

upregulation and safeguarding innate antioxidant status. Biomed Pharmacother 100, 467–477.
Robinson, J.A., Jenkins, N.S., Holman, N.A., Roberts-Thomson, S.J., Monteith, G.R., 2004. Ratiometric and non- ratiometric Ca^{2+} indicators for the assessment of intracellular free Ca^{2+} in a breast cancer cell line using a fluorescence microplate reader. J. Biochem. Biophys. Methods 58, 227–237.
Rovira-Llopis, S., Bañuls, C., Diaz-Morales, N., Hernandez-Mijares, A., Rocha, M., Victor, V.M., 2017. Mitochondrial dynamics in type 2 diabetes: Pathophysiological implications. Redox Biol. 11, 637–645.
Safi, S.Z., Qvist, R., Kumar, S., Batumalaie, K., Ismail, I.S.B., 2014. Molecular Mechanisms of Diabetic Retinopathy, General Preventive strategies, and Novel Therapeutic Targets. Biomed. Res. Int. 2014https://doi.org/10.1155/2014/801269. 801269.
Schulze, P.C., Yoshioka, J., Takahashi, T., He, Z., King, G.L., Lee, R.T., 2004. Hyperglycemia promotes oxidative stress through inhibition of thioredoxin function by thioredoxin-interacting protein. J. Biol. Chem. 279, 30369–30374.
Skarka, L., Ostadal, B., 2002. Mitochondrial membrane potential in cardiac myocytes. Physiol. Res. 51, 425–434.
Song, F., Li, H., Sun, J., Wang, S., 2013. Protective effects of cinnamic acid and cinnamic aldehyde on isoproterenol-induced acute myocardial ischemia in rats. J. Ethnopharmacol. 150, 125–130.
Spector, K.S., 1998. Diabetic cardiomyopathy. Clin. Cardiol. 21, 885–887.
Wagner, S., Rokita, A.G., Anderson, M.E., Maier, L.S., 2013. Redox regulation of sodium and calcium handling. Antioxid. Redox Signal. 18, 1063–1077.
Wang, W., Wang, Y., Long, J., et al., 2012. Mitochondrial fission triggered by hyperglycemia is mediated by ROCK1 activation in podocytes and endothelial cells. Cell Metab. 15, 186–200.
Wilson, A.P., 2000. Cytotoxicity and viability assays. In: JRW Masters, Animal Cell Culture, 3rd Ed. Oxford University, Oxford, pp. 175–219.
Yan, L.J., Christians, E.S., Liu, L., et al., 2002. Mouse heat shock transcription factor 1 deficiency alters cardiac redox homeostasis and increases mitochondrial oxidative damage. EMBO J. 21 (19), 5164–5172.
Yang, L., Wu, Q.Q., Liu, Y., Hu, Z.F., Bian, Z.Y., Tang, Q.Z., 2015. Cinnamaldehyde attenuates pressure overload-induced cardiac hypertrophy. Int. J. Clin. Exp. Pathol. 8, 14345–14354.
Yoon, Y., Galloway, C.A., Jhun, B.S., Yu, T., 2011. Mitochondrial dynamics in diabetes. Antioxid. Redox Signal. 14, 439–457.